DYNAMICS OF NEURON-SPECIFIC GENE EXPRESSION DURING DEVELOPMENT AND IN RESPONSE TO SELECTIVE LESIONS OF THE RAT CENTRAL NERVOUS SYSTEM

A Dissertation Presented

By

Richard H. Melloni, Jr.

Submitted to the Faculty of the
University of Massachusetts Graduate School of Biomedical Sciences, Worcester
in partial fulfillment of the requirements for the degree of:

DOCTOR OF PHILOSOPHY IN MEDICAL SCIENCES

April 1993

Cell Biology

DYNAMICS OF NEURON-SPECIFIC GENE EXPRESSION DURING DEVELOPMENT AND IN RESPONSE TO SELECTIVE LESIONS OF THE RAT CENTRAL NERVOUS SYSTEM

A Dissertation Presented
By
Richard H. Melloni, Jr.

Approved as to style and content by:

_____
Dr. Edward G. Fey, Chairman of Committee

_____
Dr. Robert H. Singer, Member

_____
Dr. James E. Hamos, Member

_____
Dr. Craig F. Ferris, Member

_____
Dr. Lydia Villa-Komaroff, Member

_____
Dr. Louis J. DeGennaro,
Dissertation Advisor

_____
Dr. Thomas B. Miller, Dean of
Graduate School of Biomedical Sciences

Department of Cell Biology
April 1993

In loving memory of my grandfather, Jeldino Melloni, whose lost battle with Senile Dementia of the Alzheimer's Type (SDAT) has been a constant source of inspiration.

This dissertation is dedicated to my parents, Sybil and Richard Sr.
Your sacrifice, love and friendship have made this possible.
I thank you.

ACKNOWLEDGEMENTS

It is with great pleasure that I acknowledge the many people who have helped make the work embodied in this dissertation possible. First, I would like to express my gratitude to my mentor, Dr. Louis J. DeGennaro, for providing a stimulating research environment and granting me the opportunity to pursue a research project of both personal and professional interest. I would also like to thank Lou for stimulating my growth as bench scientist and fine-tuning my skills as an author. His multitude of "red ink" suggestions have proved invaluable in training the scientific writer.

I wish to extend special thanks to Drs. Mark J. Alexander and David S. Howland for their scientific guidance and expert technical assistance. Their insight, advice and criticisms during critical stages of this project have had a significant impact on the direction and ultimately the quality of the work embodied in this dissertation. And more, I thank them for their friendship throughout. I wish to thank Dr. Edward G. Fey for assistance with SDS-PAGE and Western blotting, and for the all too frequent use of his Macintosh computer. Most especially, I would like to thank Ted for his continual interest, advice and criticisms of various aspects of the research project.

I would like to express thanks to Dr. Neil Aronin for suggesting the use of Dde I-digested cDNA probes for *in situ* hybridization, Dr. James E. Hamos for demanding a precise understanding of complex synaptic circuitry and the cellular considerations of synaptic plasticity and remodeling, and Dr. Paul R. Dobner for his advice during our combined lab meetings. I would like to express my gratitude to Drs. Brian J. Cummings and Carl W. Cotman, University of California, Irvine, for their time and resources devoted to the instruction of the perforant pathway transection procedure. Also, I wish to thank Donna Pulaski-Salo for her assistance with immunohistochemistry and for her life-saving help with the photography.

I would like to express my deepest thanks to close friends Ed Kislauskis, Walter

Nishioka, Robert Harrison, and Craig and Maria Cornwall. Their friendships have made the most grueling of processes bearable and, in many instances, actually enjoyable.

I would like to express my sincerest thank-you to my parents, Sybil and Richard Sr. I recognize them for their sacrifice through 25 years of education, and thank them for their love, support, and friendship . It is a rare instance that parents are both Mom & Dad and friend. I would also like to extend my gratitude to the members of my immediate family for their love and support through the years.

Last, but certainly not least, I wish to share this achievement with my fiance, Kimberly A. Lonis. Her love, support and persistant encouragement have made this endeavor possible. Her faith in me, without a doubt, has been the single most motivating factor in my life. Thank-you June 30, 1990.

ABSTRACT

Synapse development and injury-induced reorganization in the nervous system have been extensively characterized morphologically, although, relatively little is known regarding the molecular and biochemical events that underlie these processes. In an attempt to better understand, at the molecular level, the role of the expression of synaptic proteins during synapse establishment and regeneration, this dissertation examines the dynamics of expression of the neuron-specific gene synapsin I during development and in response to selective lesions of the rat central nervous system. Synapsin I is the best characterized member of a family of nerve-terminal specific phosphoproteins implicated in the regulation of neurotransmitter release. During development, the expression of synapsin I correlates temporally and topographically with synapse formation, and recent physiological studies by Lu *et al.*, (1992) have suggested that synapsin I may participate in the functional maturation of synapses. To better understand the temporal relationship between synapsin I gene expression and particular cellular events during development, we have used *in situ* hybridization histochemistry to localize synapsin I mRNA in the rat central and peripheral nervous systems throughout embryonic and postnatal development, and into the adult period.

During development, from the earliest embryonic time point examined (E12), the expression of the synapsin I gene was detectable in both the rat central and peripheral nervous systems. While, in general, levels of synapsin I mRNAs were high in utero, synapsin I cDNA probes revealed specific patterns of hybridization in different regions of the embryonic nervous system. To precisely determine the temporal onset of expression of the synapsin I gene during neuronal development, we examined in detail the appearance of synapsin I mRNA during the well characterized postnatal development of the cerebellum and hippocampus. In both regions, the onset of synapsin I gene expression correlated with the period of stem cell commitment to terminal differentiation. In a second phase, in accord

with prior analyses, synapsin I gene expression increases to a maximum for a given neuronal population during synapse formation.

In the adult rat brain, our data demonstrates a widespread yet regionally variable pattern of expression of synapsin I mRNA similar to that seen at earlier time points, with noteworthy exceptions. The greatest abundance of synapsin I mRNA was found in the pyramidal neurons of the CA3 and CA4 fields of the hippocampus, and in the mitral and internal granular cell layers of the olfactory bulb. Other areas abundant in synapsin I mRNA were the layer II neurons of the piriform and entorhinal cortices, the granule cell neurons of the dentate gyrus, the pyramidal neurons of hippocampal fields CA1 and CA2, and the cells of the parasubiculum. In general, the pattern of expression of synapsin I mRNA paralleled those encoding other synaptic terminal-specific proteins, such as synaptophysin, VAMP-2, and SNAP-25. Then, to determine specifically how synapsin I mRNA levels are related to levels of synapsin I protein in the adult rat brain, we employed *in situ* hybridization histochemistry and immunohistochemistry to examine in detail the local distribution of both synapsin I mRNA and protein in the hippocampus. In short, these data revealed differential levels of expression of synapsin I mRNA and protein within defined synaptic circuits of the rat hippocampus. Based on these data we hypothesized that locally high levels of synapsin I mRNA in neuronal somata may reflect the ability of the nervous system to respond to select enviromental stimuli and/or injury by producing long-term changes in synaptic circuitry.

To test this hypothesis and to better understand the regulation and putative role of synapsin I gene expression in the development of functional synapses in the central nervous system, we first examined the developmental pattern of expression of the synapsin I gene in dentate granule neurons of the dentate gyrus and their accompaning mossy fibers during the main period of synaptogenic differentiation in the rat hippocampus. The results of these studies indicate a significant difference between the temporal expression of synapsin I mRNA in dentate granule cell somata and the appearence of protein in their

mossy fiber terminals during the postnatal development of these neurons. Next, to investigate the regulation and putative role of synapsin I gene expression during the restoration of synaptic contacts in the central nervous system, we examined the expression of the synapsin I mRNA and protein following lesions of hippocampal circuitry. These studies show marked changes in the pattern and intensity of synapsin I immunoreactivity in the dendritic fields of dentate granule cell neurons following perforant pathway transection. In contrast, changes in synapsin I mRNA expression in target neurons, and in those neurons responsible for the reinnervation of this region of the hippocampus, were not found to accompany new synapse formation.

On a molecular level, both developmental and lesion data suggest that the expression of the synapsin I gene is tightly regulated in the central nervous system, and that considerable changes in synapsin I protein may occur in neurons without concommitant changes in the levels of its mRNA. From a functional standpoint, our results suggest that the appearance of detectable levels of synapsin I protein in developing and sprouting synapses does not reflect simply synaptogenesis, but coincides with the acquisition of function by those central synapses.

TABLE OF CONTENTS

LIST OF FIGURES

LIST OF TABLES

COLLABORATORS

CHAPTER III

Patricia S. Estes was involved in initial attempts to develope and implement the use of an urea based buffer as described by Sive et al., (1989) for brain punch-RNA analysis.

Dr. Paul R. Dobner provided the 18s ribosomal RNA DNA clone.

Dr. Robert H. Singer provided the α-tubulin cDNA clone.

CHAPTER VI

Dr. Paul J. Apostolides performed synapsin I-immunohistochemistry on the developing rat hippocampus.

Dr. Edward Fey provided assistance with protein extraction, SDS-PAGE, and Western blot analysis.

Dr. Paul R. Dobner provided the 18s ribosomal RNA DNA clone.

Donna Pulaski-Salo provided technical assistance with synapsin I immunohistochemistry on perforant pathway transected rat brains.

Chapter I

INTRODUCTION

Overview

Behavioral and clinical data from throughout the animal kingdom have implicated the hippocampal region of the brain in the establishment and maintenance of memory. This region within the medial temporal lobe of the cerebral cortex has been extensively studied in mammals, from rodents to primates, and is known to be involved neuropathologically in diseases that include a clinical spectrum of memory, behavioral, and cognitive dysfunction (e.g. Alzheimer's Disease (AD)). On a physiological and cellular level, it is generally accepted that neurons in the hippocampus can reorganize their synaptic connections to produce long-term changes in synaptic circuitry in response to pathological perturbations of local circuitry similar to those seen in AD, and in response to injury (reactive synaptogenesis) and/or select environmental stimuli. Reorganization occurs as surviving afferent systems innervating the afflicted zone direct local growth responses in an attempt to recapture and replace lost synaptic connections and, thereby, maintain synaptic density. Denervating lesions of the rat hippocampal formation have provided a model system suitable for the study of morphological and functional plasticity after injury. The process of reactive synaptogenesis has been extensively characterized in this system by several physiological and many morphological studies of the hippocampal region, although, to date relatively little is known regarding the molecular and biochemical events that underlie the sprouting response.

One of the main goals of the research described in this dissertation is to gain an understanding of the molecular events that are associated with and/or regulate the establishment and regeneration of synapses in the central nervous system (CNS).

Recently, data from our laboratory and the laboratories of others have characterized the nerve terminal-specific protein synapsin I as a marker of severe focal synaptic loss in the hippocampus of patients with AD (Perdahl et al., 1984; Hamos et al., 1988). Further study of this region employing more quantitative immunohistochemical methodologies suggested that synapsin I immunoreactivity may in fact be used as a sensitive indicator of neuronal sprouting during the reinnervation of the hippocampus by surviving afferent systems (J.E. Hamos, personal communication). Thus, to better understand the adaptive properties and parameters of synaptic reorganization, I have examined the expression of the synapsin I gene during development and following lesioned-induced reinnervation of the rat hippocampus.

The Hippocampal Formation: A Model for Synaptic Plasticity

In order to study the functional anatomy of the hippocampal region or hippocampal "formation" and its ability to undergo extensive remodelling during reactive synaptogenesis, it is first necessary to describe the normal circuitry of the region. The anatomy and cytoarchitecture of the hippocampal region have been studied extensively using Golgi (Cajal, 1911; Lorente de No, 1934), lesion (Blackstad, 1956, 1958; Raisman et al., 1965, 1966; Hjorth-Simonsen, 1972, 1973), physiologic transport (Swanson and Cowan, 1975, 1976, 1977; Steward, 1976; Meibach and Siegal, 1977a,b), and axonal tracing methods (Swanson et al., 1981). These studies have culminated in a detailed map of the hippocampal region, its efferent projections and incoming afferent fiber systems. In man, the hippocampal region extends along the floor of the temporal horn of the lateral ventricle and is considered a gyrus of the allocortex. In rodents, this region occupies most of the ventroposterior and ventrolateral walls of the cerebral cortex. It extends beneath the corpus callosum from the posterior level of the septal nuclei, anteriorly, to the level of the splenium, posteriorly. The organization of the hippocampal region is more simple than that of the neocortex. It is principally composed of three main structures: (1) the hippocampus

(the CA1-CA4 fields of Ammon's horn), (2) the dentate gyrus, and (3) the cortical areas collectively referred to as the subiculum and entorhinal cortex (Figure 1).

Let us focus on the hippocampus proper (including the dentate gyrus) and its afferent and efferent connections. The hippocampus is a U-shaped fold of cortex which may be subdivided into four distinct fields running along its length. They are referred to as the CA1, CA2, CA3, and CA4 fields of Ammon's horn as described by Lorente de No (1934). These fields extend from the area adjacent to the prosubliculum (most lateral aspect of the subicular complex) to the hilus of the dentate gyrus. The most remarkable cellular elements of this region of the hippocampus are the layered pyramidal cells stacked 3-5 cell layers deep formally named as cells of the *stratum pyramidale*. Hippocampal field CA1 is a field of tightly packed medium-sized cells divided into three zones, a, b, and c. Zone a is the region adjacent to the prosubiculum where scattered deep cells extend beneath the superfical packed pyramidal neurons (Bayer, 1985). Immediately following are zones b and c, distinguishable only by fiber-staining preparations. Hippocampal field CA2 is composed of a tightly packed narrow band of pyramidal neurons adjacent to CA1, itself soley distinguishable by the absence of characteristic spiny thorns of the proximal spical dendrites. Pyramidal cells of hippocampal field CA3 are divided into three zones (a, b, and c) based on the number of Schaffer collaterals supplied by each of these regions. The three regions are indistinguishable in standard Nissal preparations, however, it is important to note that CA3c pyramidal neurons lie partly within the hilar region of the dentate gyrus, their boundry marked by establishing a perpendicular from the tip of the lateral blade of the dentate gyrus to the medial blade.

The cells of hippocampal fields CA1-CA4 direct sets of axon collaterals towards both intra- and extra-hippocampal targets. For example, neurons of fields CA1, CA2, and CA3 each may send a bifurcated axon collateral out the fimbria-fornix toward extra-hippocampal targets. At the same time, the same CA1 and CA3 neurons may extend collateral axons within the hippocampus, CA1 toward the subicular complex, and CA3

Figure 1. A horizontal section of the hippocampal region in an adult rat brain to identify all major anatomical subdivisions. Amn, Ammon's horn; CA1-CA3, field CA1-CA3 pyramidal cells, each divided into a, b, and c subdivisions; DG, dentate gyrus; Ect, ectal limb of the granule cell layer of the dentate gyrus; End, endal limb; EntI, EntL, EntM, intermediate, lateral, and medial subdivisions, respectively, of the entorhinal cortex; fi, fimbria; h, hilus of the dentate gyrus (also referred to as CA4); LMlo, lacunosum moleculare layer; Mol, molecular layer of subiculum; Or, oriens layer; PaS, parasubiculum; Pros, prosubiculum; PrS, presubiculum; Py, pyramidal layer; Rad, radiatum layer; RF, rhinal fissure.

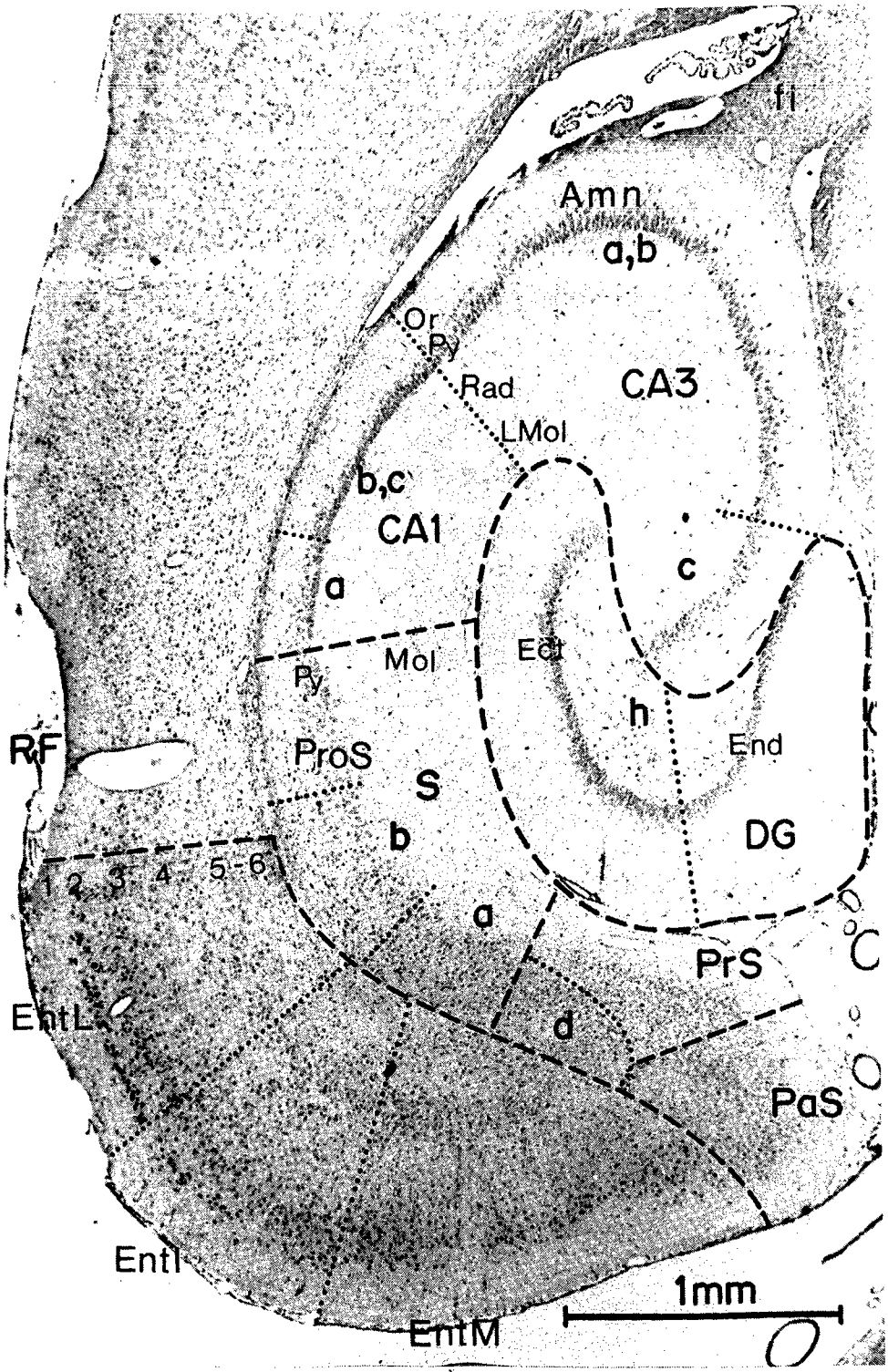

Adapted from: Bayer S.A. (1985) Hippocampal Region. In The Rat Nervous System (ed. Paxinos G.) Vol. 1. p.336 Academic Press, New York.

more locally, via the Schaffer Collateral pathway toward the *lacunosum moleculare* (a deep aspect of the CA1 and CA2 cells dendritic field).

The cells of the *stratum pyramidale* extend two sets of dendritic arborizations. They direct apical dendrites inward toward the infiltrating hippocampal fissure, terminating in the *stratum radiatum* and *lacunosum moleculare*, and they send basal dendrites outward toward the ventricular surface of the hippocampus, terminating in the *stratum oriens*. There are two types of afferents which terminate on these dendritic fields. The first type of afferents terminate diffusely over the entire dendritic surface of the neurons of Ammon's horn. These afferents originate from cells of extra-hippocampal origin such as the midbrain raphe nuclei (Conrad et al., 1974; Storm-Mathisen and Guldberg, 1974; Moore and Halaris, 1975), the locus coeruleus (Fuxe, 1965; Blackstad et al., 1967; Storm-Mathisen and Guldberg, 1974; Jones and Moore, 1977), and the medial septal-diagonal band complex (Lewis and Shute, 1967; Mellgren and Srebro, 1973; Swanson and Cowen, 1976; Meibach and Siegel, 1977). The second set of afferents terminate in specific laminae along defined segments of either apical or basal dendrites of CA pyramids. These afferents come from a variety of sources. Of particular interest are the afferents arising from (1) the cells of the medial and lateral aspects of the entorhinal cortex, via the medial and lateral perforant pathways, respectively, and (2) cells of hippocampal origin such as the dentate granule cells of the dentate gyrus. The *lacunosum moleculare* layer of pyramidal fields CA1 and CA3 receives a sparse, laminated topographic projection from cells of the entorhinal cortex. Proximal apical dendrites in the *stratum lucidum* of CA3 pyramids contain thick spiny thorns, which receive a strictly ipsilateral input from the axons of dentate granule cells termed "mossy fibers" (Cajal, 1911; Lorente de No, 1934; Blackstad et al., 1970; Gaarskjaer, 1978).

The dentate gyrus accompanies the hippocampus as a narrow band of sharply folded cortex forming a cap over the medial edge of Ammon's horn, with the fimbria above and the hippocampal fissure below (Bayer, 1985). The transitional area between the

dentate gyrus and the cells of Ammon's horn is the hilar region of the dentate gyrus, termed CA4 by Lorento de No (1934). The hilar region contains a scattered array of large, polymorphic modified pyramidal neurons, whose proximal dendritic arbors are covered by thorny spines, typical of a cell receiving input from a mossy fiber (see above). Axons from these neurons send bifurcated collaterals to extrahippocampal targets via the fimbria and, within the hippocampus, to the inner aspects of the dendritic field of dentate granule neurons (the commisural and associational (C/A) projection, see below and Figure 1.1).

The dentate granule cell layer of the hippocampus is divided into three regions. The most superficial blade of the dentate gyrus is termed the ectal wing, the medial blade is termed the endal wing. Between the two lies the crest or vertex of the dentate gyrus. The dentate gyrus cell layer contains densely packed spherical granule cells (4-10 cell layers deep) which give rise to mossy fiber axons which terminate locally upon the proximal dendrites of hilar neurons and the CA3 cells of the *stratum pyramidale* (Amaral, 1978). Dendritic arborizations of the dentate granule cells ramify in a dense synaptic plexus in the molecular layer of the dentate gyrus, delineated from the subiculum and Ammon's horn by the fold of the hippocampal fissure. The afferents onto dendrites of the dentate granule cells arise from 3 principle sources: (1) the entorhinal cortex, (2) the medial septal nucleus, and (3) the CA4 field pyramidal neurons of the hippocampus (Figures 1.1 and 2A). Laminated afferents arise almost entirely from the layer II stellate cells located in the medial and lateral entorhinal cortex. These afferents project primarily ipsilaterally, via the perforant pathway, to the outer two-thirds of the molecular layer of the dentate gyrus (referred to as the Middle and Outer Molecular Layers, MML and OML, respectively) (Cajal, 1911; Blackstad, 1958; Raisman et al., 1965; Hjorth-Simonsen, 1972; Hjorth-Simonsen and Jeune, 1972; Steward, 1976; Steward and Scoville, 1976). The ipsilateral entorhinal afferents represent a massive input to the dentate granule cells, comprising approximately 90% of the synapses on distal dendrites of granule neurons (Steward and Vinsant, 1983), and 60%-70% of their total dendritic input (Desmond and Levy, 1982).

Figure 1.1. Schematic cross-section through the hippocampus and dentate gyrus depicting the normal projection of extrinsic and intrinsic fiber systems within the rat hippocampus. CTD; crossed temporodentate pathway

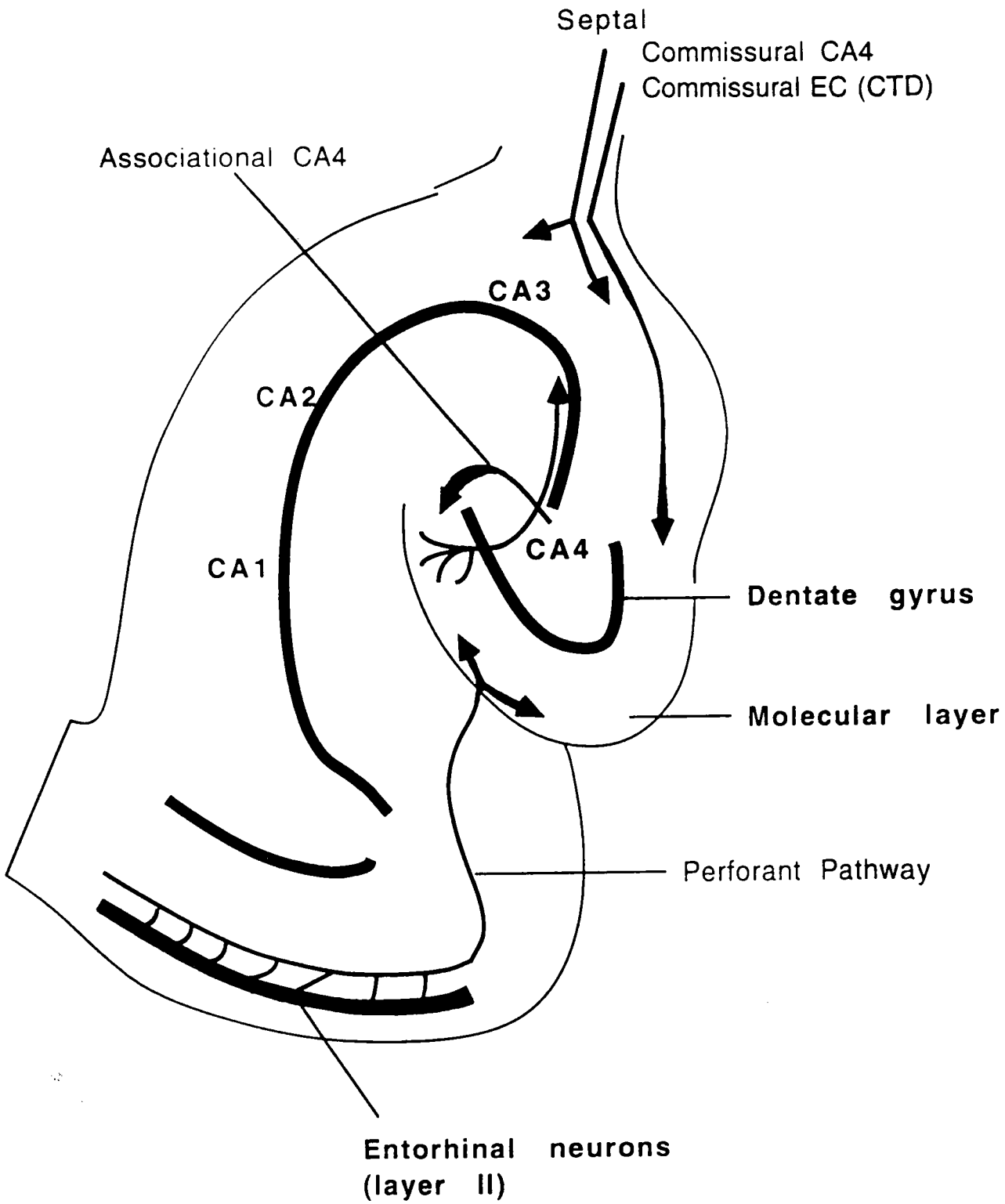
Septal
Commissural CA4
Commissural EC (CTD)
Associational CA4
CA3
CA2
CA1
CA4
Dentate gyrus
Molecular layer
Perforant Pathway
Entorhinal neurons
(layer II)

Figure 2. Summary of afferent projections onto granule cell neurons of the rat hippocampal dentate gyrus. (A) Normal dentate gyrus. (B) Denervated dentate gyrus. CA4, CA4 subfield of the hippocampus (also referred to as the hilar region).

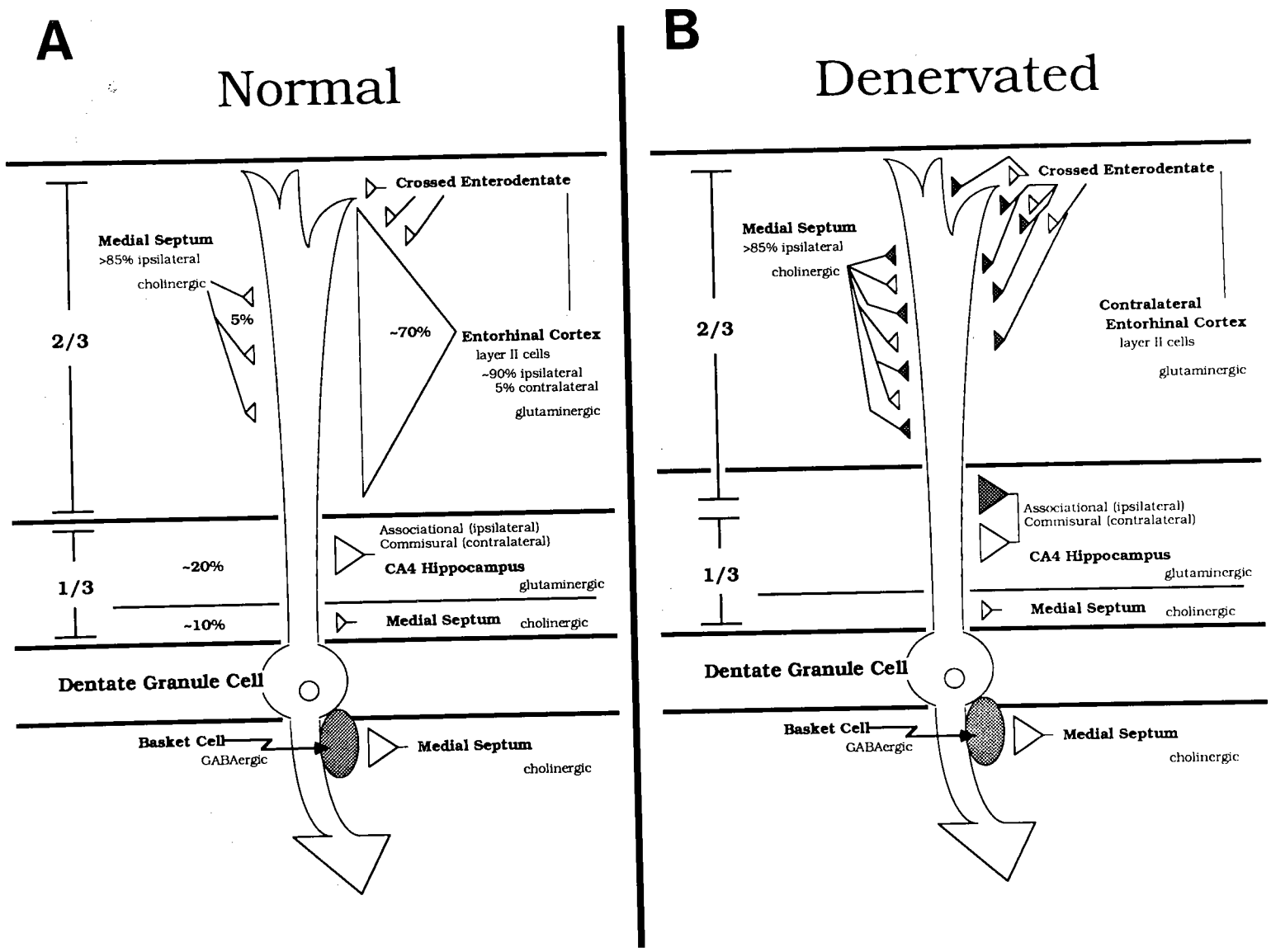
A
Normal
Medial Septum
>85% ipsilateral
cholinergic
5%
2/3
Crossed Enterodentate
~70%
Entorhinal Cortex
layer II cells
~90% ipsilateral
5% contralateral
glutaminergic
Associational (ipsilateral)
Commisural (contralateral)
CA4 Hippocampus
glutaminergic
1/3
~20%
~10%
Medial Septum
cholinergic
Dentate Granule Cell
Basket Cell
GABAergic
Medial Septum
cholinergic
B
Denervated
Medial Septum
>85% ipsilateral
cholinergic
2/3
Crossed Enterodentate
Contralateral
Entorhinal Cortex
layer II cells
glutaminergic
Associational (ipsilateral)
Commisural (contralateral)
CA4 Hippocampus
glutaminergic
1/3
Medial Septum
cholinergic
Dentate Granule Cell
Basket Cell
GABAergic
Medial Septum
cholinergic

Layer II stellate neurons of the contralateral entorhinal cortex have a sparse input to the OML of the dentate gyrus, synapsing in this region via the crossed temporo-dentate pathway (CTD; Goldowitz et al., 1975). Just below the terminal zone of the entorhinal cortex lies a band which contains both commissural (Blackstad, 1956; Laatsch and Cowan, 1967; Hjorth-Simonsen, 1977) and associational (Raisman et al., 1965; Hjorth-Simonsen, 1973) afferents. These afferents arise from cells of the contralateral and ipsilateral CA4 fields (C/A projection) (Gottlieb and Cowan, 1973; Fricke and Cowan, 1978; Swanson et al., 1981; Laurberg, 1979; Laurberg and Sorensen, 1981), and represent approximately 20%-30% of total input onto dendrites of the dentate granule cells.

Diffuse afferents to the dentate granule cells arise from cells in the brain-stem raphe nuclei, locus coeruleus, and medial septal nuclei (Fuxe, 1965; Raisman, 1966; Blackstad et al., 1967 Lewis and Shute, 1967; Melgren and Srebro, 1973; Conrad et al., 1974; Storm-Mathisen and Guldberg, 1974; Moore and Halaris, 1975; Swanson and Cowan, 1976; Jones and Moore, 1977; Meibach and Siegel, 1977). Of these three, the most significant input comes from cells in the medial septum. These cells send sparse afferents ipsilaterally, onto dendrites in the MML and OML of the dentate and more concentrated afferents (10%-20% of total input onto dendrites of the dentate granule cells) onto dendrites in the innermost one-sixth of the molecular layer of the dentate gyrus (the supragranular zone). These cells, however, do not project afferents to the zone immediately superficial to the innermost one-sixth of the molecular layer of the dentate gyrus, the field occupied by both the commissural and associational fiber afferents discussed above.

Neuronal Sprouting in the Hippocampal Formation

It is widely accepted that the central nervous system can modify its synaptic organization in response to specific CNS insults, i.e., injury-induced denervation of target neurons. One of the best studied example of synaptic reorganization after injury to the CNS is that which occurs in the dentate gyrus following damage to the projections from the

entorhinal cortex (EC). The EC provides the major source of efferent input (via the perforant path) onto the granule cell neurons of the dentate gyrus, synapsing in the outer two-thirds of its dendritic layer. As this input projects primarily in an ipsilateral fashion, an electrolytic lesion (ablation) of the EC results in the selective deafferentation of granule cell neurons in the ipsilateral dentate gyrus, resulting in a net loss of >85% of synapses on distal dendrites and approximately 60%-70% of the total synaptic input to these neurons (Mathews et al., 1976). Reorganization occurs when remaining undamaged afferent systems direct local growth responses (reactive synaptogenesis) in an attempt to reinnervate the dendritic fields of the dentate granule cell neurons (for reviews, see Cotman and Nadler, 1978; Cotman and Neito-Sampedro, 1985). In these areas, synapse replacement is achieved by the selective sprouting of residual inputs originating from neurons located in both the contralateral and ipsilateral hippocampal field CA4, layer II of the contralateral entorhinal cortex, and in the ipsilateral medial septal nucleus (Figure 2A,B).

Crossed Enterodentate Sprouting

The contralateral entorhinal cortex has been shown to project sparse inputs, via the crossed perforant pathway, into the OML of the dentate gyrus in normal rats (Goldowitz et al., 1975). In response to unilateral entorhinal cortex ablation, the undamaged fibers of this pathway have been shown to sprout and establish extensive connectional reorganization in the deafferented zone (Steward et al., 1973, 1974, 1976; Steward, 1976). Functionally, electrophysiological (Steward et al., 1973; Reeves and Smith, 1987; Reeves and Steward, 1988) and behavioral (Steward et al, 1973; Steward, 1976; Loeshe and Steward, 1977; Scheff and Cotman, 1977) studies have demonstrated that neuronal sprouting in the molecular layer of the dentate gyrus is important for the recovery of neuronal activity and of learned alternation behavior. Secondary lesion studies have confirmed that the reinnervation shown to be physiologically and behaviorally significant, originates in the contralateral entorhinal cortex, and it has thus been postulated that this

region plays a pivotal role in the recovery of the functional anatomy of the hippocampal region (Loeshe and Steward, 1977; Scheff and Cotman, 1977).

Septal Sprouting

Cholinergic afferents from the medial septum normally project in a diffuse array ipsilaterally, to the MML and OML of the dentate gyrus, and more densely to the supragranular zone, the zone of synapses immediately above the granule cell layer. In the normal brain, afferents in the MML and OML of the dentate gyrus, easily detectable with a histochemical stain for Acetylcholinesterase (AchE; Hedreen, 1985), reveal a light, homogenous pattern of staining. Upon unilateral entorhinal cortex ablation however, these afferents exhibit very dark, dense staining deposits in the MML ipsilateral to lesion (Lynch et al., 1972; Mosko et al., 1973). Confirmed by direct biochemical (Nadler et al., 1973), lesion (Cotman et al., 1973; Nadler et al., 1977) and tract tracing (Meibach and Siegal, 1977) analyses, this pattern of staining is indicative of the intense sprouting of cholinergic afferents originating in ipsilateral medial septal neurons. Interestingly, sprouting of cholinergic fibers is excluded from the region just above the supragranular zone, the region which receives glutaminergic afferents principally from cells of the contralateral and ipsilateral CA4 field of the hippocampus (Cotman et al., 1973).

Fantie and Goddard (1982) have shown that stimulation of the medial septum enhances excitatory input in the hippocampus, and that when this stimulus is paired with stimulation from the ipsilateral perforant pathway, it produces an augmentation of the entorhinal evoked dentate field potential. Thus, it is postulated that during synaptic rearrangement and sprouting following unilateral entorhinal lesion, the sprouted septal inputs may act by selectively enhancing the remaining excitatory inputs to the dentate granule cell neurons.

Commissural and Associational Sprouting

Commissural and associational (C/A) afferents to the dentate gyrus arise from cells of the contralateral and ipsilateral CA4 field, respectively. Normally, these afferents reside in the inner one-third of the molecular layer of the dentate gyrus (IML). Following entorhinal cortex ablation these afferents have been shown to sprout and expand their terminal fields outward into the MML by as much as 130%-140% of their control values (Lynch et al., 1976, 1977; Scheff et al., 1977; Zimmer, 1973). This expansion of the C/A fiber plexus can be monitored directly by various methods, including silver staining (Zimmer, 1973; Gall and Lynch, 1981) and HRP transport (Lynch et al., 1976). Autoradiographic visualization of sprouting commissural and associational fibers can be monitored indirectly by measuring the density of kainic acid (KA; a glutamate analogue) receptors in the deafferented zone. Receptors for KA appear to be selectively concentrated within the C/A pathway, and evidence from several studies has suggested that lesion-induced expansion of the C/A fiber system is paralled by an expanded distribution of KA receptors (Cotman and Nadler, 1981; Foster et al., 1981; Monaghan and Cotman, 1982; Berger and Ben-Ari, 1983; Geddes et al., 1985).

From a physiological standpoint, commissural synapses formed in the deafferented zone appear functional after 15 days following unilateral entorhinal cortex ablation, corresponding to the outgrowth of the commissural/associational fiber plexus (Cotman and Anderson, 1988). Studies measuring latency potentials produced by commissural stimulation suggest that the C/A fiber afferents may influence ipsilateral granule cell activity, possibly serving to amplify signals through this recurrent loop (West et al., 1975).

Neuronal Sprouting in Alzheimer's Disease

It is well established that the hippocampal formation plays a major role in the formation and storage of memory. Alzheimer's Disease (AD) has been characterized as a disease of neuronal deterioration associated with a classical dysfunction of memory, as well

as behavior and cognitive function. Studies on brain tissues obtained postmortem from patients with AD have demonstrated specific and focal cell loss in specific areas of the limbic system, most notably the layer II stellate cells of the entorhinal cortex (the major projection neurons of the entorhinal cortex) and pyramidal cells of the subiculum. As in the rodent, axons of layer II neurons of the human entorhinal cortex comprise the perforant pathway, the major source of input to the dentate granule cells of the hippocampal formation. It has been suggested that one of the earliest neuropathologies to appear in AD is the selective loss of neurons in the entorhinal cortex (Hyman et al., 1984; Pearson, 1985; Hamos et al., 1988; Hansen et al., 1988; Lippa et al., 1992). This loss results in the selective deafferentation of neurons of the dentate gyrus, isolating the hippocampal formation from its major source of input.

Superficially, the deafferentation that occurs in AD is somewhat analogous to that produced in experimental animals in which the dentate gyrus is deafferented by a specific entorhinal cortex lesions. In the rat entorhinal cortex lesion model, in response to deafferentation, the molecular layer of the dentate undergoes a massive reorganization of its afferent fiber systems. Evidence for the reinnervation and connectional reorganization of the molecular layer of the dentate gyrus in patients with AD has been reported (Geddes et al., 1985; Hyman et al., 1986; Gertz et al., 1987) . These data demonstrate that the human CNS is capable of growth responses in AD analogous to those seen in the experimental rodent model of neuroplasticity.

Septal Sprouting

The use of AchE activity as a marker for sprouting of cholinergic afferents in AD is often precluded by the fact that significant losses of basal forebrain cholinergic neurons occur in patients with AD (Davies and Maloney, 1976; Whitehouse et al., 1981, 1982a,b; Rossor et al., 1982; Tagliavani and Pilleri, 1983; Wilcock et al., 1983; Mann et al., 1984; Doucette et al., 1986; Rasool et al., 1986). However, several studies have shown

intensification of AchE activity in the MML and OML of the dentate in AD brains which exhibited entorhinal and subicular neuronal losses without corresponding basal forebrain losses (Geddes et al., 1985; Hyman et al., 1986). It is important to stress that this staining pattern was present only in those brains in which significant cholinergic input to the hippocampus was present. Further, in these same brains, AchE-positive plaques were identified in the denervated neuropil of the dentate gyrus, which is consistant with an aberrant sprouting response in this region (Geddes et al., 1985; Cotman and Anderson, 1988).

Ultrastructural studies quantitating dentate granule cell synaptic spine density in brains of patients with senile dementia of Alzheimer's type (SDAT) suggest a maintenence of synaptic contacts in the supragranular zone of the dentate molecular layer (Gibson, 1983). In this study the number of spines per 10-μm segment of granule cell apical dendrite in patients demonstrating significant cell loss within the medial septum and diagnonal band of Broca were evaluated. In the proximal segments (the supragranular zone) the spine density differences between SDAT and controls were not statistically significant. Since one might expect the reduction of neurons in the medial septum to lead to pronounced reductions in number of spines in their terminal zones, these data support the notion that replacement of lost cholinergic afferents occurs through the sprouting of surviving cholinergic neurons.

Commissural and Associational Sprouting

Sprouting by the C/A afferents in the hippocampus of patients with AD has been indirectly measured by examining the distribution of kainic acid (KA) receptors in the outer leaf of the IML (Cotman and Anderson, 1988). In normal human brain, the pattern and density of KA binding sites in the molecular layer of the denate gyrus was similar to that observed in normal rodent brain. In the rat brains, a high density of KA binding sites occupied the IML, analogous to the zone of innervation of the C/A fiber plexus (Gottlieb

and Cowan, 1973; Fricke and Cowan, 1978; Swanson et al., 1978; Laurberg, 1979; Laurberg and Sorensen, 1981). In the brains of AD patients however, this terminal field region was expanded by 73%, resulting in a zone of reinnervation encompassing approximately one-half of the molecular layer (ML) of the dentate gyrus. Thus, it appears that the C/A fibers in the human brain sprout in response to the disease-induced loss of neurons in the entorhinal cortex.

Additional indirect studies from our laboratory support this hypothesis. Using immunohistochemistry employing antibodies to synaptic terminal-specific proteins (synapsin I and synaptophysin) as markers for synaptic input, Hamos et al., (1988) revealed a striking decrease in synaptic staining in the MML and OML of the dentate gyrus in AD brains compared with age matched controls, where the density of synaptic terminals was uniform throughout. This pattern of immunoreactivity is consistent with the loss of synaptic input in this region from layer II stellate neurons of the entorhinal cortex. Accordingly, as discussed above, it is well established that these neurons are dramatically affected in AD, resulting in loss of as much as 95% of the normal complement of neurons found in the young adult (Lippa et al., 1992). Interestingly, quantitative densitometric analyses of synapsin I immunoreativity in the dentate molecular layer of AD brains revealed a slight increase in synaptic staining in the inner-half of this layer (Hamos et al., 1988). Further study revealed what appeared to be the expansion of this zone of synaptic staining into the proximal region of the OML in patients with AD, when compared with control brains (J.E. Hamos, personal communication). The pattern of expansion and increase in immunostaining of the IML synaptic region are consistent with those expected with the occurrence of axonal sprouting of intact connections in the ML, as has been noted during the process of lesion-induced reactive synaptogenesis in rats with entorhinal lesion (see above). Taken together with the evidence for C/A and septal sprouting, these data suggest that the human CNS responds to AD-induced denervation in a fashion similiar to that of an entorhinal cortex-lesioned rat brain, and that synapsin I immunoreactivity may be used as a

sensitive tool for the study of neuronal sprouting during the reinnervation of the central nervous system.

Synapsin I

Biochemistry

Synapsin I is the best characterized member of a family of neuron-specific phosphoproteins thought to play a fundamental role in the regulation of neurotransmitter release from the presynaptic nerve terminal. Synapsin I is the collective name for two nearly identical neuron-specific proteins, synapsin Ia and synapsin Ib, of MW 78 kd and 74 kd, respectively, which are present throughout the central and peripheral nervous systems (Ueda and Greengard, 1977; De Camilli et al., 1979; 1983a; Goelz et al., 1981; Huttner et al., 1981; McCaffery and DeGennaro, 1986; Scheibler et al., 1986). Both proteins have similar amino acid compositions and basic isoelectic points (>10). Synapsin I polypeptides Ia and Ib differ from one another in the carboxy terminal region of the peptide by the presence of 45 amino acids in synapsin Ia, compared to 9 in synapsin Ib. For the purposes of this body of work, I will refer to both synapsin I polypeptides as synapsin I.

Immunohistochemical studies have shown synapsin I to be concentrated within presynaptic nerve terminals, where it is specifically associated with the cytoplasmic surface of small (40-60 nm) synaptic vesicles (De Camilli et al., 1983a,b; Huttner et al.,1983; Navone et al., 1984; Schiebler et al., 1986; Benfenati et al., 1989). *In vitro*, synapsin I has been shown to bind to synaptic vesicles with high affinity (Kd=10nM), and subsequent phosphorylation of the protein has been shown to substantially decrease this binding (Schiebler et al., 1986).

Synapsin I protein consists of two domains, a globular collagenase resistant head region and an elongated proline-rich tail region (Ueda and Greengard, 1977; McCaffery and DeGennaro, 1986; Schiebler et al., 1986). Within these domains, the protein appears

to possess specific regions capable of associating with several components of the cytoskeleton, including microfilaments, microtubules, spectrin and actin (Baines and Bennet, 1985; 1986; Bahler and Greengard, 1987; Petrucci and Morrow, 1987; Bahler et al., 1989; 1990). In fact, synapsin I appears to contain at least two distinct actin-binding sites that allow synapsin I to bundle actin *in vitro* (Bahler and Greengard, 1987; Petrucci and Morrow, 1987; Bahler et al., 1989). Electron microscopy data provide evidence for a structural role of synapsin I in the presynaptic nerve terminal (Landis, 1988; Landis et al., 1988; Hirokawa et al., 1989). These studies suggest that synapsin I forms a fibrillar connective matrix that links synaptic vesicles to each other and to the cytoskeleton in the presynaptic nerve terminal. Synapsin I protein also possesses domains which are prominent cellular targets of several endogenous protein kinases, such as cAMP- and Ca^{2+}/calmodulin dependent protein kinases (Ueda et al. 1973; Huttner and Greengard, 1979; McGuinness et al. 1985; Nairn and Greengard, 1987). The head domain of synapsin I has been shown to be phosphorylated on a specific serine residue (amino acid #42 of the peptide sequence) by either the cAMP-dependent protein kinase (Huttner and Greengard, 1979) or the Ca^{2+}/Calmodulin-dependent protein kinase I (Kennedy and Greengard, 1981). In the tail domain of synapsin I, Ca^{2+}/Calmodulin-dependent protein kinase II has been shown to bind synapsin I (Benfenati et al., 1992) and phosphorylate the protein on two serine residues (located at amino acids #555 and #651) (Huttner and Greengard, 1979; Huttner et al., 1981). In addition, in the carboxy terminal region of the polypeptide, a newly discoved proline-directed serine/threonine kinase has been shown to phosphorylate synapsin I at a site distinct from the Ca^{2+}/Calmodulin-dependent kinase II sites (Vulliet et al., 1989; Hall et al., 1990). The binding of synapsin I to synaptic vesicles appears to be mediated by the collagenase-sensitive tail domain of the molecule (Huttner et al., 1983), as phosphorylation of this region of the molecule by Ca^{2+}/calmodulin-dependent protein kinase II decreases the affinity of synapsin I for synaptic vesicles (Schiebler et al., 1986).

Function

Several lines of evidence, including physiological and electrical stimulation studies, implicate synapsin I in the regulation of neurotransmitter release from adult presynaptic nerve terminals. For example, in the adult CNS, the affinity of synapsin I for synaptic vesicles has been shown to be regulated by conditions affecting neuronal activity. Tarelli et al. (1992) showed that electrical stimulation of the frog neuromuscular junction resulted in the dissociation of synapsin I from the synaptic vesicle. In studies by Sihra et al. (1989), K^+-evoked stimulation of neurotransmitter release from purified synaptosomes has been shown to cause the phosphorylation of synapsin I and increases the amount of the synapsin I in the cytosolic (soluble) fraction. Additionally, treatments that promote the Ca^{2+}-dependent release of neurotransmitter resulted in an increase in the pool of phosphorylated synapsin I, an effect abolished by prior phosphorylation of synapsin I by injection of Ca^{2+}/calmodulin-dependent protein kinase II (Llinas et al., 1985; 1991; Hackett et al., 1990; Lin et al., 1990; Nichols et al., 1992). The microinjection of purified dephosphorylated synapsin I into the presynaptic nerve terminal resulted in the decrease in efficiency of neurotransmitter release, whereas the injection of phosphorylated synapsin I had no effect (Llinas et al., 1985). Conversely, injection of Ca^{2+}/calmodulin-dependent protein kinase II, which results in an increase in phosphorylation of synapsin I and subsequent decrease in its affinity for synaptic vesicles, enhanced neurotransmitter release (Llinas et al., 1985).

The prevailing hypothesized role for synapsin I in the presynaptic nerve terminal is depicted in Figure 3. Cytoskeletal elements within the presynaptic nerve terminal are proposed to form a fibrillar meshwork with synapsin I mediating the link between the synaptic vesicle and the cytoskeletal matrix. Upon nerve terminal depolarization and subsequent increase in intracellular Ca^{2+}, phosphorylation of synapsin I on two sites in its carboxy terminal domain by Ca^{2+}calmodulin-dependent protein kinase II leads to a reduced

Figure 3. A schematic of the presynaptic nerve terminal and the proposed role of synapsin I in regulating neurotransmitter release, as outlined in the text.

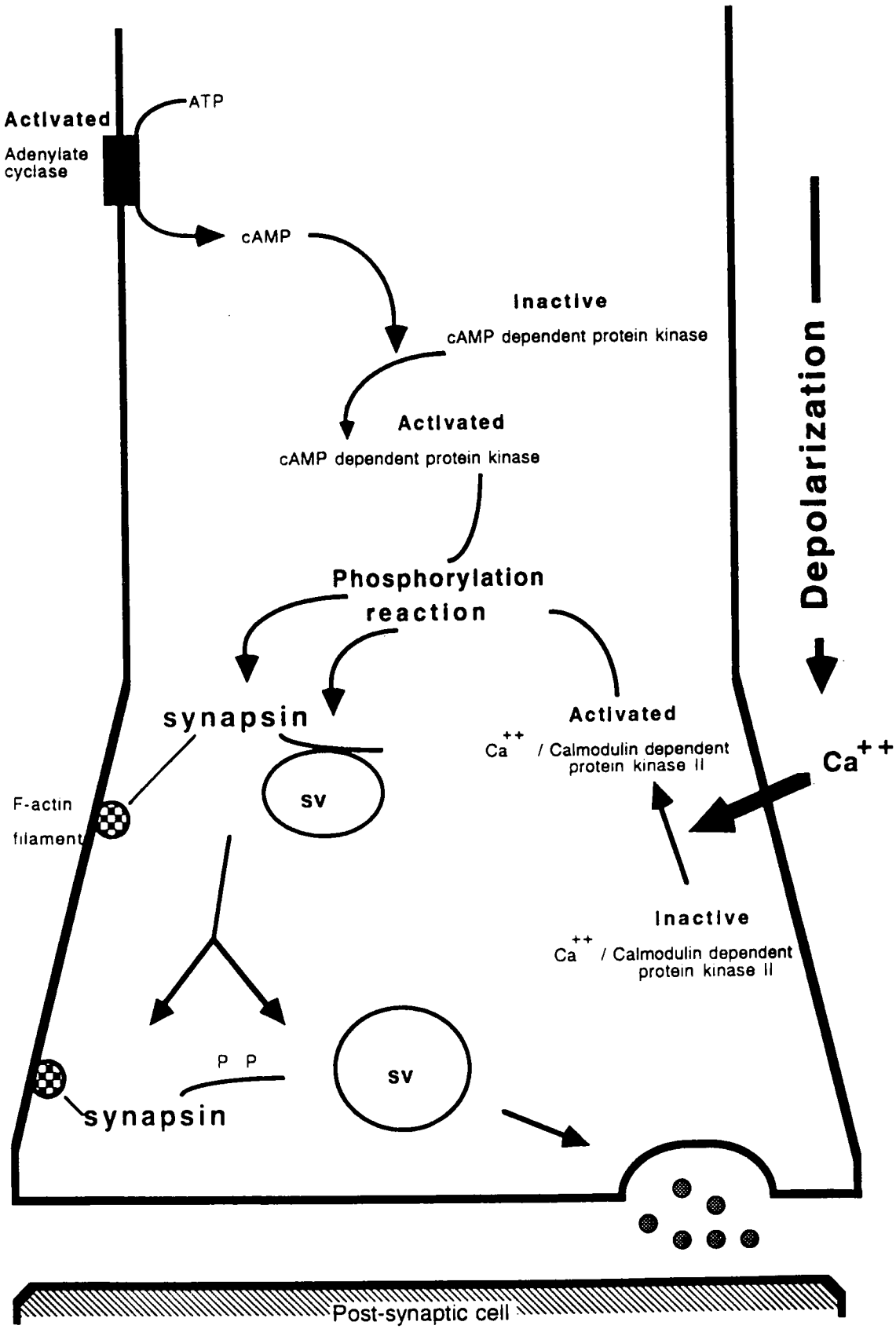
Activated
Adenylate cyclase
ATP
cAMP
Inactive
cAMP dependent protein kinase
Activated
cAMP dependent protein kinase
Phosphorylation reaction
synapsin
F-actin filament
sv
Activated
Ca++ / Calmodulin dependent protein kinase II
Depolarization
Ca++
Inactive
Ca++ / Calmodulin dependent protein kinase II
P P
synapsin
sv
Post-synaptic cell

affinity of synapsin I for the synaptic vesicle. The synaptic vesicle is then freed from the synapsin I/cytoskeletal matrix and becomes available to undergo the process of exocytosis.

Recently, biochemical and immunological evidence has established synapsin I as a diacylglycerol (DG) kinase suggesting a second role for synapsin I in the adult nerve terminal, that of a potential regulator of protein kinase C-mediated extracellular signals (Kahn and Besterman, 1991). Since the generation of DG within the neuronal membrane is believed to play an important role in the transduction of extracellular signals in the nervous system (Huang, 1989), the characterization of synapsin I as a DG kinase establishes a point of convergence between the depolarization-induced, Ca^{2+}-mediated and effector-induced, DG-mediated signal transduction pathways.

In the development of the CNS, synapsin I appears to have opposing actions to those observed in the adult. Introduction of dephosphorylated synapsin I into mature presynaptic nerve terminals results in the reduction of spontaneous and evoked neurotransmitter release (Llinas et al., 1985; 1991; Hackett et al., 1990; Lin et al., 1990), perhaps as a result of increased binding of synaptic vesicles to the presynaptic cytoskeleton. In contrast, in developing neurons when endogenous synapsin I protein levels are particularly low, Lu et al. (1992) have demonstrated that introduction of exogenous dephosphorylated synapsin I elicits marked enhancement of both spontaneous and evoked synaptic currents suggesting that endogenous synapsin I may participate in the functional maturation of synaptic function. Fletcher et al. (1991) have shown that in hippocampal cultures, the contact of presynaptic neurons with postsynaptic cells induces the rapid translocation of synapsin I to the distal site of contact. Indeed, most recent morphological studies by Han et al. (1991) have shown that overexpression of the synapsins *in vitro* may play a causal role in synaptogenesis by promoting the formation of nacent synapses.

Biosynthesis and Molecular Biology

In the adult nervous system, previous studies employing endogenous phosphorylation assays (Walaas et al., 1983, 1988), radioimmunological assays (Goelz et al., 1981), and immunohistochemistry (Bloom et al., 1979; De Camilli et al., 1983a,b; DeGennaro et al., 1989; Apostilides et al., in press) indicate that synapsin I protein is abundant in the adult rat brain. It comprises 0.4% of the total protein from cortex (Goelz et al., 1981) and 6% in a purified synaptic vesicle fraction (Huttner et al., 1983). The biosynthesis of synapsin I protein is regulated developmentally in the rodent nervous system. During the development of the rat and guinea pig CNS, Lohmann and colleagues (1978) used endogenous phosphorylation assays to demonstrate that synapsin I levels correlated with the development of synaptic structures. More recently, several studies have demonstrated that, during the developmental period, the appearance of synapsin I protein correlates temporally and topographically with synaptogenesis, both *in vivo* (De Camilli et al., 1983; DeGennaro et al., 1983; Levitt et al., 1984; and Mason, 1986; Moore and Berstein, 1989; Bergman et al., 1992) and *in vitro* (Bixby and Reichardt, 1985; Weiss et al., 1986). Together, these studies suggest that synapsin I is a precise indicator of synapse formation and that synapsin I immunoreactivity could be used as a tool for the study of synaptogenesis in the developing nervous system.

Southern blot analysis indicates that there is only a single copy of the synapsin I gene present in the haploid genome (P.D. Carroll and L.J. DeGennaro, personal communication). The gene encoding synapsin I has been localized to the X chromosome at bands XA1-XA4 in mouse, and Xp11 in man (Yang-Feng et al., 1986). Linkage analyses using repetitive DNA sequences as polymorphic markers have revealed that the synapsin I gene lies back-to-back with the A-*raf*-1 gene (the cellular homologue of a viral oncogene) on the proximal short arm of the human X chromosome (Kirchgessner et al., 1991). Additional genetic linkage studies in mouse have shown Synapsin I, A-*raf*-1, and *Timp* (the gene encoding a glycoprotein inhibitor of collagenase) to be part of a conserved cluster

on the X chromosome (Avner et al., 1987; Mullins et al., 1990; Grant and Chapman, 1991), and that Timp, only 10 kb from A-*raf*-1, actually lies within an intron of the synapsin I gene (Derry and Barnard, 1992). Detailed restriction mapping in these studies has shown that the *Timp* gene is transcribed in the same direction as A-*raf*-1 but in the opposite direction to the synapsin I gene (Derry and Barnard, 1992). Analysis of the corresponding region on the human X chromosome indicates conservation of this arrangment and further shows that the properdin (a serum glycoprotein) gene locus lies within this cluster, within approximately 5 kb of the 5'-end of the synapsin I gene (Derry and Barnard, 1992).

The gene encoding rat synapsin I is greater than 30 kb in size (L.J. DeGennaro, personal communication) and is highly homologous to the human synapsin I gene sequence (Sudhof, 1990). Both rat and human genes consist of at least 11 exons and 10 introns (L.J. DeGennaro, personal communication; Sudhof, 1990), however, due to cloning difficulties, an indepth analyses of intron/exon borders has not been established in several regions. The 5' flanking region of both the human and rat genes have been fully sequenced elucidating the 5' regulatory sequences, the start sites of transcription and translation, and the first exon (Sudhof, 1990; Howland et al., 1991). In the rat synapsin I gene, S1 nuclease and primer extension analyses suggested that the primary start site of transcription is located at an adenine residue 124 bases upstream of the ATG start site of translation, and a second, less frequent site is located at adenine residue +14 (Howland et al., 1991). Inspection of the DNA sequence immediately upstream of the transcription start site revealed that the rat synapsin I gene promotor is comprised of a GC-rich sequence lacking the consensus TATA and CAAT box elements. The sequence surrounding the transcription start site is identical to the functional initiator control element (5'-CTCANTCT-3') present in the murine lymphocyte-specific terminal deoxynucleotidyltransferase (TdT) and adenovirus major late (AdML) genes (Smale and Baltimore, 1989). Such a sequence in the synapsin I gene promotor may function in promoting transcription initiation in the absence

of a TATA box (Blake et al., 1990; Howland et al., 1991). Interestingly, similar sequence motifs are found in several genes lacking TATA boxes that are known to be developmentally regulated (Smale and Baltimore, 1989; and below). Further inspection of the rat synapsin I promotor revealed several homologies to recognizable sequence elements including a cyclic-AMP response element (located at -151 bp), and an AP-1 site (-1397 bp).

Functional dissection of the rat synapsin I gene promotor in PC12 cells, a clonal line derived from a rat adrenal medullary pheochromocytoma, and the neuroblastoma cell line NS20Y, have identified both positive- and negative-acting promotor sequences which regulate the neuron-specific expression of the rat synapsin I gene (Howland et al., 1991). In these studies, deletion analyses revealed the presence of a positive acting regulator element between -349 bp and +110 bp of the synapsin I 5' promotor. This fragment was shown to be 33 times more active in PC12 cells than in HeLa cells when fused to the bacterial chloramphenicol acetyltransferase (CAT) reporter gene (Sauerwald et al., 1990; Howland et al, 1991). Reporter plasmids containing up to 4.4 kb of rat synapsin I gene promotor resulted in a significant reduction in CAT activity in PC12 cells. Further dissection of this region by deletion analysis revealed that the reduction in CAT activity was attributable to a negative regulator positioned between -349 bp and -1341 bp in the rat synapsin I promotor (Howland et al, 1991).

The rat synapsin I gene directs the concerted expression of two classes of mRNA of 3.4 kb and 4.5 kb, respectively (Haas and DeGennaro, 1988). Polymerase chain reaction (PCR) data reveal that the 4.5 kb class of mRNA includes the unspliced last exon at the 3'end of the synapsin I gene (P.D. Carroll and L.J. DeGennaro, personal communication), however, the complete sequence and role of the 4.5 kb form of synapsin I mRNA has not yet been determined. cDNA cloning (Kilimann and DeGennaro, 1985) and sequence analysis (McCaffery and DeGennaro, 1986; Sudhof et al., 1989) have shown that the 3.4 kb mRNA is composed of two similarly sized alternatively spliced species of mRNA

encoding both the synapsin Ia and Ib polypeptides.

The expression of the two synapsin I mRNA classes is differentially regulated during the development of the rat brain and cerebellum (Haas and DeGennaro, 1988). By RNA blot analysis, the 4.5 kb transcript was shown to be expressed in the rat cerebellum until postnatal day 7, after which it decreased to undetectable levels. The 3.4 kb mRNA was detected throughout development and into the adult. The expression of this form of mRNA was shown to peak at postnatal day 20 in the developing cerebellum, coincident with the peak period of synaptogenesis in the cerebellum (Haas and DeGennaro, 1988). By *in situ* hybridization, synapsin I mRNA was localized over the developing internal granule cell layer of the cerebellum, but not over Purkinje cells (Haas and DeGennaro, 1988). This pattern of expression suggests that the developmentally regulated expression of the neuron-specific synapsin I gene correlates with the synaptogenic differentiation of particular subsets of neurons in the rat central nervous system.

Synapsin I and the Molecular Changes Associated with Neuronal Sprouting and Alzheimer's Disease

Data from our laboratory and the laboratories of others have characterized the neuron-specific protein synapsin I as a marker of severe focal synaptic loss in the hippocampus of patients with AD (Perdahl et al., 1984; Hamos et al., 1988). Further semi-quantitative densitometric analyses of synapsin I immunostaining in the molecular layer (ML) of the dentate gyrus (the hippocampal region deafferented by AD pathology) revealed an increase in the density and area of staining in the IML, perhaps indicative of a sprouting response by surviving afferent systems in this region (Hamos et al., 1988). Recent *in vitro* studies by Han et al. (1991) indicate that the regulation of synapsin expression could be involved in chronic changes in neuronal signalling, and that the synapsins may contribute to both short-term and long-term synaptic plasticity.

Recently it has been shown that the same afferent systems responsible for the

reinnervation of the rat hippocampus following entorhinal cortex ablations undergo remarkably similiar plastic responses in chronic neurodegenerative pathologies such as Alzheimer's Disease and Senile Dementia of Alzheimer's Type (SDAT). Since the process of hippocampal reinnervation has been well characterized at the cellular level in rats with acute lesions of the entorhinal cortex, this system may serve as a useful model for some of the chronic changes observed in AD, most notably, the neuronal sprouting response of undamaged afferent fiber projections. Further study of this system at the level of gene expression may serve to elucidate the putative cellular and molecular mechanisms underlying neuronal plasticity (sprouting) and their relationship to neurodegenerative diseases such as AD/SDAT.

As described above, neuronal sprouting in the rodent hippocampus in response to entorhinal cortex ablation has been extensively characterized by standard morphological methods, although relatively little is known regarding the molecular and biochemical events that underlie the sprouting response. Recently, several studies have shown that changes in gene expression (Whittemore et al., 1987; Geddes et al., 1990a,b; May et al., 1990; Phillips and Steward, 1990; Poirier et al, 1990; Steward et al., 1990; Gibbs et al., 1991; Laping et al., 1991; Nichols et al., 1991; Poirier et al., 1991a,b; Chen and Hillman, 1992), protein synthesis (Nieto-Sampedro et al., 1982; Caceres et al., 1988; Lapchak, 1991;), membrane composition (Masco and Seifert, 1990), and the levels and/or distribution of cellular components (McWilliams and Lynch, 1981; Caceres et al., 1988; Steward, 1983) occur with particular neurons in the rat brain in response to lesions of the entorhinal cortex. These studies suggest that massive deafferentation of a subset of neurons within the CNS results in a myriad of cellular and molecular responses within both pre- and postsynaptic compartments. One of these responses may be a recapitulation of the original developmental mechanisms of axonal guidance and growth in those cells whose remaining undamaged afferent fiber projections sprout in response to lesion (Geddes et al., 1990c; Poirer et al., 1991b), Another response may be the attenuation of neuronal signaling

between effector and target neurons (Taxt and Storm-Mathisen, 1984; Anderson et al., 1991). Since the neuron-specific expression of synapsin I is (1) regulated in a coordinate fashion with synaptogenesis in the developing nervous system (2) involved in signaling between neuronal populations and (3) involved in chronic pathological and subsequent plastic changes in hippocampal circuitry in AD, we believed it would be of tremendous interest to examine the *in vivo* expression of the synapsin I gene and its protein products during development and following entorhinal lesion-induced changes in hippocampal synaptic circuitry.

Objective and Experimental Approach

The main objective of the research described in this dissertation is to study the relationship between the regulation of synapsin I gene expression and neuronal sprouting by examining molecular and cellular events which occur in presynaptic and postsynaptic compartments of selected nerve cells in the rat brain in response to entorhinal cortex lesion. As previously described, the hippocampal formation of rodents demonstrates a remarkable degree of plasticity following entorhinal cortex ablation. In this model system, every afferent fiber system which borders on or terminates within the MML and OML of the dentate gyrus shows marked growth responses following the removal of entorhinal afferents. Our strategy was to study the expression of synapsin I mRNA and protein in the defined synaptic circuitry of the hippocampus and its incoming afferent systems following deafferentation by surgical knife-cut transection of the perforant pathway; selectively severing the primary source of afferent connections to the dendritic field of the dentate granule neurons of the rodent hippocampus. Knife-cut transection of the perforant pathway was chosen as a preferred means of deafferenting the hippocampus for several reasons. The principle advantages of this procedure are that it typically spares both the cell bodies of the transected neurons and their terminal fields, and it avoids overt post-lesion epileptiform seizures induced by electrolytic lesions or the injection of toxic compounds

such as kainic acid. This characteristic is particularly advantageous, since seizure activity itself, has been shown to evoke dramatic and specific increases in mRNA encoding the cellular oncogenes *c-fos* (Morgon et al., 1987; Dragunow et al., 1992), Fos B, Fos-related proteins (FRAs), c-jun, jun B, jun D and krox-24 (NGF1A) (Dragunow et al., 1992), and the transcripts of several other genes including heat shock protein 73 (hsp 73) (Wong et al., 1992), nerve growth factor (NGF), brain-derived neuro-tropic factor (BDNF), neurotrophin-3 (NT3) (Rocamora et al., 1992), and prodynorphin and proenkephalin (Douglass et al., 1991). Since the knife-cut transection procedure avoids post-surgical seizure activity in lesioned rats, subsequent analysis of gene expression in those regions of interest should select for molecular events associated with changes of synaptic wiring in the brain, events potentially obscured by seizure-induced molecular changes. Additionally, since the wire knife transection protocol is inherently less destructive, animals suffer less and recovery times are shortened.

As a prelude to examining the regulation of expression of the synapsin I gene during the synaptic reorganization of the deafferented hippocampus, it was first necessary to develop and implement rapid and sensitive assay systems for the analysis of synapsin I gene expression in the rat nervous system. Thus far, the analysis of the expression of the synapsin I gene in rat central nervous system had been restricted to observations by standard RNA blot and only limited *in situ* hybridization analyses during the postnatal development of the rat cerebellum (Haas and DeGennaro, 1988), with little or no data available detailing the pattern and level of expression of the synapsin I gene elsewhere in brain. Chapter III of this thesis reports the development of an RNA blot procedure for the direct analysis of steady-state mRNA levels in microgram quantities of frozen mammalian tissues, with particular emphasis on synapsin I mRNAs from rat brain. The punch-and-load procedure described is rapid, extremely sensitive and reproducibly results in excellent recovery, detection, and quantification of intact synapsin I mRNA from discrete regions of brain. Chapters IV and V report the development of an extremely sensitive and

reproducible hybridization procedure for the detection of synapsin I mRNAs *in situ*. This procedure was used to define the normal patterns of expression of the synapsin I gene in the developing and adult rat brain. The developmental studies, presented in Chapter IV, further serve to elucidate the temporal onset of expression of the synapsin I gene in relation to the state of differentiation of particular types of neurons during the development of the rat cerebellum and hippocampus. Studies of synapsin I gene expression in the adult rat central nervous system presented in Chapter V, detail the comparative levels of expression of expression of synapsin I mRNA in the adult rat, providing a map of the intensity of expression of synapsin I mRNA throughout brain.

As a prelude to an analysis of synapsin I gene expression in the restoration of synapses in the rat hippocampus, the next series of experiments focused in detail on the expression of the synapsin I gene (mRNA and protein) during the normal development of the rat hippocampus. Specifically, in these experiments, presented in the latter part of Chapter V and in the first part of Chapter VI of this dissertation, a comparison of the patterns of expression of synapsin I mRNA and protein in the developing and adult rat hippocampus by *in situ* hybridization and immunohistochemistry were carried out to determine specifically how synapsin I mRNA levels are related to levels of synapsin I protein during the establishment and maintenence of synapses in rat central nervous system.

Finally, to investigate the regulation of the synapsin I gene (mRNA and protein) during the restoration of functional synaptic contacts in the rat central nervous system, lesion studies were designed to evoke neuronal sprouting and synaptic reorganization in the hippocampal formation. In these studies, presented in the latter part of Chapter VI, the expression of synapsin I protein and mRNA were measured in presynaptic and postsynaptic neurons at varying survival times following transection of the perforant path. Of particular interest is the documentation of molecular changes in neurons which occur concommitant with neuronal sprouting and the restoration of synaptic function.

Compendium of Manuscripts

Chapters III, IV, V, and VI were taken, in part, from the following manuscripts:

Chapter III

Melloni, R.H., Jr., Estes, P., Howland, D.S., and DeGennaro, L.J. (1992) A Method for the direct measurement of mRNA in discrete regions of mammalian brain. Anal. Biochem. 200:95-99.

Chapter IV

Melloni, R.H., Jr., and DeGennaro, L.J. (submitted for publication) Temporal onset of synapsin I gene expression coincides with neuronal differentiation during the development of the rat nervous system.

Chapter V

Melloni, R.H., Jr., Hemmendinger, L.M., Hamos, J.E., and DeGennaro, L.J. (1993) Synapsin I gene expression in the adult rat brain with comparative analysis of mRNA and protein in the hippocampus. J. Comp. Neurol. 327(4): 507-520.

Chapter VI

Melloni, R.H., Jr., Apostolides, P.J., Hamos, J.E., and DeGennaro, L.J. (submitted for publication) Dynamics of neuron-specific gene expression during the establishment and restoration of functional synapses in the rat hippocampus.

Chapter II

MATERIALS AND METHODS

Animals, Surgical Procedures and Tissue Preparation

All animal work was carried out in accordance with the Policy on Animal Treatment regarding the care and use of experimental animals, as approved by the Society for Neuroscience, April 1984.

Developmental studies. Sprague-Dawley rat pups (n=2-4 per time point) (Charles River, Wilmington, MA), from each of thirteen different time points embryonic (E) days 12, 14, 16 and 19, and postnatal (P) days 0, 3, 6, 9, 11, 14, 21, 31 and adult {P90}) were used. For *in situ* hybridization on embryonic rat tissue, rat pups were frozen by immersion in dry-ice-supercooled 2-methylbutane (Aldrich), warmed to -16°C in a cryostat, and sectioned whole at 16 µm in the sagittal plane. For *in situ* hybridization on postnatal rat tissue, the animals were sacrificed by carbon dioxide asphyxiation and decapitation. The brains were removed according to the protocol of Palkovits and Brownstein (1988), frozen in dry-ice-supercooled (-30°C to -40°C) 2-methylbutane (Aldrich), and stored in plastic bags at -70°C. Just before use, the brains were then warmed to -16°C, and 16 µm cryostat sections were cut in the coronal, horizontal, and parasagittal planes. Sections were thaw-mounted on precooled slides coated with Vectabond® reagent (Vector Laboratories, Burlingame, CA) and stored at -70°C until use. For RNA (n=3 per time point) and Western blot (n=2 per time point) analyses, rat brains were frozen as above and warmed to -9°C. Cryostat sections were cut at 250 µm, and the sections were used for brain punch microdissection (Palkovitz and Brownstein, 1988). For immunohistochemistry (n=2-4 per time point), rats were anesthetized by exposure to ether or by injection of pentobarbital, and then perfused transcardially with 100 ml 0.9% saline followed by 400 ml cold 2%

paraformaldehyde-lysine-periodate in 0.1 M phosphate buffer (PB; pH 7.4). The brains remained exposed to fixative for the 15-20 minute length of the perfusion, followed by 2-4 hours of postfixation at 4°C. The brains were then removed and transferred to 30% sucrose in 0.1 M phosphate buffered saline (PBS; pH 7.4) for cryoprotection at 4°C.

Adult studies. Male Sprague-Dawley rats (n=6) from Charles River Breeding Laboratories (Wilmington, MA), 90-120 days old and weighing 250-300 grams, were used in this study. For *in situ* hybridization and RNA and Western blot analyses, the animals were sacrificed by carbon dioxide asphyxiation and decapitation. Brains were removed, frozen in dry-ice-supercooled 2-methylbutane (Aldrich), and stored in plastic bags at -70°C. For immunohistochemistry, the animals were perfused transcardially with a saline flush, followed by 0.01M periodate-0.075 M lysine-4% paraformaldehyde in 0.037 M phosphate buffer, pH 7.2 ("PLP fixative", McLean and Nakane, 1974). Brains were postfixed for 2 hours at room temperature and passed through ascending concentrations of sucrose in 0.2 M phosphate buffer, pH 7.2 (PB), at 4°C for cryoprotection. The brains were subsequently stored in 30% sucrose in 0.2 M PB until their use.

For *in situ* hybridization, the brains were warmed to -16°C, and 16 µm cryostat sections were cut in coronal, parasagittal, and horizontal planes. The sections were thaw-mounted on precooled slides coated with Vectabond® reagent (Vector Laboratories, Burlingame, CA) and stored at -20°C. For RNA and Western blot analyses, rat brains were warmed to -9°C and cryostat sections were cut at 250 µm. The sections were thaw mounted onto baked RNAase-free glass slides and subsequently used for brain punch microdissection (Palkovitz and Brownstein, 1988) and punch-and-load RNA (Melloni et al., 1992) or Western (Towbin et al., 1979) blot analyses. For immunohistochemical staining, immediately before use, horizontal sections of rat brain were cut free-floating at 40 µm on a sliding microtome and placed in 0.1 M phosphate-buffered saline (pH 7.4) (PBS).

For perforant path transection studies, male Sprague-Dawley rats (250-300g) from

Charles River Breeding Laboratory were randomly divided into 3 groups. Animals in groups 1 and 2 were anesthetized with 0.1 mg/kg pentobarbitol and placed in a stereotaxic device with incisor bar at -3.3 mm. Animals in group 3 were unoperated controls.

Group #1 ($n \geq 7$ per time point) received a unilateral knife cut transecting the perforant path starting at 0.7 mm anterior to lambda and 5.7 mm lateral to midline. A Scouten adjustable wire knife cannula (David Kopf, Ind.) was lowered 5 mm below the duramater and the wire knife blade extruded 3.2 mm medially (total cut length = 2.5 mm). The wire knife blade was then raised 4.5 mm resulting in a coronal knife cut made 2.5 mm medial-lateral and 4.5 mm dorsal-ventral. A second cut at a predetermined angle (60^{o} off the coronal plane) was made laterally to a total cut length of 2.3 mm.

Group #2 (n=11) received sham surgical procedures which entailed soley the lowering of the Scouten wire knife cannula to the level of the duramater.

Group #3 (n=8) were unoperated (naive) controls.

Animals in groups #1 and #2 were allowed to survive 1, 2, 4, 7, 14, and 31 days post knife-cut and were sacrificed as described above. The brains were then removed and levels of synapsin I protein were examined by immunohistochemistry and steady state levels of synapsin I mRNA were examined by *in situ* hybridization and RNA blot analysis as described.

Construction of Synapsin I cDNA Vector pSPT 18E2

The EcoRI 1.7 kb fragment of synapsin I cDNA was subcloned from pSyn 5 (Kilimann and DeGennaro, 1985) into the transcription vector pSPT 18 (Boehringer Mannheim). The 1.7 kb fragment of synapsin I cDNA spans the midsection of the synapsin I cDNA sequence from nucleotides 694 to 2445. Briefly, the synapsin I cDNA plasmid pSyn 5 was cut with the restriction enzyme Eco RI (Boehringer Mannheim) and the digestion products displayed on a 1% agaraose gel (Maniatis et al., 1982). The 1700 bp fragment, 5E2, was excised from the gel, purified with Gene-Clean (Bio 101, Inc.,

LaJolla, CA), and ethanol precipitated. After resuspension, the fragment was subsequently ligated to an Eco RI-digested pSPT 18 transcription vector and transformed into Escherichia coli strain HB101 using the calcium chloride method of Cohen et al. (1972). Standard protocols were used to amplify and culture bacterial transformants and isolate plasmid DNA (Maniatis et al., 1982). Two transcription plasmids were verified by restriction enzyme analysis, and plasmid nomenclature was chosen to emphasize the fragment origin and orientation derived from plasmid pSyn 5 containing the parent synapsin I cDNA clone. For instance, pSPT18E2(+) denotes that the synapsin I cDNA sequence 5E2, from parent vector pSyn5, resides 3' to 5' from the SP6 promotor in the transcription vector pSPT18. pSPT18E2(-) denotes the 5E2 fragment in the 5' to 3' orientation from the SP6 promotor. Thus, *in vitro* transcription using SP6 polymerase (Boehringer Mannheim) and the vector pSPT18E2(-) results in the production of a sense synapsin I synthetic RNA strand for potential use as a standard in such procedures as RNA blot or RNAse protection assays.

Synthesis of cDNA Probes for FUV-RNA Blot Analysis

Several probes were used to identify RNAs on FUV-RNA blots. Most significantly for our use was the isolation and subsequent use of synapsin I cDNA fragment 5E2 as a probe to analyze the integrity of synapsin I mRNA transcripts in punch-and-load processed rat brain samples. To isolate synapsin I cDNA fragment 5E2, the synapsin I transcription plasmid pSPT18E2(-) was digested the restiction enzyme EcoRI (Boehringer Mannheim) and the 1.7 kb fragment containing synapsin I cDNA sequences 694-2445 was purified by electroelution from a 1% (w/v) agarose gel (Maniatis et al., 1982). The cDNA fragment was then labeled to a specific activity of 0.6 to 1.2 x 10^9 dpm per µg by random oligonucleotide priming (Feinberg and Vogelstein, 1983; 1984) using a commercial kit (Boehringer Mannheim) with [α-^{32}P] dCTP (New England Nuclear Research Products, 3000Ci/mmol). Unincorporated nucleotides were removed by

Sephadex G25 column chromatography using commercially available spin columns (Boehringer Mannheim). Finally, cDNAs for α-tubulin (Cleveland and Sullivan, 1985) and 18s ribosomal RNA (Katz et al., 1983) were obtained and used as cDNA probes in subsequent experiments. These cDNA plasmids were labeled to a specific activity of 0.8 to 1.5 x 10^9 dpm per μg by random oligonucleotide priming with [α-^{32}P] dCTP as previously described.

RNA Analysis

All materials were molecular biology grade or of the highest purity. All glassware was baked at 180°C for >4 hours to inactivate ribonucleases (Maniatis et al., 1982), and aqueous solutions were treated with 0.1% DEPC and autoclaved before use. The FUV-denaturing gel loading buffer was a modified urea lysis buffer (Sive et al., 1989). The FUV-buffer contained 2.2M formaldehyde, 7M urea, 20mM vanadyl ribonucleoside complex (VRC), 0.5% sodium dodecyl sulfate (SDS), and 1X 3-[N-Morpholino]propane-sulfonic acid (MOPS). A urea stock solution minus formaldehyde and VRC was made and stored at room temperature for no longer than one week. Formaldehyde (37%) and VRC were added just prior to sample processing.

FUV-RNA Blot Analysis - Normal Adult Rat Brain

Total rat brain RNA was extracted and purified from rat tissues by the method of Chirgwin *et al.* (1979), or analyzed by the punch-and-load procedure described below.

Punch-and-Load Procedure. Stainless steel hypodermic tubing (Small Parts Inc., Miami, FL.) was used to sample punches of tissue 0.5 - 1.0 mm in diameter from 250 μm thick cryostat sections of rat brain, kidney, and liver (approximately 50 - 200 μg tissue (Palkovitz and Brownstein, 1988)). The micropunches were immediately solublized by pestle homogenization using a Kontes reusable CTFE/stainless steel pestle attached to a Skiltwist cordless screwdriver motor unit. Homogenization was carried out in 50 μl FUV-

buffer in Kontes 500 µl polypropylene microtubes and samples were placed on ice. Samples were then centifuged in an Eppendorf microfuge for 15 seconds at room temperature, heated at 65°C for 20 minutes, and returned to ice. Ethidium bromide, to a final concentration of 25 ng/µl, and bromophenol blue (4%) loading dye were added to each tube, and the samples were applied directly to a 2.2M formaldehyde-agarose (1.2%) gel for electrophoresis (Maniatis et al., 1982). The gel was then photographed under ultraviolet illumination to visualize the 28s ribosomal RNA band as a qualitative measure of RNA integrity.

Hybridization. RNA was blotted onto Zetabind nylon membrane (American Bioanalytical) by capillary action using 10X SSC (1X SSC = 0.16M NaCl, 0.015M $Na_3C_6H_7{\cdot}2H_20$, pH 7.0) as the transfer buffer (Maniatis et al., 1982). Membranes were UV cross-linked for 1 minute (Pauli et al., 1991), and baked at 80°C for 1 hour. For prehybridization, membranes were incubated for 4-6 hours at 50°C in hybridization buffer (50% formamide, 0.5M Na_2HPO_4 pH 7.5, 7% SDS, and 250 µg/ml heat-denatured Escherichia coli DNA). Membranes were then hybridized to [α^{32}P]-dCTP random-primed labeled (Boehringer Mannheim) synapsin I (Kilimann and DeGennaro, 1985), α-tubulin (Cleveland and Sullivan, 1985), and/or 18s ribosomal RNA (Katz et al., 1983) cDNA probes at 3 - 10 x 10^6 cpm/ml. Hybridizations were carried out in hybridization buffer at 50°C overnight (>16 hours). Membranes were then washed at room temperature for 20 minutes in two changes of 2X SSC, 0.1% SDS, 0.1% $Na_4P_2O_7$; followed by 1X SSC, 0.1% SDS, 0.1% $Na_4P_2O_7$; and 0.3X SSC, 0.1% SDS, 0.1% $Na_4P_2O_7$, each preheated to 65°C. RNA blots were then exposed to Kodak XAR-5 film for >4 days at -70°C with a Dupont Cronex intensifying screen.

Standardization. Prior to tissue sampling, an unlabeled sense synapsin I synthetic RNA was added to the FUV-buffer to serve as external standard (Heumann and Thoenen, 1986). Briefly, a 1.7kb synapsin I sense RNA transcript was synthesized *in vitro* by using the synapsin I transcription vector pSPT18E2(-) and SP6 polymerase (Dunn and Studier,

1983) with the aid of a commercial SP6/T7 Transcription Kit (Boehringer Mannheim). The RNA was purified by repeated ethanol precipitation (Maniatis et al., 1982), and a known amount was added to punch samples to control for differences in RNA recovery, degradation, blotting, and hybridization.

FUV-RNA Blot Analysis - Developing and Lesioned Rat Brain

RNA was prepared from brain punches obtained from various subregions of rat brain. For developmental studies, a 0.3 mm stainless steel punch was used to sample the dentate granule cell layer of the hippocampus bilaterally from several consecutive sections of rat brains aged 14, 21, and 31 days postnatally. For perforant pathway transection studies, a 0.3 mm punch was used to sample the dentate granule cell layer and the CA4 region of the hippocampus, the medial septal nucleus, and the superficial entorhinal cortex bilaterally from several consecutive sections of lesioned, sham operated, and naive control animals. Multiple brain punches were pooled and total RNA was prepared by a modification of the method of Chomczynsky and Sacchi (1987) and analyzed by formaldehyde-agarose gel electrophoresis utilizing the FUV buffer as previously described (Melloni et al., 1992, 1993). The RNA was blotted onto Zetaprobe® nylon membrane (Bio-Rad) as described by Thomas (1980), and hybridized for >16 hours at 50°C in 50% (v/v) formamide, 7% (w/v) SDS, 0.5 M Na_2HPO_4, pH 7.5, 250 µg/ml heat-denatured *Escherichia coli* DNA and 10 ng/ml rat synapsin I and/or 18s ribosomal RNA cDNA fragments, labeled as described. Membranes were then washed to high stringency through several changes of SSC, and exposed to Kodak XAR-5 film for >4 days at -70°C with a Dupont Cronex intensifying screen.

Synthesis of Synapsin I cDNA Probes for *In Situ* Hybridization.

Synapsin I Dde I-digested cDNA fragment 5E2 was used as cDNA probe for *in situ* hybridization. Briefly, synapsin I cDNA plasmid pSyn 5 (Kilimann and DeGennaro,

1985) or pSPT18E2 (+/-) was cut with the restriction enzyme Eco RI (Boehringer Mannheim) and the 1700 bp fragment, 5E2 (nucleotides 694-2445 of the synapsin I cDNA sequence), was purified by electroelution from a 1% (w/v) agarose gel (Maniatis et al., 1982). Fragment 5E2 was then redigested with the restriction enzyme Dde I (Boehringer Mannheim) and the digestion products were purified by ethanol precipitation. These fragments were labeled to a specific activity of 2 - 3 x 10^8 dpm per µg by random primed labeling (Boehringer Mannheim) in the presence of [α-^{35}S]dCTP as previously described. Before use, unincorporated nucleotides were removed by chromatography over a Sephadex G25 spin column (Boehringer Mannheim).

In Situ Hybridization Histochemistry

All materials were molecular biology grade or of the highest purity. All glassware was baked at 180°C for >4 hours to inactivate ribonucleases (Maniatis et al., 1982), and aqueous solutions were treated with 0.1% DEPC and autoclaved prior to their use.

Synapsin I *In Situ* Hybridization Histochemistry

Fixation and Tissue Preparation. Slide-mounted brain sections were warmed to room temperature, post-fixed in 4% formaldehyde (Polysciences, Inc.) in 0.1 M phosphate buffer (pH 7.4) for 5 minutes at 0°C, rinsed in phosphate buffered saline (PBS), and treated with 0.25% acetic anhydride (in 0.1 M triethanolamine, pH 8.0) for 10 minutes at room temperature. After rinsing in 2 X SSC and dehydration (2.5 minutes each) through a graded series of alcohols (75%, 95%, and then 100%), the sections were delipidated in chloroform (Fisher Scientific) for 5 minutes at room temperature. The sections were subsequently rehydrated to 95% ethanol in descending concentrations of alcohols and then air dried. Processed slides were kept in light-tight slide boxes at room temperature until use.

Hybridization Conditions and Post-Hybridization Washes. For hybridization, probe (2-3 x 10^6 cpm) was applied in 65 µl hybridization buffer (50% formamide, 10% dextran sulfate, 2 X Denhardt's solution, 5 X SSC, 50 mM DTT, 0.1% SDS, 100 µM dNTPs, and 0.1% $Na_4P_2O_7$), and the slides were coverslipped and incubated at 50°C overnight (>16hrs.) in a moist chamber. Following hybridization, coverslips were removed in 2 X SSC, 0.1% $Na_4P_2O_7$ at room temperature, and the slides were washed for 30 minutes each in two changes each of: 2 X SSC, 0.1% $Na_4P_2O_7$ at room temperature; 2 X SSC, 0.1% $Na_4P_2O_7$ at 42°C; 0.5 X SSC, 0.1% $Na_4P_2O_7$ at room temperature; 0.1 X SSC, 0.1% $Na_4P_2O_7$ at room temperature; and 0.1 X SSC, 0.1% $Na_4P_2O_7$ at 42°C. After a final wash in 0.1 X SSC, 0.1% $Na_4P_2O_7$ for 15 minutes at room temperature, the sections were dehydrated through a graded series of alcohols in which water was replaced by 0.6 M ammonium acetate. The slides were then air dried and exposed to Kodak XAR-5 film for 7 days at room temperature.

Autoradiography. For emulsion autoradiography, selected slides were coated with photographic emulsion (NTB2; Eastman Kodak, Rochester, NY; diluted 1:1 with 0.6 M ammonium acetate). Briefly, in total darkness NTB2 photographic emulsion was melted at 40°C and diluted with warm 0.6 M ammonium acetate. Diluted emulsion was then equilibrated to 40°C in a Dip-Miser emulsion dipping chamber (Electron Microscopy Sciences, Inc.) and selected slides were dipped twice and allowed to dry standing upright, at room temperature in total darkness. Slides were then stored with dessicant in plastic slide boxes wrapped three times in aluminum foil to keep light tight. Sections were allowed to expose for 14 days at 4°C, before developing.

Before the development of slides, D19 developing (Eastman Kodak; diluted 1:1 with water), a water rinse, and Kodak Fixer solutions were precooled to 15°C-16°C in an ice bath. Room temperature slides were placed in cooled D19 developer for 4 minutes with gentle agitation. Slides were then rinsed in prechilled water for 10 seconds and placed in Kodak Fixer for 5 minutes. After fixation, slides were rinsed in running water (~16°C) for

30 minutes.

Cresyl-Violet Acetate Counterstain. To identify neuronal somata, slides processed for emulsion autoradiography were counterstained with 0.04% cresyl-violet acetate (Eastman Kodak). Slides were immersed in 0.1 M sodium acetate buffer (pH 3.5) for 1 minute then stained in 0.04% cresyl-violet (in 0.1M ammonium acetate, pH 3.5) for approximately 10 seconds. They were differentiated in water for 1-2 minutes and then dehydrated through 70%, 95%, and 100% ethanol for 2 minutes each. Slides were subsequently placed in xylene for 2 minutes and coverslipped with Permount (Fisher Scientific).

Antibodies for Western Blot Analysis and Immunohistochemistry

Synapsin I polyclonal antibodies used in these experiments were contained in antisera prepared in rabbits against purified rat synapsin I protein (Kilimann and DeGennaro, 1985). To raise the antibody, synapsin I was purified from rat brain by a modification (Hunter et al., 1981) of the original protocol (Ueda et al., 1977). Two different non-immune rabbit sera, including one from an animal subsequently immunized against synapsin I, served as controls. The polyclonal antibodies used in these studies have been extensively characterized (Kilimann and DeGennaro, 1985), and used previously to localize synapsin I protein in a number of immunohistochemical studies (Hamos et al., 1988; Smith et al., in press; Apostolides et al., in press). At dilutions of 1:500 - 1:2000, the synapsin I antiserum reacts specifically with synapsin I on Western blots of rat brain protein (Kilimann and DeGennaro, 1985 and Figure X), and on rat and human brain sections processed for immunohistochemistry (Hamos et al., 1988; Smith et al., in press; Apostolides et al., in press).

Western Blot Analysis

Adult Studies. Total protein was extracted from the neocortex of an adult rat brain

by a modification of the method of Klose and Zeindl (1984). Briefly, brain punches, 1 mm diameter x 250 µm thickness, were homogenized in 500 µl of tissue extraction buffer [2% Nonidet P-40, 9.5 M urea, 1% ß-mercaptoethanol, and 200 mM K_2CO_3 (pH 9.5)] and then centifuged in an Eppendorf microfuge for 10 minutes at room temperature. The supernatant was collected and a Coomassie Plus protein assay (Pierce, Rockford Ill.) was performed to determine protein concentration.

Western blots were performed according to the method of Towbin et al. (1979). Briefly, 8% polyacrylamide gels were run according to the method of Laemmli (1970). Gels were blotted onto Immobilon-P (Millipore, Bedford, MA) using the semidry blotting technique of Kyhse-Anderson (1984), washed with TBST (25 mM Tris [pH 8.0], 137 mM NaCl, 2.7 mM KCl, 0.05% Tween 20), and blocked with TBST containing 5% nonfat dry milk (NFDM). Synapsin I polyclonal antibody was diluted 1:1000 in TBST containing 1% NFDM (antibody buffer) and incubated with the blot for 1 hour at room temperature. Blots were washed extensively in TBST and incubated with secondary antibody (alkaline phosphatase conjugated goat anti-rabbit IgG, Sigma) at a dilution of 1:3000 in antibody buffer for 1 hour at room temperature. The blots were washed in three changes of TBST for 5 minutes each, rinsed in TBS, and then developed with the Immune-Lite chemiluminescent detection system (Bio-Rad, Richmond, CA) according to manufactures' instructions.

Developmental studies. Total protein was extracted from the hippocampus of rat brains of postnatal days 21 and 31, and Western blot analysis was performed as previously described. Briefly, brain punches 1 mm diameter x 250 µm thickness were obtained from the dentate gyrus and accompaning mossy fiber zone as described by Palkovits and Brownstein (1988). Multiple punches were pooled and total protein was extracted by a modified procedure of Klose and Zeindl (1984). Duplicate aliquots of total dentate protein were electrophoresed in an 8% polyacrylamide gel according to the method of Laemmli (1970). After electrophoresis the gel was divided and one half was fixed and stained with

Daiichi silver stain (Enprotech), while the proteins in the second half were electroblotted onto Immobilon-P (Millipore, Bedford, MA) using the semidry blotting technique of Kyhse-Anderson (1984). Subsequently, Western blots were performed according to the method of Towbin et al. (1979) as described above (Melloni et al., 1993).

Immunohistochemistry

Thirty-five micron horizontal or parasagittal sections, cut on the freezing stage of a sliding microtome, were collected as free-floating sections in 0.1 M PBS (pH 7.4). Every fourth section in the series was preincubated for 30 minutes in 0.01% H_2O_2 in methanol, rinsed twice for 10 minutes each in PBS, 0.03% Triton X-100 (Sigma) (PBST), and then incubated for 1 hour in blocking buffer [20% nonimmune goat serum in PBS containing 0.3% Triton X-100]. Sections were then reacted overnight, at 4°C, with the synapsin I primary antibody at a dilution of 1:1000 in PBS, 0.3% Triton X-100, 3% nonimmune goat serum. On the following day, antibody binding was revealed by using the avidin-biotin complex method of peroxidase labeling (Vector Laboratories, Burlingame, CA). Briefly, sections were rinsed twice for 30 minutes each in PBST, incubated for one hour in biotinylated goat anti-rabbit immunoglobulins (secondary antibody) in PBST, rinsed again twice for 15 minutes each in PBST, and incubated for 1 hour in avidin-biotin-peroxidase complex. The peroxidase label was revealed by using 3,3'-diaminobenzidine (DAB) (Sigma; 0.05% in 50 mM Tris, pH 7.4) as a chromogen. The immunostained sections were mounted on gelatin-coated slides, dehydrated in a graded series of alcohols and xylene, and coverslipped with Permount. Adjacent sections were stained with cresyl violet acetate.

Experimental controls were performed on representative sections and included either the substitution of nonimmune rabbit sera for the primary antibody, omission of the primary antibody, omission of the secondary antibody, or preabsorption of anti-synapsin I IgGs from total rabbit serum using a 100-fold excess of purified synapsin I. Additionally,

adjacent sections that had not been processed through the immunohistochemical protocol were mounted in series and stained for neuronal somata with 1% cresyl violet acetate.

Acetylcholinesterase Histochemistry

To determine the extent of lesion-induced neuronal sprouting in the molecular layer of the dentate gyrus, 16 μm sections adjacent to those used for *in situ* hybridization and 35 μm sections adjacent to those used for immunohistochemistry were processed for acetylcholinesterase (AChE) histochemistry (Hedreen et al., 1985). Sections were incubated in AChE media for >48 hours. After incubation, sections were washed extensively in 0.1 M PBS, then placed in 1% ammonium sulfide developing solution for 2-4 minutes. The sections were then washed extensively in water, dehydrated through a graded series of alcohols, and coverslipped. All incubations were carried out at room temperature.

Image Analysis

In developmental studies, the relative levels of synapsin I protein immunoreactivity and mRNA hybridization we assessed on an IBAS 2000 Image Analysis System linked to a Zeiss Axioplan light microscope. On immunohistochemically stained sections, grey-level density values of synapsin I immunoreactivity were obtained from the mossy fiber zone of the rat dentate gyrus. In these analyses, an average of five readings of grey-level density were taken from a 100 X 100 pixel area on a scale of 0 (black, i.e., very immunoreactive) to 255 (white, i.e., no immunoreactivity) in each of 3 animals from 5 developmental time points. In each case, the grey-level density values obtained were standardized relative to the average density of background staining in the corpus callosum. On *in situ* hybridization sections, the relative levels of synapsin I hybridization in the dentate granule cell layer were assessed from autoradiographic films. In these analyses, the dentate gyrus was outlined, and as above, an average of five readings of grey-level dentsity were obtained in each of 3

animals from 8 developmental time points. In each case, the grey-level densities were standardized relative to background hybridization; e.g., average grey-level density values obtained from the corpus callosum. The data presented represent the relative levels of synapsin I immunoreactivity and hybridization as compared with the signal found in white matter fiber tracts known to be void synapsin I protein and mRNA. Values are presented ± SEM per developmental time point.

Chapter III

DEVELOPMENT OF A METHOD FOR THE DIRECT MEASUREMENT OF SYNAPSIN I mRNA IN DISCRETE REGIONS OF MAMMALIAN BRAIN

Introduction

Hybridization analysis of steady state mRNA levels as a reflection of differential gene expression is a procedure commonly used in molecular neurobiology. For such analyses to be truly quantitative and reproducible, RNA isolation and purification protocols typically must yield intact RNA with high efficiency and good recovery. Several difficulties arise in the application of current methods which meet these criteria to the study of gene expression in the discrete subregions of the mammalian brain. First, these methods invariably require moderate amounts of tissue, which precludes their use in the analysis of mRNA levels in tissue samples where quantities are limited. Furthermore, due to the elaborate nature of conventional RNA preparation protocols, the analysis of large numbers of RNA samples can be tedious and often very time consuming. Recently, several reports of rapid, small scale preparations of nuclear, cytoplasmic, poly $(A)^+$ and total cellular RNA have been published (Chen et al., 1983; Dziadek and Andrews, 1983; Ilaria et al., 1985; Chomczynski and Sacchi, 1987; Badley et al., 1988; Emmet and Petrack, 1988; Gough, 1988; Meirer, 1988; Wilkinson, 1988a,b; Rappolee et al., 1989). These reports detail RNA extraction protocols from both isolated- and cultured- cell suspensions and fresh tissues, using as little as 10^5 cells or 3 mg tissue, respectively. However, consistently poor yields indicate many of these methods are unsuitable for the rapid analysis of multiple RNA samples from microgram amounts (approximately 50 - 200 μg) of intact tissue.

An alternate method of measuring mRNA levels in small amounts of tissue has

recently been published by Sive *et al.* (1989). The authors describe the use of an urea lysis buffer (7M Urea, 0.5% SDS, 1X MOPS) to solubilize small amounts of freshly dissected *Xenopus* embryo parts. To measure steady state mRNA levels directly, the solubilized tissue samples were added to a formaldehyde-agarose gel for electrophoresis and subsequent RNA blot analysis. In our hands, however, complications with RNA degradation and incomplete denaturation proved this buffer unsuitable for use with small quantities of frozen mammalian brain tissue.

In this chapter, the main objective was to develope a procedure for the direct analysis of mRNA levels in microgram quantities of frozen mammalian tissues, with particular emphasis on RNAs from brain. The resulting protocol, the punch-and-load procedure, is extremely rapid, results in excellent recovery of RNA, and allows the direct assay of mRNA levels in discrete regions of cryostat cut tissue sections.

Results

Ethidium Bromide Staining of FUV-RNA Formaldehyde-agarose Gel

Figure 4A shows the ethidium bromide-stained 2.2M formaldehyde-agarose (1.2%) gel of duplicate punches of rat brain frontal cortex. Punch samples of 0.5 mm in diameter (approximately 50 μg tissue, lanes 3 and 4) and 1.0 mm in diameter (approximately 200 μg tissue, lanes 5 and 6) were processed by the punch-and-load procedure and photographed under ultraviolet illumination. The 28s ribosomal RNA band of the FUV-denatured punches comigrates with those of purified rat brain (lane 1) and liver (lane 2) RNA. This similarity in migration and band pattern signifies complete denaturation of intact RNA present in the lysed punches and demonstrates the suitability of this RNA for hybridization analysis. Subsequent densitometric and/or hybridization analysis of the 28s ribosomal RNA offer alternative means of quantitating relative amounts of RNA present per FUV-

Figure 4. Electrophoretic and RNA blot analysis of FUV-denatured punch samples from rat brain frontal cortex. Purified total rat brain RNA (1.0 μg, lane 1), rat liver RNA (4.0 μg, lane 2), and duplicate sample punches of rat frontal cortex, 0.5 mm in diameter (approximately 50 μg tissue, lanes 3 and 4) or 1.0 mm in diameter (approximately 200 μg tissue, lanes 5 and 6) x 250 μm in thickness, were solubilized in FUV-buffer and electrophoresed on a 2.2M formaldehyde-agarose (1.2%) gel as described in the text. The gel (A) was photographed under ultraviolet illumination to visualize 28s ribosomal RNA as a measure of RNA integrity, and then the RNA transferred to Zetabind nylon membrane and affixed by ultraviolet irradiation for 1 minute and baking at 80°C for 1 hour. The filter was hybridized to a rat synapsin I cDNA probe, washed as described, and exposed to Kodak XAR-5 film with a Dupont Cronex intensifying screen at -70°C. The filters were then stripped of synapsin I probe in two washes of 20 minutes each in boiling 0.1X SSC, 0.5% SDS; followed by a 0.1X SSC rinse, and rehybridized to a 18s ribosomal RNA cDNA probe; both probes were labeled with [^{32}P]-dCTP. The autoradiogram (B) shows both 3.4kb and 4.5kb rat synapsin I mRNA species in rat total RNA (lane 1) and in rapid punch-and-load processed rat brain frontal cortex samples (lanes 3-6) when hybridized with rat synapin I cDNA as probe, and (C) a 1.8kb 18s ribosomal RNA when rehybridized with 18s ribosomal RNA cDNA as probe.

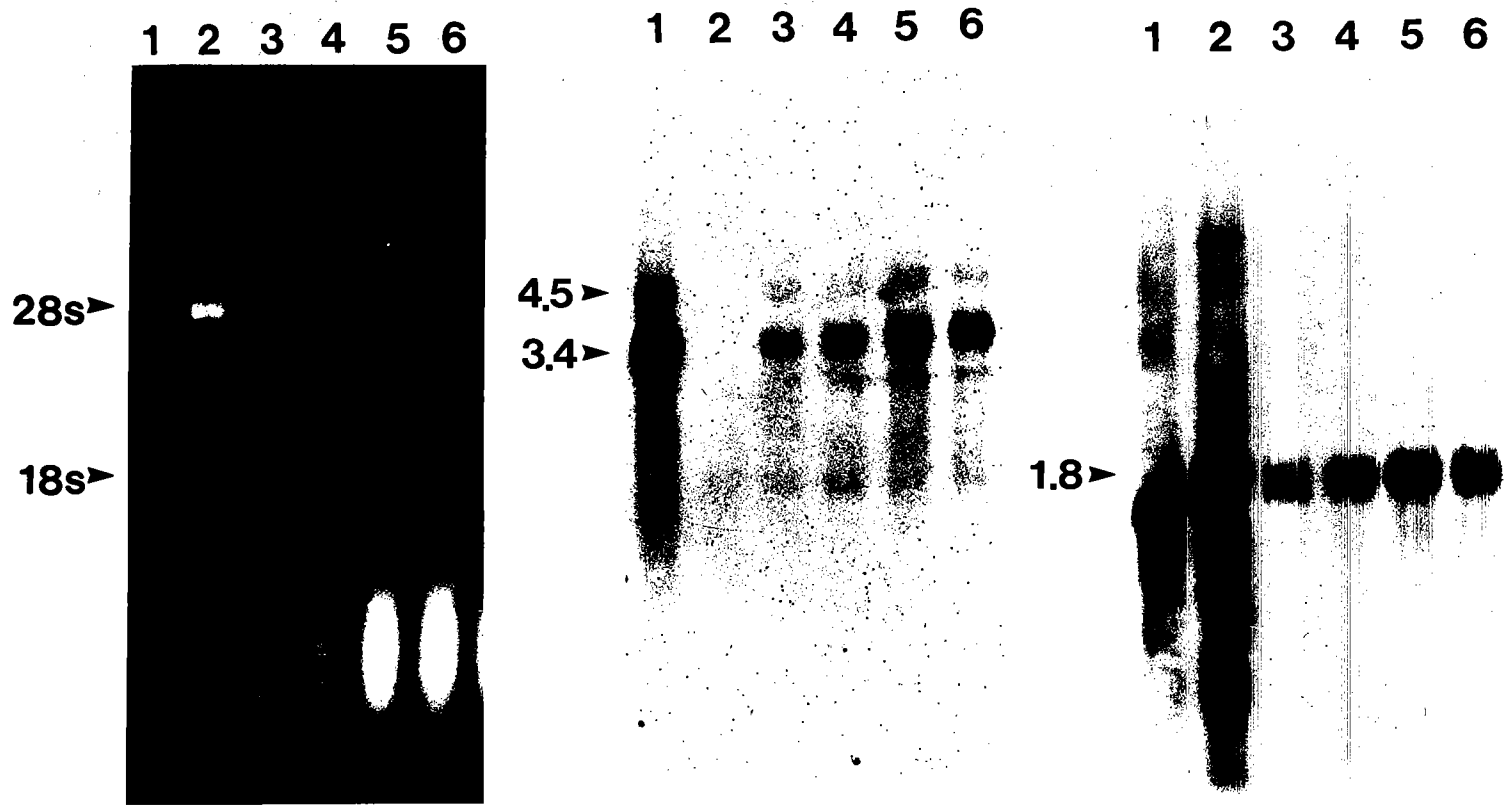
1 2 3 4 5 6
28s
18s
1 2 3 4 5 6
4.5
3.4
1 2 3 4 5 6
1.8

denatured punch. The ethidium-bromide fluoresence at the bottom of each sample most likely represents a mixture of transfer RNAs, solubilized proteins, and cellular debris, present since whole tissue homogenates are being applied directly to the formaldehyde-agarose gel.

Synapsin I and 18s Ribosomal RNA in Rat Brain Frontal Cortex

Total RNA isolated by the method of Chirgwin *et al.* (1979) and the punch-and-load procedure have been used for the detection and quantitation of mRNAs of the neuron-specific rat synapsin I gene and 18s ribosomal RNA. Figure 4B shows an autoradiogram of the formaldehyde-agarose gel depicted in Figure 4A after hybridization to a ^{32}P-labeled rat synapsin I cDNA probe. Both synapsin I mRNAs of 3.4kb and 4.5kb (Haas and DeGennaro, 1988) were identified with little or no smearing in each of the four punch-and-load samples (lanes 3-6). The sharp banding pattern seen in Figure 4B indicates that the synapsin I mRNAs are intact and suggests efficient inactivation of cellular RNAses during the homogenization step of the punch-and-load procedure. Liver RNA (lane 2), added as a negative control, shows no hybridization signal with synapsin I cDNA as probe. Figure 4C illustrates the same RNA blot rehybridized to a ^{32}P-labeled 18s ribosomal RNA cDNA probe. Hybridization in the punch-and-load samples is detected as a single discrete band migrating at approximately 1.8kb in length. No hybridization signals were detected in the wells of the RNA blots with either the synapsin I or the 18s ribosomal RNA cDNA probes. The above results demonstrate the capacity of the FUV-denaturing gel loading buffer to thoroughly and reproducibly solubilize and denature different RNA species within the same sample.

Synapsin I mRNA in Discrete Regions of Rat Brain

The punch-and-load procedure has been used in our laboratory to quantitate synapsin I mRNAs from discrete regions of rat brain. Figure 5 presents a RNA blot

Figure 5. RNA blot autoradiogram of RNA from punch-and-load processed samples from various regions of rat brain. Purified total rat brain RNA (3.3 μg, lane 1) and duplicate 1.0 mm x 250 μm sample punches (lanes 2-7) were processed, electrophoresed, and blotted as described in the text. The filter was hybridized to a rat synapsin I cDNA probe labeled with [^{32}P]-dCTP. The filter was exposed to Kodak XAR-5 film with a Dupont Cronex intensifying screen for >4 days at -70°C. In all samples, intact synapsin I mRNAs of 3.4kb and 4.5kb were identified on the autoradiogram, along with a 1.7kb synapsin I internal cRNA standard (20 pg) added prior to sample homogenization to control for mRNA recovery. The rat brain regions sampled were frontal cortex (lanes 2 and 3), dentate gyrus (lanes 4 and 5), and the lateral and medial amygdaloid nuclei (lanes 6 and 7).

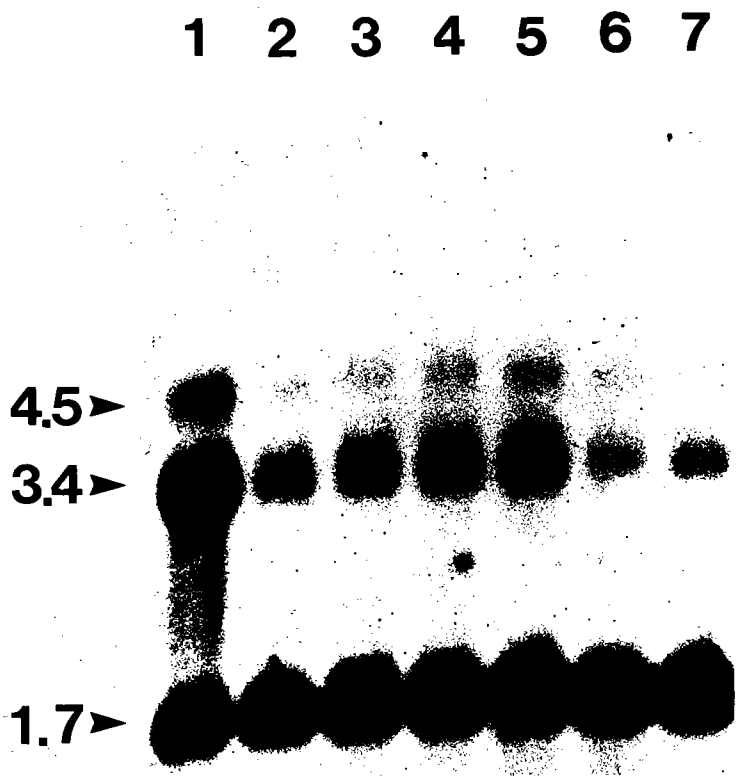
1 2 3 4 5 6 7
4.5
3.4
1.7

analysis of duplicate 1.0 mm FUV-denatured punches from various regions of rat brain (lanes 2-7). Hybridization of synapsin I cDNA probes identified intact synapsin I mRNAs of 3.4 kb and 4.5 kb, respectively, and a 1.7kb synapsin I internal cRNA standard (20pg) added to control for mRNA recovery. Consistent with the RNA blot results described earlier, sufficient RNA was present in one 50 - 200 μg punch from each of the dissected brain areas to quantitate reproducibly the steady state levels of synapsin I mRNA. Subsequent rehybridization of the blot to alternative probes of interest offers a quantitative measure of differential gene expression in focal, discrete subregions of the mammalian brain, a level of analysis previously hindered by a lack of rapid and reproducible RNA microisolation techniques.

Punch-and-Load RNA in Multiple Tissue Types

The general applicability of the punch-and-load procedure for the analysis of mRNAs in tissues other than rat brain has also been tested. Figure 6A shows the ethidium-bromide stained gel of FUV-denatured punches of rat liver (lanes 2 and 3) and kidney (lanes 4 and 5) compared with purified rat liver RNA (lane 1). Both the 28s ribosomal RNA band and the 18s ribosomal RNA band are visible in the liver punch samples. Such clear banding patterns in liver suggests an increased solubilization efficiency of the FUV-buffer in this tissue. Since densitometric and hybridization analyses can be performed on both ribosomal RNA species, RNA quantitation and standardization per punch are even more reliable in this case. Figure 6B presents a RNA blot analysis of the gel in Figure 6A using a ^{32}P-labeled 18s ribosomal RNA cDNA as probe. Similiar results are obtained to those shown in Figure 4C, where a sharp, distinct band of 1.8kb in length representing intact 18s ribosomal RNA was easily identified.

Technical Considerations

Significant problems surfaced in the analysis of mRNA levels from pancreatic and

Figure 6. Electrophoresis and RNA blot analysis of punch samples from tissues other than rat brain. Purified rat liver RNA (4.0 μg, lane 1) and duplicate 1.0 mm x 250 μm sample punches of rat liver (lanes 2 and 3) and kidney (lanes 4 and 5) were solubilized in FUV-buffer and electrophoresed as described in the text. The gel (A) was photographed under ultraviolet illumination as a measure of RNA quality. Note the integrity of both the 28s ribosomal band and the 18s ribosomal band present in the liver punch samples. The RNA was transferred to Zetabind nylon membrane and hybridized to a [^{32}P]-dCTP labeled 18s ribosomal RNA cDNA probe. Hybridization is detected as a single, discrete band of 1.8kb in length with no apparent smearing on the autoradiogram.

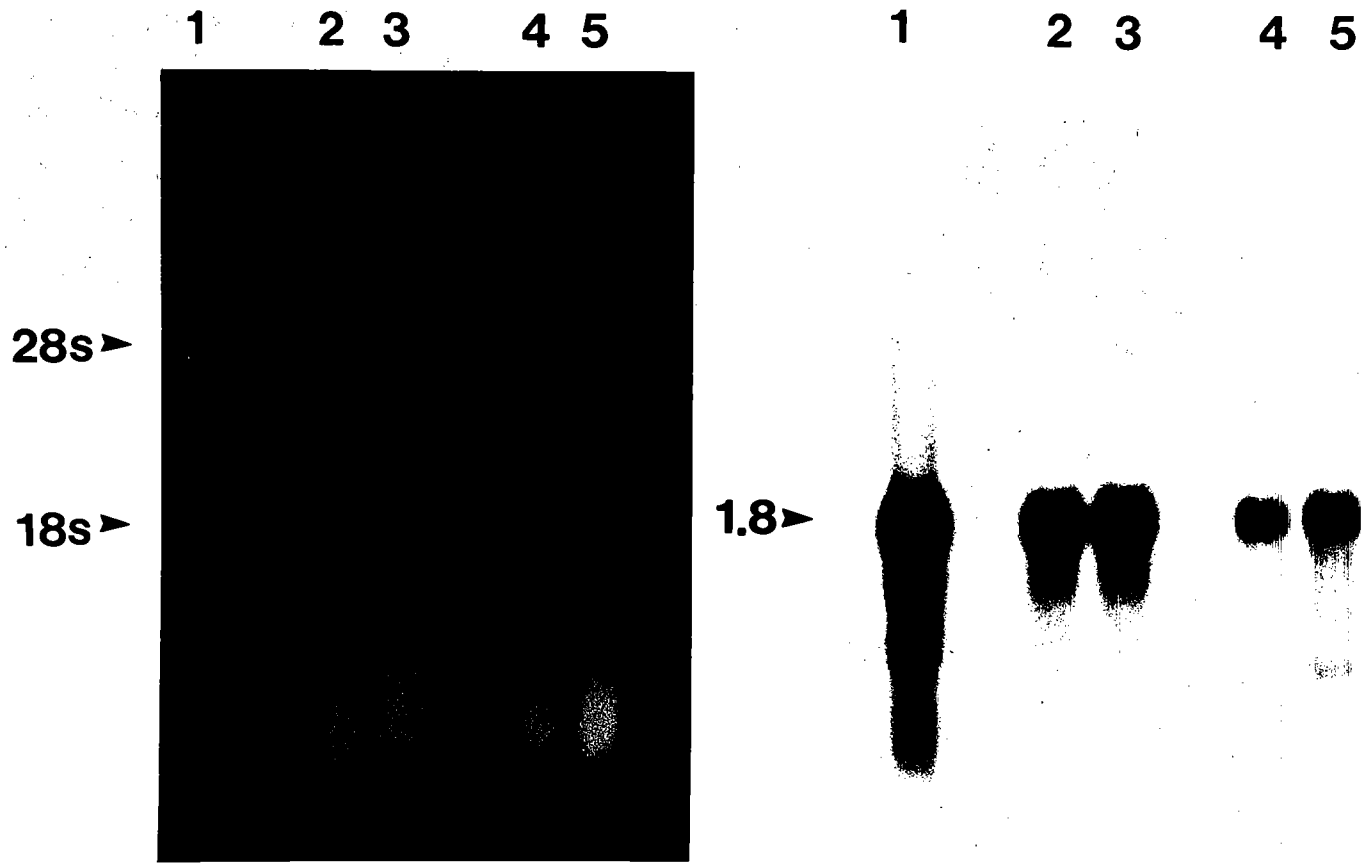
1 2 3 4 5
28s
18s
1 2 3 4 5
1.8

striated muscle tissue. In the pancreas, high levels of RNAse activity overwhelmed the FUV-buffer, resulting in degraded mRNA, as evidenced by a smeared or often non-existent hybridization signal obtained when punch samples were probed with an alpha-tubulin cDNA probe (data not shown). Striated muscle tissue presented considerable problems in the homogenization step of the technique, as indicated by a persistence of cellular precipitates after homogenization. Subsequent electrophoretic analysis showed incomplete denaturation of mRNAs on both the ethidium bromide stained formaldehyde-agarose gel and alpha-tubulin probed RNA blot (data not shown).

Variation in hybridization signal seen in lanes 3 and 4, Figure 4C, and lanes 4 and 5, Figure 6B, suggest different levels of 18s ribosomal RNA in duplicate 1 mm punches. In general, this variation was found to be due to inconsistant tissue sampling, where differences in cell number between duplicate punches translate into differences in RNA levels. To control for reproducible sampling of a cell cluster, punch positions should be chosen that are similiar in cell density and number, with defined boundries and landmarks. Additionally, a punch should be chosen whose internal diameter falls within the borders of the cell cluster rather than one that samples the entire field.

One cannot rule out variation in hybridization signals which may be due to problems at the level of RNA blotting. The results presented demonstrate that the punch-and-load method is reproducibly useful for the detection and quantification of relatively large mRNAs. However, smaller mRNAs which migrate near or within the smear of cellular debris present at the bottom of each formaldehyde-agarose gel may not transfer efficiently. Further, hybridization to these RNAs may be hindered by the presence of this same material on the RNA blot. Accordingly, to minimize problems inherent in RNA blot analysis and to control for differences in hybridization efficiencies, accurate normalization of RNA levels should be carried out with control probes which recognize RNA species of a size similiar to that of the mRNA of interest.

Discussion

The main objective was to develop a simple and reliable procedure for the direct analysis of mRNA levels in microgram quantities of frozen mammalian brain. The principle advantages of the punch-and-load procedure over conventional methods are several. First, the procedure is extremely rapid. This minimizes time constraints inherent in conventional RNA preparation methods and becomes especially useful for the simultaneous processing of multiple samples. Second, it utilizes very small quantities of tissue, approximately 50 - 200 μg vs. >3 mg for rapid procedures, and >1-2 g for most conventional RNA isolation and purification protocols. This is of particular significance to the molecular neurobiologist, since it affords the researcher the opportunity to compare specific mRNA levels in discrete brain areas or nuclei where tissue quantities are severly limited. Third, the procedure is quantitative and reproducible, as mRNA levels from duplicate samples can be easily normalized by hybridization to a known amount of added synthetic cRNA external standard and/or relative amounts of 18s and 28s ribosomal RNA. Fourth, the procedure is sensitive and results in excellent recovery of intact RNA. In our hands, the punch-and-load technique can reproducibly detect on the order of 15-50 molecules of synapsin I mRNA per neuron. The degradation and loss of RNA is minimized by the limited processing of samples in this procedure. The lack of hybridization anywhere on the RNA blots other than to specifically targeted mRNAs suggests complete recovery of both exogenous and endogenous RNAs. Finally, because the rapid punch-and-load procedure is very simple, it circumvents the tedious and often difficult nature of conventional RNA preparation protocols. Electrophoresis of multiple samples can be underway within 30 minutes of tissue sectioning.

Chapter IV

SYNAPSIN I GENE EXPRESSION DURING THE DEVELOPMENT OF THE RAT NERVOUS SYSTEM

Introduction

In the adult rodent, biochemical (Walaas et al., 1983, 1988), immunological (Goelz et al., 1981), and immunohistochemical (Bloom et al., 1979; De Camilli et al., 1983a,b; DeGennaro et al., 1989; Sudhof et al., 1989; Apostilides et al., (in press)) studies all indicate that synapsin I protein is widely, but not uniformly, distributed throughout the central nervous system. During development, the appearance of synapsin I protein in the neuropil coincides temporally and topographically with synaptogenic differentiation both *in vivo* (Lohman et al., 1978; De Camilli et al., 1983; DeGennaro et al., 1983; Levitt et al., 1984; and Mason, 1986; Moore et al., 1989) and *in vitro* (Bixby and Reichardt, 1985; Weiss et al., 1986), and recent morphological and physiological studies by Han *et al.* (1991) and Lu *et al.* (1992) suggest that the synapsins may participate in synaptogenic differentiation and the functional maturation of synapses in the developing nervous system.

Given the various postulated roles for synapsin I in the development and function of the nervous system, it is of particular importance to define and characterize the temporal and spatial expression of the synapsin I gene during the development of distinct neuronal populations. Thus far, the analysis of the expression of the synapsin I gene in development has been limited to observations by RNA blot and *in situ* hybridization analyses in the postnatal rat cerebellum (Haas and DeGennaro, 1988). In that study, the peak expression of synapsin I mRNA in the developing cerebellum was shown to coincide with the major period of synaptogenesis, occuring at approximately postnatal day 20 in the

rat. The results reported are limited, however, in that they (1) do not detail the developmental pattern of expression of the synapsin I gene across the entire central and peripheral neuraxis, and more focally, (2) failed to resolve with precision the time of onset of expression of the synapsin I gene.

In this chapter, the first extensive *in situ* hybridization study describing the regional and cellular localization of synapsin I mRNA throughout the rat central and peripheral nervous systems during embryonic and postnatal development is presented. This study was then extended to determine the precise time of onset of synapsin I gene expression during the emergence of particular types of neurons in the developing central nervous system. These results present a detailed description of the temporal and spatial expression of the synapsin I gene during the embryonic and postnatal development of the nervous system, as well as provide insight into the temporal onset of expression of the synapsin I gene in relation to the state of differentiation of granule cell neurons of the hippocampus and cerebellum.

Results

Specificity of Detection of Synapsin I mRNA in the Nervous System

In rat brain, the gene encoding synapsin I directs the synthesis of two classes of mRNA of 3.4kb and 4.5kb in length, respectively (Haas and DeGennaro, 1988). The 3.4kb mRNA is comprised of two alternatively spliced transcripts encoding synapsin Ia and Ib polypeptides (Sudhof et al., 1989). The complete sequence of the 4.5kb mRNA has not been determined. To ensure that the Dde-I digested synapsin I cDNA probes used in this study were specific for synapsin I mRNAs, RNA blot analysis was performed on total RNA purified from adult rat brain. Figure 7 shows a RNA blot of 3.3 μg of guanidium isothiocyanate-purified total rat brain RNA hybridized with radioactively-labeled Dde-I

Figure 7. RNA blot autoradiogram demonstrating specificity of Dde I-digested synapsin I cDNA probes. Purified total rat brain RNA (3 μg) was prepared, electrophoresed, blotted and hybridized as described in text. The synapsin I cDNA probes recognized exclusively synapsin I mRNAs of 3.4 kb and 4.5 kb.

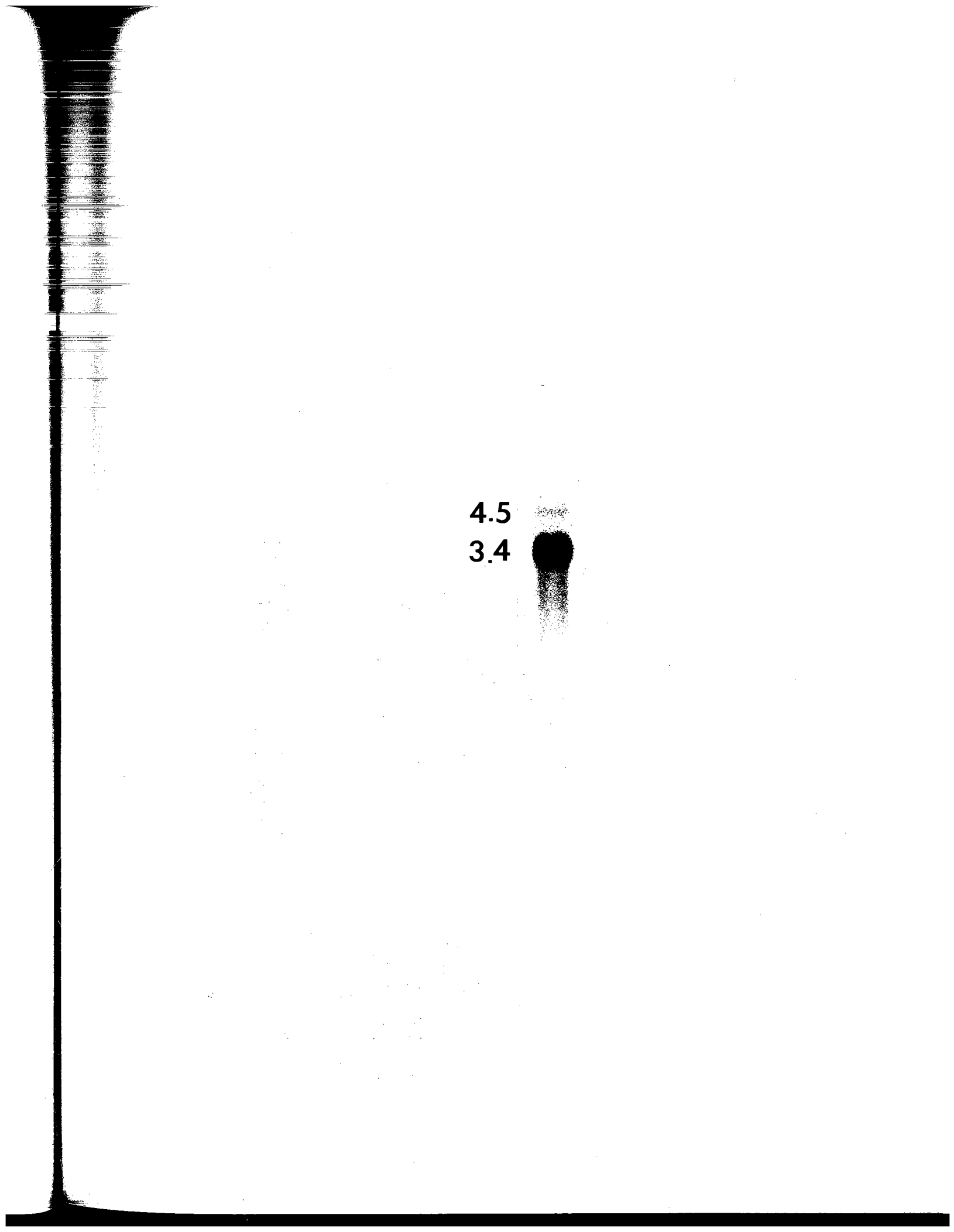
4.5
3.4

digested synapsin I cDNA probe. Here synapsin I cDNA hybridized specifically with both classes of synapsin I mRNAs, 3.4 kb and 4.5 kb, respectively. No hybridization was detected on blots in which synapsin I cDNA was hybridized to liver and kidney RNA (data not shown).

To compare the relative levels of expression of synapsin I mRNA in different areas of the rat central nervous system, RNA blot analysis was performed on RNA prepared from various subregions of rat brain. Figure 8A presents RNA blot analysis of duplicate 1.0 mm tissue punches from discrete regions of the adult rat brain. The synapsin I cDNA probes recognized exclusively synapsin I mRNAs of 3.4 kb and 4.5 kb, and a 1.7 kb synapsin I external RNA standard, in purified rat brain RNA (RB) and RNA from all brain areas sampled (Ctx-MS). The strength of the hybridization signal obtained varied in different brain regions, with the highest signal in the RNAs from the dentate gyrus and the neocortex and the lowest in the RNA from the caudate nucleus.

The hybridization signals obtained by RNA blot analysis (Figure 8A) corresponded with the pattern and strength of synapsin I mRNA hybridization localized in discrete regions of rat brain by *in situ* hybridization (Figure 8B, C). Strong radioactive labeling of granule cell neurons in the dentate gyrus (Figure 8C) corresponded to the highest level of synapsin I mRNA detected by RNA blot analysis (Figure 8A). Lower hybridization signals were obtained, in decreasing order of intensity, in the neocortex, central/lateral amygdala, medial septum, and the caudate nucleus. In these areas, as above, the strength of the hybridization signals revealed by *in situ* hybridization corresponded to the intensity of signals obtained by RNA blot analysis.

This specificity is also apparent after hybridization, *in situ*, to sections of rat brain. Emulsion autoradiography revealed that, throughout the brain, hybridization was restricted to neuronal profiles and was essentially absent in white matter fiber tracts, meningies, blood vessels, and the neuropil (Figure 9). For example, a comparison of dark- and bright-field images of an emulsion autoradiogram of the dentate gyrus revealed

Figure 8. RNA blot analysis and *in situ* hybridization of synapsin I mRNA in rat brain. (A) RNA blot autoradiogram of synapsin I mRNA levels in different brain regions. Purified total rat brain RNA (3 μg) and RNAs prepared from various regions of brain were processed, separated by electrophoresis, blotted and hybridized as described in text. The strength of the hybridization signal obtained varied in different brain regions, with the highest signal in the RNAs from the dentate gyrus and the neocortex and the lowest in the RNA from the caudate nucleus. (B-C) X-ray autoradiograms of coronal sections of adult rat brain hybridized with ^{35}S-labeled synapsin I cDNA probes. In these sections, the strength of the hybridization signals revealed by *in situ* hybridization corresponded to the intensity of signals obtained by RNA blot analysis. Amy, central/lateral amygdala; CPu, caudate/putamen; Ctx, neocortex; DG, dentate gyrus; MS, medial septum; RB, total rat brain RNA. Blots were exposed to Kodak XAR-5 film for 4 days. Sections were exposed to Kodak XAR-5 film for 10 days. Scale bar; B and C, 1.5 mm.

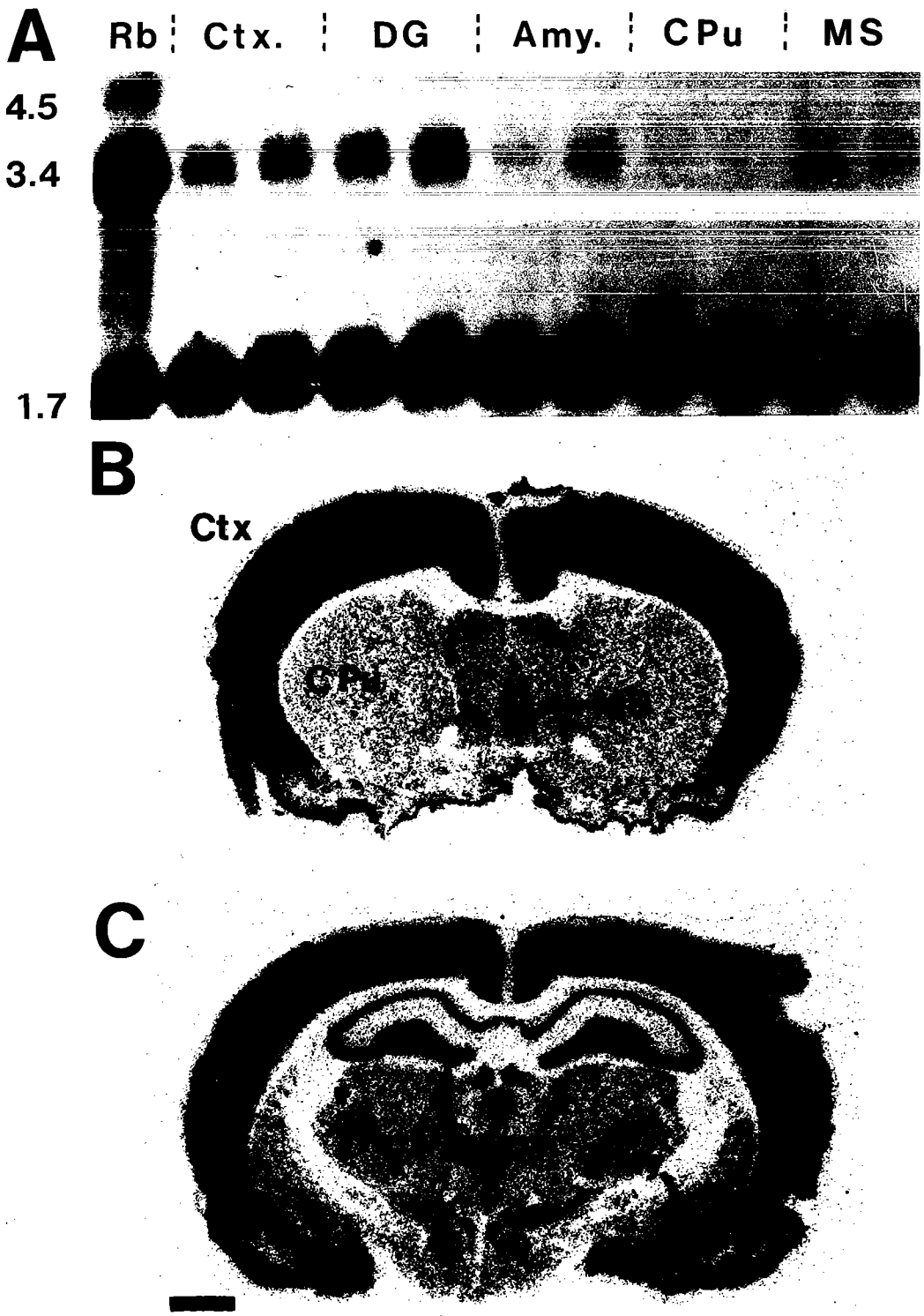
A
Rb
Ctx.
DG
Amy.
CPu
MS
4.5
3.4
1.7
B
Ctx
CPu
C

hybridization over the somata of granule cell and hilar neurons in this region (Figure 9A, B). Labeling was distributed evenly over neurons of the granule cell layer and appeared consistent along the entire length of the dentate gyrus. Examination of the cells of the hilus at high magnification showed labeling to be present over individual neuronal somata in this region (Figure 9C).

To ensure that labeling of sections was specific to synapsin I mRNA, some sections were co-incubated with a mixture of radioactively-labeled synapsin I cDNA probe and a 100-fold excess of unlabeled synapsin I cDNA probe. In all control sections, no detectable hybridization signals were obtained (data not shown).

Temporal and Spatial Distribution of Synapsin I Transcripts

To define the pattern of expression of the synapsin I gene during the development of the rat nervous system, the distribution and cellular localization of synapsin I mRNA were examined in the developing rat central nervous system from embryonic (E) day E14 through postnatal (P) day P21 by *in situ* hybridization. A series of (>5) *in situ* hybridization studies were conducted in coronal (Figures 8 and 9), parasagittal (Figures 10 and 11), and horizontal (Figures 11-15) planes of section. The hybridization signals were characterized as light (+), moderate (++), and high (+++), as estimated by visual comparisons of several autoradiographic films of sections hybridized to radioactively-labeled synapsin I cDNA probes of comparable specific activities. After visual inspection of autoradiographic signals, selected slides were processed for emulsion autoradiography to examine more precisely the cellular localization of synapsin I mRNA.

Mapping of Synapsin I mRNA Throughout the Embryonic Rat Central and Peripheral Nervous Systems

Synapsin I mRNA was detected in the nervous system by *in situ* hybridization from the earliest time points assayed in the embryonic period (by embryonic day 12-14).

Figure 9. Emulsion autoradiograms demonstrating specificity of synapsin I cDNA probes for neurons in the adult rat central nervous system. (A and B) Dark-field and bright-field photomicrographs of an emulsion autoradiogram of granule cell neurons of the dentate gyrus hybridized to synapsin I cDNA probes. Synapsin I hybridization is specific for neuronal profiles of the granule cell layer and hilar region of the dentate gyrus. (C) High magnification bright-field photomicrograph of an emulsion autoradiogram of cells of the hilar region of the dentate gyrus. Clusters of silver grains indicate hybridization to synapsin I probes is specific for neuronal somata and not glial components of the CNS. bv, blood vessel; DG, dentate gyrus; gl, glial cell; Hilar, dentate hilar neuron; Exposure time of the emulsion-coated sections was 2 weeks. Scale bars: A and B, 300 μm; C, 120 μm.

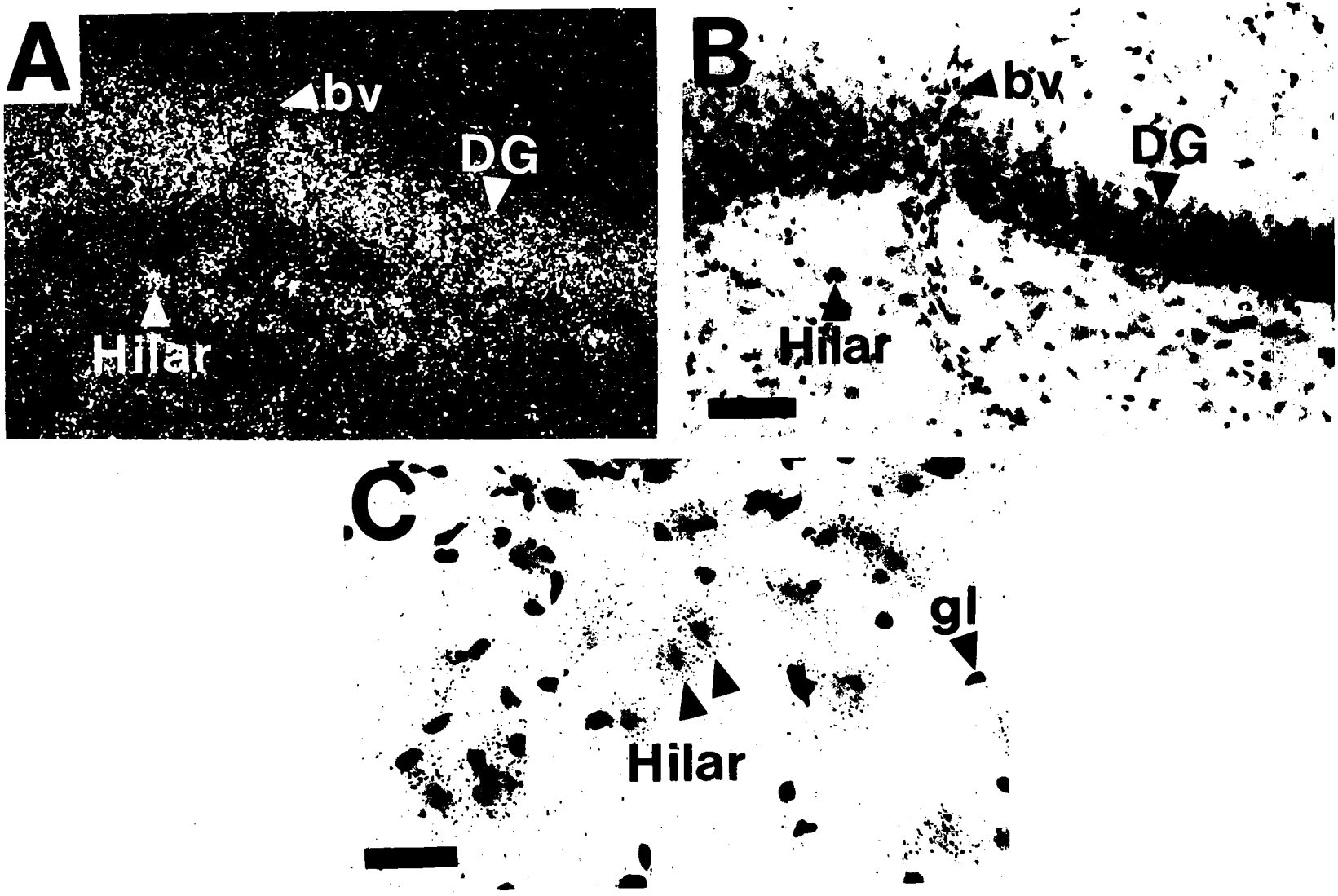
A
bv
DG
Hilar
B
bv
DG
Hilar
C
gl
Hilar

Already by this stage of development, synapsin I mRNA was expressed heterogenously throughout the central and peripheral nervous systems, and was most abundant in distinct nuclei of the developing Mes-, Met-, and Myelencephalon (Figure 10). By comparison, the Di- and Telencephalon displayed more moderate levels of synapsin I hybridization. In the central nervous system, areas high in synapsin I mRNA by E16 were the hypothalamic neuroepithelium, the anterior and intermediate thalamic neuroepithelium, the anterobasal nucleus, the pons, the medulla, as well as the developing spinal cord (Figure 10). Areas displaying moderate levels of synapsin I hybridization were the superior and inferior colliculus, the septum, the basal telencephalic plate, and the cortical neuroepithilium.

By embryonic day 14 through 16, synapsin I-specific hybridization was clearly apparent in various ganglia in the peripheral nervous system of the embryonic rat. Moderate levels of synapsin I hybridization were observed in the head of the rat in a region identified as the sphenopalatine ganglion. More peripherally, synapsin I hybridization was observed in moderate levels in the celiac and superior mesenteric ganglia of the gut, and at higher levels in the dorsal root ganglia and sympathetic trunk.

By embryonic day 19, hybridization of synapsin I cDNA probes to neurons forming distinct nuclei and recognizable tracts of cells in the rat central nervous system was notably more apparent (Figure 11). In the telencephalon, hybridization appeared high in the mitral cell layer of the olfactory bulb (Figure 11A), the CA3 field of the hippocampus (Figure 11B, E), the cortical plate (Figure 11B), the piriform cortex (Figure 11D), and the lateral septum (Figure 11B). Moderate synapsin I hybridization signals were detected in the cortical subplate (Figure 11E) and in the medial septum (Figure 10C). Light hybridization signals were observed in the caudate nucleus and putamen (Figure 11C). In the diencephalon, labeling of synapsin I mRNA was high in the thalamus (Figures 11C, F), the hypothalamus (Figure 11F) and the posterior pituitary (Figure 11E). In the midbrain, synapsin I hybridization signals were high in the pontine nucleus (Figure 11G), while the brainstem nuclei such as the superior and inferior colliculi displayed moderate

Figure 10. Expression of synapsin I mRNA in parasagittal sections of whole rat embryos. X-ray autoradiograms of sections of E14 and E16 embryos hybridized to ^{35}S-labeled synapsin I cDNA probes. AB, anterobasal nucleus; Bt, basal telencephalic plate; CB, cerebellum; Celiac, celiac ganglia; Ctx, neocortex; Di, Diencephalon; DRG, dorsal root ganglia; H, hypothalamus; IC, inferior colliculus; Mes, mesencephalon; Met, metencephalon; Myel, myelencephalon; SC, superior colliculus; Sept, septum; SMes, superior mesenteric ganglia; Sphpal, sphenopalatine ganglia; Sp. cord, spinal cord; Symp, sympathetic trunk; Tel, telencephalon; Th, thalamus.

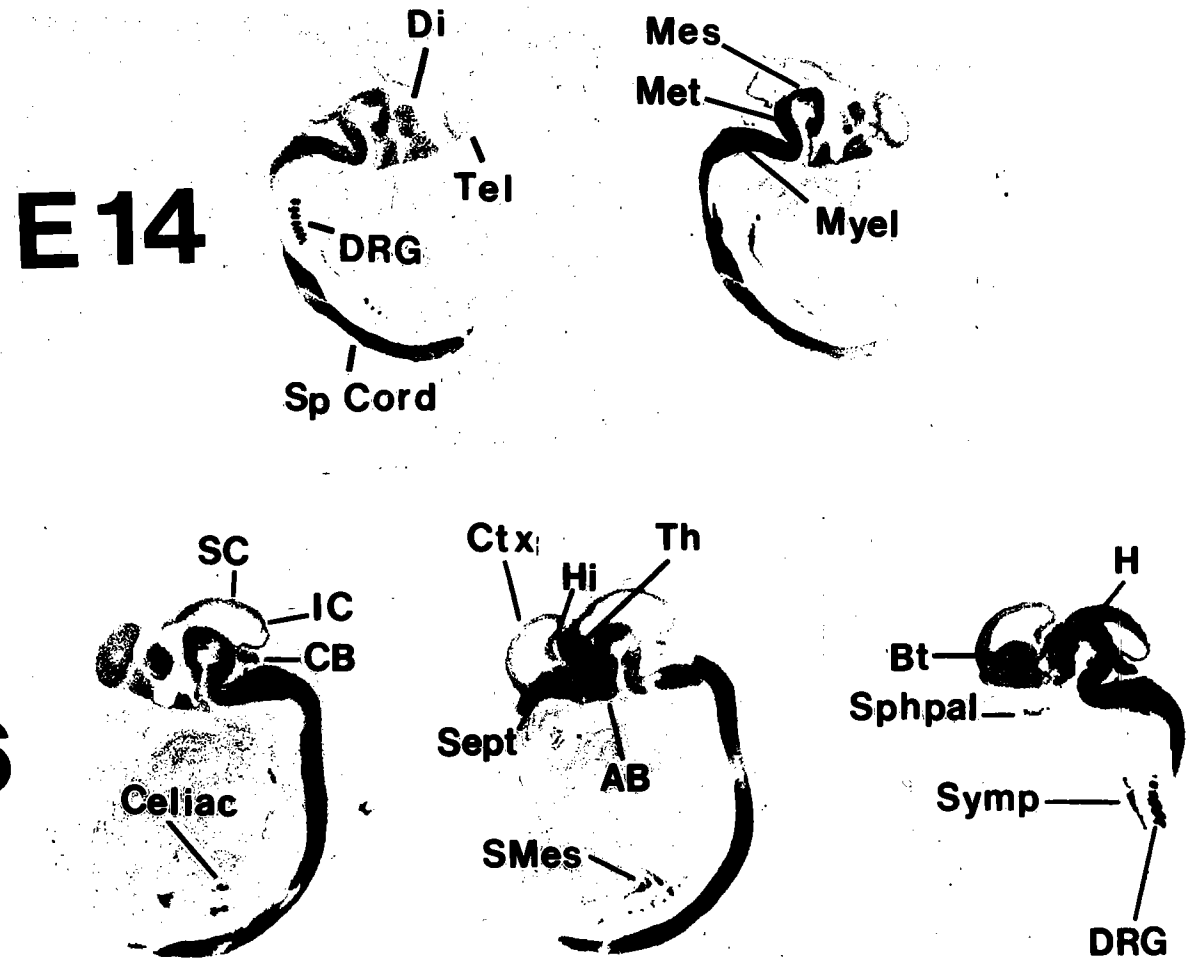
E14
Di
Tel
DRG
Sp Cord
Mes
Met
Myel
E16
SC
IC
CB
Celiac
Ctx
Hi
Th
Sept
AB
SMes
H
Bt
Sphpal
Symp
DRG

Figure 11. Expression of synapsin I mRNA in E19 rat head by *in situ* hybridization. X-ray autoradiograms of horizontal (A-D) and parasagittal (E-F) sections hybridized to ^{35}S-labeled synapsin I cDNA probes. Cb, cerebellum; CPu, caudate/putamen; CxP, cortical plate; CxS, cortical subplate; H, hypothalamus; Hi, hippcampus; LS, lateral septum; MS, medial septum; OB, olfactory bulb; Pir, piriform cortex; Pit, pituitary; Pons, pontine nuclei; RGn, retinal ganglion cell layer; SC, superior colliculus; Sphpal, sphenopalatine ganglion; Th, thalamus. Sections were exposed to Kodak XAR-5 film for 10 days.

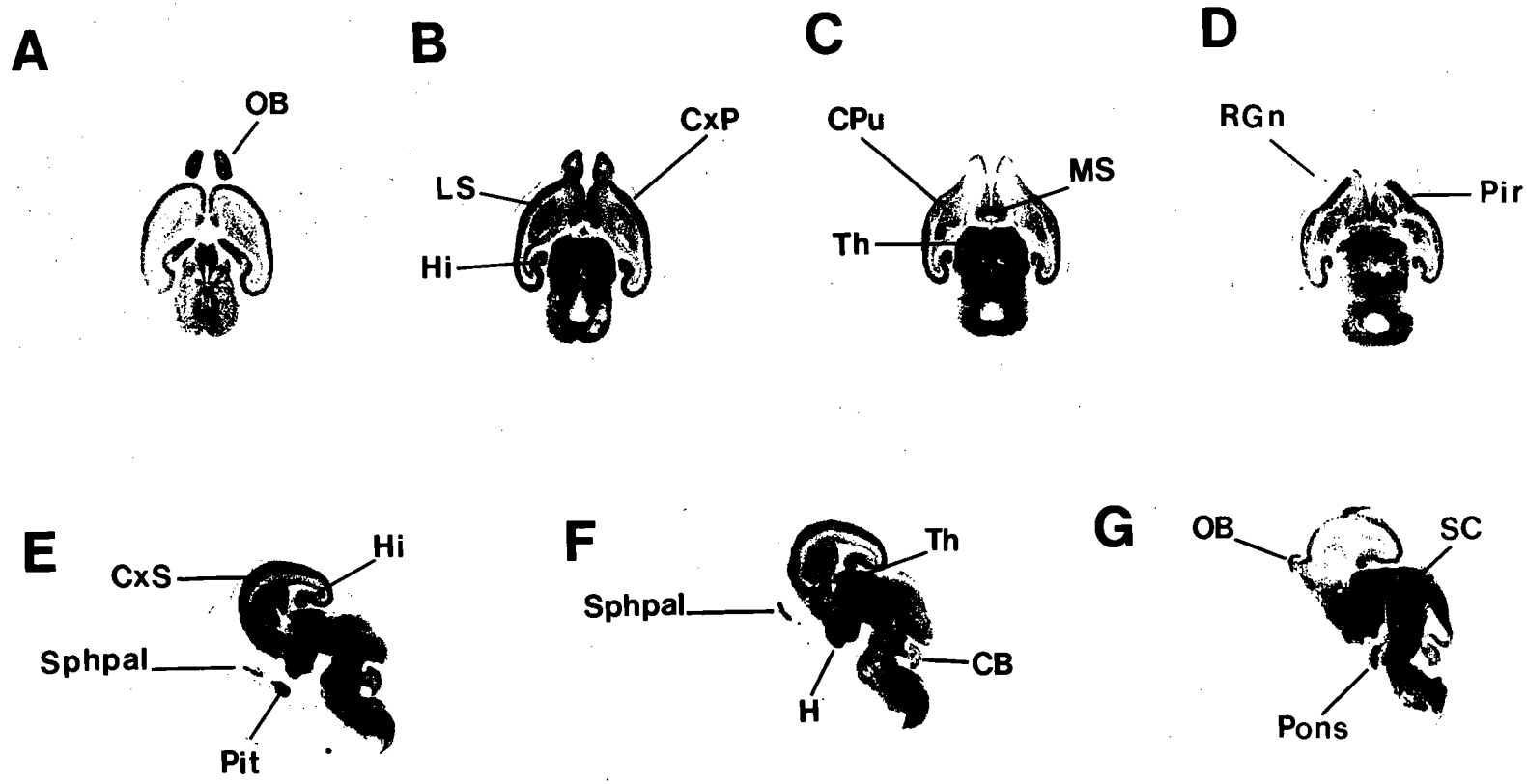
A
OB
B
CxP
LS
Hi
C
CPu
MS
Th
D
RGn
Pir
E
Hi
CxS
Sphpal
Pit
F
Th
Sphpal
CB
H
G
OB
SC
Pons

levels of synapsin I mRNA (Figure 11G). In the developing cerebellum, very light, if any, labeling of synapsin I mRNA was observed (Figure 11F).

Hybridization to synapsin I cDNA probes was observed in regions of the rat head outside of the brain. This hybridization signal was primarily restricted to cells of the sphenopalatine ganglia (Figures 11E, F) and to the retinal ganglion cells (Figure 11D) located in the innermost aspect of the retinal lamination.

Mapping of Synapsin I mRNA Throughout the Postnatal Development of the Rat Brain

In situ hybridization to synapsin I mRNA at various stages of the postnatal development of the rat brain (Figure 12) revealed similiar patterns of hybridization to those observed in the adult (see Chapter V). As predicted by the pattern of expression at embryonic day 19, synapsin I transcripts were already widely distributed in the rat brain at postnatal day 0 (P0; day of birth). Furthermore, in a number of brain regions, the level of expression of synapsin I mRNA observed at P0 were comparable to those seen in the adult rat brain, with the noteworthy exceptions (see below). The expression of the synapsin I gene was particularly high in the mitral cells of the olfactory bulb (Figures 12A, D), the cortex (including the entorhinal, piriform, cingulate and frontal corticies, Figures 12A-F), the hippocampus (CA1-CA3 sectors, Figures 12A-F), the amygdala (Figure 12C), and the red nucleus (Figure 12D). Other areas high in synapsin I hybridization not depicted in Figure 12 are; the olfactory tubercle, paraventricular thalamic nuclei, the medial habenula, the ventromedial nucleus of the hypothalamus, the substantia nigra compacta, and the pontine nucleus. Synapsin I mRNA was expressed at lower levels in medial septum (Figures 12A-F), the bed nucleus of the stria terminalis (Figure 12D), the parafascicular nucleus (Figure 12F), the caudate nucleus (Figure 12A-F), and the putamen (Figure 12A-F). Areas not shown which displayed lower hybridization signals are; the diagonal band of Broca, dorsal lateral geniculate nucleus, the lateral habenula, the paraventricular

Figure 12. *In situ* hybridization of synapsin I mRNA in horizontal sections of postnatal developing rat brain at the level of the medial septum. (A-F) X-ray autoradiograms of sections hybridized to ^{35}S-labeled synapsin I cDNA probes. BST, basal nucleus of the stria terminalis; CA, CA fields of the hippocampus; Cb, cerebellum; CPu, caudate-putamen; Ctx, neocortex; DG, dentate gyrus; EC, entorhinal cortex; Gl, glomerular layer of the olfactory bulb; LS, lateral septum; M, mitral cell layer of the olfactory bulb; MS, medial septum; OB, olfactory bulb; PF, parafasicular nucleus; Th, thalamic nucleus. Sections were apposed to Kodak XAR-5 film for 10 days.

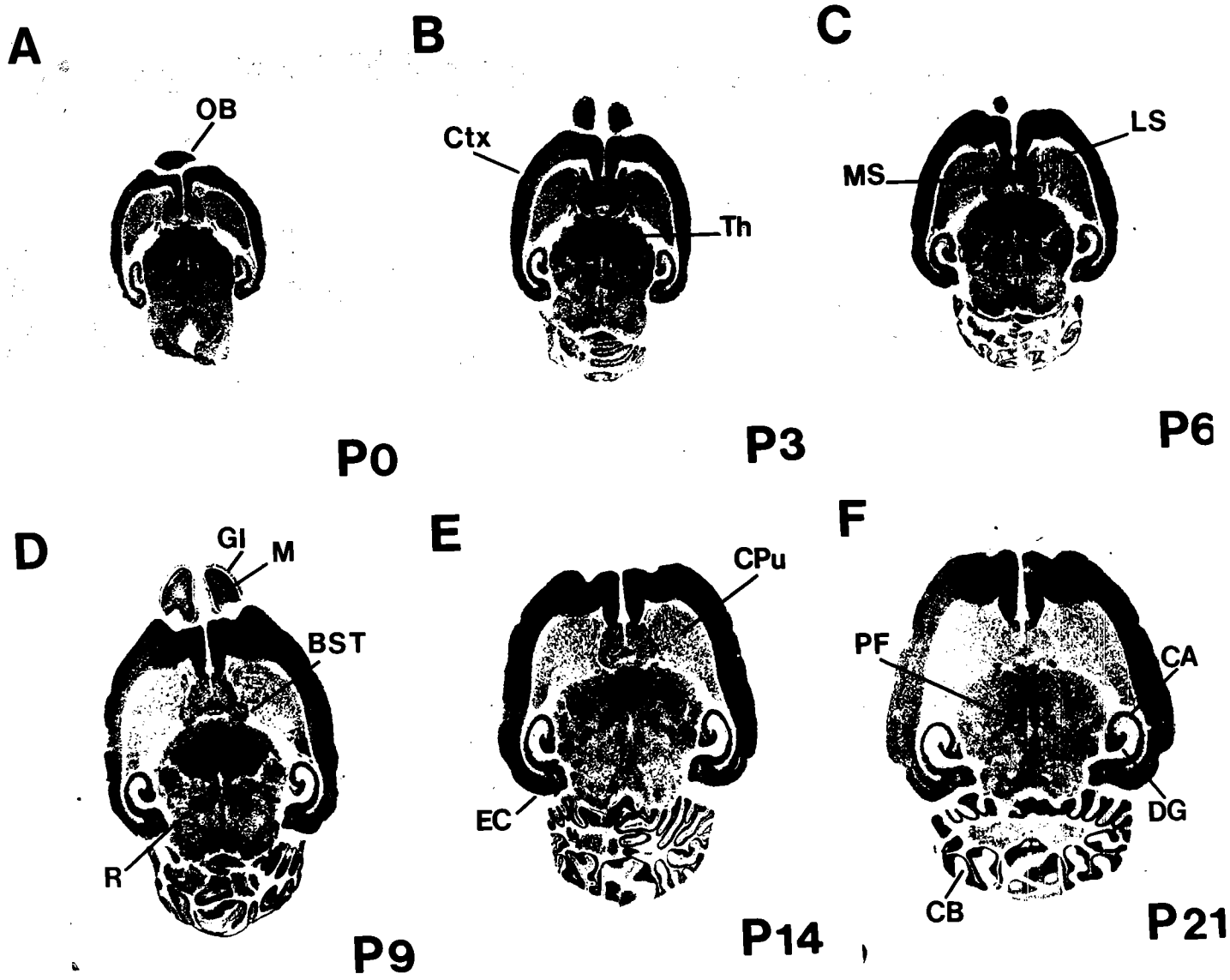
A
OB
P0
B
Ctx
Th
P3
C
LS
MS
P6
D
Gl
M
BST
R
P9
E
CPu
EC
P14
F
PF
CA
DG
CB
P21

hypothalamic nucleus, and the superior and inferior colliculi.

In certain areas, the overall patterns of synapsin I mRNA expression underwent extensive remodeling during the first two-to-three postnatal weeks. For example, in the postnatal development of the lateral septum and the anterior portions of the thalamus, synapsin I hybridization intensity decreased dramatically between postnatal days 3 and 14 (Figures 12B-E). By contrast, the intensity of synapsin I hybridization signal increased slowly over the entire developing cerebellum from birth and, after postnatal day 14, hybridization to synapsin I probes increased dramatically in the developing granule cell layer of the cerebellum (Figures 12B-F). Likewise, the intensity of hybridization to synapsin I probes increased in the dentate granule cells of the developing hippocampus in the postnatal period. Here, the hybridization signal in the hilus and dentate granule cell layer increased rapidly to peak levels by postnatal day 6. From postnatal day 6 and onward, hybridization remained at high, near adult levels in the developing dentate granule cell layer, while synapsin I hybridization fell dramatically in the hilar region of dentate gyrus (see below and Figure 14).

Expression of the Synapsin I Gene in the Postnatal Development of the Cerebellum and Hippocampus

The main histogenetic events in the development of the rat cerebellum and hippocampus have been extensively characterized (Altman and Das, 1965, 1966; Altman, 1972a,b,c; Bayer and Altman, 1974; Schlessinger et al., 1975; Stanfield and Cowan, 1979; Bayer, 1980; Gaarskjaer, 1981, 1985; Crespo et al., 1986). These studies have shown that granule cells in the developing rat cerebellum and hippocampus undergo the processes of neurogenic and synaptogenic differentiation postnatally in the rat brain. Due to their well characterized postnatal development and simple cytoarchitecture, the rat cerebellum and hippocampus were chosen as *in vivo* model systems to study the temporal and spatial appearance of synapsin I mRNA. Specifically, to correlate the onset of expression of the

synapsin I gene with the state of differentiation of particular types of neurons in the developing rat central nervous system, *in situ* hybridization was performed on serial sections of rat brain from animials ranging in age from embryonic day 19 to postnatal day 21.

Temporal Onset of Expression of the Synapsin I Gene During the Postnatal Development of the Rat Cerebellum

The overall changes in the distribution and intensity of synapsin I hybridization in the developing rat cerebellum are illustrated in Figure 13. The *in situ* localization of synapsin I mRNA in young cerebella (P6) showed that synapsin transcripts were present at high levels in cells located at the boundry to the immature internal granule cell layer, and in lower, but still detectable, levels in the immature internal granule cell layer itself (Figure 13A). High power bright-field microscopy of this region revealed that the majority of silver grains were concentrated over cells of the Purkinje cell layer (Figure 13B). No synapsin I-specific hybridization signal was observed in the external granule cell layer or in the primative molecular layer. During this period, Purkinje cells are beginning to differentiate beneath the thin underdeveloped molecular layer, undifferentiated granule cells reside in the external granule cell layer and the mature layered structure of the cerebellum has not yet formed.

From postnatal day 11 through 14, synapsin I-specific hybridization throughout the cerebellum was more intense than at earlier time points, with the most notable increase observed in the cells of the developing internal granule cell layer (Figures 13C-F). Additionally, during this period of development, hybridization to synapsin I cDNA probes was observed in the external granule cell layer of the cerebellum. Within the external granule cell layer, synapsin I mRNA was primarily detected in cells immediately adjacent to the molecular layer. Cells in this region of the external granule cell layer make up the premigratory zone, the portion of the external granule cell layer where undifferentiated

Figure 13. Low magnification dark-field photomicrographs of emulsion autoradiograms of cells of the developing rat cerebellum hybridized to ^{35}S-labeled synapsin I cDNA probes. EGL, external granule cell layer; IGL, internal granule cell layer; ML, molecular layer; PCL, Purkinje cell layer. Emulsion-coated sections were exposed for 2 weeks.

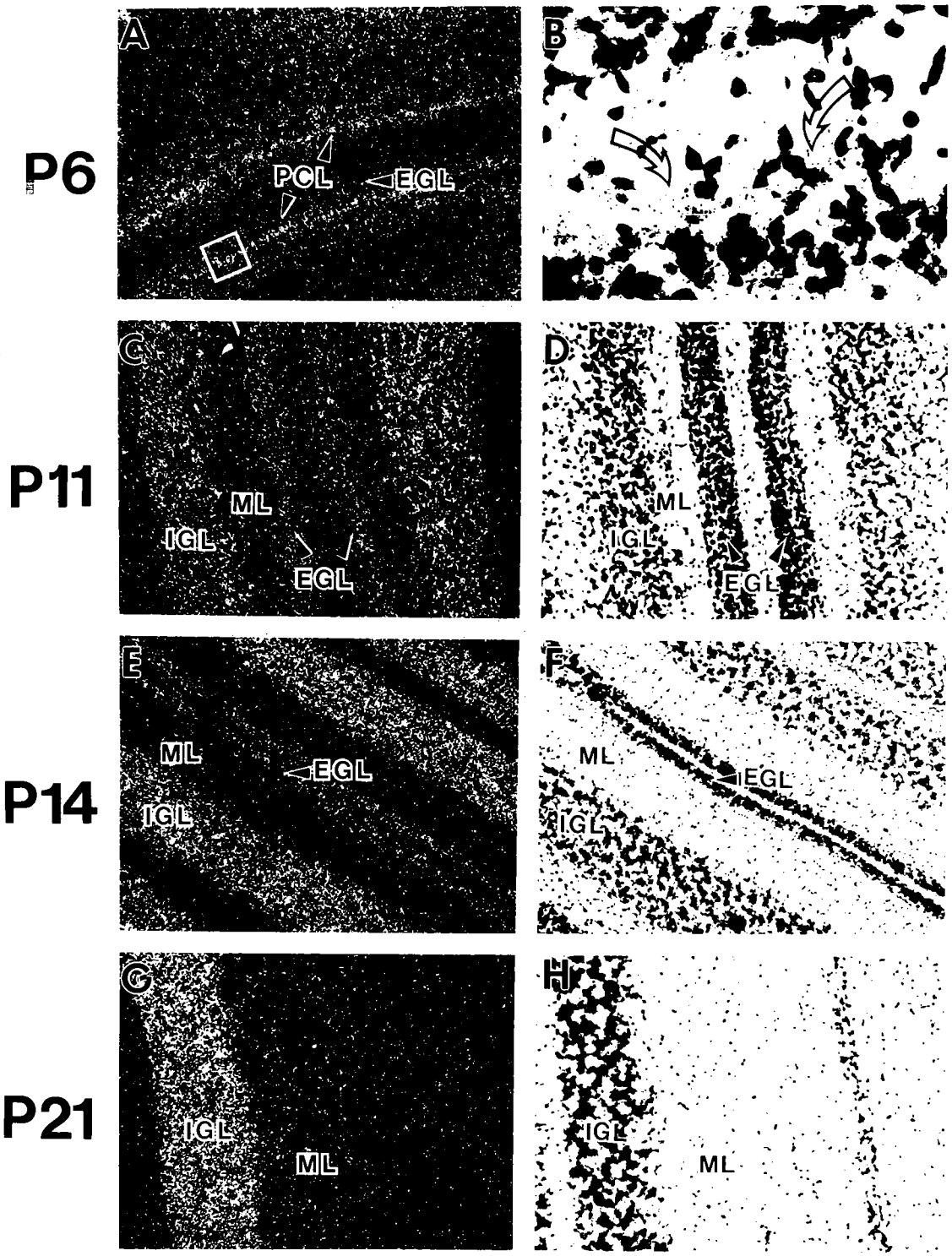
P6
A
PCL
EGL
B
P11
C
ML
IGL
EGL
D
ML
IGL
EGL
P14
E
ML
EGL
IGL
F
ML
EGL
IGL
P21
G
IGL
ML
H
IGL
ML

granule cell precursors begin to undergo the process of neuronal differentiation. However, no synapsin I-specific hybridization signal was observed in the overlying cells of the proliferative zone, the region of the external granule cell layer comprised entirely of undifferentiated, mitotic stem cells. At postnatal day 14, synapsin I gene expression continued in the premigratory zone of the external granule cell layer, although, the width of this region has decreased as cells within this zone continue to differentiate and migrate into the internal granule cell layer (Figures 13E, F).

From postnatal day 21 onward, synapsin I gene expression was detectable in the internal granule and the Purkinje cell layers, but not in the external granule cell layer, as only remnants of this cell layer remain at this time in the development of the rat cerebellum (Figures 13G, H). In accord with prior analyses (Haas and DeGennaro, 1988), we found the synapsin I-specific hybridization signal increased significantly at postnatal day 21 in the internal granule cell layer of the developing rat cerebellum, coinciding with a population of granule cells undergoing a particular phase of differentiation, i.e., synaptogenesis (Figure 13G).

Temporal Onset of Expression of the Synapsin I Gene During the Postnatal Development of the Rat Hippocampus

In the fetal rat brain (E19), hybridization to synapsin I probes was observed in all subregions of the hippocampus (Figure 14). In particular, hybridization was high in the CA3 field of the hippocampus, while hybridization in the CA1 zone is more moderate and scattered (Figure 14A). In the zone which is to become the hilus (the region where dentate granule neurons originate in development), the synapsin I-specific hybridization signal was low and diffusely scattered (Figure 14A). At this stage of development the laminar structure of the dentate gyurs has not formed as the undifferentiated granule cell precursors still reside in the zone which is to become the hilus.

In the neonatal hippocampus (P0 and P3), while the overall pattern of hybridization

Figure 14. Expression of synapsin I mRNA in horizontal sections of the developing rat hippocampus. (A-F) Dark-field photomicrographs of emulsion-coated sections of the developing rat hippocampus (E19 - P21) hybridized to ^{35}S-labeled synapsin I cDNA probes. CA3; CA3 field of the hippocampus; DG, dentate granule cell layer; H, hilar region. Emulsion-coated sections were exposed for 2 weeks.

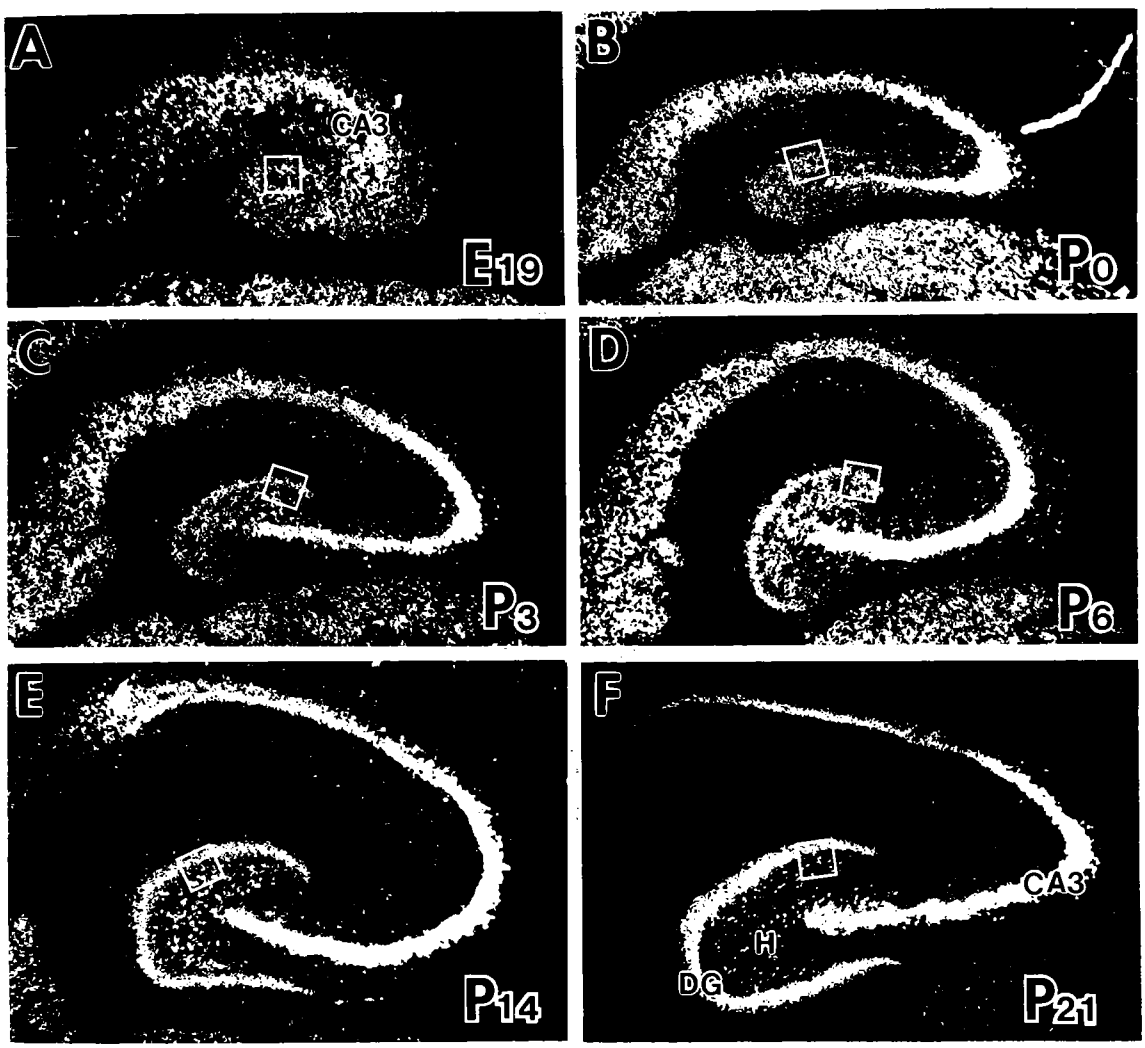
A
CA3
E19
B
P0
C
P3
D
P6
E
P14
F
CA3
H
DG
P21

to synapsin I probes remained similar to that seen at fetal time points, the synapsin I-specific hybridization signal changed in particular subregions. For example, hybridization in hippocampal subfield CA1 displayed a thinner, more concentrated signal than at earlier time points, while high levels of synapsin I-specific hybridization were relatively unchanged in CA3 (Figures 14B,C). Also, in the dentate gyrus, synapsin I-specific hybridization signal was now observed in the developing ectal blade of the dentate gyrus, as well as in the cells of the hilar region (Figures 14B,C). In these regions, emulsion autoradiography revealed hybridization over the somata of individual granule cell neurons in the hilus and the ectal blade of the developing dentate gyrus. In fact, examination of the cells of the hilus and the ectal dentate gyrus at high magnification revealed silver grains deposited over a variety of granule cell types in this region, as well as over the larger polymorphic hilar neurons (Figures 15B,C). More specifically, synapsin I-specific labeling was present over mature, differentiated granule cell neurons which reside in the superficial aspects of the granule cell layer of the dentate gyrus (superficial dentate gyrus) as well as over spindle-shaped, immature differentiating granule cells situated in the more basal portions of the dentate granule cell layer (basal dentate gyrus) and in the hilus. No appreciable labeling was observed over undifferentiated precursors or glial cells in these regions.

By the end of the first week of postnatal development, approximately between postnatal days 6 and 9, hybridization to synapsin I probes changed dramatically in the dentate gyrus and hilar region of the hippocampus (Figure 14). On or around postnatal day 6, coinciding with the peak period of granule cell neurogenesis, a strong burst of hybridization to synapsin I probes was observed in the hilar region of the dentate gyrus (Figure 14D). This dramatic increase in synapsin I-specific hybridization signal in the hilus was accompanied by a parallel increase in hybridization signal in the granule cell layer of the dentate gyrus (Figure 14D). In fact, at this developmental time point, synapsin I-specific hybridization signal reached its high, near adult level in the developing dentate

granule cell layer (Figures 12, 14D-E, and 15D-E). High magnification photomicrographs revealed accumulations of silver grains deposited over individual hilar neurons and the majority of granule cells in the hilus and the dentate gyrus proper (Figure 15D). As at earlier stages in the neurogenic development of the granule cell layer of the dentate gyrus, high-to-intense hybridization signal was observed over mature, differentiated granule cells in the superficial dentate gyrus, and at lower, but still high levels in the immature spindle-shaped differentiating granule cells in the basal dentate gyrus.

By postnatal days 14 through 21, the burst of synapsin I-specific hybridization in the hilus has subsided, as the peak period of neuronal differentiation of granule cells in the hilar region of the dentate gyrus has passed. As evidenced by heavy accumulations of silver grains, intense levels of expression of synapsin I mRNA were now observed in individual large polymorphic neurons in the hilar region (Figures 14E and 15E) and mature, differentiated granule cells in the superficial dentate gyrus (Figure 15E). Additionally, during this period of hippocampal development, elevated levels of synapsin I-specific hybridization were now observed in the more intermediate and basal aspects of the developing dentate gyrus. Hybridization to immature, differentiating granule cells was also evident still in the basal dentate gyrus.

Discussion

Several recent studies have postulated a role for the synapsins in the development of the nervous system (Han et al., 1991; Lu et al., 1992). Taken together, these studies suggest that these proteins may play a causal role in synaptogenesis by promoting synapse differentiation and the functional maturation of developing synapses in the nervous system. To better understand the relationship between synapsin I and particular cellular events during development *in vivo*, *in situ* hybridization histochemistry was used to localize the

Figure 15. High magnification autoradiographic location of synapsin I mRNA in regions boxed in Figure 7. Emulsion autoradiograms of cells of the developing rat dentate gyrus hybridized to ^{35}S-labeled synapsin I cDNA probes. DG, dentate granule cell layer; H, hilar region.

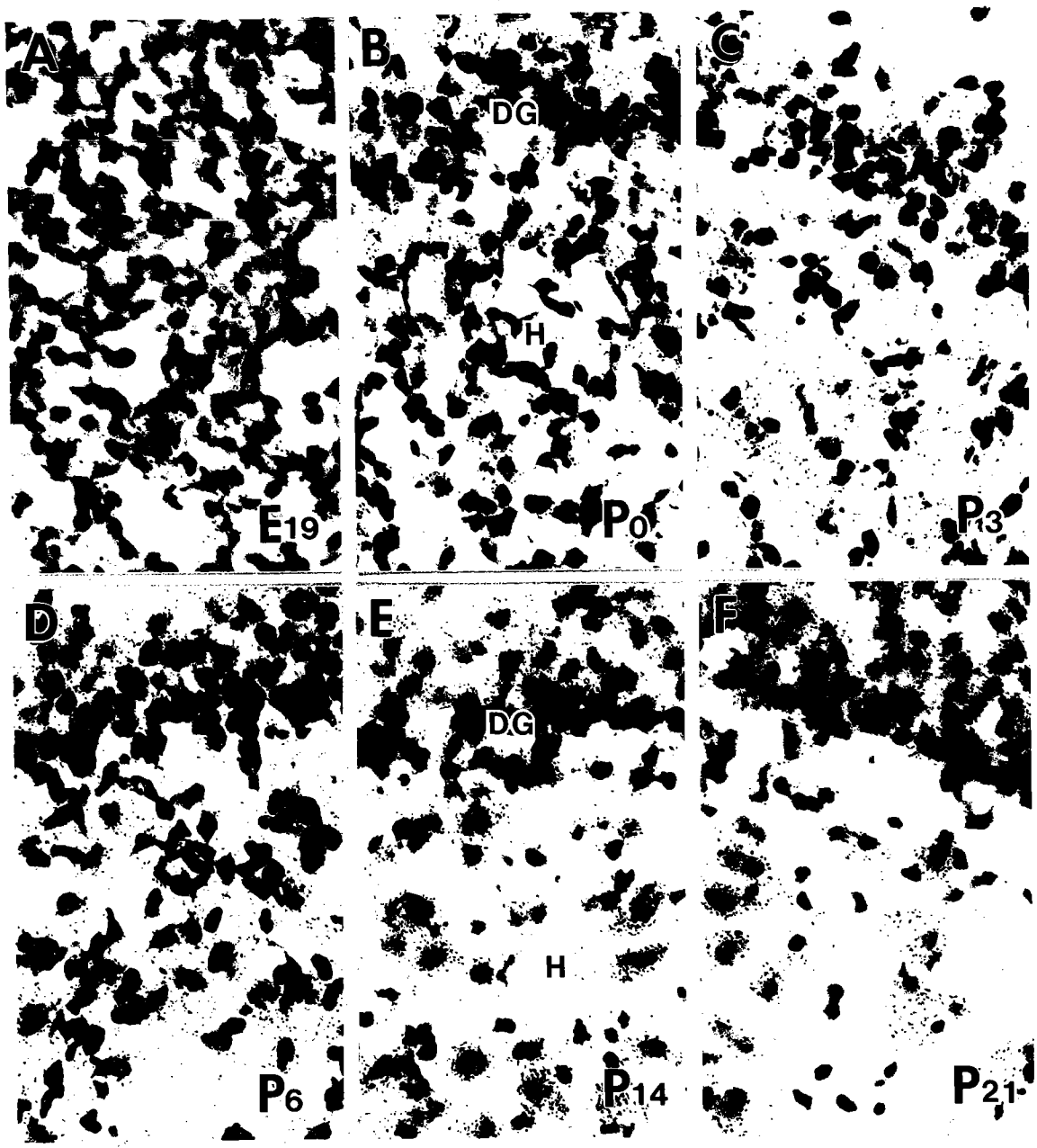
A
B
DG
H
C
E19
P0
P13
D
E
DG
H
F
P6
P14
P21

expression of the synapsin I gene throughout the rat central and peripheral nervous systems through embryonic and postnatal development. These studies were then extended to determine precisely the temporal onset of expression of the synapsin I gene during nervous system development. The results present a detailed description of the spatial distribution of synapsin I mRNA during the development of the entire central and peripheral neuraxis, as well as provide insight into the temporal onset of expression of the synapsin I gene in relation to the state of differentiation of particular types of neurons in the developing rat central nervous system.

Localization of Synapsin I mRNA

Synapsin I cDNA probes revealed specific patterns of hybridization in different regions of the rat brain by RNA blot analysis and *in situ* hybridization. By RNA blot analysis, synapsin I cDNA probes recognized exclusively synapsin I mRNAs of 3.4kb and 4.5kb. The intensity of synapsin I mRNA hybridization varied in RNA prepared from different regions of the rat brain, suggesting differential levels of expression of synapsin I mRNAs in these areas. By *in situ* hybridization, similiar patterns of hybridization emerged, and the intensity of synapsin I mRNA labeling in discrete subregions of the rat brain revealed by *in situ* hybridization corresponded with the strength of the hybridization signals obtained by RNA blot analysis (Figure 7). Synapsin I mRNA labeling was clearly neuron-specific (Figure 8), consistent with previous immunocytochemical and limited *in situ* hybridization data showing that synapsin I protein (De Camilli et al., 1983a,b; Huttner et al., 1983) and mRNA (Haas and DeGennaro, 1988) are present only within neurons in the central nervous system.

Synapsin I mRNA in the Embryonic and Postnatal Nervous System

The *in situ* hybridization data presented clearly indicate that the synapsin I gene is expressed in nervous tissue throughout the various stages of the development of the rat

embryo from the earliest embryonic time point examined (E12-data not shown). In general, the regional levels of synapsin I mRNAs were high in utero, although synapsin I cDNA probes revealed specific patterns of hybridization in different regions of the embryonic rat central and peripheral nervous systems. For example, by embryonic day 14-16, areas notably abundant in synapsin I mRNA were the hypothalamic neuroepithelium, the anterior and intermediate thalamic neuroepithelium, the anterobasal nucleus, as well as the spinal cord.

Later in the development of the nervous system, by embryonic day 19 - postnatal day 0 (day of birth), more subtle differences in the levels of synapsin I mRNA expression could be observed. Through this period of development, an abundance of synapsin I mRNA was found in the CA3 field of the hippocampus, the mitral cell layer of the olfactory bulb, the piriform cortex, and the posterior pituitary (at E19), however, other areas notably abundant in synapsin I mRNA at this stage in development were the thalamus, the hypothalamus, the lateral septum, and the developing neocortex. Together with the recent morphological and physiological studies by Han et al. (1991) and Lu et al. (1992), these data can be taken as strong indication for a role of the encoded protein in very early nervous system development.

During postnatal development, the appearance of synapsin I protein in the neuropil coincides with the peak period of synapse formation throughout the forebrain and cerebellum (Lohman et al., 1978; Mason, 1986; Moore and Bernstein, 1989). Data presented here reveals that, from the earliest stages of the postnatal development of the rat brain, the distribution of synapsin I mRNA is remarkably similiar to the pattern of hybridization observed in the adult (Figure 12 and see Chapter V, Figure 16). The fact that high levels of synapsin I mRNA are already present by P0 (the day of birth) throughout most of the developing rat forebrain, and by postnatal days 6 - 11 in the Purkinje, and internal and external granule cell layers of the developing cerebellum, suggests that the temporal onset of synapsin I gene expression precedes the process of synaptogenesis,

which occurs mainly between postnatal days 7 - 30 in the developing forebrain (Aghajanian and Bloom, 1967), and between postnatal days 18 - 30 in the developing rat cerebellum (Altman, 1972c). A correspondence of these results with those obtained from previous studies of the expression of synapsin I protein throughout the development of the rat brain is not immediately evident, however. For example, synapsin I protein levels, as assessed by endogenous phosphorylation (Lohman et al., 1978) and *in vitro* translation (DeGennaro et al., 1983) assays, are low in the brains of newborn rats, yet the results presented here show clearly that synapsin I mRNAs are abundant throughout the entire neuraxis by this stage in development. Although caution must be exercised when comparing differences between levels of mRNA localized *in situ*, and protein generated or modified *in vitro*, the discrepancy between mRNA and protein levels opens the possibility of post-transcriptional control of synapsin I gene expression. In this regard, more focused studies examining in detail the relative levels of synapsin I mRNA and protein present in the somata and presynaptic terminal fields of developing and adult neurons will be necessary to decipher at what further level synapsin I gene expression is regulated.

Correlation of Synapsin I Gene Expression with Neuronal and Synapse Differentiation in the Developing Rat Central Nervous System

When synapsin I cDNA probes were used for *in situ* hybridization on sections of whole rat embryos, synapsin I mRNAs were detected heterogenously throughout the central and peripheral nervous systems from the earliest time points assayed (see Figure 10). Thus, to link the onset of synapsin I gene expression to particular cellular events in the development of the nervous system, it was necessary to study a population of neurons whose birth and maturation occured later in development, preferably occuring during the postnatal period. As *in vivo* model systems, the granule cell neurons of the developing cerebellum and hippocampus meet these criteria; the cerebellum developing primarily between postnatal days 5 and 21, and the hippocampus between embryonic day 17 and

postnatal day 14. Therefore, to decipher the temporal onset of expression of the synapsin I gene in development, we performed *in situ* hybridization histochemistry with radioactively-labeled synapsin I cDNA probes on horizontal sections of postnatal rat cerebella and embryonic and postnatal rat hippocampus.

Correlation of Synapsin I Gene Expression with Neuronal and Synapse Differentiation in the Developing Rat Cerebellum

The neurogenesis and morphogenesis of the cerebellum in the developing rodent central nervous system has been extensively studied and characterized (Altman and Das, 1966; Altman, 1972a,b,c). These studies have shown that cells in the rat cerebellum undergo the processes of neurogenic and synaptogenic differentiation postnatally. The adult rat cerebellar cortex is composed of three principle layers: (1) a superficial cell-free molecular layer composed of a dense plexus of fiber processes, (2) a thick internal granule cell layer (IGL), and at the interface between the two, (3) a single-cell-thick layer of Purkinje cells. At birth (P0), however, the composition of the cerebellar cortex differs from that of the adult in that there exists a fourth layer of cells, the external granule cell layer (EGL), which is composed primarily of small, darkly staining, often mitotic, cells. At this stage of development, directly beneath the external granule cell layer resides a thin underdeveloped molecular layer, and then a layer of undifferentiated Purkinje cells, several cell layers thick, which merge with the underlying internal granule cell layer.

In the postnatal development of the cerebellum, the Purkinje cells are the first cell population to differentiate. By postnatal day 6 undifferentiated Purkinje cell precursors stacked 2-3 cells deep in the Purkinje cell layer begin to differentiate directly beneath the still very thin, underdeveloped molecular layer (Altman and Das, 1966; Altman, 1972b). At this stage of development the external granule cell layer is composed primarily of undifferentiated granule cells and the layered structure of the cerebellum has not yet formed. As development proceeds, the Purkinje cell layer decreases in thickness until

about postnatal day 20 when the Purkinje cells assume their normal distribution in a single cell layer positioned at the interface between the molecular and internal granule cell layers. The beginning of the development of the internal granule cell layer coincides with the development of the Purkinje cell layer. From this stage in development, granule cells in the premigratory zone of the external granule cell layer (inner 2/3) differentiate, become motile, and migrate through the molecular layer, to the internal granule cell layer (Atman and Das, 1966; Altman, 1972a,c). This process of differentiation and migration continues resulting in the dissolution of the external granule cell layer until only vestiges of it remain at postnatal day 20. By postnatal day 20 the superficial molecular layer and the internal granule cell layer have essentially assumed their adult appearance.

The *in situ* hybridization data presented here revealed two phases of synapsin I gene expression in the developing rat cerebellum. First, the temporal onset of expression of the gene (the onset of appearance of synapsin I transcripts) coincides with the period of neurogenesis, between postnatal days 5 and 21 of rat cerebellar development. The heavy accumulation of silver grains present over individual Purkinje cell bodies in young cerebella (P6) reflects the production of synapsin I mRNA concommitant with the period of neurogenic differentiation of these cells (Figures 13A, B). At this stage of development, no synapsin I-specific hybridization signal was observed in the external granule cell layer, and very little in the internal granule cell layer.

From postnatal day 11, synapsin I mRNA was localized to both the internal and external granule cell layers, as well as in the Purkinje cell layer. Here, the pattern of hybridization observed is consistent with the onset of the expression of synapsin I mRNA occuring during the period of neurogenic differentiation of granule cells in the external granule cell layer of the developing cerebellum. At postnatal day 11 synapsin I mRNA was detected in the premigratory zone of the external granule cell layer (a zone comprised of differentiating granule cell neurons) but not in the overlying proliferative zone (the region of the external granule cell layer comprised entirely of undifferentiated, mitotic stem cells).

The width of the synapsin I-specific hybridization signal in the external granule cell layer is greatest at postnatal day 11 as a large number of precursor cells in this region become postmitotic and begin to differentiate (Figures 13C, D). By postnatal day 14, the width of the synapsin I-specific hybridization signal in the external granule cell layer is thinner, as a number of differentiated granule cell neurons have exited from this zone and migrated to their final position within the internal granule cell layer (Figures 13E, F). Additionally, a general increase of synapsin I mRNA was detected in the internal granule cell layer as the number of granule cell neurons residing in this cell layer increases through this period of cerebellar development. Subsequently, by postnatal day 21, synapsin I hybridization in the external granule cell layer has disappeared as only remnants of this region exist by this point in development. Therefore, through postnatal development of the rat cerebellum, the temporal onset of synapsin I gene expression is consistent with the neurogenic pattern of differentiation of the Purkinje and granule cell neurons.

By postnatal day 21, the neurogenic and morphogenic development of the cerebellum has ended and the internal granule cell layer, the Purkinje cell layer, and the molecular layer have essentially assumed their adult appearance. From this stage of development, *in situ* hybridization revealed the second phase of synapsin I gene expression in the rat cerebellum. In accord with prior Northern blot and *in situ* hybridization analyses (Haas and DeGennaro, 1988), a sharp increase in the synapsin I-specific hybridization signal was observed in the internal granule cell layer of the developing rat cerebellum (Figures 12 and 13). By emulsion autoradiography, examination of the cells of the internal granule cell layer at high magnification revealed a heavy, clustered accumulation of silver grains over individual granule cell neurons (data not shown). As detailed by Haas and DeGennaro (1988), the pattern and intensity of synapsin I-specific hybridization in the internal granule cells at this stage in their development is consistent with an increase in synapsin I mRNA production during the period of synaptogenic differentiation of the granule cell parallel fibers on the dendrites of cerebellar Purkinje cells and with the

accumulation of synapsin I protein in the molecular layer of the cerebellum during this same phase of cerebellar development (De Camilli et al., 1983; Mason et al., 1986).

Correlation of Synapsin I Gene Expression with Neuronal and Synapse Differentiation in the Developing Rat Hippocampus

As in the cerebellum, the cytogenesis and morphogenesis of the hippocampus has been extensively studied in the rodent central nervous system (CNS). One feature of hippocampal neurogenesis which has emerged from these studies is that 80-90% of the granule neurons of the dentate gyrus are generated and mature during well established developmental periods, characteristically occuring postnatally in the mouse and rat. In the rat, the first granule cell precursors are born of neuroepithelial origin in the adjoining ventricular system between embryonic days 14 and 17 (Hine and Das, 1974; Schlessinger et al 1975, Bayer, 1980a). These cells migrate to the tip of the developing CA3 field of the hippocampus and establish a new proliferatve zone in the region that is to become the hilus, from which new granule cells (>85%) continue to be produced beyond postnatal day 18 (Bayer 1980a) and into the adult period (Altman and Das, 1965; Bayer and Altman, 1974; Kaplan and Hinds, 1977; Bayer et al., 1982). During hippocampal development, the morphogenesis of the dentate granular layer follows the pattern of neurogenesis. By the day of birth (P0), undifferentiated granule cell precursors and immature differentiating granule cells migrate radially from the hilus and gradually accumulate in the granular layer, stacked in ordered fashion such that later-generated cells are added to the base of the granule cell layer (Altman and Das, 1965; 1966; Altman, 1966; Bayer and Altman, 1974; Schlessinger et al., 1975; Bayer, 1980; Crespo et al., 1986). As development continues, the morphogenesis of the dentate gyrus proceeds from the tip of the lateral (ectal) wing to the medial (endal) wing, as in general, earlier formed neurons are destined for the ectal wing of the dentate and later forming neurons are distributed to the crest and the endal wing, respectively (Bayer and Altman, 1974; Schlessinger et al., 1975; Bayer, 1980).

Between postnatal days 5 - 8, during the peak period of cell proliferation and neuronal differentiation in the hilar region of the developing dentate gyrus, it is probable that as many as 30% - 40% of the total number of granule cells to be generated are born. By postnatal day 21 approximately 80% of adult level of mature granule cells are acquried by the granule cell layer, and the morphological pattern is essentially that observed in the adult (Bayer and Altman, 1974, Bayer 1980, Gaarskjaer, 1985).

As in the developing rat cerebellum, the temporal onset, pattern and intensity of expression of the synapsin I gene coincides with the neurogenic, morphogenic, and synaptogenic patterns of differentiation and development of the granule cell population of the hippocampus. From embryonic day 19 to the day of birth (P0), the low levels of synapsin I mRNA expressed in the hilar region and dentate granule cell layer reflect the amount of neurogenesis occuring within that zone, as <14% of mitotic stem cell precursors have differentiated into granule cell neurons. Perhaps the most compelling evidence that the temporal onset of expression of the synapsin I gene coincides with dentate granule cell neurogenesis is the sudden burst of synapsin I mRNA expression observed in the hilar region of the hippocampus on or around postnatal day 6 of development (Figure 14C,D). This developmental stage (postnatal day 5-8) is characterized typically by a burst of cell proliferation and neuronal differentiation in this region resulting in the birth of at least 50,000 granule cell neurons each day (Bayer and Altman, 1974; Schlessinger et al., 1975). Then, by postnatal day 14, as the peak period of neurogenic differentiation in the hilus passes, the burst of synapsin I mRNA expression observed in this region decreases dramatically, as <15% of the granule cells found in the adult dentate gyrus are born between postnatal days 12 and 15.

At postnatal day 21, synapsin I mRNA expression within the hilus is restricted primarily to large hilar neurons scattered throughout this region. By this stage in the development of the hippocampus, the overall pattern of expression of the synapsin I gene is reminiscent of that in the adult (as described in Chapter V of this dissertation), where high-

to-intense levels of synapsin I mRNA were detected in "mossy" or hilar neurons and the granule cell neurons of the dentate gyrus. As previously stated, by postnatal day 21, approximately 80% of the adult level of mature granule cells are positioned in the granule cell layer, and the morphological pattern is essentially that observed in the adult. Thus, through the postnatal development of the hippocampus, the onset and pattern of synapsin I gene expression are consistent with both the neurogenic and morphogenic patterns of differentiation and development of granule cells of the dentate gyrus.

Further, as seen in the developing cerebellum, the intensity of hybridization to synapsin I cDNA probes in the granule cell neurons suggests that the expression of the synapsin I gene is regulated additionally by synaptogenic differentiation of neurons in the central nervous system (Haas and DeGennaro, 1988). Studies by Gaarskjaer (1978, 1981, 1985) and Amaral and Dent (1981) have shown that in the adult dentate gyrus, the granule cell axons or "mossy fibers" of earlier formed granule cells are longer and more divergent than the fibers from granule cells that form later, and that during development it is the earliest forming granule cell neurons that are the first to undergo the process of synaptogenesis by directing the outgrowth of pioneer fibers locally within the hilar region. Since earlier-formed neurons are positioned in the more superficial aspects of the developing dentate granule cell layer (Altman and Das, 1965; 1966, Altman, 1966; Bayer and Altman, 1974; Schlessinger et al, 1975; Bayer, 1980; Crespo et al., 1986), it is these neurons that are the first to establish synaptic contact in the hilar region. In the rat, the process of synaptogenesis of dentate granule cell neurons begins prenatally and continues into the third postnatal week of development (Gaarskjaer, 1981, 1985). Thus, if synapsin I gene expression is also modulated concurrently with synaptogenic differentiation in the granule neurons in the developing dentate granule cell layer, neurons in the superficial dentate gyrus should express elevated levels of synapsin I mRNA early during postnatal development, whereas levels in the intermediate and basal regions of the dentate gyrus should increase later in development.

Between postnatal days 6 and 14, emulsion autoradiography revealed heavy accumulations of silver grains present over older, more mature and differentiated granule cells residing in the superficial dentate gyrus, with lower levels distributed over spindle-shaped, immature differentiating granule cells located throughout the hilus and basal dentate gyrus (Figure 14). As development proceeds (postnatal days 14 through 21), heavy accumulations of silver grains were observed over neurons in the more intermediate and basal portions of the dentate granule cell layer, as more neurons in these regions become fully mature and begin to undergo synaptogenic differentiation. These results reveal elevated levels of synapsin I gene expression are correlated with the synaptogenesis of granule cell neurons in the developing hippocampus, as well as cerebellum.

In conclusion, the data presented in this chapter identify two distinct phases of synapsin I gene expression during the development of the rat central nervous system. The first phase of expression reflects the temporal onset of expression of the synapsin I gene. The *in situ* hybridization data presented in this chapter clearly show that the temporal onset and pattern of synapsin I gene expression are consistent with the neurogenic patterns of differentiation of individual populations of neurons in the developing nervous system, most notably the granule cell neurons of the developing rat cerebellum and hippocampus. Furthermore, it was shown that a second phase of synapsin I gene expression correlates with the synaptogenic differentiation of neurons. That is, by *in situ* hybridization it was confirmed that the level of expression of the synapsin I gene is also regulated in a fashion coordinate with the major period of synaptogenesis in the developing cerebellum as reported by Haas and DeGennaro (1988), and further demonstrated the presence of elevated levels of synapsin I gene expression in cells undergoing synaptogenesis in the dentate granule cell layer of the developing rat hippocampus.

The appearance of synapsin I mRNA immediately upon the neurogenic differentiation of precursor cells supports the suggestion that synapsin I protein plays a role in the morphological and functional maturation of neurons and of the neuronal secretion

mechanism. Viewed from the standpoint of neuronal competition, high levels of synapsin I gene expression before synaptogenesis may preload neurons to allow for rapid synapse formation upon contact with a limiting number of targets. Further study, detailing a comparision between the expression synapsin I mRNA and protein during the development of defined circuits of the brain, as well as perhaps the production of transgenic mouse mutants of the synapsin I gene, will be necessary to better understand the precise role of the synapsin I protein in the development of the nervous system.

Chapter V

SYNAPSIN I GENE EXPRESSION IN THE ADULT CENTRAL NERVOUS SYSTEM WITH COMPARATIVE ANALYSIS OF mRNA AND PROTEIN IN THE HIPPOCAMPUS

Introduction

Synapsin I protein is widely distributed in nerve terminals throughout the mammalian central nervous system (De Camilli et al., 1983a,b; DeGennaro et al., 1989; Sudhof et al., 1989; Apostolides et al., in press). The pattern of distribution, however, is not uniform across the neuraxis, and it has been postulated that this differential distribution reflects differences in the functional properties of central synapses (Sudhof et al., 1989; Apostolides et al., in press). At present no data are available which detail the spatial distribution and comparative levels of expression of the synapsin I gene (mRNA and protein) in the adult central nervous system. Such a map of the intensity of synapsin I gene expression would provide insight into the specific properties and functional requirements of those neurons whose termini comprise central synapses. In this chapter, *in situ* hybridization histochemistry employing radioactively-labeled synapsin I cDNA probes was performed to examine the regional and cellular distribution of synapsin I mRNA in the adult rat central nervous system. Then, focusing on the rat hippocampus as a model system, *in situ* hybridization and immunohistochemistry were employed to compare the relative levels of expression of synapsin I mRNA and protein within defined synaptic circuits of the brain.

Results

Mapping of Synapsin I mRNA Throughout the Adult Rat Brain.

To detail the distribution of synapsin I mRNA in the adult rat brain, several (>7) *in situ* hybridization studies were conducted in horizontal (Figures 16, 18, and 20), and parasagittal (Figure 17) planes of section. In this study, hybridization signals were characterized as light (+), moderate (++), high (+++) and intense (++++), as estimated by visual comparison of several autoradiographic films of sections hybridized to radioactively-labeled synapsin I cDNA probes of comparable specific activities (Table 1). In each *in situ* hybridization run, this relative scale was used to describe the intensity of the hybridization signals from the different rat brain regions. This scale consistently assigned the CA3 neurons of the rat hippocampus the highest hybridization intensities and the caudate nucleus the lowest. After visual inspection of autoradiographic films, selected slides were processed for emulsion autoradiography to examine more accurately synapsin I mRNA distribution and cellular localization.

Telencephalon

Olfactory bulb. Intense labeling was observed in discrete layers of the olfactory bulb (Figures 16 and 17). Intense labeling was seen over the cells of the mitral and internal granular layers (Figures 16G, 17E). Light-to-moderate labeling was observed over cells of the glomerular layer (Figures 16F, G). Little or no labeling was detected over the external plexiform and olfactory nerve layers.

Cortex. Synapsin I mRNAs were concentrated in the entorhinal, piriform, cingulate, and frontal cortices (Figures 16-18, 21). High-to-intense synapsin I mRNA levels were detected in neocortical lamina II and the upper parts of lamina V (Figures 16B, 18A,B). The parasubiculum was intensely labeled (Figures 16B-E, 21B), as were the lamina II neurons of the piriform cortex (Figures 16I, 17A, 18D) and laminae II and V of

the entorhinal cortex (Figures 16C, 18C, 21B). Moderate synapsin I hybridization signals were observed primarily in laminae III, IV and VI of the neocortex (Figures 16B-E, 18A, B).

Basal forebrain and basal ganglia. In the basal forebrain, labeling of synapsin I mRNA was high in the olfactory tubercle and moderate in the bed nucleus of the stria terminalis, diagonal band of Broca, and medial septum (Figure 16F-H). Light hybridization was observed in the lateral septum (Figures 16C-G). In the basal ganglia the caudate-putamen was among the lightest hybridizing areas of the rat brain (Figures 16B-H, 18).

Amygdala. Both the anterior basolateral and the lateral nucleus of the amygdala exhibited high levels of synapsin I mRNA (Figures 16G-I, 17A), while the medial division of the central nucleus contained moderate amounts (Figures 16F-I). The least pronounced hybridization in the amygdala came from the lateral division of the central nucleus (Figures 16F-I).

Hippocampus. The large pyramidal neurons of hippocampal fields CA3 and CA4 consistently revealed the highest density of hybridization throughout the adult rat brain (Figures 16, 18G, 21B). Similiarly, high-to-intense levels of synapsin I mRNA were detected in the "mossy cells" or hilar neurons of the dentate gyrus (Figures 16E, 21B). Labeling of synapsin I mRNA was notably high over pyramidal cells in layers CA1 and CA2 and the granule cells of the entire dentate gyrus (Figures 16D, 17C, 18E, F, 21B).

Diencephalon

Thalamus. High hybridization signals were present in the anterodorsal and paraventricular thalamic nuclei (Figures 16C, D and 17D). In contrast, light-to-moderate labeling was generally observed in most remaining thalamic nuclei, including both the ventrolateral and the dorsomedial divisions of the anteroventral nucleus, and the parafasicular nucleus (Figure 16E). Particularly light labeling was observed in the ventral

Figure 16. Distribution of synapsin I mRNA in horizontal sections of adult rat brain by *in situ* hybridization. (A-I) X-ray autoradiograms of sections hybridized to ^{35}S-labeled synapsin I cDNA probes. V, lamina V of the neocortex; AD, anterodorsal thalamic nucleus; BSTM, bed nucleus of the stria terminalis, medial; CA3, CA3 field of the hippocampus; Cb, cerebellum; CG, central gray; CPu, caudate/putamen; Ctx, neocortex; DG, dentate gyrus; Dtg, dorsal tegmental nucleus; EC, entorhinal cortex; Gl, glomerular layer; GP, globus pallidus; IC, inferior colliculus; IGr, internal granular layer; La, lateral amygdala; LS, lateral septum; M, mitral cell layer; MHb, medial habenula; MS, medial septum; PaS, parasubiculum; PF, parafasicular thalamic nucleus; Pir, piriform cortex; PVA, paraventricular thalamic nucleus, anterior part; R, red nucleus; SC, superior colliculus; SNC, substantia nigra pars compacta; STh, subthalamic nucleus; Tu, olfactory tubercle; VLG, ventral lateral geniculate nucleus; VM, ventromedial thalamic nucleus. Sections were exposed to Kodak XAR-5 film for 10 days. Scale bar, 4 mm (for all panels).

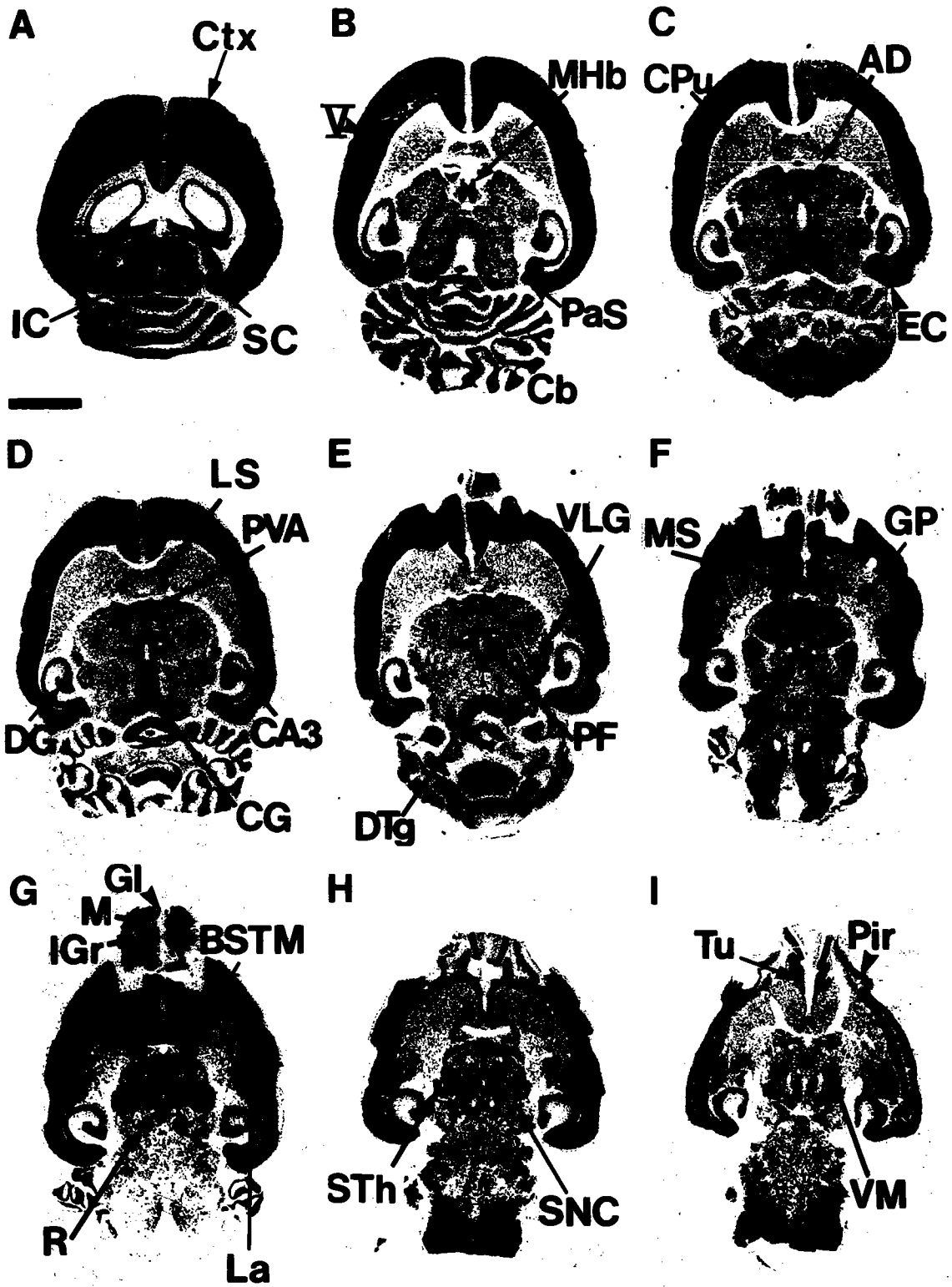
A
Ctx
IC
SC
B
MHb
V
PaS
Cb
C
CPu
AD
EC
D
LS
PVA
DG
CA3
CG
E
VLG
PF
DTg
F
MS
GP
G
Gl
M
IGr
BSTM
R
La
H
STh
SNC
I
Tu
Pir
VM

Figure 17. *In situ* hybridization of synapsin I mRNA in parasagittal sections of adult rat brain. (A-F) X-ray autoradiograms of sections hybridized to ^{35}S-labeled synapsin I cDNA probes. V, lamina V of the neocortex; 7, facial nucleus; AD, anterodorsal thalamic nucleus; AHi, amygdalohippocampal area; CA3, CA3 field of the hippocampus; Cb, cerebellum; CGD, central gray, dorsal part; CGPn, central gray of the pons; DG, dentate gyrus; DLG, dorsal lateral geniculate nucleus; IC, inferior colliculus; LA, lateroanterior hypothalamic nucleus; MCLH, magnocellular nucleus of the lateral hypothalamus; MGD/V, medial geniculate nucleus, dorsal and ventral parts; MS, medial septum; OB, olfactory bulb; Pir, piriform cortex; PMV, premammillary nucleus, ventral part; Pn, pontine nuclei; RtTg, reticulotegmental nucleus of the pons; STh, subthalamic nucleus; VMH, ventromedial hypothalamus; VPL, ventral posterolateral thalamic nucleus; VTA, ventral tegmental area; VTg, ventral tegmental nucleus; ZI, zona incerta. Sections were apposed to Kodak XAR-5 film for 10 days. Scale Bar, 4 mm (for all panels).

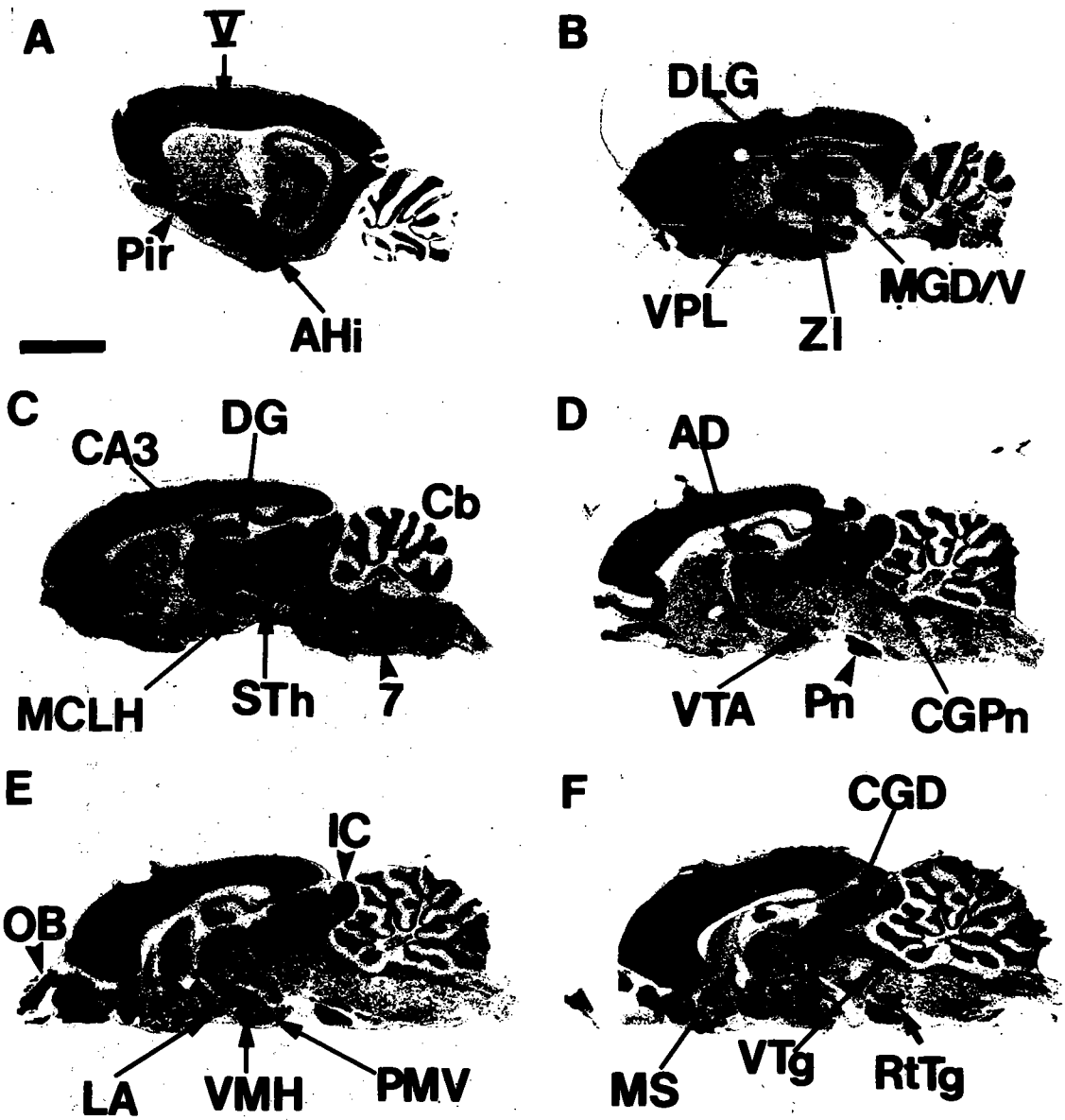
A
V
Pir
AHi
B
DLG
VPL
ZI
MGD/V
C
CA3
DG
Cb
MCLH
STh
7
D
AD
VTA
Pn
CGPn
E
IC
OB
LA
VMH
PMV
F
CGD
MS
VTg
RtTg

posterolateral thalamic nucleus and the dorsal lateral geniculate nucleus (Figure 17B).

Habenula. The medial habenula contained moderate-to-high levels of synapsin I mRNA (Figure 16B), while the lateral habenula contained lesser amounts.

Hypothalamus. In the hypothalamus, high levels of synapsin I mRNA were observed in the ventromedial nucleus (Figure 17E). Specifically, hybridization was high in the dorsomedial and ventrolateral divisions of the ventromedial nucleus (data not shown). Similiarly high levels were seen in the ventral premammillary nucleus and in the subthalamic nucleus (Figures 16H and 17C, E). Lower levels of synapsin I mRNA were present in most other hypothalamic regions, including the arcuate nucleus, the paraventricular nucleus, the lateral anterior nuclei, the lateral magnocellular nucleus, and the preoptic nucleus.

Midbrain

Moderate-to-high amounts of synapsin I mRNA were present in the red nucleus and in the substantia nigra pars compacta (Figure 16G, H). Light-to-moderate levels of synapsin I mRNA were observed in most other midbrain regions. For example, the dorsal central gray (Figure 17F) and the ventral tegmental area (Figure 17D) were moderately labeled. Synapsin I mRNAs were expressed homogenously across the inferior and superior colliculi. Here, both the dorsal cortex of the inferior colliculus and the superficial gray layer of the superior colliculus were lightly labeled (Figures 16A, 17E).

Brainstem

In the brainstem, high levels of synapsin I mRNA were present in the pontine nucleus (Figure 17D), the reticulotegmental nucleus (Figure 17F), the ventral tegmental nucleus (Figure 17F), the pontine central gray (Figure 17D), and the facial nerve nucleus (Figure 17C). Many brainstem nuclei, such as the ventral cochlear nucleus and the nucleus of the trapezoid body were moderately labeled.

Table 1. Relative abundance of synapsin I mRNA in different regions of rat brain. Hybridization signals were characterized as light (+), moderate (++), high (+++) and intense (++++), as estimated by visual comparison of several autoradiographic films of sections hybridized to radioactively-labeled synapsin I cDNA probes of comparable specific activities.

Relative abundance of synapsin I mRNA in different regions of rat brain

Area	Abundance
olfactory bulb, mitral cell layer	++++
internal granular cell layer	++++
glomerular cell layer	+
cortex, layers II-III, neocortex	++-+++
layer V, neocortex	+++-++++
piriform, layer II	++++
entorhinal, layer II and V	++++
frontal/cingulate	+++/+++
pre-/para-subiculum	++/+++-++++
basal forbrain, bed nucleus of stria terminalis	++
diagonal band of Broca	++
olfactory tubercle	+++
septum, medial	++
lateral	+
basal ganglia, caudate/putamen	+
amygdala, basolateral, anterior	+++
central, lateral/medial divisions	+/++
lateral	+++
hippocampus, CA 1	+++
CA 3	++++
CA 4	++++
dentate gyrus	+++
hilar neurons	++++
thalamus, anterodorsal nucleus	+++
paraventricular nucleus	+++
anteroventral nucleus, ventrolateral	++
dorsomedial	++
parafasicular nucleus	++
geniculate nucleus, ventral lateral, magnocellular part	++
medial	+
precommisural nucleus	+++
hypothalamus, ventromedial nucleus	+++
paraventricular nucleus	++
lateral anterior nuclei	++
lateral, magnocellualar nucleus	++
preoptic nucleus	++
arcuate nucleus	++
premammillary nucleus, ventral	++
subthalamic nucleus	+++
habenula, medial	++
colliculi, inferior	+
superior	+
red nucleus	+++
central grey, dorsal	++
pontine	+++
substantia nigra pars compacta	+++
tegmental nucleus, ventral	++
anterior	+++
pontine nucleus	+++
ventral cochlear nucleus, anterior part	++
cerebellum	
granule cell layer	+++
deep cerebellar nuclei	++-+++

Figure 18. High magnification dark-field and bright-field photomicrographs of emulsion autoradiograms of cells of the parietal neocortex (A and B), entorhinal cortex (C), piriform cortex (D), dentate granule cell neurons of the dentate gyrus (E), and the pyramidal cells of the hippocampus (F and G) hybridized to ^{35}S-labeled synapsin I cDNA probes. Hybridization intensities were greatest in layer V of the parietal, layers II and V of the entorhinal, and layer II of the piriform cortex. The highest hybridization signals detected throughout the rat brain were present in the CA3 neurons of the hippocampus. I-VI, layers of the cerebral cortex; CA1, CA1 field neurons of the hippocampus; CA3, CA3 field neurons of the hippocampus; DG, dentate gyrus. Emulsion-coated sections were exposed for 2 weeks. Scale bars: A and B, 1 mm; C-G, 300 μm.

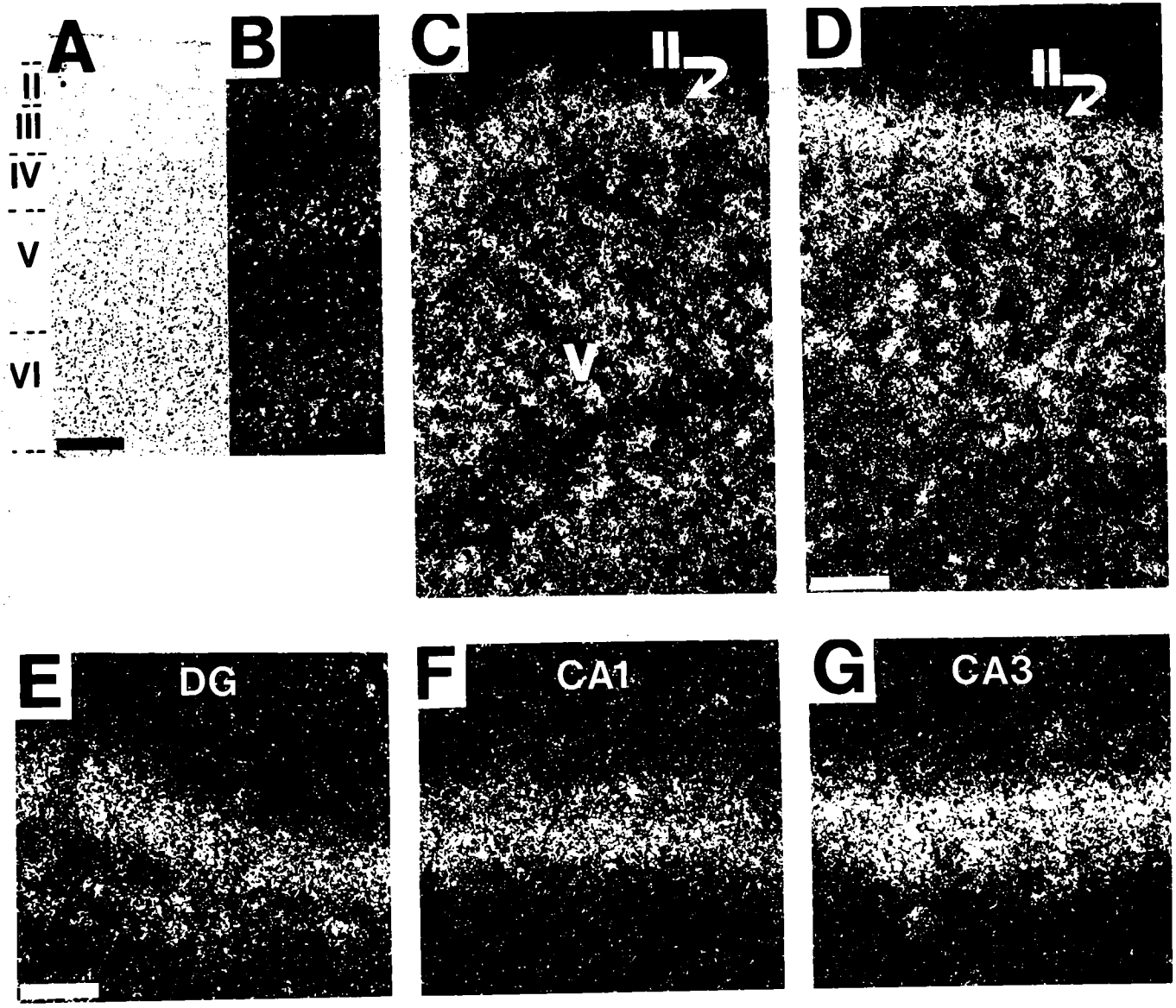
A
II
III
IV
V
VI
B
C
II
V
D
II
E
DG
F
CA1
G
CA3

Cerebellum

In the cerebellum, high-to-intense labeling was present over the cerebellar granule cells (Figures 16A-D, 17B-F). The intense labeling of granule cells made it difficult to determine, on X-ray film and by emulsion autoradiography, how much of the synapsin I hybridization signal was attributable to Purkinje cells. Light-to-moderate labeling was observed over the remainder of the cerebellar layers (Figures 16A-D, 17B-F), while the deep cerebellar nuclei showed moderate-to-high labeling over individual neurons scattered throughout the region (data not shown).

Synapsin I mRNA and Protein: Comparative Analysis of Expression

Previous studies have indicated that synapsin I protein is present in high levels in the rodent hippocampus (Bloom et al., 1979; Goelz et al., 1981; De Camilli et al., 1983a,b; Walaas et al., 1983; 1988; DeGennaro et al., 1989; Apostilides et al., in press). No studies however, have been reported which correlate protein data with the cellular distribution and patterns of expression of synapsin I mRNA in these areas. To examine the distribution of synapsin I mRNA and compare the relative levels of synapsin I mRNA and protein in rat hippocampus, *in situ* hybridization and immunohistochemistry were performed on horizontal sections of adult rat brain (Figure 21).

To ensure the specificity of the synapsin I polyclonal antibody, we performed Western blot anlysis with protein from adult rat neocortex (Figure 19). At the dilutions used for immunohistochemistry, 1:500 - 1:2000, the synapsin I antibodies recognized exclusively synapsin Ia and Ib polypeptides.

Immunohistochemistry using polyclonal antibodies to synapsin I revealed extremely low levels of synapsin I protein in the somata of all neurons, as evidenced by weak synapsin I immunostaining in the pyramidal cell layers of the hippocampus, the dentate

Figure 19. Western blot demonstrating specificity of synapsin I polyclonal antibody. Purified rat total neocortical brain protein was prepared, electrophoresed, and blotted as described in text. Synapsin I polyclonal antibodies were bound and immunoreactive bands were visualized. Antibodies recognized exclusively synapsin Ia and Ib polypeptides, of 78 Kd and 74 Kd, respectively, and a small amount of synapsin I proteolysis products.

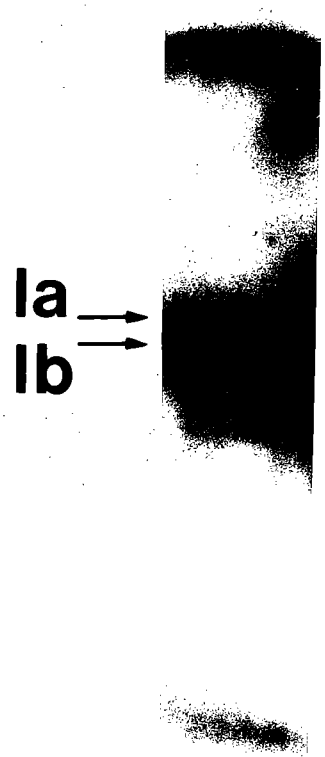
Ia
Ib

gyrus, and the layer II cells of the entorhinal cortex (Figures 20, 21C). In the dentate gyrus, granule cells give rise to mossy fiber afferents which terminate solely upon neurons of the hilar zone and the proximal dendrites of the CA3-CA4 cells of the hippocampus (see Figure 1.1). In this circuit, *in situ* hybridization and immunohistochemistry revealed a direct correspondence between high levels of synapsin I mRNA in granule cell somata and intense synapsin I protein staining in their mossy fiber terminals (Figure 21B, C). In contrast, *in situ* hybridization revealed intense levels of synapsin I mRNA in the somata of layer II neurons of the entorhinal cortex, while only moderate synapsin I protein staining was observed in the outer molecular layer of the dentate gyrus, the terminal field of these layer II neurons (Figure 21B, C). These results suggest differential levels of expression of synapsin I mRNA and protein within neurons which compose a defined synaptic circuit in the adult rat brain.

Discussion

In this chapter, the first extensive *in situ* hybridization study describing the regional and cellular distribution of synapsin I mRNA in the adult central nervous system is described. These data reveal the widespread but regionally variable distribution of synapsin I mRNA throughout the adult rat brain. Further, using the rat hippocampus as a model system, specific neurons were identified in which the level of synapsin I mRNA in neuronal parikarya correlates directly with the level of synapsin I protein in the synaptic termini of those cells, and other neurons within the same synaptic circuit in which synapsin I mRNA and protein levels do not correspond.

Figure 20. Low magnification photomicrographs of synapsin I immunoreactivity in parasagittal section of the adult rat brain (from Localization of Synapsin I in the Adult Rat Central Nervous System. Apostolides, P.J., DeGennaro, L.J., Melloni Jr., R.H., Pulaski-Salo, D., and Hamos, J.E. Synapse. (in press)).

AOB, accessory olfactory bulb; AON, accesssory olfactory bulb, CA3, CA3 field of the hippocampus; Cgr, granule cell layer, cerebellum; Cml, molecular layer, cerebellum; CPu, caudate-putamen; IC, inferior colliculus; ICj, island of Calleja; LPBlateral parabrachial nucleus; LSO, lateral superior olive; SC, superior colliculus; scp, superior cerebellar peduncle; SNR, substantia nigra, reticulata; Thal, thalamus; VP, ventral pallidum.

B

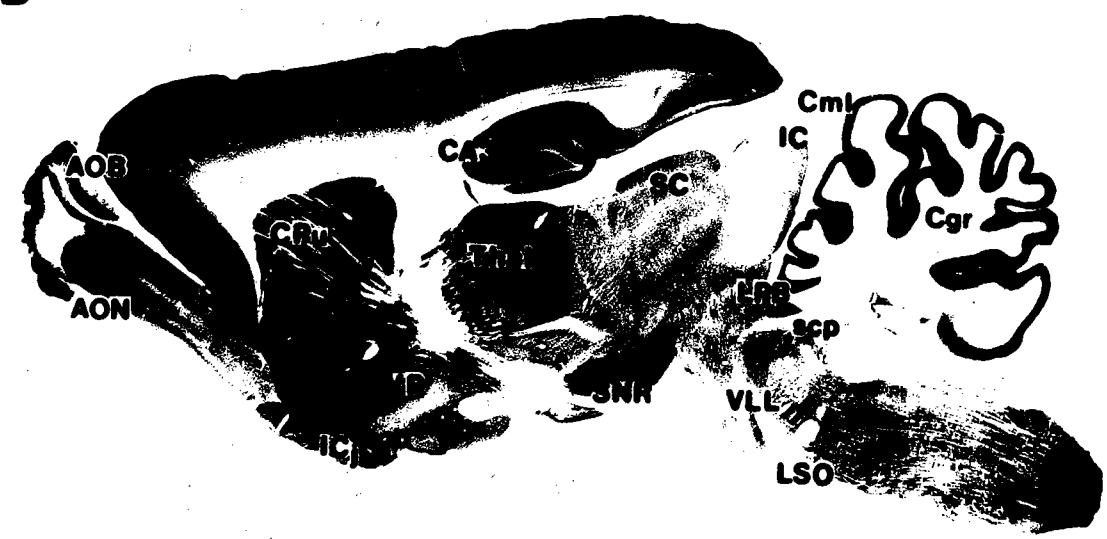

Figure 21. Expression of synapsin I mRNA and protein in horizontal sections of the adult rat hippocampus. (A) Cresyl violet stained section of rat hippocampal area to identify neuronal perikarya. (B) Dark-field photomicrograph of an emulsion-coated section of the rat hippocampal area hybridized to ^{35}S-labeled synapsin I cDNA probes. Hybridization intensity is greatest over the pyramidal cells of CA3 and CA4, and the layer II neurons of the medial entorhinal cortex. (C) Immunocytochemical localization of synapsin I protein in the rat hippocampus. Sections were immunostained with a polyclonal antibody raised against purified synapsin I protein. Intense immunoreactivity was apparent in the mossy fiber terminals, while moderate immunoreactivity was present in the molecular layer of the dentate gyrus. Immunoreactivity was weak in neuronal parikarya and in white matter fiber tracts. alv, alveus of the hippocampus; CA1, CA1 field neurons of the hippocampus; CA3, CA3 field neurons of the hippocampus; CA4, CA4 field neurons of the hippocampus; DG, dentate gyrus; EC, entorhinal cortex; mf, mossy fiber terminals; ml, molecular layer of the dentate gyrus. Emulsion-coated sections were exposed for 2 weeks. Scale bars: A, 55 μm; B, 65 μm; C, 70 μm.

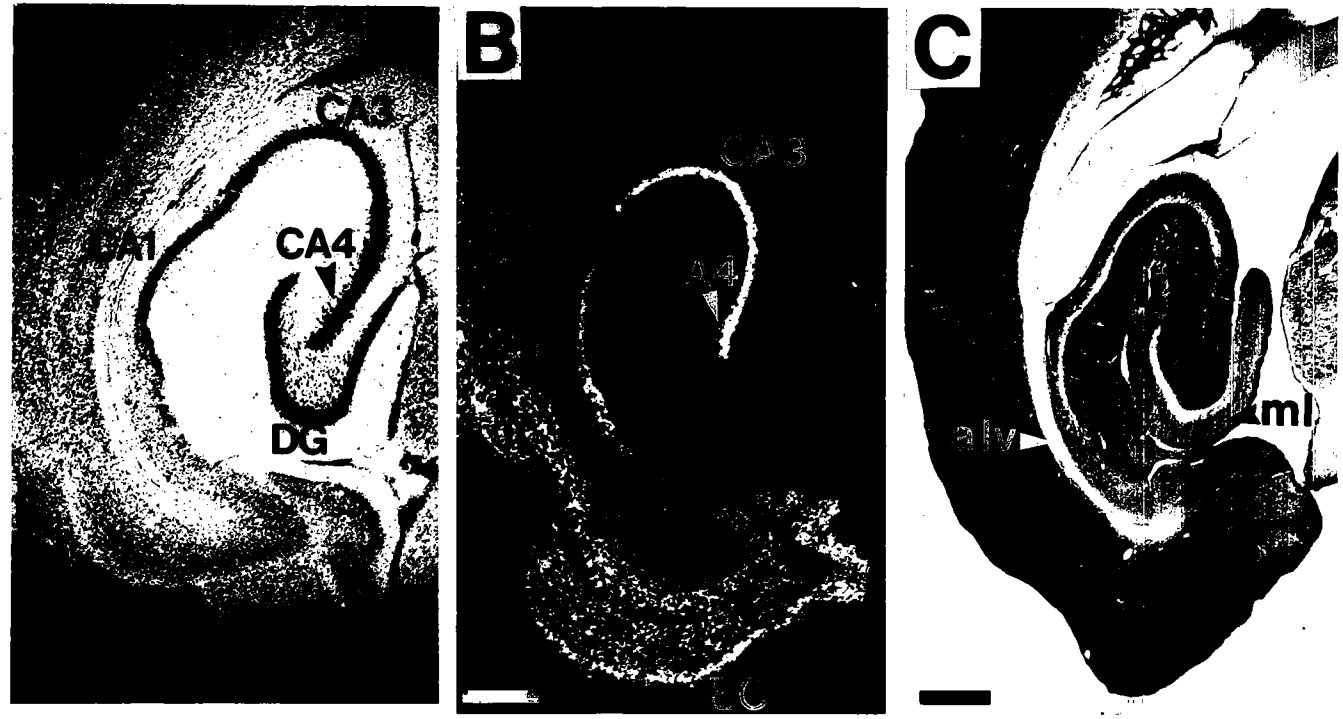
CA3
CA1
CA4
DG
B
CA3
CA4
C
alv
ml

Synapsin I In Situ Hybridization Patterns Correlate with the Distribution of mRNAs Encoding Other Neuron-Specific Synaptic Vesicle Proteins

Immunohistochemical studies have shown that synapsin I and synaptophysin, a synaptic vesicle integral membrane protein, display similiar distributions in the rat central nervous system (Sudhof et al., 1989). Recently the distribution and cellular localization of synaptophysin mRNA in the rat brain has been reported (Marqueze-Pouey et al., 1991). By comparison, a striking correlation between the patterns of expression of synapsin I and synaptophysin mRNAs in specific regions of the adult rat brain are observed. High levels of both mRNAs are present in layers IV-V of the neocortex, in the mitral cell layer of the olfactory bulb, in all fields of the hippocampus proper and the dentate gyrus, the medial habenula, the paraventricular nucleus of the thalamus, and in the granule cells of the cerebellum. Additionally, light-to-moderate levels of both mRNAs were localized in the striatum, the basal forebrain, and in widespread areas of the thalamus. No correlation however, was observed between the localization of synapsin I and synaptophysin transcripts in the internal granule cell layer of the olfactory bulb. Here, synapsin I mRNAs were present at high levels, while little or no synaptophysin mRNAs were detected. In this cell layer however, a good correlation was observed between the localization of synapsin I and synaptoporin, a novel synaptophysin variant (Marqueze-Pouey et al., 1991).

Synapsin I mRNA distribution correlates well with the pattern of expression of mRNAs encoding other synaptic vesicle proteins. VAMP-2 is another abundant synaptic vesicle protein whose mRNA expression pattern and distribution has been reported in rat central nervous system (Elferink et al., 1989; Trimble et al., 1990). Both the VAMP-2 and synapsin I genes express high levels of mRNAs in the substantia nigra pars compacta, the anterodorsal thalamus, the basolateral amygdala, the piriform cortex, and in all fields of the hippocampus proper and the dentate gyrus. Similiarly, the hippocampal localization and distribution of the mRNA for synaptosomal-associated protein, 25kD, (SNAP-25), parallels that of synapsin I mRNA (Geddes et al., 1990). In the adult rat hippocampus, the

greatest abundance of SNAP-25 mRNA was in the large pyramidal neurons of CA3, with a lower density of hybridization signal in the CA1 pyramidal cells and in the granule cells of the dentate gyrus.

Heterogeneous Distribution of Synapsin I mRNA

Together, RNA blot (Chapter III, Figure 8) and *in situ* hybridization data provide biochemical and histochemical evidence of regional variability in the level of synapsin I mRNA in the central nervous system. At least two possibilities exist to explain the heterogeneous distribution of synapsin I mRNA throughout the adult rat brain. One possibility is that strong hybridization signals reflect the number and density of neuronal somata per field. The mitral and internal granular cell layers of the olfactory bulb, the granule cell layer of the dentate gyrus, and the CA1 field of the hippocampus are all examples of densely packed layers of cells which exhibit high levels of synapsin I mRNA labeling. Densely packed nuclei also display strong labeling of synapsin I mRNA. The anterodorsal and paraventricular thalamic nuclei, the medial habenula, the subthalamic nucleus, and the substantia nigra pars compacta all display similiarly high hybridization signals by *in situ* hybridization. The cell types in each of these areas varies widely, from small spherical granule cells to large pyramidal neurons, densely packed in clusters forming a nucleus or tract of cells. In these regions, strong synapsin I mRNA hybridization signals are most probably related directly to cell packing.

A second possibility is that strong hybridization signals in discrete regions of rat brain reflect differences in the levels of synapsin I mRNA expressed in those cells. In these regions, hybridization intensity cannot be attributed solely to the number and packing density of neuronal perikarya. For example, Figure 18B shows high levels of synapsin I mRNA in the perikarya of neurons in layer V of the parietal neocortex. Although this region is low in cell number and packing density (Figure 18A), these medium-sized neurons express high amounts of synapsin I mRNA, as evidenced by the sharp band of

hybridization seen in Figures 16B-E, 17A-C, and 18B. Similiarly, the small and medium-sized cells in layer V of the medial entorhinal cortex express notably high levels of synapsin I mRNA (Figures 16C-E, 18C, 21B). Other examples of areas which appear to express levels of synapsin I mRNA not apparently related to packing density, are the pyramidal neurons of hippocampal field CA3, the layer II stellate cells of the entorhinal cortex, and the neurons of the parasubiculum. The large pyramdial neurons of CA3 are significantly less densely packed than the pyramidal neurons of the neighboring CA1 field and the granule cells of the dentate gyrus. The CA3 neurons, however, express appreciably higher levels of synapsin I mRNA (Figures 18E-G) than cells in the other two regions. The layer II stellate neurons of the entorhinal cortex form a continuous layer of cells in the medial aspect of the parahippocampal gyrus. Here, although somewhat less densely packed than neurons of the dentate gyrus and CA1, the stellate cells display consistently higher hybridization signals (Figures 21A, B). In fact, hybridization to synapsin I mRNA in these neurons was nearly equal in intensity to that in neurons of the CA3 field of the hippocampus (Figure 21B). The parasubiculum lies adjacent to the medial entorhinal cortex and is characterized by a superficial layer of moderately packed medium-sized cells. The presubiculum lies next to the parasubiculum and is characterized typically by a lamina of densely packed small cells. Although significantly more densely packed, the presubiculum appears less labeled than its neighbor, suggesting different levels of expression of synapsin I mRNA between the two cell populations (Figures 18B, 21B). The areas mentioned above contain neurons of various cellular profiles which form less densely packed and occasionally pale fields of neurons. These neurons however, exhibit strong hybridization to synapsin I cDNA probes by *in situ* hybridization. Thus, these data reflect differences in synapsin I mRNA levels in individual neurons representative of a specific region of the rat brain.

Dissimiliar Expression Patterns of Synapsin I mRNA and Protein in the Rat Hippocampus

To address directly the possibility that high levels of synapsin I mRNA in discrete subsets of neurons may reflect the amount of synapsin I protein present in the presynaptic terminal fields of those neurons, the patterns of expression of synapsin I mRNA and protein in the defined synaptic circuitry of the rat hippocampus were compared. The rat hippocampus is a fold of cortex divided into four distinct fields, CA1-CA4, respectively (Figure 21A). Accompanying the hippocampus is the dentate gyrus, a layer of densely packed granule cells whose dendritic arborizations ramify in a dense synaptic plexus in the molecular layer of the dentate gyrus. The major source of afferent inputs to the dentate granule cells is the large stellate cells of layer II of the medial entorhinal cortex (Desmond and Levy, 1982). These afferents project ipsilaterally, via the perforant path, to the outer two-thirds of the molecular layer of the dentate gyrus. The dentate granule cells, then, extend mossy fiber axons locally to the mossy cells scattered throughout the hilus of the dentate gyrus and to the proximal dendritic field of ipsilateral CA3 neurons of the hippocampus.

Synapsin I mRNA and protein are present in neurons of the rat dentate gyrus and entorhinal cortex (Figure 21). Synapsin I transcripts are expressed at notably high levels in granule cells of the dentate gyrus and at intense levels in the layer II neurons of the entorhinal cortex (Figure 21B). Synapsin I protein, however, exhibits remarkably dissimiliar patterns of expression in the presynaptic terminal fields of these two cell populations (Figure 21C). Synapsin I protein is present in intense amounts in the mossy fiber terminal fields of dentate granule neurons. In contrast, the protein is present in only moderate amounts in the outer two-thirds of the molecular layer of the dentate gyrus, the terminal field of layer II entorhinal neurons. One possible explanation for the discrepancy between levels of synapsin I mRNA and protein in the somata and termini of specific neurons of the hippocampal region is that these levels may reflect simply the synaptic

density or amount of terminal arborization of those cells. However, a review of synaptic density, as measured by quantitative ultrastructural analyses, suggests that the number of synapses per unit area is relatively invariant across the hippocampal neuraxis (Amaral et al., 1981; Scheff et al., 1985; Scheff et al., 1991). Therefore, local differences in synaptic density cannot adequately explain the variability in synapsin I protein staining in the terminal fields of neurons of the dentate gyrus and entorhinal cortex. Furthermore, the markedly dissimiliar patterns of expression of synapsin I mRNA and protein in the neurons of the dentate gyrus and entorhinal cortex suggest that synapsin I mRNA levels cannot reflect simply the amount of synapsin I protein present in the terminal arborizations of central neurons. Alternatively, it is proposed that the differential levels of expression of synapsin I mRNA and protein in these synaptic circuits reflect differences in the functional properties and/or requirements of neurons which form these central synapses. For example, studies on the restoration of synaptic connections in response to selective nervous system lesions have demonstrated that the hippocampal formation possesses a robust potential for synaptic regrowth (see review by Cotman and Nieto-Sampedro, 1984). In these studies, synapse replacement is achieved by the selective sprouting of residual inputs; in the case of unilateral entorhinal lesions, originating in hippocampal fields CA3c-CA4, layer II of the contralateral entorhinal cortex, and in the medial septum. Thus, locally high levels of synapsin I mRNA in hippocampal and entorhinal somata may reflect the ability of the system to be plastic and respond to injury and/or select environmental stimuli by producing long-term synaptic circuitry changes. Other neurons, in which synaptic plasticity is not a major necessity (ie. dentate granule neurons), might still require locally high levels of synapsin I mRNA to maintain correspondingly high levels of synapsin I protein in their presynaptic terminal fields. In these neurons, high levels of synapsin I gene expression (mRNA and protein) might be required to maintain high rates of activity that characterizes the circuits in which they participate.

In conclusion, the data presented in this chapter provide a detailed map of the

intensity of synapsin I gene expression across the adult rat neuraxis. These studies show that synapsin I mRNA exhibits widespread, yet regionally variable, levels of expression throughout the adult rat central nervous system. Further study, employing more quantitative *in situ* hybridization procedures and probes able to distinguish individual synapsin I mRNA subtypes, will be necessary to quantitate precisely the levels of the different isoforms of synapsin I mRNAs expressed in these areas. Additionally, *in situ* hybridization and immunohistochemistry demonstrated differential levels of expression of synapsin I mRNA and protein within the defined synaptic circuitry of the adult rat hippocampus. Studies of the expression of synapsin I mRNA and protein duing the synaptic development of the hippocampus and following selective lesions of this brain region may provide insight into the regulation of, and functional requirement for, synapsin I gene expression during the establishment and restoration of synaptic contacts in the central nervous system.

Chapter VI

SYNAPSIN I mRNA AND PROTEIN DURING THE ESTABLISHMENT AND RESTORATION OF FUNCTIONAL SYNAPSES IN THE RAT HIPPOCAMPUS

Introduction

As detailed in the previous chapters, numerous reports of the neuron-specific expression of synapsin I protein in the adult rodent CNS have been described. These studies employing endogenous phosphorylation assays (Walaas et al., 1983, 1988), radioimmunological assays (Goelz et al., 1981), and immunohistochemistry (Bloom et al., 1979; De Camilli et al., 1983a,b; DeGennaro et al., 1989; Melloni et al., 1993; Apostilides et al., in press) all indicate that synapsin I protein is present at extremely high levels in neuropil regions of the hippocampus. During development of the rodent nervous system, the appearance of synapsin I protein in the neuropil has been shown to correlate temporally and topographically with synaptogenesis (Lohman et al., 1978; De Camilli et al., 1983; DeGennaro et al., 1983; Levitt et al., 1984; and Mason, 1986; Moore and Berstein, 1989; Bergman et al., 1992). Recently, *in situ* hybridization histochemistry has been used to describe the pattern of expression of synapsin I mRNA in the developing and adult rat hippocampus (Melloni and DeGennaro, submitted, see Chapter IV; Melloni et al., 1993, see Chapter V). These studies revealed that during the development of the hippocampus the temporal onset and the peak expression of the synapsin I gene coincides, respectively, with neuronal and synaptogenic differentiation of granule cell neurons of the dentate gyrus. Coupled with recent morphological and physiological data by Han *et al.*, (1991) and Lu *et al.*, (1992), these data suggest a possible role for the encoded protein in the establishment

and maintenence of synapses in the early development of the nervous system. However, while our previous work provided strong evidence for high levels of synapsin I gene activity during hippocampal development, they also suggested that synapsin I mRNA levels did not reflect simply the amount of synapsin I protein present in the terminal arborizations of central neurons (Melloni et al., 1993, see Chapter IV). Based on these results we hypothesized that locally high levels of synapsin I mRNA in neuronal somata may reflect the ability of the nervous system respond to select environmental stimuli and/or injury by producing long-term changes in synaptic circuitry.

To test this hypothesis and to better understand the regulation and putative role of synapsin I gene expression in the development of functional synaptic contacts in the CNS, immunohistochemistry and *in situ* hybridization were employed to compare the patterns of expression of synapsin I protein and mRNA during the main period of synaptogenic differentiation in the developing rat hippocampus. Then, to examine the regulation and putative role of synapsin I gene expression during the restoration of synaptic contacts in the CNS, a second set of experiments involving knife cut transection of the perforant pathway were designed to evoke synaptic reorganization in local hippocampal circuitry. Synapsin I immunoreactivity and mRNA expression were then examined in target and sprouting neurons in response to and during the denervation and reinnervation of the hippocampus.

Results

The expression of synapsin I protein and mRNA during the development of the rat hippocampus

Previous studies employing diverse biochemical and histochemical techniques have indicated that the appearance of synapsin I protein during development coincides with synaptogenic differentiation both *in vivo* (Lohman et al., 1978; De Camilli et al., 1983a,b;

DeGennaro et al., 1983; Levitt et al., 1984; Mason, 1986; Moore and Bernstein, 1989) and *in vitro* (Bixby and Reichardt, 1985; Weiss et al., 1986). None of these studies, however, correlate the developmental patterns of expression of synapsin I protein and mRNA in the nervous system. To determine how synapsin I mRNA levels are related to levels of synapsin I protein during the establishment of synapses in the rat CNS, a comparison was carried out using the developing rat hippocampus as a model system. Specifically, to correlate the onset of appearance of detectable levels of synapsin I protein in the mossy fiber terminal fields with the expression of synapsin I mRNA in hippocampal granule cell neurons, immunohistochemistry and *in situ* hybridization were performed on serial sections of rat brains of postnatal ages P5/6, P11, P21, P31, and adult (P90).

Synapsin I protein in the developing rat hippocampus

Immunohistochemistry. In the adult rat, synapsin I immunoreactivity conformed to well-known features of hippocampal circuitry (see Chapter V, Figures 20 and 21). Staining was found primarily within the neuropil, while neuronal somata remained unstained; an observation particularly evident in the granule cell layer of the dentate gyrus or the pyramidal cell layer of the hippocampus. The highest density of synapsin I staining was found in the hilus and in the CA3 field, within the mossy fiber terminal zone of dentate granule cells. In this zone, dense staining was distributed evenly in the hilar region and appeared consistent along the entire length of the proximal CA3 dendritic field.

The overall changes in distribution and intensity of synapsin I immunostaining in the mossy fiber terminals of the rat hippocampus through a range of postnatal days 5 - 31 are illustrated in Figure 22. At the earliest postnatal time points examined (P0 - P2), the entire hippocampus showed very little, if any, immunoreactivity with synapsin I antibodies (data not shown) and, although cresyl violet staining of dentate granule somata revealed the near adult morphology by postnatal day 5 (Figure 22A), synapsin I immunoreactivity in the hilar region remained diffuse and very light (Figure 22B). Other areas within the

Figure 22. Immunohistochemical localization of synapsin I protein in the developing rat hippocampus. (A,C,E,G,) High magnification photomicrographs of the developing rat hippocampus stained with cresy violet acetate to identify neuronal perikarya. (B,D,F,H,) High power photomicrographs of synapsin I immunoreactivity in the developing rat hippocampus. No appreciable synapsin I immunostaining was present between postnatal days 5 and 11 (arrows in B and D). Note marked increase in synapsin I immunoreactivity in the mossy fiber zone and along the proximal dendrites of CA3 between postnatal days 21 and 31 (arrows in F and G). (A,B) postnatal day 5. (C,D) postnatal day 11. (D,E) postnatal day 21. (G,H) postnatal day 31.

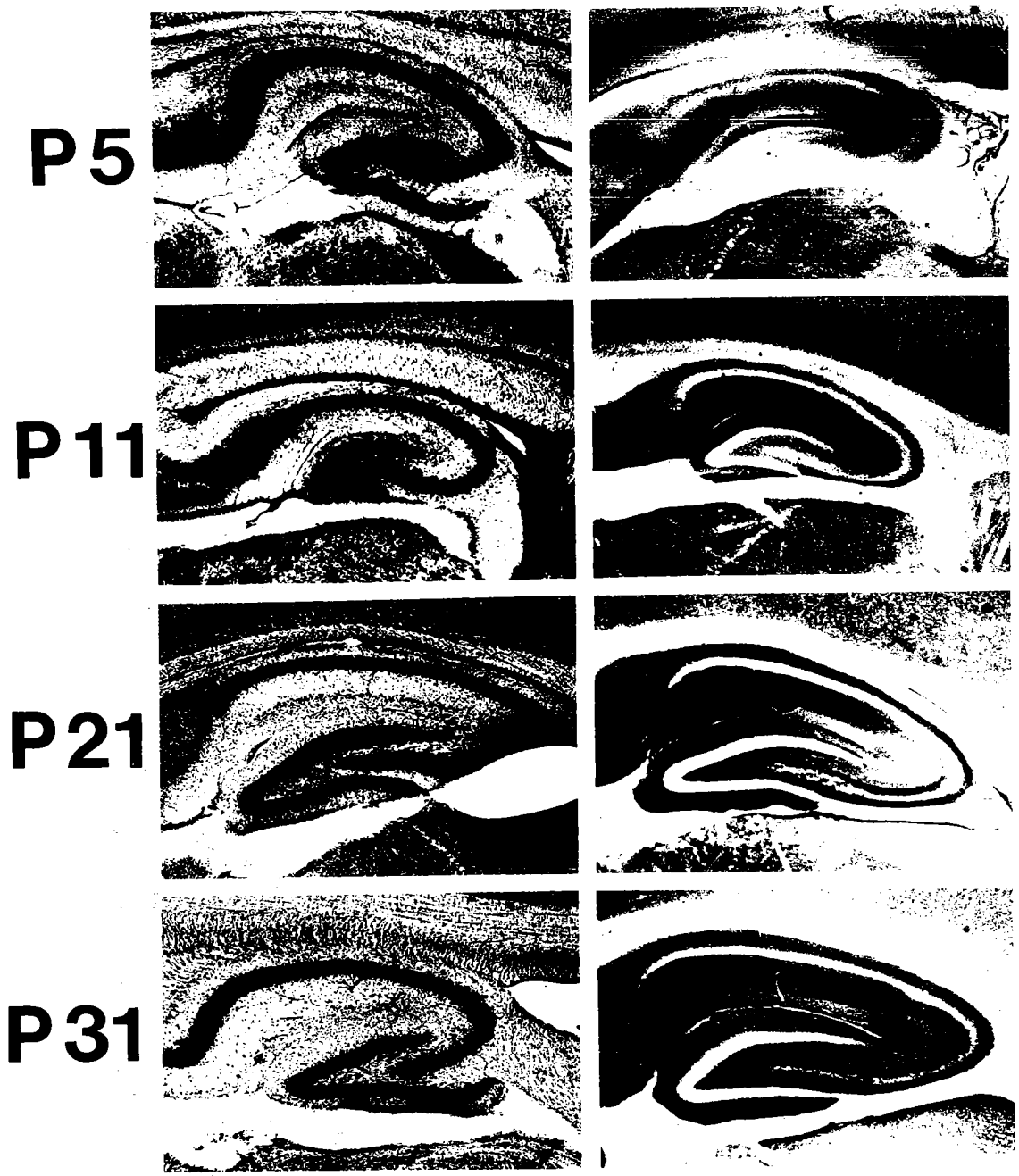
P5
P11
P21
P31

hippocampus, however, showed much higher levels of synapsin I immunoreactivity. For example, the *stratum radiatum* and *stratum oriens* of Ammon's horn, and the molecular layer of the suprapyramidal blade of the dentate gyrus showed modest, diffuse staining. While synapsin I immunostaining in the hippocampus at this early time point was relatively light compared with adult staining, many other regions of the neuraxis, such as the olfactory bulb and the ventral forebrain, have already reached their adult level of synapsin I immunoreactivity (unpublished observations).

By postnatal day 11 (Figure 22C,D), the adult morphology of the hippocampus was well established and synapsin I staining throughout the hippocampus was more apparent than at earlier time points. At this time, although other subfields of the hippocampus showed the adult distribution and intensity of synapsin I staining, the mossy fiber terminal zone had not yet attained its extremely dark, adult level of dense immunoreactivity. A slight, but increasing, gradient of punctate synaptic staining could, however, be identified within the hilus and along the distal regio inferior at this postnatal time point.

By postnatal day 21, the intensity and pattern of synapsin I immunoreactivity had changed markedly (Figure 22E,F). The mossy fiber terminal zone in the hilus and CA3 field was now moderately-to-darkly stained for synapsin I protein, but not at the intense levels that typically characterize the adult mossy fibers. At this time in development, synapsin I immunoreactivity within the mossy fiber terminal zone revealed two patterns of staining. Synapsin I immunostaining was slightly more intense in the hilus and the distal CA3 field, while staining was moderate in the proximal CA3 mossy fibers. Additionally, punctate synapsin staining is more obvious at this time point as several individual mossy fiber terminals appear densely stained.

By postnatal day 31, the pattern and intensity of synapsin I immunostaining had once again changed dramatically, as the mossy fiber terminal zone in the hilus and CA3 fields has reached the adult level of synapsin I immunoreactivity (Figure 22G,H). At this

time, mossy fibers showed remarkably intense synapsin I immunostaining reflecting very high levels of synapsin I protein in the large mossy fiber termini within this region. This dense pattern of immunostaining was homogeneous across the hilus and along the entire length of the regio inferior.

Semi-quantitative analysis of synapsin I immunoreactivity substantiated the qualitative observations (Figure 26). Densitometric analysis, carried out on five sections from at least three experimental animals per developmental time point, indicated that synapsin I immunoreactivity in the mossy fiber terminal zone did not begin to increase from its lowest levels until after nearly two weeks of postnatal development. Moreover, in correspondence with immunohistochemical data, synapsin I immunoreactivity does not reach its high, adult level of intensity in the hilar region until approximately postnatal day 31 of development.

Western blot analysis. To measure more quantitatively the changing levels of synapsin I protein observed in the hilar region by immunohistochemistry, Western blot analysis was performed with protein isolated from dentate granule neurons and their accompaning mossy fiber terminals at postnatal ages 21 and 31 days (Figure 23). Silver staining of total proteins present in dentate granule neurons and their mossy fiber terminals at these two time points revealed a series of protein bands strikingly similar in position and intensity, with the exception of one band (MWr ~74 kd) which was dramatically increased (Figure 23, lanes 2 and 3). The increased band co-migrated with purified synapsin I protein (lane 4). Immunoblots probed with synapsin I-specific antibody (lanes 5-7) revealed that the increased band was synapsin I and that, synapsin I protein increased at least 2-5 fold in the mossy fiber terminals of dentate granule neurons between postnatal days 21 and 31.

To determine whether this change was specific to synapsin I or indicative of more general changes in the complement of synaptic proteins, immunoblot duplicates of lanes 2 and 3 were probed with monoclonal antibodies directed against the neuron-specific protein synaptophysin (lanes 8 and 9). Synaptophysin (previously referred to as p38) is a major

Figure 23. Western blot of total protein extracted from dentate granule neurons and their accompaning mossy fiber terminals from punched sections of rat brain of postnatal ages 21 and 31 days. Purified rat total dentate protein was prepared, electrophoresed, and blotted as described in the text. Lane 1: markers. Lanes 2 and 3: Diiachi silver staining of total proteins present in dentate granule neurons and their mossy fiber terminals in rat pups of postnatal ages 21 (lane 2) and 31(lane 3) days. Lane 4: Diiachi silver staining of purified synapsin I protein (4 μg). Lanes 5-7: immunoblot of duplicates of lanes 2-4 probed with synapsin I-specific (SYN) antibodies. Note the 2-5 fold increase in synapsin I immunoreactive bands between postnatal days 21 and 31. Lanes 8 and 9: immunoblot of duplicates of lanes 2 and 3 probed with synaptophysin-specific (SYT) antibodies. Synaptophysin immunoreactive bands increased 2 fold between postnatal days 21 and 31.

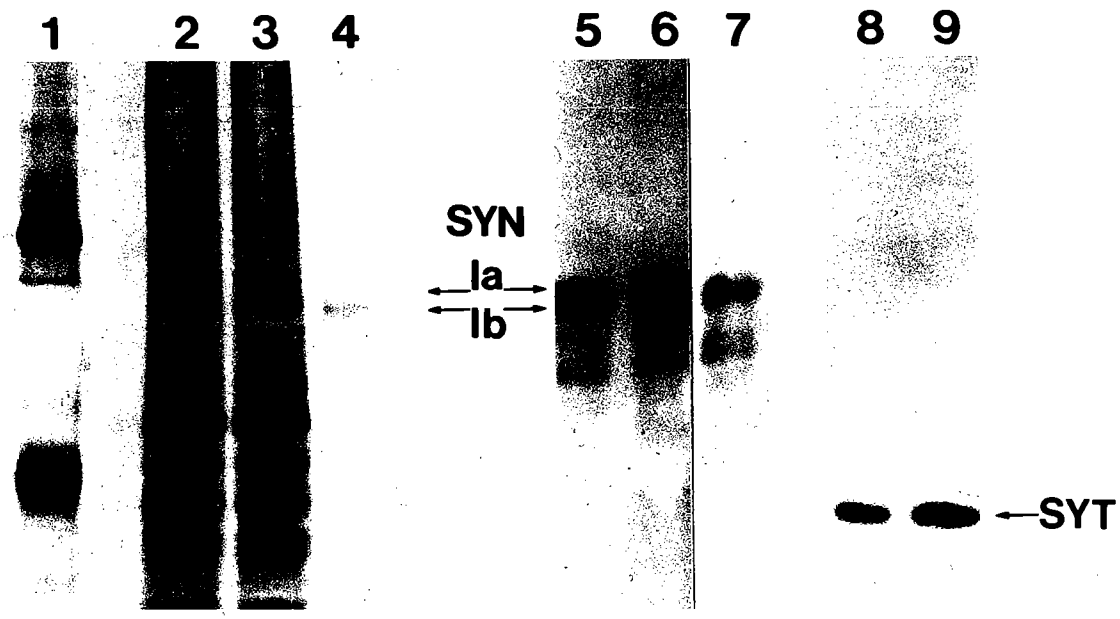
1
2
3
4
5
6
7
8
9
SYN
Ia
Ib
SYT

integral membrane protein of the synaptic vesicle membrane, believed to participate in the formation of an exocytotic fusion pore, which ultimately leads to the release of neurotransmitter (Jahn et al., 1985; Wiedenmann and Franke, 1985; Sudhof et al., 1987; Thomas et al., 1988). Immunoblots probed with synaptophysin-specific antibody revealed that synaptophysin protein increases approximately 2 fold in dentate granule neurons and their mossy fiber terminals between postnatal days 21 and 31.

Synapsin I mRNA in the developing rat hippocampus

In situ hybridization. In the adult rat hippocampus, synapsin I hybridization highlights well-known features of hippocampal anatomy (see Chapter V, Figure 21). In general, hybridization was restricted to neuronal somata while the white matter, neuropil and meninges remained devoid of signal. Synapsin I hybridization signal was intense in neurons throughout the hippocampal fields CA1-CA4, with highest levels in CA3. Hybridization to synapsin I probes was also observed at notably high levels in the granule cell neurons of the dentate gyrus.

During the postnatal development of the hippocampus, the expression of synapsin I mRNA in cells of the dentate gyrus paralleled the neurogenic and morphogenic patterns of differentiation and development of dentate granule cell neurons (Figure 24). From the earliest times examined in the postnatal period (P0-P2), synapsin I mRNA is expressed in hippocampal fields CA1-CA3, and the developing neurons of the rat dentate gyrus (Figure 24A, B). In fact, already by this stage of development (P0), high (near adult) levels of hybridization to synapsin I cDNA probes were observed in hippocampal fields CA2 and CA3. As evidenced by the thin line of hybridization in the lateral blade of the developing dentate gyrus, synapsin I hybridization also revealed the earliest stages of the morphogenic development of the dentate granule cell layer.

At postnatal day 6, hybridization to synapsin I probes changed dramatically in particular areas of the rat hippocampus, while high levels of hybridization remained in

Figure 24. Expression of synapsin I mRNA in sections of the developing rat hippocampus. (A,C,E,G,I) High magnification photomicrographs of the developing rat hippocampus stained with cresy violet acetate to identify neuronal perikarya. (B,D,F,H,J) Dark-field photomicrographs of emulsion-coated sections of the developing rat hippocampus hybridized to ^{35}S-labeled synapsin I cDNA probes. High, near adult levels of synapsin I hybridization are present in dentate granule neurons by postnatal day 6 (arrow in D). (A,B) postnatal day 0 (DOB). (C,D) postnatal day 6. (E,F) postnatal day 11. (G,H) postnatal day 21. (I,J) postnatal day 31. CA3; CA3 field of the hippocampus; DG, dentate granule cell layer; H, hilar region. Emulsion-coated sections were exposed for 2 weeks.

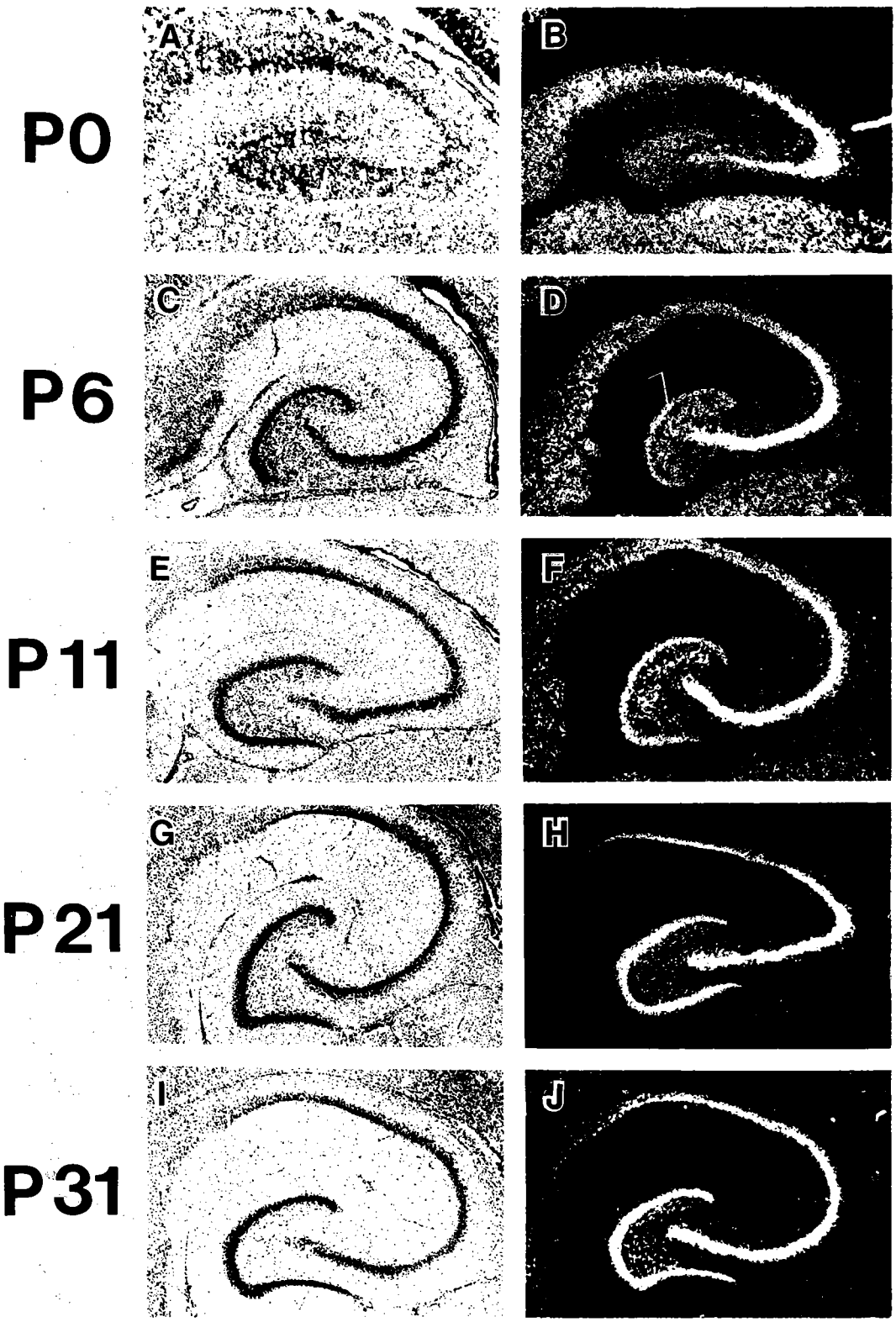
P0
P6
P11
P21
P31
A
B
C
D
E
F
G
H
I
J

hippocampal fields CA1-CA3. For example, in the dentate gyrus, the pattern of synapsin I hybridization now clearly reveals high levels of synapsin I mRNA expression (Figure 24C,D) Through this period of hippocampal development, synapsin I hybridization continues to delineate the development of the dentate granule cell layer as both the lateral (ectal) and medial (endal) blades of the dentate granule cell layer hybridized to synapsin I probes. In fact, at this time in development , hybridization signals in the dentate granule cell layer appeared near equal in intensity to those observed in the adult animal. In addition, hybridization was notably increased in the hilar region of the hippocampus, as cells in this area undergo a massive burst of neurogenic differentiation between postnatal day 5 and postnatal day 8 (Schlessinger et al., 1975).

At postnatal day 11, hybridization to synapsin I probes displayed similar patterns to those observed at earlier time points, with few notable exceptions (Figure 24E,F). Synapsin I hybridization revealed high levels of synapsin I mRNA in neurons along the entire length of the developing granule cell layer of the dentate gyrus . The pattern and strength of hybridization seen at this time was clearly equal in intensity to those observed in the adult rat dentate gyrus. Elevated levels of synapsin I hybridization remained in the hilus of the hippocampus, as neurogenesis remains high that region throughout this developmental time period (Altman and Das, 1965). The adult pattern of intense hybridization to synapsin I probes was also observed in hippocampal fields CA1-CA3 at this time point.

From postnatal day 21 and beyond, the pattern and intensity of hybridization to synapsin I probes seen in the hippocampus differs slightly from that seen at earlier time points (Figures 24G-J). Hybridization was notably high in granule cell neurons of the dentate gyrus and intense in the pyramidal neurons of hippocampal fields CA3. In contrast, the overall levels of hybridization in the hilus were markedly lower than at earlier time points, as hybridization in the hilar region at this time was restricted to large polymorphic neurons. From this stage of development, in general, hybridization to

synapsin I cDNA probes in the hilus and in the granule cell layer of the dentate gyrus were analogous to those observed in the adult rat hippocampus

Semi-quantitative analysis of film autoradiograms substantiated the patterns and intensity of synapsin I hybridization observed in the developing dentate gyrus (Figure 26). Film densitometry was carried out on five sections from at least three experimental animals per developmental time point. These analyses indicated that synapsin I mRNA hybridization reached its high, adult level of intensity in the dentate gyrus by postnatal day 6 of development, preceding by over 20 days, the time at which synapsin I protein reached its adult level.

RNA blot analysis. To confirm more quantitatively the pattern of expression of synapsin I mRNA observed in neurons of the developing dentate gyrus by *in situ* hybridization, RNA blot analysis was performed with RNA isolated from dentate granule cell neurons at postnatal ages 14, 21, and 31 days (Figure 25). In these samples, synapsin I cDNA probes detected two mRNAs of the predicted size (4.5 kb and 3.4 kb) and ratio. In accord with prior analysis, the relative levels of synapsin I mRNA (both the 4.5 kb and 3.4 kb mRNAs) did not change significantly in the dentate granule cell layer through this period of hippocampal development.

Lesion-induced alterations in hippocampal innervation

In adult rats, the perforant pathway was transected in order to induce the sprouting of fibers originating from the hippocampal CA4 region, entorhinal cortex, and the medial septal nucleus. Histological examination verified that the unilateral knife cut had severed completely the perforant pathway connecting the medial and lateral entorhinal cortex to the ipsilateral hippocampus. To verify that our knife cuts had induced sprouting in the hippocampus, AChE histochemistry was employed to demonstrate alterations in the cholinergic innervation to the dendritic fields (the molecular layer) of dentate granule cell neurons (Figure 27). AChE staining of the control (contralateral) side of a knife cut animal

Figure 25. Synapsin I mRNA in developing dentate granule neurons of the hippocampus. (A) Quantitation of the relative amounts of synapsin I mRNA in dentate granule neurons from the hippocampus of rats of postnatal ages 14, 21, and 31, respectively. Blots, generated as in (B), were scanned by densitometry. Data are means ± SEM. (B) RNA blot analysis of synapsin I mRNA and 18s ribosomal RNA in developing dentate granule neurons of the hippocampus. The same filters were used for both probes.

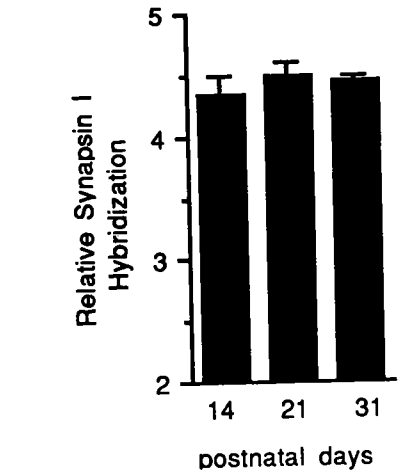
5
4
3
2
Relative Synapsin I Hybridization
14
21
31
postnatal days

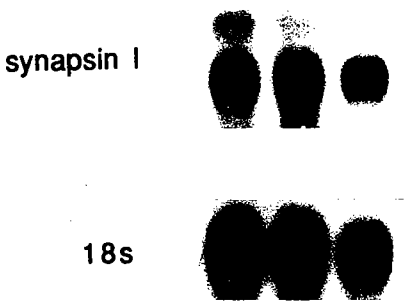
synapsin I
18s

Figure 26. Semi-quantitative evaluation of synapsin I mRNA and protein in developing dentate granule cell neurons and their mossy fiber terminals by *in situ* hybridization and immunohistochemistry, respectively. DG mRNA data represent film densitometry readings of synapsin I cDNA hybridization taken from the dentate granule cell layer. Mossy fiber protein data represent densitometry of synapsin I immunoreactivity taken from the hilar region of the dentate gyrus. Data are means ± SEM.

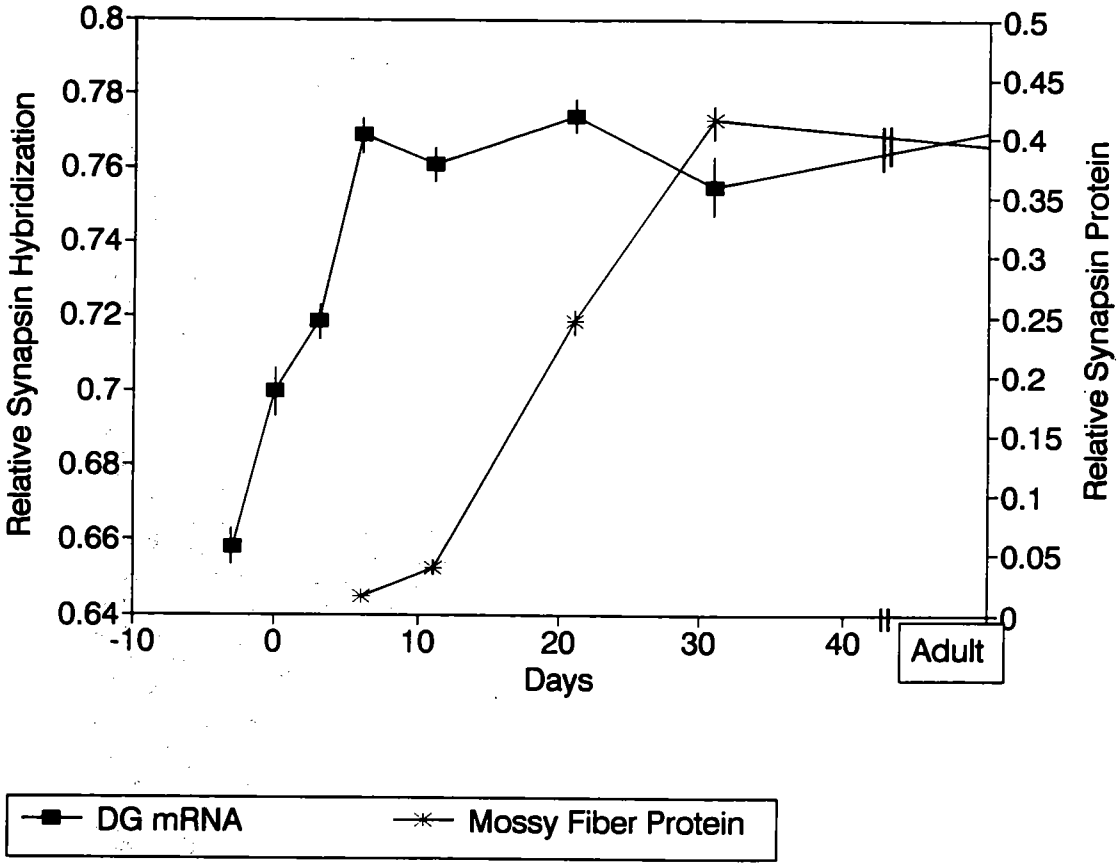
0.8
0.78
0.76
0.74
0.72
0.7
0.68
0.66
0.64
Relative Synapsin Hybridization
0.5
0.45
0.4
0.35
0.3
0.25
0.2
0.15
0.1
0.05
0
Relative Synapsin Protein
-10
0
10
20
30
40
Adult
Days
DG mRNA
Mossy Fiber Protein

(Figure 27C) demonstrated a staining pattern similiar to that observed in an unoperated naive control animal (data not shown). In these sections there was a dense zone of AChE staining in the most proximal aspect of the inner molecular layer of the dentate gyrus (the supragranular zone), and light homogeneous staining throughout the remainder of the molecular layer. In contrast, on the perforant pathway transection (ipsilateral) side of a knife cut animal, AChE histochemistry at 7, 14, and 31 days post lesion revealed a dense band of AChE-stained fibers within the middle molecular of the dentate gyrus (Figure 27B). The changes in AChE staining observed within the molecular layer reflect the reorganization and sprouting of cholinergic afferents from the ipsilateral medial septal nucleus, in response to the loss of afferents originating from the entorhinal cortex, thus confirming that the knife cut had denervated the hippocampus. The AChE reaction observed in response to perforant pathway transection was similar in intensity to those seen with electrolytic (Lynch et al., 1972) or aspirative (Nadler et al., 1977) entorhinal lesions.

The expression of synapsin I protein and mRNA following perforant pathway transection

It has been previously shown that lesions of the entorhinal cortex produce a myriad of cellular and molecular responses in pre- and postsynaptic components of the perforant pathway (Whittemore et al., 1987; Geddes et al., 1990a,b,c; May et ., 1990; Phillips and Steward, 1990; Poirier et al., 1990; Steward et al., 1990; Gibbs et al., 1991; Laping et al., 1991; Nichols et al., 1991, Poirier et al., 1991a,b; Chen and Hillman, 1992). One of these responses may be the recapitulation of the original developmental mechanisms of axonal guidance and growth in those cells whose remaining efferent fiber projections sprout in response to lesion (Geddes et al., 1990; Poirer et al., 1991). Another response may be the attenuation of membrane bound receptors, ultimately altering the signalling between effector and target neurons (Taxt and Storm-Mathison, 1984; Anderson et al., 1991)

Recently, it has been suggested that the regulation of synapsin expression may be

Figure 27. Changes in AChE staining in the molecular layer of the dentate gyurs 14 days following transection of the perforant pathway. (A) Camera-lucida drawing at the horizontal level from which AChE staining was photographed. The extent of the perforant pathway knife cut is indicated by a dashed line and arrowheads. (B) Section of the dentate gyrus from the ipsilateral side of a knife cut animal stained with acetylcholinesterase histochemistry. In this section, there is a dense band of staining within the molecular layer, confirming that the knife cut deafferented the hippocampus. (C) Section of the dentate gyrus from the contralateral side of the same animal in (B) stained with acetylcholinesterase. This section reveals homogeneous staining throughout the molecular layer. g, granule cell layer, hippocampus; Hp, hippocampus; i, inner molecular layer, dentate gyrus; m, middle molecular layer, dentate gyrus; MS, medial septal nucleus; o, outer molecular layer, dentate gyrus.

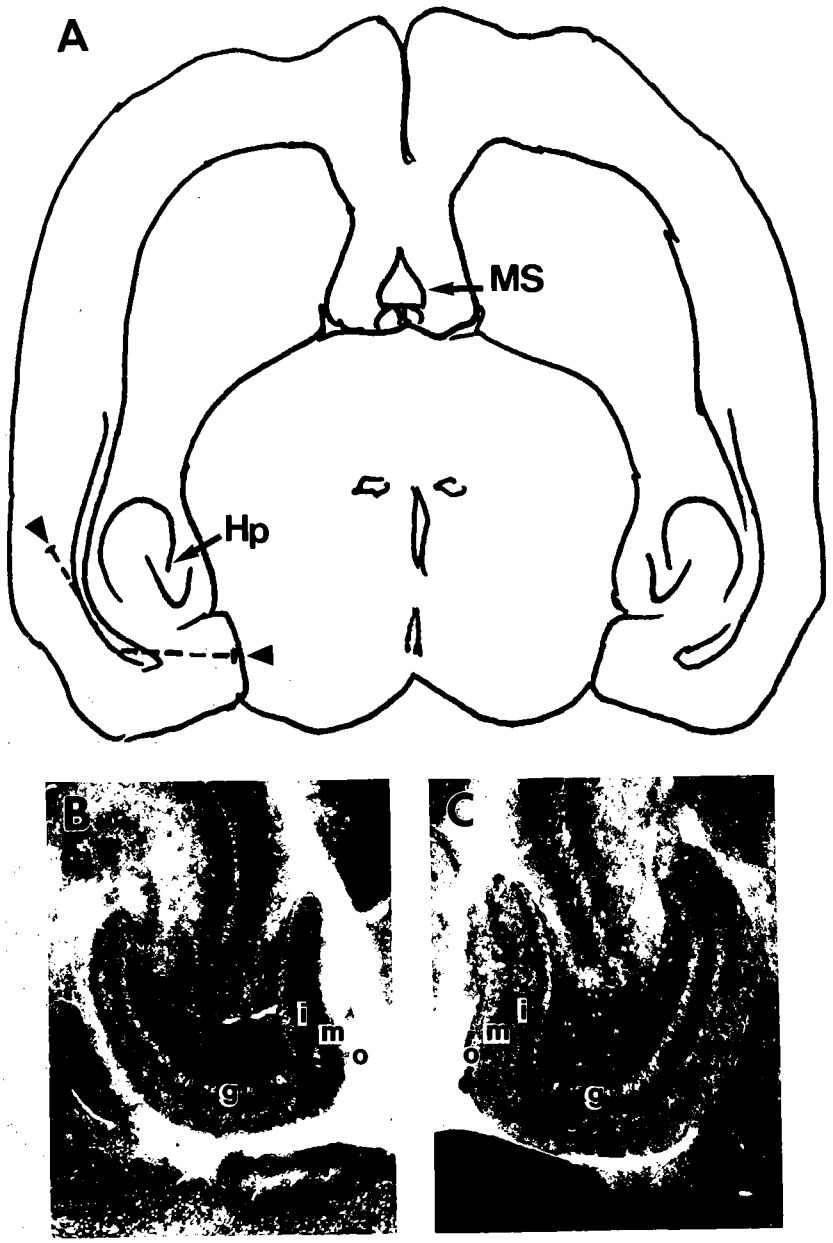
A
MS
Hp
B
m
o
g
C
m
o
g

involved in chronic changes in neuronal signalling, and that the synapsins may contribute to a neuron's capacity for short- and long-term synaptic plasticity (Han et al., 1991; Melloni et al., 1993 and Chapter V). Thus, to examine the regulation and putative role of synapsin I gene expression during the restoration of functional synaptic contacts within the CNS, the perforant pathway was surgically transected in adult rats, and anterograde and retrograde neuronal populations were assayed for relative levels of synapsin I protein and mRNA.

Synapsin I protein following perforant pathway transection

Immunohistochemistry. Following unilateral perforant pathway transection, axons travelling to the molecular layer of the ipsilateral dentate gyrus degenerate, and the normal pattern of synapsin I immunoreactivity in this brain region is significantly altered (Figure 28). In unoperated control animals, the molecular layer of the dentate gyrus displayed a moderate, relatively uniform pattern of immunoreactivity with synapsin I antibodies (Figures 28A,B, see Chapter V, Figure 21). Following transection of the perforant pathway, the distribution and intensity of synapsin I immunostaining in the molecular layer changed in a very ordered fashion (Figure 28C-H). When compared with control sections, the pattern of synapsin I immunoreactivity in the molecular layer was unaffected 1 day post-perforant pathway transection (Figure 28C). The molecular layer revealed a homogenous plexus of immunoreactivity, indicative of the uniform synaptic input along dendrites of the granule cell neurons.

From the second day post-transection, however, synapsin I immunostaining in the molecular layer changed dramatically. In sharp contrast to the homogenous pattern of staining observed throughout the molecular layer in control and 1 day post-transection tissue, the relative levels of synapsin I immunoreactivity decreased in the outer two-thirds of the molecular layer (the middle and outer molecular layers) between 2 and 4 days post-perforant pathway transection, reflecting the zone of deafferentation (Figures 28D and E).

Figure 28. Immunohistochemical localization of synapsin I in the molecular layer of the dentate gyrus following transection of the perforant pathway. (A) Low magnification of the distribution of synapsin I protein in control hippocampus. The area boxed represents the region of the dentate gyrus analyzed. (B) The distribution of synapsin I obtained in a control molecular layer. The molecular layer of the dentate gyrus displays a moderate, relatively uniform pattern of immunoreactivity with synapsin I antibodies. (C-H) The distribution of synapsin I obtained in the molecular layer of dentate gyrus ipsilateral to perforant pathway transection 1-31 days post-knife cut. (C) Synapsin I protein levels were unaffected in the molecular layer 1 day post perforant pathway transection. (D,E) Clearing of synapsin I immunoreactivity from the MML and OML, 2 and 4 days post-perforant pathway transection. (F-G) Increase in immunoreactivity to synapsin I in the OML and MML indicative of reactive synaptogenesis in these zones, 7 and 14 days post-perforant pathway transection, respectively. (H) By 31 days post-perforant pathway transection, the molecular layer revealed a moderate, near homogenous pattern of synapsin I immunoreactivity, similar to that seen in control tissue. The arrowhead in each panel denotes the hippocampal fissure. DG, dentate granule cell neurons; IML, innermolecular layer; ML, molecular layer; MML, middle molecular layer; OML, outer molecular layer; H, hilar region.

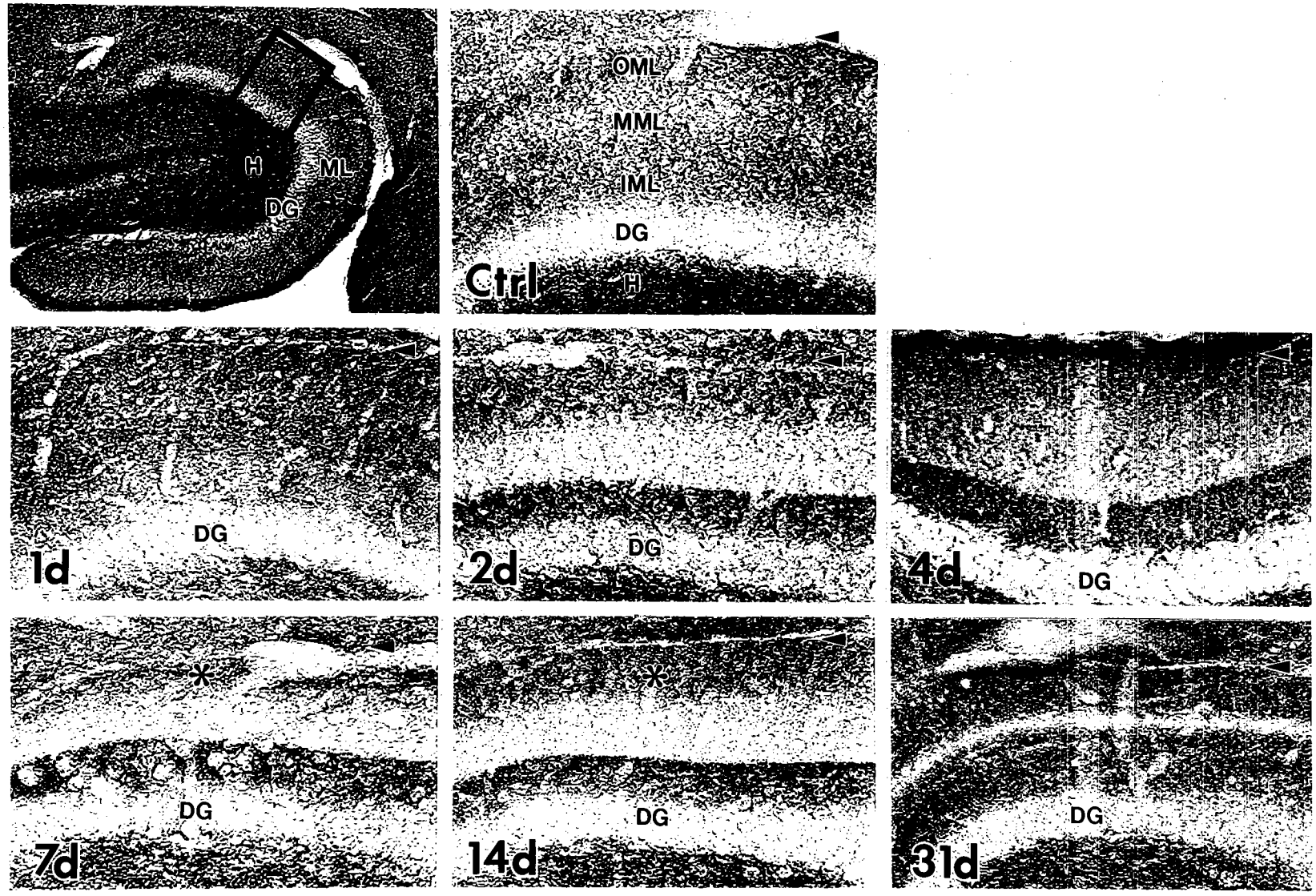
H
ML
DG
OML
MML
IML
DG
Ctrl
H
1d
DG
2d
DG
4d
DG
7d
*
DG
14d
*
DG
31d
DG

The inner molecular layer remained moderately immunoreactive, while the middle and outer molecular layers retained only a fraction of their normal immunoreactivity.

From day 4 onward, following perforant pathway transection, a relative increase in immunoreactivity to synapsin I antiserum was observed in particular subregions of the molecular layer which varied with survival time. By 7 days post-transection, a slight increase in synapsin I immunoreactivity was observed in the outer molecular layer, however, the middle molecular layer remained only lightly stained (Figure 28F). Staining in the outer molecular layer increased through 14 days post-transection as synapsin I specific immunostaining in this region became wider and more intense than at earlier time points (Figure 28G). By 31 days post-transection, a striking change in distribution and intensity of synapsin I immunostaining was observed in the molecular layer of the dentate gyrus, as this region now revealed a moderate, near homogenous pattern of immunoreactivity to synapsin I antibodies, similar to that seen in control tissue (Figure 28H). Within this region, however, the molecular layer was divided by a very thin zone of light staining separating two uniformly stained regions. In some regions of the molecular layer this border was barely discernable. Although there were significant overall changes in the pattern and intensity of synapsin I immunoreactivity in the molecular layer of the dentate gyrus ipsilateral to perforant pathway transection during the 30 days post-transection, no comparable changes were observed in the contralateral hippocampus, or in either hippocampal region of sham-operated or naive control animals.

Synapsin I mRNA following perforant pathway transection

In situ hybridization. In contrast to the dramatic changes observed in the pattern and intensity of synapsin I immunostaining in the molecular layer of the dentate gyrus following perforant pathway transection, the levels of synapsin I-specific hybridization did not change significantly during denervation and reinnervation of dentate granule neurons (Figures 29-33). In fact, *in situ* localization of synapsin I mRNA in sections throughout

the brains of animals that had survived 1-31 days post-perforant pathway transection displayed control, steady-state levels of synapsin I mRNA expression in all areas affected by the lesion (Figure 29). For example, the distribution and intensity of hybridization to synapsin I probes within the deafferented dentate gyrus (ipsilateral) was indistinguishable from labeling in the dentate gyrus contralateral to transection and the bilateral hippocampi of sham operated and naive control rats (Figure 29C,D). Further, tissue from perforant pathway transected and control rats showed no contralateral/ipsilateral differences in synapsin I-specific hybridization intensity in neurons of the medial septal nucleus (Figure 29B) or CA4 neurons of the hippocampus (Figure 29C,D), those regions responsible for the changing pattern of distribution of synapsin I immunoreactivity during the reorganization and sprouting of afferents to the molecular layer of the dentate gyrus. However, not suprisingly, labeling intensity was slightly decreased in the entorhinal cortex ipsilateral to perforant pathway transection (Figure 29C,D), as this surgical procedure results in an approximate 28% loss of large layer II stellate neurons in the medial entorhinal cortex (Cummings et al., 1992).

RNA blot analysis. *In situ* hybridization data were independently confirmed by RNA blot analysis. These analyses showed no significant difference in the levels of expression of both the 4.5kb and 3.4kb forms of synapsin I mRNAs in deafferented (ipsilateral) and contralateral regions of experimental animals and sham-operated- and naive control animals, sacrificed at varied survival times post-perforant pathway transection (Figure 30). Further, there were no significant differences in the level of expression of synapsin I mRNA in neurons in either the hippocampal subfield CA4 (Figure 31) or the medial septal nucleus (Figure 32). There was, however, a slight, although insignificant, decrease in synapsin I mRNA observed in layer II stellate neurons of the ipsilateral entorhinal cortex (Figure 33).

Figure 29. Expression of synapsin I mRNA in medial septal, hippocampal, and entorhinal neurons by *in situ* hybridization 31 days following transection of the perforant pathway. (A) Camera-lucida drawing of the regions from which synapsin I mRNA was analyzed (Boxes). (B-D) Dark-field photomicrographs of emulsion-coated horizontal sections obtained from the medial septum (B) and the hippocampus ipsilateral (C) and contralateral (D) to perforant pathway transection. Note the uniform levels of expression of synapsin I mRNA in the medial septal and hippocampal CA4 neurons ipsilateral and contralateral to lesion. The apparent increase in synapsin I mRNA in the contralateral layer II cells of the entorhinal cortex reflects cell loss in the same area ipsilateral to lesion. DG, dentate gyrus; EC, entorhinal cortex; MS, medial septal nucleus.

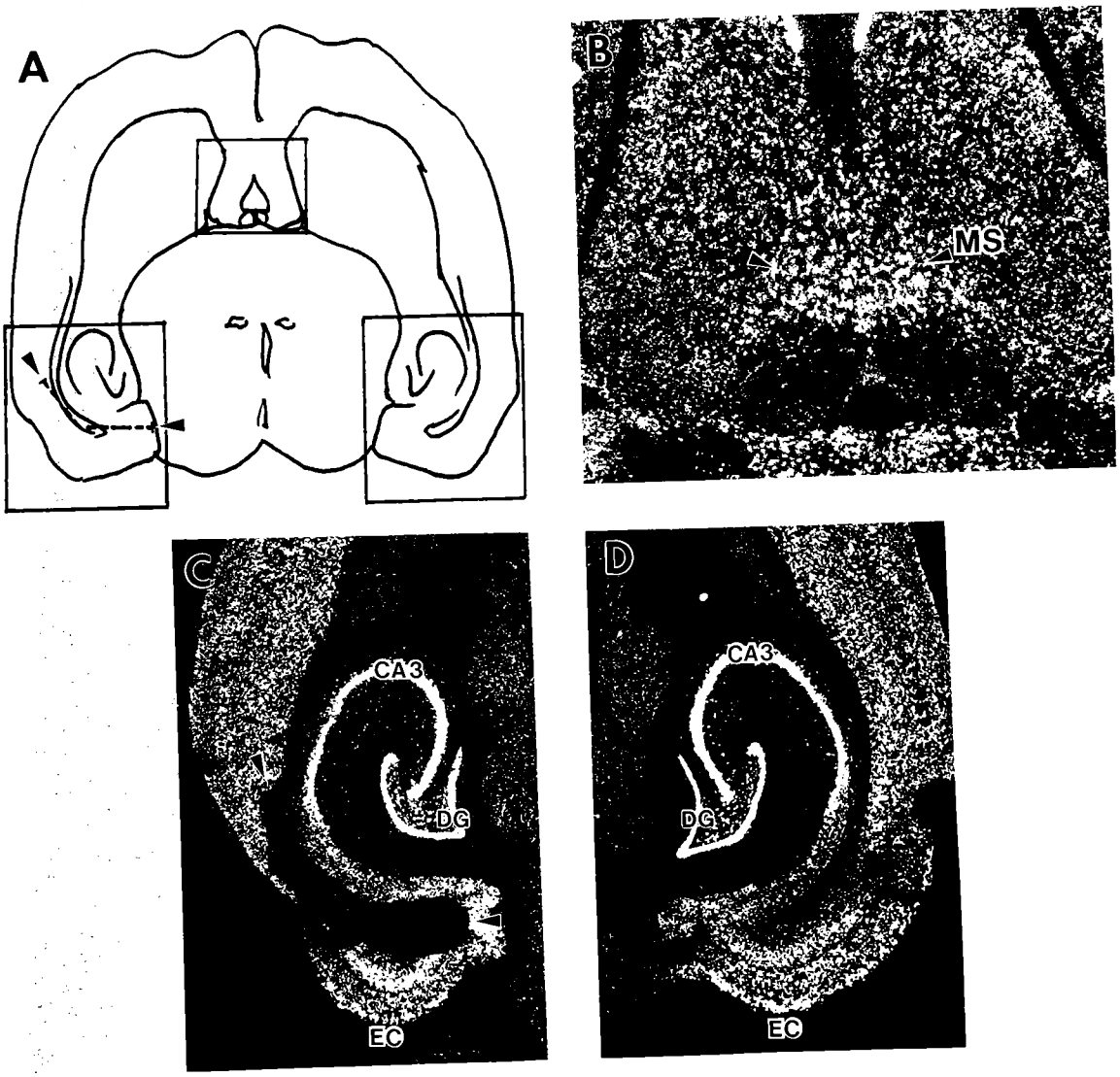
A
B
MS
C
CA3
DG
EC
D
CA3
DG
EC

Figure 30. Time course of the effects of perforant pathway transection on synapsin I mRNA expression in the dentate granule neurons. Lower half of the figure shows original RNA blot from brain punches hybridized with synapsin I or 18s ribosomal RNA specific probes. Bar graph shows changes in synapsin I mRNA levels in neurons ipsilateral and contralateral to lesion with time post-lesion, normalized against 18s rRNA signal.

DENTATE GRANULE NEURONS

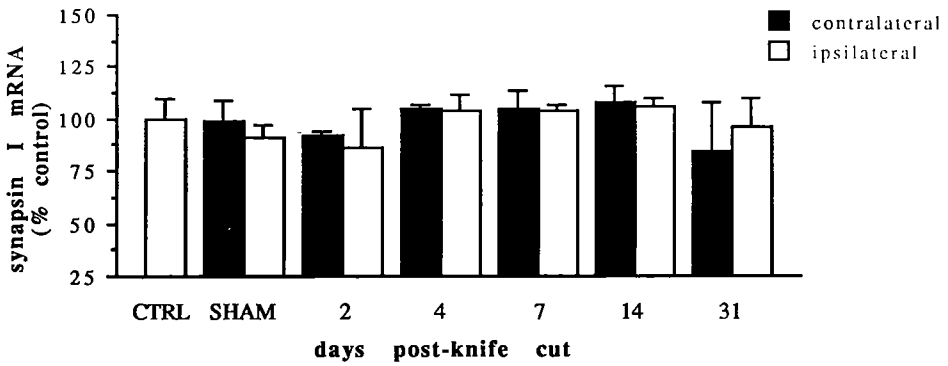

Figure 31. Time course of the effects of perforant pathway transection on synapsin I mRNA expression in hippocampal CA4 neurons. Lower half of the figure shows original RNA blot from brain punches hybridized with synapsin I or 18s ribosomal RNA specific probes. Bar graph shows changes in synapsin I mRNA levels in neurons ipsilateral and contralateral to lesion with time post-lesion, normalized against 18s rRNA signal.

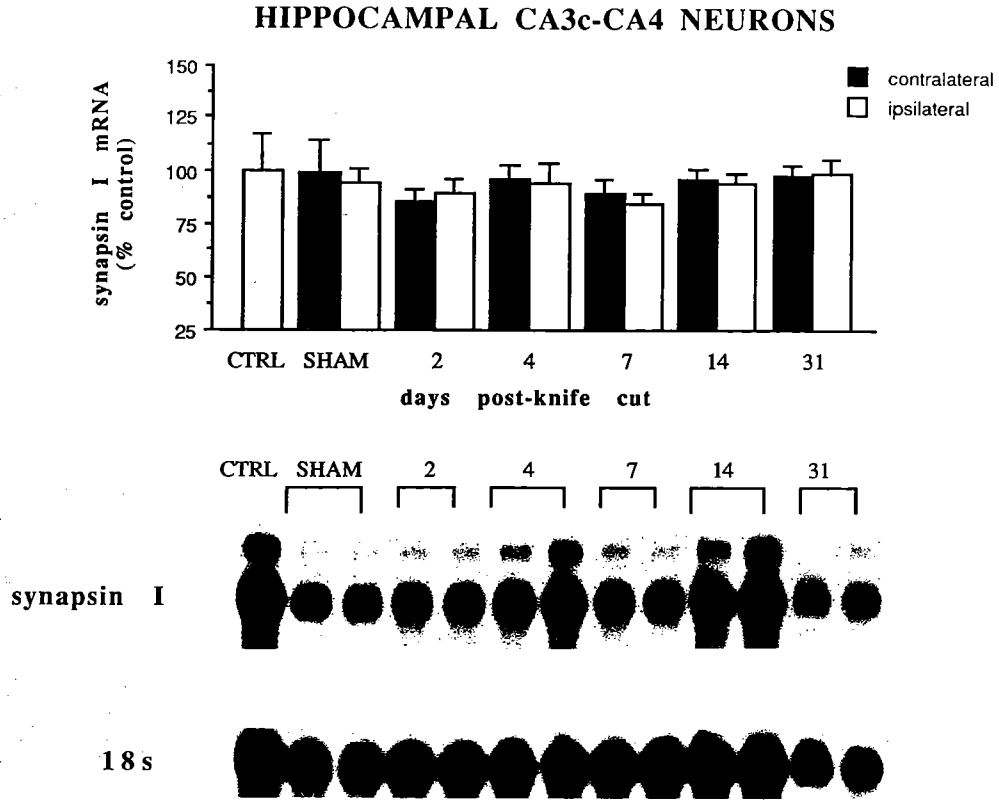
HIPPOCAMPAL CA3c-CA4 NEURONS
synapsin I mRNA (% control)
150
125
100
75
50
25
contralateral
ipsilateral
CTRL SHAM 2 4 7 14 31
days post-knife cut
CTRL SHAM 2 4 7 14 31
synapsin I
18s

Figure 32. Time course of the effects of perforant pathway transection on synapsin I mRNA expression in the medial septal neurons. Lower half of the figure shows original RNA blot from brain punches hybridized with synapsin I or 18s ribosomal RNA specific probes. Bar graph shows changes in synapsin I mRNA levels in neurons ipsilateral and contralateral to lesion with time post-lesion, normalized against 18s rRNA signal.

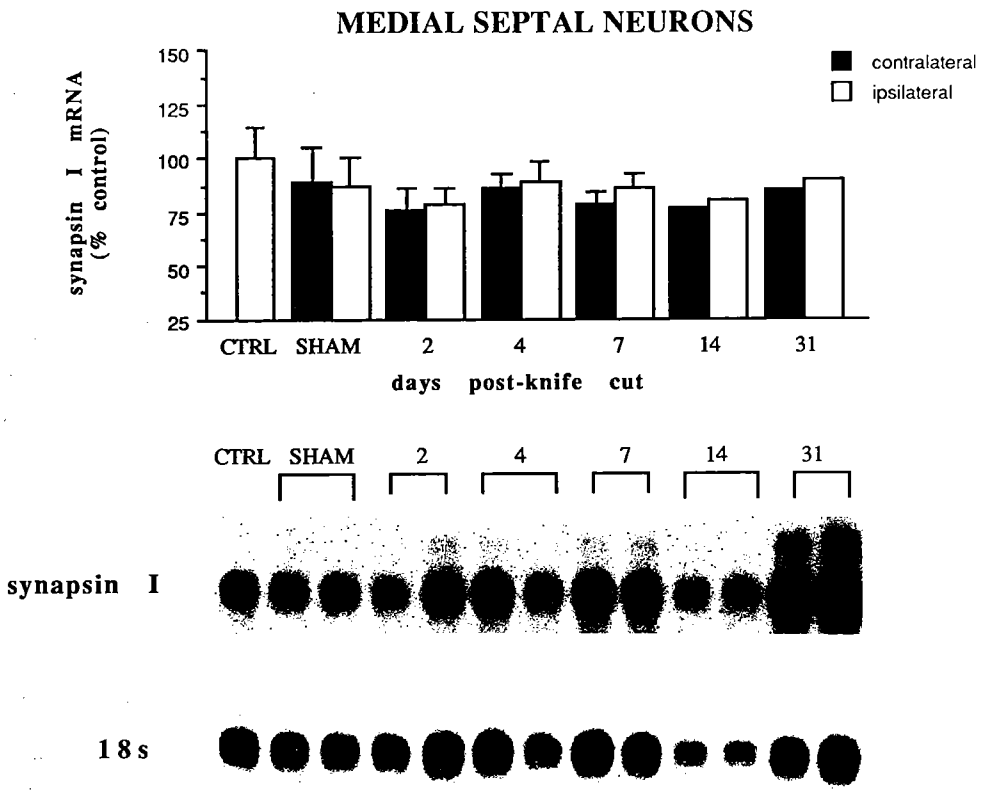
MEDIAL SEPTAL NEURONS
contralateral
ipsilateral
synapsin I mRNA
(% control)
150
125
100
75
50
25
CTRL
SHAM
2
4
7
14
31
days post-knife cut
CTRL SHAM 2 4 7 14 31
synapsin I
18s

Figure 33. Time course of the effects of perforant pathway transection on synapsin I mRNA expression in layer II cells of the entorhinal cortex. Lower half of the figure shows original RNA blot from brain punches hybridized with synapsin I or 18s ribosomal RNA specific probes. Bar graph shows changes in synapsin I mRNA levels in neurons ipsilateral and contralateral to lesion with time post-lesion, normalized against 18s rRNA signal.

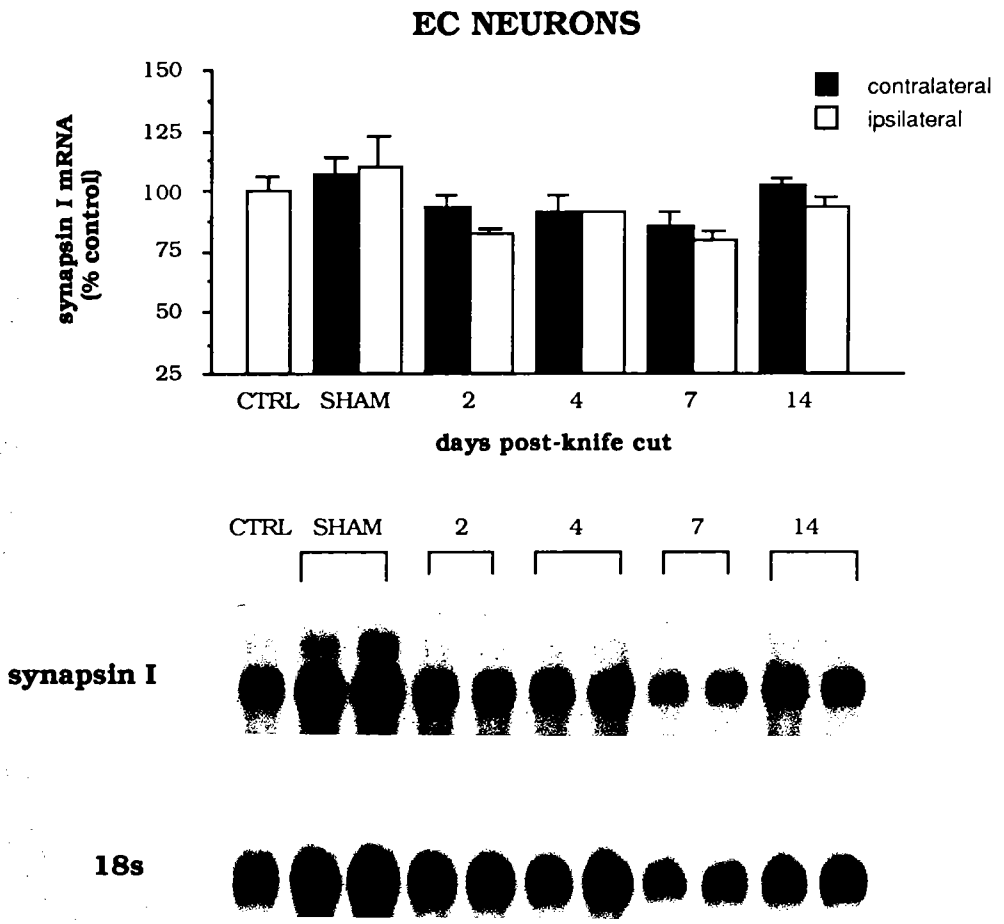
EC NEURONS
150
125
100
75
50
25
synapsin I mRNA
(% control)
contralateral
ipsilateral
CTRL
SHAM
2
4
7
14
days post-knife cut
CTRL
SHAM
2
4
7
14
synapsin I
18s

Discussion

Although the specific molecular mechanisms underlying the release of neurotransmitter from presynaptic nerve terminals remain unknown, several lines of evidence implicate synapsin I in the regulation of the release process (for reviews, see Sudhof and Jahn, 1991; Greengard et al., 1993). Likewise, during CNS development, while recent studies *in vitro* have provided evidence suggesting a role for synapsin I in the functional maturation of peripheral synapses, its precise physiological role in the development of the central nervous system has not been elucidated. To better understand the relationship between the expression of the synapsin I gene (mRNA and protein) and particular cellular events during development, i.e., the establishment of synaptic contacts in the central nervous system, immunohistochemistry and *in situ* hybridization histochemistry were employed to localize the expression of synapsin I protein and mRNA throughout the development and reinnervation of the rat hippocampus. These data demonstrate that synapsin I protein levels change dramatically during the establishment of synaptic contacts in the developing hippocampus and during the process of reinnervation of deafferented dentate granule cell neurons after perforant pathway transection, while changes in the levels and pattern of expression of synapsin I mRNA were not found to accompany new synapse formation.

Synapsin I mRNA and protein during the development of dentate granule neurons and their mossy fiber terminals

The morphogenic, neurogenic, and synaptogenic development of the dentate granule cell neurons of the hippocampus have been extensively studied in the rodent CNS (Altman and Das, 1965; Bayer and Altman, 1974; Hine and Das, 1974; Schlessinger et al 1975; Kaplan and Hinds, 1977; Bayer, 1980a,b). The morphogenesis of the dentate gyrus

follows from the pattern of neurogenic differentiation of dentate granule neurons in the developing hippocampus, as undifferentiated granule cell precursors and immature, differentiated granule cell neurons migrate radially from the hilus and gradually accumulate in the granule cell layer (Altman and Das, 1965,1966; Altman, 1966; Bayer and Altman 1974; Schlessinger et al, 1975; Bayer, 1980a; Crespo et al., 1986). This pattern of development proceeds from the tip of the lateral (ectal) blade to the medial (endal) blade of the dentate gyrus, such that by postnatal day 21, >80% of adult level of mature granule cells are acquried by the granule cell layer, and the morphological pattern is essentially that observed in the adult (Bayer and Altman, 1974; Bayer, 1980; Gaarskjaer, 1985).

The pattern of synapsin I mRNA expression revealed by *in situ* hybridization is entirely consistent with the morphogenic pattern of development of the dentate granule cell layer (Figure 24). At the time of birth (P0), as the morphogenesis of the dentate gyrus begins, synapsin I mRNA is already present in the lateral blade of the developing dentate granule cell layer (Figure 24A, B). As development proceeds through postnatal day 5/6 (Figure 24C, D), the level of synapsin I mRNA increases in the hilar zone and the distinct lateral and medial blades of the dentate gyrus become evident. Hybridization intensity in the hilar region is greatest between postnatal day 5 and postnatal day 8, during the peak period of neurogenic differentiation of the developing granule cell neurons of the dentate gyrus. During this time, at least 50,000 neurons are being generated per day, in total, representing >25% of the complement of the adult dentate gyrus (Schlessinger et al., 1975). Synapsin I mRNA levels are high in both the lateral (ectal) and medial (endal) blades of the dentate gyrus already by this time in postnatal development, nearly equal to those observed in the adult. By postnatal day 11 and beyond, the segregated appearance, pattern, and relative intensity of hybridization to synapsin I probes in the dentate gyrus indicate that synapsin I mRNA levels are equal to those observed in the adult rat central nervous system (Figure 24E-J). Further, RNA blot analysis shows adult, steady state levels of both the 4.5 kb and 3.4 kb forms of synapsin I mRNA are present by postnatal

day 14 and continue through postnatal day 31 in the dentate granule cells of the developing dentate gyrus. These data confirm our observations *in situ*, that adult levels of synapsin I mRNA are present in dentate granule neurons in the second postnatal week.

From the viewpoint of neuronal competition, the appearance of high levels of synapsin I mRNA immediately upon the neurogenic differentiation of dentate granule cell precursors suggests that synaspin I gene expression may preload neurons to allow for rapid synapse formation upon contact with a limiting number of targets during synaptogenesis. However, the appearance of detectable levels of synapsin I protein by immunohistochemistry does not conform to the developmental pattern of expression suggested by the levels of its mRNA. Synapsin I mRNA in granule cell neurons of the developing dentate gyrus reached its high, near adult levels of expression by postnatal day 6. In contrast, very little, if any, synapsin I protein was present in the mossy fiber terminal fields of these neurons at this time in development. In fact, synapsin I protein does not begin to accumulate in mossy fiber terminals until approximately postnatal day 21, or reach its adult concentration in these terminals until around postnatal day 31.

The comparatively late appearance of synapsin I protein in the hilar region of the dentate gyrus during development could have several explanations. One possible explanation for this discrepancy is that mossy fiber terminals of dentate granule neurons are not present until later in the developmental period, beyond postnatal day 21. However, histochemical as well as fluorescent tracing studies suggest that mossy fiber terminals establish synaptic contact with the cells in the hilar region and with proximal dendrites of adjacent pyramidal neurons of hippocampal zones CA3 (regio inferior) very early in the developmental period, and that the mossy fiber zone has the adult segregated appearance at the outset of postnatal life (Stirling and Bliss, 1978; Zimmer and Haug, 1978; Amaral and Dent, 1981, 1985). Further, Gaarskjaer (1985) and Amaral and Dent (1981) have shown that the mossy fibers and their connections are, in principle, fully matured morphologically, by postnatal day 10-15, although a more subtle and protracted development of the system

persists long into adulthood.

High levels of synapsin I mRNA in dentate granule cell neurons coupled with a lack of immunostaining of synapsin I protein in their mossy fiber terminals early in the postnatal developmental period could suggest that the protein is produced at adult levels in neurons of the developing dentate gyrus but not localized to and concentrated in the presynaptic nerve terminals until relatively late in the development of those cells. However, in contrast to the uniform level of synapsin I mRNA expressed in the dentate gyrus during this period of granule cell development, Western blot analysis of protein prepared from dentate granule neurons and their mossy fiber terminals clearly shows that levels of synapsin I protein present at postnatal day 31 are 2-5 fold higher than those present 10 days earlier at postnatal day 21. Thus, although the synapsin I gene establishes its high adult level of mRNA expression early in the development of the dentate gyrus, by P6-P11, synapsin I protein does not reach its extremely high, adult levels in the presynaptic nerve terminals of granule cell neurons until well into the postnatal developmental period, around postnatal day 31. Differences in the turnover of synapsin I mRNA and/or protein may result in the developmental patterns of expression observed in the dentate granule neurons. Since our studies measure steady-state levels of synapsin I mRNA and protein, the extent to which differences in mRNA and protein stability are involved remains unknown.

Alternatively, the comparatively late postnatal appearance and accumulation of synapsin I protein in the mossy fiber terminals of dentate granule neurons could suggest that synapsin I gene products mediate different functions in the developing and adult nervous systems. Recently, it has been proposed that synapsin I may participate in the functional maturation of developing peripheral synapses by promoting the maturation of secretion mechanisms during development (Lu et al., 1992). A review of the development and maturation of the dentate area and the mossy fiber projection system suggests that cells of this region form a morphologically mature structure relatively early in the developmental period, acquiring >80% of its cells by postnatal day 21, and the mature complement of its

synaptic staining and dendritic expansions between postnatal days 10-15(18) (Zimmer and Haug, 1978; Amaral and Dent, 1981; Gaarskjaer, 1981, 1985). Electrophysiological studies suggest that mossy fiber synapses do not elicit mature synaptic events until or after postnatal day 15, as population spikes may only be reliably elicited after this stage of hippocampal development (Bliss et al., 1974). Since detectable levels of synapsin I protein begin to appear in the mossy fiber terminals of dentate granule neurons on or around postnatal day 21 of development (and not at adult levels until after this time), the lag in detection suggests that synapsin I protein is only fully accumulated in presynaptic nerve terminals during the functional maturation of their synapses. Further, this phenomenon may be a general property of the expression of synaptic terminal proteins, as the synaptic vesicle protein, synaptophysin, increases as well in the mossy fiber zone through this period of hippocampal development.

Synapsin I protein and mRNA in target and sprouting neurons following transection of the perforant pathway

Lesions of hippocampal circuitry produce strikingly similar observations to those made during hippocampal development. Following entorhinal cortex ablation and/or perforant pathway transection, fibers originating from extra- and intrahippocampal neurons reinnervate the deafferented dentate gyrus, restoring active synapses to the outer and middle molecular layers of its dendritic field (Lynch et al, 1972; Lynch et al., 1973, 1977; Zimmer, 1973; Zimmer and Hjorht-Simonsen, 1975; Steward and Vinsant, 1983). This process begins a few days after deafferentation (3-4 days), until virtually all the lost inputs are replaced, and the synaptic density of middle and outer molecular layers is approximately 80% of their prelesion values, by 2-6 months post-lesion (Hoff et al., 1982; Steward and Vinsant, 1983).

From a functional standpoint, physiological and behavioral studies (Steward et al., 1973; Loeshe and Steward, 1977; Steward, 1981; Reeves and Steward, 1988) have

demonstrated that neuronal sprouting in the molecular layer of the dentate gyrus is important for the recovery of unit activity of neurons in the dentate granule cell layer and of learned alternation behavior after unilateral entorhinal cortex lesions, and most significantly, that these activities recover to levels comparable to prelesion controls between 8-14 days post-lesion. A comparison between the time course and pattern of synapsin I immunoreactivity and sprouting-related physiological and behavioral changes suggests that the reappearance of synapsin I protein in the molecular layer of the dentate gyrus correlates, temporally and topographically, with the recovery of synaptic function in this region. Synapsin I immunoreactivity increases during the reinnervation of the molecular layer, beginning first in the outer molecular layer around 7 days post-lesion and increasing to control levels in this region by 14 days post-lesion. This increase in synapsin I in the outer molecular layer correlates with the proliferation of the crossed temporodentate pathway (CTD), a functionally homologous pathway originating in the contralateral entorhinal cortex. This pathway is known to participate in the physiological and behavioral recovery of function following unilateral entorhinal cortex lesions (Steward et al., 1973; Steward, 1976; Loeshe and Steward, 1987). Further, the post-lesion time course of increase in synapsin I protein in the outer molecular layer correlates precisely with the time course of post-lesion increases in CTD evoked potentials (Reeves and Smith, 1987) and the recovery of T-maze alternation performance (Loeshe and Steward, 1977), reaching prelesion values by 14 days post-lesion. By 31 days post-lesion, well before the process of reinnervation establishes pre-lesion synaptic density, but after the restoration of physiological and behavioral function, the molecular layer revealed a moderate, near homogenous pattern of synapsin I immunoreactivity, similar to that seen in sham-operated and naive control tissue. In accord with the developmental studies, these data suggest that during the establishment/restoration of functional synaptic contacts in the lesioned hippocampus, the appearance of synapsin I protein in the neuropil does not reflect simply synaptogenesis, but coincides temporally and topographically, with the functional maturation of newly created

synapses in the central nervous system.

Previously our laboratory has shown that the peak expression of synapsin I mRNA coincides with the major period of synapse formation of the granule cell population in the developing rat cerebellum (Haas and DeGennaro, 1988). More recently, we have confirmed these observations in the granule cells of the developing rat hippocampus (Melloni and DeGennaro, submitted; see Chapter IV). Therefore, since it appears that synapsin I gene expression is regulated in a coordinate fashion with synaptogenesis, it might be predicted that this expression would undergo changes in both target and sprouting neurons in response to and during the denervation and reinnervation of the hippocampus.

Recently, several studies have shown changes in the expression of mRNAs such as prodynorphin and proenkephalin (Xie et al., 1990), SNAP-25 (Geddes et al., 1990b,c), Tα-tubulin (Geddes et al., 1990ab; Poirier et al., 1990, 1991), and SGP2 (May et al., 1990), in the hippocampus in response to variations in neuronal activity and connectivity. In contrast, during the early period of denervation following entorhinal cortex ablation and through the time that innervation is reestablished as a result of neuronal sprouting, hippocampal type II calcium calmodulin-dependent protein kinase, β-NGF and α-actin mRNAs levels have been shown not to change (Whittmore et al., 1987; Benson et al., 1992). By *in situ* hybridization and RNA blot analysis, our data revealed that the level of expression of synapsin I mRNA in granule cell neurons of the contra- and ipsilateral dentate gyrus did not significantly differ following perforant pathway transection from that of naive or sham-operated control animals. As deafferentation of the dentate gyrus by EC lesion results in the removal of approximately 60% of the total innervation to dentate granule cell neurons, reducing the ongoing activity of those neurons by an average of 60%-80% at early post-lesion intervals (1-4 days post-lesion) (Reeves and Steward, 1988), the most straightforward interpretation of these results is that neuronal activity is not necessary for the maintenence of high levels of synapsin I gene expression in neurons of the dentate granule cell layer of the adult hippocampus, and that neuron-target interactions are not

important in synapsin I gene regulation in the adult animal.

During the reinnervation of the denervated dentate gyrus, those neurons responsible for forming active synapses in the deafferented zone have been shown to express elevated levels of Tα1 tubulin, SNAP-25, and $p75^{NGFR}$ mRNAs (Geddes et al., 1990ab; Gibbs et al., 1991). In contrast, by *in situ* hybridization and RNA blot analysis, our studies revealed no significant changes in the relative levels of synapsin I mRNA in neurons in those brain regions responsible for the sprouting response following perforant pathway transection. Since dramatic changes in the pattern and intensity of synapsin I immunoreactivity were observed in the molecular layer during its reinnervation, this observation implies that increased synthesis of synapsin I mRNA is not necessary for the large increases in synapsin I protein observed in the terminal fields of sprouting neurons. Rather, it is likely that the synapsin I gene is stably expressed in mature, differentiated neurons in the adult animal, undergoing very little, if any, further regulation after development. Studies of synapsin I gene expression *in vitro* support this conclusion, as expression of the synapsin I gene in PC12 cells shows only modest increases (approximately 2 fold) upon treatment with agents that promote neuronal differentiation (Howland et al., 1991). In fact, inspection of the 5' flanking promotor region of the rat synapsin I gene reveals a GC-rich sequence lacking the conventional TATA and CAAT box elements (Howland et al., 1991). Such promotor sequences share striking homology to elements in a large subclass of stably expressed genes, including several housekeeping genes (Smale and Baltimore, 1989; Blake et al., 1990). It is reasonable to conclude then, that the synapsin I gene is further regulated at some post-transcriptional or translational level during development and hippocampal reinnervation, as differential levels of synapsin I protein occur without concommitant changes in levels of synapsin I mRNA.

In conclusion, the data presented in this chapter present a detailed comparision of the time course and pattern of hippocampal synapsin I gene expression (mRNA and protein) during development and in response to selective denervating lesions. On a

molecular level, both developmental and lesion data suggest that the expression of the synapsin I gene is tightly regulated in the CNS, as considerable changes in synapsin I protein occur in neurons without concommitant changes in levels of its mRNA. From a functional standpoint, the data suggests that the appearance/reappearance of synapsin I protein in the neuropil of developing and sprouting neurons does not reflect simply synaptogenesis, but coincides temporally and topographically, with the period of the functional maturation of those central synapses. Thus, examination of synapsin I immunoreactivity in the brain may be used as a sensitive indicator of the establishment/maintenence and/or the loss/recovery of functional synapses in the CNS. As such, this phenomenon may be useful in investigating alterations in neural circuitry in response to CNS injury and in variety of neuropathological conditions such as temporal lobe epilepsy and Alzheimer's disease.

Chapter VII

DISCUSSION

As discussed in the previous chapters, there is a growing body of evidence which suggests that the expression of the neuron-specific phosphoprotein synapsin I plays an important role in the establishment and maintenance of synapses in the developing nervous system and in the restoration of synapses in the pathologically damaged nervous system. However, until now, the regulation of the expression of the synapsin I gene and its relationship to the expression of synapsin I protein during the formation of functional synapses in the CNS had not been described. To this end, experiments presented in this dissertation examine (1) the patterns of expression of the synapsin I gene in the normal developing and adult rodent nervous systems, (2) the relationship between the levels of expression of synapsin I mRNA and protein during the development and maintenance of synapses in the neonatal and adult rodent hippocampal formation, (3) the regulation of synapsin I gene expression (mRNA and protein) during synaptic turnover and reorganization in the hippocampal formation following lesions of the perforant pathway. The results of these experiments, their significance, and the implications for future work are discussed below.

Synapsin I gene expression *in vivo*.

Developmental studies of synapsin I gene expression

In vivo, synapsin I protein was found to appear in neuropil regions of the nervous system coincident with the peak period of synaptogenesis (Lohman et al., 1978; De Camilli et al., 1983a,b; DeGennaro et al., 1983). In fact, studies by Mason (1986) reveal the presence of the protein in growth cones of basket cell neurons in the developing

cerebellum. Based on these data it is possible that synapsin I plays a role in the very early development of the rat nervous system. Indeed, recent studies by Han et al. (1991) and Lu et al. (1992) provide evidence that the synapsins participate in the morphological and functional maturation of secretion mechanisms.

We have used *in situ* hybridization to localize the expression of the synapsin I gene throughout the embryonic and postnatal development of the rat nervous system. These data reveal that the expression of the synapsin I gene is high in utero, and remains high in the central nervous system throughout postnatal life in the rat. Our localization of synapsin I mRNA during CNS development provides insight into the temporal and spatial expression of the synapsin I gene in relation to the state of differentiation of particular types of neurons. Given the time frame of expression, our data clearly show that the temporal onset of synapsin I gene expression precedes the process of synaptogenesis, which constitutes a late event in brain development, occuring mainly between the first and fourth postnatal week in the rat (Aghajanian and Bloom, 1967; Lohmann et al., 1978). Studies of synapsin I gene expression during the early postnatal development of the rat cerebellum and hippocampus reveal a biphasic pattern of expression of the gene in developing neurons. In the cerebellum, the first phase of synapsin I gene expression (the temporal onset of expression of synapsin I mRNA) is shown to be coincident with the period of terminal differentiation of Purkinje and granule cell precursors after their final cell division (neurogenesis). This observation is confirmed in the developing granule cell population of the rat hippocampus, as a burst of synapsin I-specific hybridization is observed coincident with neurogenesis in the proliferative zone of the hilus. The postnatal onset of expression of the synapsin I gene in the granule cells of the hippocampus and cerebellum suggests it belongs to a class of "late onset" mRNAs, whose appearance correlates with the terminal differentiation of neuronal precursors. The onset of expression of the synapsin I gene during the final stage of neuronal maturation is similar to several neuron-specific genes whose protein products are expressed predominently postnatally such as Thy-1 (Barclay,

1979), neuron-specific enolase (Marongos et al., 1980), rat nervous system antigen G5 (Akeson et al., 1983), DARPP-32 (Lewis et al., 1983), MIT-23 (Hawkes et al., 1982), tau-microtubule associated proteins (Ginzburg et al., 1982), αββ'-spectrin (Lazarides and Nelson, 1983), 1B236 (Lenoir et al., 1986), α- and β-tubulin (Bhattacharya et al., 1987), and inositol 1,4,5-triphosphate 3-kinase (Mailleux et al., 1993).

Developmental studies of the time course of expression of synapsin I protein in cerebellum by Mason (1986) support the early expression of the synapsin I gene product in postnatal development. In these studies, synapsin I protein was shown to be expressed in axonal growth cones in neonatal mouse brain. At these ages, the entire terminal arbors of growing axons are synapsin I-positive, in contrast to later postnatal and adult periods, when only synaptic boutons express synapsin I. Thus, for synapsin I protein to exist in developing growth cone structures before the development of classical synaptic terminals, the temporal onset of expression of the synapsin I gene must occur prior to the process of synaptogenesis. However, as this analysis of synapsin I localization in growing axons is one of few reported, only limited information is available regarding the regulation of the expression of synapsin I *in vivo*. *In vitro* analyses suggest that synapsin I protein levels are extremely low in the brains of neonatal rats, yet our results clearly show that the level of expression of synapsin I mRNA is high by this stage in development. Although caution must be exercized in the interpretation of these data, the most straightforward interpretation of this discrepancy between mRNA and protein levels opens the possibility of post-transcriptional control in the regulation of synapsin I expression during the development of the rat CNS. Further study of the direct relationship between levels of synapsin I mRNA and protein (e.g. mRNA stability and pulse-chase studies) are needed to elucidate the precise molecular mechanism of synapsin I gene regulation during the development and adult life of the rat.

In the second phase of synapsin I gene expression, (previously characterized in the cerebellum by Haas and DeGennaro, 1988) synapsin I mRNA increases to a maximum for

a given neuronal population during the peak period of synapse formation (synaptogenesis) of those neurons. We have extended these earlier studies using the developing rat hippocampus as model system. We have found that synapsin I gene expression is modulated concurrently with synaptogenic differentiation in the granule neurons in the developing dentate granule cell layer. This conclusion, which is consistant with the postulated role of the encoded protein in promoting the functional maturation of developing synapses in the rat nervous system, is supported by three independent lines of evidence. First, *in vitro* translation assays have shown previously that polysome-associated synapsin I mRNA activities were highest between 1 and 4 weeks of postnatal life, coinciding with a period of rapid formation of recognizable synapses in developing brain (DeGennaro et al., 1983). Second, in endogenous phosphorylation assays, synapsin Ia and Ib polypeptides were shown to increase markedly during the time of major synaptogenesis in rat and guinea pig cerebrum (Lohmann et al., 1978). Third, in cerebellar axons, the restriction to and concentration of synapsin I protein in the presynaptic terminal bouton follows axon arrival, and coincides with the appearance of elementary synapses, accompaning the transformation of growing tips into stereotypic synaptic boutons (Mason, 1986). Together, these data suggest that the early expression of the synapsin I gene is required for the normal development of synaptic structures in the rat central nervous system.

As such, these studies indicate that the expression of the synapsin I gene in particular populations of cells could be used as a molecular marker of differentiated neurons during the development of the nervous system. However, the coincidence of synapsin I gene expression with the peak periods of neurogenic and synaptogenic differentiation in the developing nervous system raises the question of whether the synapsin I gene product is absolutely crucial for proper differentiation and development of neurons and their central synapses, or whether its function is restricted to its hypothesized role as a regulator of synaptic transmission in the nervous system. Further investigation establishing direct comparisons between synapsin I mRNA and protein expression during development or in

response to pathophysiological events, may provide an answer to this question. In addition, the production of transgenic mice, mutant in different segments of the synapsin I gene, and subsequent analysis of the development of well characterized structures in the brain (both neuronal and synaptic) will be necessary to better understand the precise role of synapsin I in nervous system development. Such experiments may prove useful for characterizing functional domains of the synapsin I protein as they pertain to the development of the nervous system *in vivo*.

Adult studies of synapsin I gene expression

Synapsin I protein is known to be widely, but not uniformely, distributed throughout the rat central and peripheral nervous systems, and the relative level of synapsin I in neuropil regions across the adult rat neuraxis has been postulated to reflect the functional properties of those central synapses (Sudhof et al., 1989; Apostolides et al., in press). Although the heterogeneous distribution of synapsin I protein has been well-characterized, the pattern and relative levels of expression of the synapsin I mRNA have been unknown. To gain insight into the specific properties and functional requirements of those neurons whose termini comprise central synapses, I have used *in situ* hybridization histochemistry and RNA blot analysis to examine the regional and cellular distribution and relative levels of synapsin I mRNA in the adult rat central nervous system. These data represent the first extensive report published detailing the expression of the synapsin I gene in the rodent brain (Melloni et al., 1993).

Together the RNA blot and *in situ* hybridization data provide biochemical and histochemical evidence of regional variability in the level of synapsin I mRNA in the rat central nervous system. By *in situ* hybridization, the synapsin I gene was found to display a widespread yet regionally variable pattern of expression throughout the adult brain, similar to the distribution of mRNAs encoding the neuron-specific synaptic terminal proteins synaptophysin (Marqueze-Pouey et al., 1991), VAMP-2 (Elferink et al., 1989;

Trimble et al., 1990), and SNAP-25 (Geddes et al., 1990). Synapsin I mRNA was expressed in all neurons in the central nervous system, which is consistent with previous immunohistochemical data showing that synapsin I protein is present in virtually all presynaptic terminals examined, regardless of the type of neurotransmitter contained within (De Camilli et al., 1983a,b; Huttner et al., 1983; Navone et al., 1984; Benfenati et al., 1989).

In discrete regions of the rat brain, particular subsets of neurons express different levels of synapsin I mRNAs. In some areas of the brain, the pattern and intensity of synapsin I-specific hybridization parallel the cell density in the region, while in others the levels of expression of synapsin I mRNA reflect differences representative of the neuron-specific expression of the gene. The best example of the former case are the neurons of the anterodorsal nucleus of the thalamus. In this region, neurons are packed tightly into a cluster forming a nucleus of cells. As a result of this morphology, hybridization intensity in this region appears extremely high, although, unfortunately, a detailed analysis of the levels of synapsin I mRNA on a per cell basis are precluded by the sheer density of neurons in the region. In the latter case are the superficial layer V pyramidal neurons of the rat somatic sensory-motor (SSM) neocortex. Although all pyramidal neurons possess conical cell bodies and apical and basal dendrites, the size and location of their cell bodies vary greatly (Lorente de No, 1938; O'Leary, 1943; Lund, 1973). Layer V neurons of the rat SSM cortex can be subdivided into two sublaminae. The deeper layer, Vb, contains many large pyramidal neurons. The more superficial layer Va, mainly contains small to medium-sized pyramidal neurons and is cell sparse in the SI cortex. In comparision to their neighboring neuronal populations (layer IV, Vb, and layer VI), layer Va neurons appear to express elevated levels of synapsin I mRNA. Retrograde labeling (Jones et al., 1977; Wise and Jones, 1977; Donoghue and Kitai, 1981) and electrophysiological (Donoghue and Kitai, 1981) studies have indicated that these small-to-medium-sized neurons located in the upper part of laminia V of the rat SSM cortex form the main, if not the sole, population of

cortical neurons that project directly to the neostriatum and the thalamus, regions previously shown to express high-to-intense levels of synapsin I immunoreactivity (Apostolides et al., in press, see Chapter V, Figure 20). In turn, although these neurons display a very confined dendritic field, they posess an extensive dendritic spine network and subsequently receive the most thalamocortical synapses of any pyramidal cell examined in layer V of the SSM cortex (Hersch and White, 1981). These data lead to the speculation that the high levels of synapsin I mRNA in neuronal somata is correlated with high levels of synapsin I protein in their presynaptic terminal boutons, and that the extent of direct synaptic circuitry can influence the level of synapsin I gene expression.

Regulated expression of synapsin I mRNA and protein

Normal adult rat hippocampus

To address directly the possibility that high levels of synapsin I mRNA in discrete subsets of neurons may reflect the amount of synapsin I protein present in the presynaptic terminal fields of those neurons, I examined in detail the local distribution and relative levels of expression of both synapsin I mRNA and protein in defined synaptic circuits of the adult rat hippocampus. Those circuits examined were the first and second synapses in the trisynaptic circuit of the hippocampus, most notably the entorodentate (entorhinal cortex to dentate gyrus) and mossy fiber (dentate gyrus to CA3-CA4) synapses. In these regions, the layer II stellate neurons of the entorhinal cortex and the granule cell neurons of the dentate gyrus express comparable levels of synapsin I mRNA. However, immunohistochemistry revealed different levels of expression of synapsin I protein in the presynaptic terminal fields of these two cell populations. Thus, the level of synapsin I mRNA present in the somata of adult hippocampal neurons does not reflect simply the amount of synapsin I protein present in their presynaptic terminal fields. We propose that the different levels of expression of synapsin I mRNA and protein in these synaptic circuits may reflect differences in the functional properties and/or requirements of neurons which

form these central synapses. We further speculate that the discrepancy between the levels of expression of mRNA and protein may specify the use of post-transcriptional mechanisms in the regulation of the expression of the synapsin I gene in the CNS.

Developmental and Lesion Studies

To examine the regulation of the synapsin I gene during the establishment and reorganization of synapses in the CNS, studies of the expression of synapsin I mRNA and protein during hippocampal development and in response to lesions of hippocampal circuitry were performed. Developmental studies employing *in situ* hybridization and RNA blot analysis revealed that synapsin I mRNA was expressed at its high, near adult level in the dentate granule cell layer by the end of the first postnatal week of the developmental period. By comparison, however, the level of synapsin I protein present in mossy fiber terminals of dentate granule cell neurons during this period of development was sufficiently low to be undetectable by standard immunohistochemical techniques. In fact, there is a significant time lag between the expression of high (adult) levels of synapsin I mRNA and the appearance of detectable amounts of synapsin I protein in the synaptic termini of these neurons during development. Further, adult levels of protein in mossy fiber terminals were not observed until considerably later in development, around the fourth postnatal week. The most straightforward interpretation of these data suggests that synapsin I mRNA levels are stable in developing neurons of the central nervous system, and that regulation by post-transcriptional mechanisms are responsible for the lag in expression of synapsin I protein in developing mossy fiber synapses. Further, as subsequent immunohistochemical and Western blot experiments have indicated, the amount of synapsin I protein is 2-5 fold greater in P31 dentate granule neurons and their mossy fiber synapses than in P21 neurons. These data suggest that post-translational regulation at the level of protein modification and/or translocation is unlikely, and that regulation most likely occurs utilizing post-transcriptional and/or translational regulatory mechanisms.

Studies of lesions of adult hippocampal circuitry support this conclusion. Following lesions of the perforant pathway, the molecular layer of the dentate gyrus is reinnervated by the selective sprouting of surviving afferent systems in the zone of denervation. By immunohistochemistry, we observed dramatic changes in the pattern and intensity of synapsin I protein in the presynaptic terminal fields of sprouting neurons, and since we have previously established that the expression of synapsin I mRNA is up-regulated during the process of synaptogenesis, it was predicted that the expression of the synapsin I gene would be up-regulated in sprouting neurons in the central nervous system. However, *in situ* hybridization and RNA blot analyses revealed no significant changes in the relative levels of expression of synapsin I mRNA in those neurons responsible for the changing patterns of synapsin I immunoreactivity following lesion. These results, coupled with the data compiled in the developmental studies, imply that increased synthesis of synapsin I mRNA is not necessary for the large increases in synapsin I protein observed in the terminal fields of developing and/or sprouting neurons. Rather, it is likely that the expression of the synapsin I gene is stable in neurons, and undergoes very little, if any, transcriptional regulation after synapse development. Together with our previous data showing that the expression of synapsin I mRNA is initiated during the neurogenic differentiation of neuronal precursors, and upregulated during the peak period of synapse formation (see Haas and DeGennaro, 1988; and above), we speculate that synapsin I gene expression is regulated by multiple molecular mechanisms *in vivo*, including transcriptional as well as post-transcriptional and/or translational mechanisms. This phenomenon is not uncommon, as several neuron-specific genes such as tyrosine hydroxylase (Gizang-Ginsberg and Ziff, 1990; Miller et al., 1991), peripherin (Lindenbaum et al, 1988), neurofilament (Thompson and Ziff, 1989), and growth-associated protein 43 (GAP-43) (Nedivi et al., 1991; 1992; Perrone-Bizzozero et al., 1993) have recently been shown to be regulated by transcriptional and post-transcriptional mechanisms.

Several possibilties for the transcriptional activation and up-regulation of synapsin I

gene expression during neurogenesis and synaptogenesis exist. However, the most likely mechanism for the neuron-specific activation of the synapsin I gene during development is one of selective derepression, similar to that seen in several other developmentally regulated neuron-specific genes, including the SCG10 (Mori et al., 1990) and type II sodium channel (Maue et al., 1990). This mechanism implicates a factor(s) present in neuronal precursor and nonneuronal cells that acts in *trans* by selectively binding a silencer element(s) in the promotor region of neuronal genes. This binding to the silencer element confers dominant negative regulation and selectively suppresses the expression of neuronal genes in neuronal precursor and nonneuronal cells. Subsequently, the activation of neuronal expression involves the release of repression of neuron-specific genes in cells of neuronal lineages during the process of neuronal differentiation (Mori et al., 1990). The presence of silencer elements have been identified in several eukaryotic genes. Some, like those in the SCG10 and type II sodium channel genes, have been shown to promote cell type-specific expression (Muglia et al., 1986; Nir et al., 1986; Winoto and Baltimore, 1989). As such, the initial derepression of synapsin I gene expression may be conferred by the presence of a neuronal silencer in its distal 5' promotor.

A comparison of the 5' promotor DNA sequences of the SCG10, type II sodium channel, and synapsin I genes indicates similar elements which may regulate the tissue-specific and developmental-stage specific expression. Mori et al., (1992) identified a short sequence homology conserved between the 5' promotor regions of the SCG10, type II sodium channel and the synapsin I genes. This region in the synapsin I promotor shows >90% sequence identity to a sequence in the SCG10 5' promotor known as the neural-restrictive silencer element (NRSE). Although the neuron-specific expression of the synapsin I gene is known to be regulated by the region of the synapsin I promotor encompassing these sequences, it had not been clear whether it contained functional silencer elements (Sauerwald et al., 1990; Howland et al., 1991; Thiel et al., 1991). Just recently Li *et al.*, (February, 1993) have shown that the putative NRSE sequence in the

human synapsin I gene contains a functional silencer element. This element, located at positions -231 to -211 in the human synapsin I 5' promotor region, selectively represses the transcription of the synapsin I gene in nonneuronal cells. Further, these studies demonstrated the presence of a sequence-specific synapsin I silencer-binding protein in nonneuronal cell extracts whose binding, *in vitro*, correlated well with the repression of transcription of the synapsin I gene *in vivo*. These studies went further to propose the existence of additional cis-acting element(s) within the promotor region that also contribute to the neuron-specific expression of the synapsin I gene.

As is the case for a number of silencer elements identified thus far (Weinberger et al., 1988; Savagner et al., 1990; Weissman and Singer, 1991), the synapsin I NSRE may function in concert with cell type-specific positive-acting elements to achieve neuron-specific expression of the synapsin I gene. For example, is the lineage-specific transcriptional activation of the synapsin I gene influenced by environmental signals such as nerve growth factor (NGF) or other NGF-like trophic factors? As detailed previously, the synapsin I 5' promotor region posses specific sequence regulatory elements such as a cyclic AMP responsive element (CRE) and an AP-1 site, located at -151 bp and -1397 bp, respectively (Howland et al., 1991). AP-1 sequence elements have been shown to bind several combinations of the immediate early gene (IEG) family products, cellular proto-oncogenes known to act as transcription factors in eukaryotes. During development, a variety of trophic factors such as NGF, brain-derived neurotrophic factor (BDNF), ciliary neurotrophic factor (CNTF), and fibroblast growth factors (aFGF and bFGF) have been shown to influence the survival and differentiation of neuronal cells (Barde, 1989). These factors act through binding to membrane associated receptors. These receptors are typically coupled to signal transduction pathways which generate second messengers such as cAMP, which activate IEG products. These proteins bind as homodimers to the specific sequence elements utlimately resulting in activation and/or increase in target gene expression. For example, NGF, which is normally expressed in target tissues and retrogradely transported

to neuronal somata (retrograde signaling), has been shown to promote the phenotypic conversion of adrenal chromaffin cells to sympathetic neurons (Greene and Shooter, 1980). One of the earliest responses to NGF in PC12 cells is the rapid, transient, and protein synthesis-independent induction of several genes encoding members of the IEG family. This rapid activation of IEG expression has led to the proposal that these proteins initiate a cascade of transcriptional events which culminate in neuronal differentiation (Greenberg et al., 1985; Sheng, 1990). With regard to synapsin I gene expression, it is distinctly possible that retrograde and receptor-coupled enviromental cues are also involved in the activation of synapsin I gene expression during neurogenesis. Moreover, since the neuronal and synaptic milieu of both the cerebellum and hippocampus are extremely diverse later in development, we speculate that these cues may also influence or direct the up-regulation of synapsin I gene expression during the process of synaptogenesis in the developing brain.

In addition to the presence of NRSE sequences in the promotor regions of the type II sodium channel (Maue et al., 1990) and synapsin I (Howland et al., 1991) genes, sequence analyses indicate that the promotors of these genes are GC-rich and lack strong TATA box elements, sequence elements that specify transcription initiation in many other genes (Blake et al., 1990). Further, the SCG10, type II sodium channel, and synapsin I promotors contain multiple transcription initiation sites (Maue et al., 1990; Mori et al., 1990, Howland et al., 1991). Although the functional significance of multiple start sites is unknown, many genes that are regulated during differentiation (Anderson et al., 1988; Biggin and Tjian, 1988), as well as a variety of housekeeping genes which lack strong TATA homologies, are encoded by transcripts with different 5' ends. Further dissection of the synapsin I distal and proximal 5' promotor regions and subsequent reporter gene analysis as well as production of transgenic mouse mutants of the synapsin I promotor should provide insight into the developmentally-regulated expression of the synapsin I gene.

As with the case for the transcriptional regulation, there exist several possibilities for the post-transcriptional and/or translational regulation of the synapsin I gene. Post-transciptional regulation can occur by several mechanisms operating at multiple levels in eukaryotic cells. The regulation of primary RNA transcripts can occur at such levels as splicing and processing, or at the level of transport from the nucleus to the cytoplasm. Subsequently, cytoplasmic mRNAs can be subject to regulation at the level of mRNA turnover, itself dependent upon such factors as inherent mRNA stability and degradation via the absence or presence of intrinic (passive turnover) and extrinsic (regulated turnover) factors (see review by Peltz et al., 1991).

We speculate that one possible mechanism for the post-transcriptional regulation of the synapsin I gene during establishment and remodeling of central nervous system synapses is similar to that seen in the neuron-specific gene, GAP-43 (Brown et al., 1992; Kohn and Perrone-Bizzozero, 1992). GAP-43 is a developmentally regulated phosphoprotein which has been linked to the development, regeneration, and remodeling of axonal connections (for reviews see Skene, 1989; Benowitz and Perrone-Bizzozero, 1991). High GAP-43 mRNA and protein levels are typically associated with axonal growth during development and following neuronal injury (Neve et al., 1987; Perrone-Bizzozero et al, 1991). Following transection of the mouse inferior gluteal nerve, collateral sprouting of the uninjured superior gluteal (SGN) nerve fibers serve to reinnervate the adjacent zone of denervation (Brown et al., 1992). During this process, marked increases in GAP-43 protein were detected within collateral sprouting fibers of the SGN. However, when fluorogold (a retrograde tracer) was applied to the surface of the muscle to identify sprouting motorneurons with axons in the superior nerve, fluorescent cells had mRNA levels indistinguishable from those of motorneurons in other parts of the motor column. Thus, in a similar fashion to synapsin I, the increased synthesis of GAP-43 mRNA is not necessary for the large increases in GAP-43 protein observed in the presynaptic terminal fields of sprouting motoneurons. As we have speculated for synapsin I, the regulation of

GAP-43 gene expression appears to be mediated at both the transcriptional (Nedivi et al., 1991; 1992) and post-transcriptional levels (Irwin et al., 1991; Kohn and Perrone-Bizzozero, 1992; Perrone-Bizzozero et al., 1993). At the post-transcriptional level, GAP-43 expression appears regulated by protein kinase C-dependent stabilization of the mRNA (Perrone-Bizzozero et al., 1993). Sequence dissection of the 3'untranslated region (UTR) of GAP-43 mRNA revealed the presence of a highly conserved sequence element (UUUCCCACCCA-14bps-UGUGUGGCAAA). Further studies investigating RNA-protein interactions between this conserved region of the 3'UTR of GAP-43 mRNA and cytosolic brain proteins have implicated sequences in the 3'UTR in the post-transcriptional regulation of GAP-43 gene expression (Kohn and Perrone-Bizzozero, 1992). Subsequently, three GAP-43 mRNA binding proteins have been identified whose putative function in the post-transcriptional regulation of the stabilty of GAP-43 mRNA is currently under investigation.

Although the 3'UTR of the synapsin I mRNAs contain no such obvious AU-rich regions or GAP-43-like consensus stem-loop sequence elements, the transcripts do contain a highly conserved sequence repeat. The 3'UTRs of both the bovine and human synapsin I messages contain a 100-nucleotide repeat that is 65% identical and starts immediately after the termination codon (nucleotides 4520-4617 and 4635-4748) (Sudhof, 1990). This conservation of the nucleotide sequences in the 3'UTR seems unusual (see "Discussion" in Hobbs et al., 1985), and suggests a possible regulatory role of these sequences. We speculate that this region of the synapsin I mRNA may confer mRNA stability regulation in a fashion similar to that identified for GAP-43. Further study investigating the putative role of these conserved repeats in the post-transcriptional regulation of synapsin I gene expression includes experiments similar to those outlined above.

Functional Correlates of Synapsin I Gene Expression

Normal adult rat hippocampus

In the adult rat hippocampus, the markedly dissimilar patterns of expresssion of synapsin I mRNA and protein in the neurons of the dentate gyrus and entorhinal cortex suggest that synapsin I mRNA levels cannot refect simply the amount of synapsin I protein present in the terminal arborizations of central neurons. We propose that the different levels of expression of synapsin I mRNA and protein in these synaptic circuits may reflect differences in the functional properties and/or requirements of neurons which form these central synapses. As detailed previously, studies on the restoration of synaptic connections in response to selective nervous system lesions have demonstrated that the hippocampal formation possesses a robust potential for synaptic regrowth (see review by Cotman and Nieto-Sampedro, 1984). In this system, synapse replacement in the molecular layer of the dentate gyrus is acheived by the selective sprouting of surviving afferent systems. Thus, locally high levels of synapsin I mRNA in hippocampal CA4 and layer II entorhinal neurons may reflect the abiltity of the system to be plastic and respond to injury and/or select enviromental stimuli by producing long-tem synaptic circuitry changes. Other neurons, such as granule cell neurons of the dentate gyrus, might still require locally high levels of synapsin I mRNA to maintain correspondingly high levels of synapsin I protein in their presynaptic terminal fields. In dentate granule cell neurons, high levels of synapsin I gene expression (mRNA and protein) may reflect the ability of these neurons to respond to stimuli by producing a long-lasting enhancement in the synaptic efficacy of transmission. This example of plasticity, known as long-term potentiation (LTP), is a well-characterized property of dentate granule neurons, and reflects an ability of these cells to elicit an increased amplitude of synaptic potentials following afferent stimulation (Baskys et al., 1991). It has been proposed that this particular property of dentate granule neurons in the hippocampal formation is a strong candidate for a cellular mechanism underlying learning and memory. Studies invoking LTP in dentate granule neurons by microiontophoretic

application of NMDA (a gluatamate analog, Kauer et al., 1988), or stimulation of the lateral amygdala (Henke, 1990; Racine et al., 1983) or perforant pathway (Baskys et al., 1991) could be used to elucidate the possible involvement of synapsin I expression in hippocampal LTP.

Developmental and Lesion Studies

A review of the neurogenic and synaptogenic development of the dentate granule cell neurons and their presynaptic terminal fields suggests that these cells establish synaptic contact in the hilar region early in postnatal development (by P0-P3), and that the majority of the mossy fiber synapses become mature, at least morphologically, between postnatal days 10-15 (Zimmer and Haug, 1978; Amaral and Dent, 1981; Gaarskjaer, 1981, 1985). However, it is after this stage of mossy fiber synaptogenesis that mature patterns of synaptic profiles are first observed, indicating the beginning of the functional maturation of these central synapses (Bliss et al., 1974). While it is clear that by this stage of development the mossy fibers are, for the most part, fully mature, a more subtle and protracted structural and functional development of the mossy fiber system persists long into the adult life of the animal (Gaarskjaer, 1985; Bliss et al., 1974).

Our analyses indicate that detectable levels of synapsin I protein become localized and concentrated in mossy fiber synapses, beginning around postnatal day 21. The adult level of protein, however, is not present until later in development of these synapses, around postnatal day 31. Since detectable levels of synapsin I protein begin to appear in mossy fiber terminals after postnatal day 15, we conclude that synapsin I protein is only fully accumulated in presynaptic mossy fiber terminals during the functional maturation of their synapses. Indeed, in addition to its putative role in regulating neurotransmitter release from mature nerve terminals, recent evidence suggests that synapsin may promote the formation and functional maturation of new synapses. Morphological studies by Han *et al.*, (1991) have shown that overexpression of synapsin IIb in cultured neuroblastoma-

glioma hybrid cells resulted in marked increases in the number of neuritic varicosities and the numbers of small clear synaptic vesicles and large dense core vesicles per varicosity. In addition, those transfected cells gained the ability to form synapse-like cell-to-cell contact with one another. Moreover, those cells showed a specific increase in the expression of endogenous synaptic vesicle-associated proteins, including synapsin I, synapsin II and synaptophysin. Most recently, physiological studies by Lu *et al.*, (1992) have shown that exogenously added synapsin I may play a causal role in synaptogenesis by promoting the acceleration of the establishment of quantal-secretion mechanisms. In these studies, performed in *Xenopus* spinal neurons, injected synapsin I was shown to enhance both spontaneous and evoked transmitter release as measured by both sponteneous (SSC) and evoked (ESC) synaptic currents. Previous studies had shown that evoked synaptic responses at immature synapses have relatively low and variable amplitude and exhibit frequent failures (Evers et al., 1989). However, in synapsin I-loaded spinal neurons a significant increase in the ESC amplitude as well as a reduced variability was observed, indicating that more mature and reliable synapses were established. Thus, the exogenous synapsin I appeared to promote the functional maturation of these synapses (Lu et al., 1992). In the same studies, using cell manipulation techniques, enhanced neurotransmitter release from synapsin I-loaded neurons was shown to occur at the onset of synaptogenesis, suggesting a presynaptic developmental action of synapsin I prior to synaptic contact.

A detailed comparision of the time course and pattern of hippocampal synapsin I immunostaining and sprouting-related physiological and behavioral changes reveal striking parallels. An analysis of the pattern and intensity of synapsin I immunoreactivity during the reinnervation of the molecular layer of the dentate gyrus following perforant pathway transection suggests that the reappearance of synapsin I protein in the neuropil correlates, temporally and topographically, with the recovery of synaptic function. From a functional standpoint, physiological and behavioral studies (Steward et al., 1973; Loeshe and Steward, 1977; Steward, 1981; Reeves and Steward, 1988) have demonstrated that

neuronal sprouting in the molecular layer of the dentate gyrus is important for the recovery of unit activity of neurons in the dentate granule cell layer and of learned alternation behavior after unilateral entorhinal cortex lesions, and most significantly, that these activities recover to levels comparable to prelesion control between 8-14 days post-lesion. Synapsin I protein in the neuropil increases during the reinnervation of the molecular layer, beginning first in the outer molecular layer around 7 days post-lesion and increasing to control levels in this region by 14 days post-lesion. This increase in synapsin I in the outer molecular layer correlates with the proliferation of the crossed temporodentate pathway (CTD), a functionally homologous pathway originating in the contralateral entorhinal cortex known to participate in the physiological and behavioral recovery of function following unilateral entorhinal cortex lesions (Steward et al., 1973; Steward, 1976; Loeshe and Steward, 1987). Further, this post-lesion time course of increase in synapsin I protein in the OML correlates precisely with the time course of post-lesion increases in CTD evoked potentials (Reeves and Smith, 1987) and the recovery of T-maze alternation performance (Loeshe and Steward, 1977), reaching prelesion values by 14 days post-lesion. By 31 days post-lesion, well before the process of reinnervation establishes pre-lesion synaptic density, but after the restoration of physiological and behavioral function, the molecular layer revealed a moderate, near homogenous pattern of synapsin I immunoreactivity, similar to that seen in sham-operated and naive control tissue. In accord with the developmental studies, these data indicate that during the establishment/restoration of functional synaptic contacts in the lesioned hippocampus, the appearance of synapsin I protein in the neuropil does not reflect simply synaptogenesis, but coincides temporally and topographically, with the period of the functional maturation of newly created synapses in the central nervous system.

SUMMARY

The data presented in this thesis demonstrate clearly that the temporal onset of expression of the synapsin I gene coincides with neuronal differentiation in the rat central nervous system. Further, studies of the postnatal development of the cerebellum and hippocampus reveal that expression of synapsin I mRNA is further modulated by particular cellular events during development, e.g., synaptogenesis. These studies provide a temporal and spatial map of the expression of the synapsin I gene throughout the developmental life of the rodent nervous system. This map reveals the widespread yet regionally variable levels of expression of the synapsin I gene accross the entire neuraxes. In particular regions, the level of synapsin I gene expression appears related to the density of neuronal somata, whereas in other regions the levels of synapsin I hybridization appear to reflect differences in synapsin I mRNA levels in individual neurons representative of a specific region of the rat brain. In addition, we have extended these studies to determine precisely, the relationship between the levels of expression of synapsin I mRNA and protein during the development and restoration of functional synaptic contacts in the defined synaptic circuitry of the rat hippocampus. These data revealed the differential levels of expression of synapsin I mRNA in neuronal somata and synapsin I protein in their presynaptic terminal fields, suggesting a further level of regulation of the synapsin I gene, by post-transcriptional and/or translational mechanisms. These studies further reveal that the appearance of synapsin I protein in the hippocampal neuropil does not reflect simply synaptogenesis, but coincides temporally and topographically, with the functional maturation of synapses in the central nervous system.

LITERATURE CITED

Aghajanian G.K. and F.E. Bloom (1967) The formation of synaptic junctions in developing rat brain: A quantitative electron microscopic study. Brain Res. 6:716-727.

Akeson R.A., Rodman J.S., and A Roberts (1983) Induction of expression of the rat G5 nervous system antigen occurs postnatally. Dev. Brain Res. 7:327-336.

Altman J. and G.D. Das (1965) Autoradiographic and histological evidence of postnatal hippocampal neurogenesis in rats. J. Comp. Neurol. 124:319-336.

Altman J. and G.D. Das (1966) Autoradiographic and histological studies of postnatal neurogenesis. I. A longitudinal investigation of the kinetics, migration and transformation of cells incorporating tritiated thymidine in neonate rats, with special reference to postnatal neurogenesis in some brain regions. J. Comp. Neurol. 126:337-390.

Altman J. (1966) Autoradiographic and histological studies of postnatal neurogenesis. II. A longitudinal investigation of the kinetics, migration and transformation of cells incorporating tritiated thymidine in infant rats, with special reference to postnatal neurogenesis in some brain regions. J. Comp. Neurol. 128:421-474.

Altman J. (1972a) Postnatal development of the cerebellar cortex in the rat. I. The external germinal layer and the transitional molecular layer. J. Comp. Neurol. 145:353-398.

Altman J. (1972b) Postnatal develolpment of the cerebellar cortex in the rat. II. Phases in the maturation of Purkinje cells and of the molecular layer. J. Comp. Neurol. 145:399-464.

Altman J. (1972c) Postnatal development of the cerebellar cortex in the rat. III. Maturation of the components of the granular layer. J. Comp. Neurol. 145:465-513.

Amaral D.G. (1978) A Golgi study of cell types in the hilar region of the hippocampus in the rat. J. Comp. Neurol. 182:851-914.

Amaral D.G.and J.A. Dent (1981) Development of the mossy fibers of the dentate gyrus: I. A light and electron microscopy study of the mossy fibers and their expansions. J. Comp. Neurol. 195:51-86.

Anderson K.J., Bridges R.J., and C.W. Cotman (1991) Increased density of excitatory amino acid transport sites in the hippocampal formation following entorhinal lesion. Brain Res. 562:285-290.

Anderson S.J., Chow H.S., and D.Y. Lon (1988) A conserved sequence in the T-cell receptor β-chain promotor region. Proc. Natl. Acad. Sci. U.S.A. 85:3551-3554.

Angevine J., Jr., (1965) Time of neuron origin in the hippocampal region. An autoradiographic study in the mouse. Exp. Brain Res. Suppl. 2:1-70.

Apostolides P.J., DeGennaro L.J., Melloni, Jr. R.H., Pulaski-Salo D., and J.E. Hamos Localization of synapsin I in the adult rat central nervous system. Synapse. (in press).

Avner P., Bucan M., Arnaud D., Lehrach H., and U Rapp (1987) A-*raf* oncogene

localizes on mouse X chromosome to a region some 10-17 centimorgans proximal to hypoxanthine phosphoribosyltransferase gene. Somat. Cell Mol. Genet. 13:267-272.

Badley J. E., Bishop G. A., St. John T., and J. A. Frelinger (1988) A simple, rapid method for the purification of poly A+ RNA. Biotechniques 6(2):114-116.

Bahler M. and P. Greengard (1987) Synapsin I bundles F-actin in a phosphorylation-dependent manner. Nature 326:704-707.

Bahler M., Benfenati F., Valtorta F., Czernik A.J., and P Greengard (1989) Characterization of synapsin I fragments by cysteine-specific cleavage: a study of their interactions with F-actin. J. Cell Biol. 198:1841-1849.

Bahler M., Benfenati F., Valtorta F., and P. Greengard (1990) The synapsins and the regulation of synaptic function. Bioessays 12:259-263.

Baines A.J. and V. Bennet (1985) Synapsin I is a spectrin-binding protein immunologically related to erythrocyte protein 4.1. Nature 315:410-413.

Baines A.J. and V. Bennet (1986) Synapsin I is a microtubule-bundling protein. Nature 319:145-147.

Barclay N. (1979) Localization of the Thy-1 antigen in the cerebellar cortex of rat brain by immunofluorescence during postnatal development. J. Neurochem. 32:1249-1257.

Barde Y.-A. (1989) Trophic factors and neuronal survival. Neuron 2:1525-1534.

Baskys A., Carlen P.L., and J.M. Wojtowicz (1991) Long-term potentiation of synaptic responses in the rat dentate gyrus is due to increased quantal content. Neurosci. Letts. 127(2):169-172.

Bayer S.A. and J. Altman (1974) Hippocampal development in the rat: cytogenesis and morphogenesis examined with autoradiography and low-level X-irradiation. J. Comp. Neurol. 158:55-80.

Bayer S.A. (1980a) Development of the hippocampal region in the rat. I. Neurogenesis examined with 3H-thymidine autoradiography. J. Comp. Neurol. 190:87-114.

Bayer S.A. (1980b) Development of the hippocampal region in the rat. II. Morphogenesis during embryonic and early postnatal life. J. Comp. Neurol. 190:115-134.

Bayer S.A. (1982) Changes in the total number of dentate granule cells in juvenile and adult rats: A Correlated volumetric and 3H-thymidine autoradiographic study. Exp. Brain Res. 46:315-323.

Bayer S.A., Yackel J.W., and P.S. Puri (1982) Neurons in the rat dentate gyrus granular layer substantially increase during juvenile and adult life. Science 216:890-892

Bayer S.A. (1985) Hippocampal Region. In *The Rat Nervous System* (ed. Paxinos G.) Vol. 1. pp.335-352. Academic Press, New York.

Benfenati F., Bahler M., Jahn M., and P. Greengard (1989) Interactions of synapsin I with small synaptic vesicles: distinct sites in synapsin I bind to vesicle phospholipids and vesicle proteins. J. Cell Biol. 108:1863-1872.

Benfenati F., Valtorta F., Rubenstein J.L., Gorelick F.S., Greengard P., and A.J. Czernik (1992) Synaptic vesicle-associated Ca2+/calmodulin-dependent protein kinase II is a binding protein for synapsin I. Nature 359:417-420.

Benson D.L., Gall C.M., and P.J. Isackson (1992) Dendritic localization of type II calcium calmodulin-dependent protein kinase mRNA in normal and reinnervated rat hippocampus. Neuroscience 46(4):851-857.

Berger M. and Y. Ben-Ari (1983) Autoradiographic visualization of [^{3}H] kainic acid receptor subtypes in the rat hippocampus. Neuroscience Letts. 39:237-242.

Bergman H., Browning M., and A.C. Granholm (1992) Development of synapsin I and synapsin II in intraocular hippocampal transplants. Hippocampus 2(4):339-348.

Bhattacharya B., Mandal C., Basu S., and P.K. Sarkar (1987) Regulation of α- and β-tubulin mRNAs in rat brain during synaptogenesis. Mol. Brain Res. 2:159-162.

Biggin M.D. and R. Tjian (1988) Transcription factors that activate the *Ultrabithorax* promotor in developmentally staged extracts. Cell 53:699-711.

Birnboim, H. C. (1988) Rapid extraction of high molecular weight RNA from cultured cells and granulocytes for northern analysis. Nucl. Acids Res. 16(4):1487-1497.

Bixby J. and L.F. Reichardt (1985) The expression and localization of synaptic vesicle antigens at neuromuscular junctions in vitro. J. Neurosci. 5:3070-3080.

Blackstad T.W. (1956) Commissural connectins of the hippocampal region in the rat, with special references to their mode of termination. J. Comp. Neurol. 105:417-537.

Blackstad T.W. (1958) On the termination of some afferents to the hippocampus and fascia dentata. An experimental study in the rat. Acta. Anat. 35:202-214.

Blackstad T.W., Fuxe K., and T. Hokfelt (1967) Noradrenalin nerve terminals in the hippocampal region of the rat and the guinea pig. Z. Zellforsch. 78:463-473.

Blakstad T.W., Brink K., Heim J., and B. Jeune (1970) Distribution of hippocampal mossy fibers in the rat. An experimental study with silver impregnation methods. J. Comp. Neurol. 138:433-450.

Blake M.C., Jambou R.C., Swick A.G., Kahn J.W., and J. Clifford-Azizkhan (1990) Transcription initiation is controlled by upstream GC-box interactions in a TATAA-less promotor. Mol. and Cell. Biol. 10(12):6632-6641.

Bloom F.E., Ueda T., Battenberg E., and P. Greengard (1979) Immunocytochemical localization, in synapses, of protein I, an endogenous substrate for protein kinase in mammalian brain. Proc. Natl. Acad. Sci. U.S.A. 76:5982-5986.

Bliss T.V.P., Chung S.H., and R.V. Stirling (1974) Structural and functional development of the mossy fiber system in the hippocampus of the postnatal rat. J. Physiol. (Lond.) 239:92-94P.

Brown M.C., Booth C.M., Bisby M.A., and W. Tetzlaff (1992) Motorneuron sprouting

is not associated with increases in GAP-42 mRNA. Soc. Neurosci. Abstr. 18:605.
Caceres A., Busciglio J., Ferreira A., and O. Steward (1988) A immunocytochemical and biochemical study of the microtubule-associated protein MAP-2 during post-lesion dendritic remodeling in the central nervous system of adult rats. Mol. Brain Res. 3:233-246.

Cajal S. Ramon y (1911) *Histologie du systeme nerveux de l'homme et des vertebres.* Vol. 2. Institute Ramon y Cajal, Madrid.

Chen C.L., Dionne F.T., and J.T. Roberts (1983) Regulation of the pro-opiomelanocortin mRNA levels in rat pituitary by dopaminergic compounds. Proc. Natl. Acad. Sci. USA 80:2211-2215.

Chen S. and D.E. Hillman (1992) Transcient c-fos expression and dendritic spine plasticity in hippocampal granule cells. Brain Res. 577:169-174.

Chirgwin J.M., Przybyla A.E., MacDonald R.J., W.J. Rutter (1979) Isolation of biologically active ribonucleic acid from sources enriched in ribonuclease. Biochemistry 18:5294-5299.

Chomczynski P. and N. Sacchi (1987) Single-step method of RNA isolation by acid guanidinium thiocyanate-phenol-chloroform extraction. Anal. Biochem. 162:156-159.

Cleveland D. W. and K. F. Sullivan (1985) Molecular biology and genetics of tubulin. Ann. Rev. Biochem. 54, 331-365.

Conrad L.C.A., Leonard C.M., and D.W. Pfaff (1974) Connections of the median and dorsal raphe nuclei in the rat: An autoradiographic and degeneration study. J. Comp. Neurol. 156:179-206.

Cotman C.W. and J.V. Nadler (1978) Reactive synaptogenesis in the hippocampus. In *Neuronal Plasticity* (ed. Cotman C.W.), pp.227-271. Raven Press, New York.

Cotman C.W. and J.V. Nadler (1981) Glutamate and aspartate as hippocampal transmitters: Biochemical and pharmacological evidence. In *Glutamate: Transmitter in the Central Nervous System.* (eds. Roberts P.J., Storm-Mathisen J., and Johnston G.A.R), pp. 117-154. John Wiley, London.

Cotman C.W. and N. Nieto-Sampedro (1984) Cell biology of synaptic plasticity. Science 225:1287-1294.

Cotman C.W. and K.J. Anderson (1988) Synaptic plasticity and functional stabilization in the hippocampal formation: Possible role in Alzheimer's Disease. In *Advances in Neurology: Functional Recovery in Neurological Disease.* (ed. Waxman S.G.) Vol. 47, pp. 313-335. Raven Press, New York.

Crespo D., Stanfield B.B., and W.M. Cowan (1986) Evidence that late-generated granule cells do not simply replace earlier formed neurons in the rat dentate gyrus. Exp. Brain Res. 62:541-548.

Cummings B.J., Yee G.J., and C.W. Cotman (1992) bFGF promotes the survival of entorhinal layer II neurons after perforant path axotomy. Brain Res. 591:271-276.

Davies P. and A.J.F. Maloney (1976) Selective loss of central cholinergic neurons in

Alzheimer's disease. Lancet 2:1403

De Camilli P., Ueda T., Bloom F.E., Battenberg E., and P. Greengard (1979) Widespread distribution of protein I in the central nervous system. Proc. Natl. Acad. Sci. U.S.A. 76(11):5977-5981.

De Camilli P., Cameron R., and P. Greengard (1983a) Synapsin I (protein I), a nerve-terminal specific phosphoprotein. I. Its general distribution in the synapses of the central and peripheral nervous system demonstrated by immunofluorescence in frozen and plastic sections. J. Cell Biol. 96:1337-1354.

De Camilli P., Harris S.M., Huttner W.B., and P. Greengard (1983b) Synapsin I (protein I), a nerve terminal-specific phosphoprotein. II. Its specific association with synaptic vesicles demonstrated by immunocytochemistry in agarose-embedded synaptosomes. J. Cell Biol. 96:1355-1373.

De Camilli P., and P. Greengard (1986) Synapsin I: a synaptic vesicle-associated phosphoprotein. Biochem. Pharmacol. 35:4349-4357.

De Camilli, P., F. Benfenati, F. Valtorta, and P. Greengard (1990) The synapsins. Annu. Rev. Cell. Biol. 6:433-460.

DeGennaro L.J., Kanazir S.D., Wallace W.C., Lewis R.M., and P. Greengard (1983) Neuron-specific phosphoproteins as models for neuronal gene expression. Cold Spring Harbor Symp. Quant Biol. 48:337-345.

DeGennaro L.J., Apostolides P.J., Pulaski-Salo D., and J.E. Hamos (1989) Localization of synapsin I in adult rat brain. Soc. Neurosci. Abstr. 15:680.

Derry J.M.J. and P.J. Barnard (1992) Physical linkage of the A-raf-1, properdin, synapsin I, and TIMP genes on the human and mouse X chromosomes. Genomics 12:632-638.

Desmond N.L. and W.B. Levy (1982) A quantitative anatomical study of the granule cell dendritic fields of the rat dentate gyrus using a novel probabilistic method. J. Comp. Neurol. 212:131-145.

Donoghue J.P. and S.D. Kitai (1981) A collateral pathway to the neostriatum from corticofugal neurons of the rat sensory-motor cortex: An intracellular HRP study. J. Comp. Neurol. 201:1-13.

Doucette R., Fisman M., Hachinski V.C., and H. Mersky (1986) Cell loss from the nucleus basalis of meynert in Alzheimer's disease. Can. J. Neurol. Sci. 13:435-440.

Dragunow M., Yamada N., Bilkey D.K., and P. Lawlor (1992) Induction of immediate-early gene proteins in dentate granule cells and somatostatin interneurons after hippocampal seizures. Mol. Brain Res. 13:119-126.

Douglass J., Grimes L., Shook J., Lee P.H.K., and J.-S. Hong (1991) Systemic administration of kainic acid differentially regulates the levels of prodynorphin and proendephalin mRNA and peptides in the rat hippocampus. Mol. Brain Res. 9:79-86.

Dziadek M. A. and G. K. Andrews (1983) Tissue specificity of alphafetoprotein messenger RNA expression during mouse embryogenesis. EMBO J. 2:549-554.

Elferink L.A., Trimble W.S., and R.H. Scheller (1989) Two vesicle-associated membrane protein genes are differentially expressed in the rat central nervous system. J. Biol. Chem. 264:11061-11064.

Emmet M. and B.Petrack (1988) Rapid isolation of total RNA from mammalian tissues. Anal. Biochem. 174:658-661.

Evers J., Laser M., Sun Y., Xie Z., and M-m. Poo (1989) Studies of nerve-muscle interactions in *Xenopus* cell culture: Analysis of early synaptic currents. J. Neurosci. 9:1523-1539.

Fantie B.D., and G.V. Goddard (1982) Septal modulation of the population spike in the fascia dentata produced by perforant path stimulation in the rat. Brain Res. 252:227-237.

Feinberg A.P. and B. Vogelstein (1983) A technique for radiolabeling DNA restriction endonuclease fragments to high specific activity. Anal. Biochem. 132:6-13.

Feinberg A.P. and B. Vogelstein (1984) Addendum: A technique for radiolabeling DNA restriction endonuclease fragments to high specific activity. Anal. Biochem. 137:266-267.

Fletcher T.L., Cameron P., De Camilli P., and G.A. Banker (1991) The distribution of synapsin I and synaptophysin in hippocampal neurons developing in culture. J. Neurosci. 11:1617-1626.

Foster A.C., Mena E.E., Monaghan D.T., and C.W. Cotman (1981) Synaptic localization of kainic acid binding sites. Nature 289:73-75.

Fricke R. and W.M. Cowan (1978) An autoradiographic study of the development of the entorhinal and commissural afferents to the dentate gyrus of the rat. J. Comp. Neurol. 173:231-250.

Fuxe K. (1965) Evidence for the existence of monoamine neurons in the central nervous system. I. Distribution of monoamine nerve terminals. Acta Physiol. Scand. Suppl. 64,247:37-85.

Gall C. and G. Lynch (1981) Fiber architecture of the dentate gyrus following ablation of the entorhinal cortex in rats of different ages: Evidence for two forms of axon sprouting in the immature brain. Neuroscience 6(5):903-910.

Gaarskjaer F.B. (1978) Organization of the mossy fiber system of the rat studied in extended hippocampi. II. Experimental analysis of fiber distribution with silver impregnation methods. J. Comp. Neurol. 178:73-88.

Gaarskjaer F.B. (1981) The hippocampal mossy fiber system of the rat studied with retrograde tracing techniques. Correlation between topographic organization and neurogenetic gradients. J. Comp. Neurol. 203:717-735.

Gaarskjaer F.B. (1985) The development of the dentate area and the hippocampal mossy fiber projection of the rat. J. Comp. Neurol. 241:154-170.

Geddes J.W., Monaghan D.T., Cotman C.W., Lott I.T., Kim R.C., and H.C. Chui (1985) Plasticity of hippocampal circuitry in Alzheimer's disease. Science 230:1179-1181.

Geddes J.W., Hess E.J., Hart R.A., Kesslak J.P., Cotman C.W., and M.C. Wilson (1990a) Lesions of hippocampal circuitry define synaptosomal-associated protein-25 (SNAP-25) as a novel presynaptic marker. Neuroscience 38:515-525.

Geddes J.W., Wilson M.C., Miller F.D., and C.W. Cotman (1990b) Molecular markers of reactive plasticity. In *Excitatory Amino Acids and Neuronal Plasticity*. (ed. Ben-Ari Y.), pp. 425-431. Plenum Press, New York.

Geddes J.W., Wong J., Choi B.H., Kin R.C., Cotman C.W., and F.D. Miller (1990c) Increased expression of the embryonic form of a developmentally regulated mRNA in Alzheimer's disease. Neurosci. Lett. 109:54-61.

Gertz H.J., Cervos-Navarro J., and V. Ewald (1987) The septo-hippocampal pathway in patients suffering from senile demential of Alzheimer's type. Evidence for neuronal plasticity. Neuroscience Letts. 76:228-232.

Gibbs R.B., Chao M.V., and D.W. Pfaff (1991) Effects of fimbria-fornix and angular bundle transection on expression of the $p75^{NGFR}$ mRNA by cells in the medial septum and diagonal band of Broca: Correllations with cell survival, synaptic reorganization and sprouting. Mol. Brain Res. 11:207-219.

Gibson P.H. (1983) EM study of the numbers of cortical synapses in the brains of ageing people and people with Alzheimer-type dementia. Acta Neuropathol. 62:127-133.

Ginzburg I., Scherson T., Giveon D., Behar L., and U.Z. Littauer (1982) Modulation of mRNA for microtubule-associated proteins during brain development. Proc. Natl. Acad. Sci. U.S.A. 79:4892-4896.

Gizang-Ginsberg E. and E.B. Ziff (1990) Nerve growth factor regulates tyrosine hydroxylase gene transcription through a nucleoprotein complex that contains c-fos. Genes and Devel. 4:477-491.

Goelz S.E., Nestler E.J., Chehrazi B., and Greengard P. (1981) Distribution of protein I in mammalian brain as determined by a detergent-based radioimmunoassay. Proc. Natl. Acad. Sci. U.S.A. 78:2130-2134.

Gottlieb D.I. and W.M. Cowan (1973) Autoradiographic studies of the commissural and ipsilateral association connections of the hippocampus and dentate gyrus of the rat. I. The commissural connections. J. Comp. Neurol. 149:393-422.

Gough N. M. (1988) Rapid and quantitative preparation of cytoplasmic RNA from small numbers of cells. Anal. Biochem. 173:93-95.

Grant S.G. and K. Chapman (1991) Detailed genetic mapping of the A-*raf*-1 proto-oncogene on the mouse X chromosome. Oncogene 6:397-402.

Greenberg M.E., Greene L.A., and E.B. Ziff (1985) Nerve growth factor and epidermal growth factor induce rapid transcient changes in proto-oncogene transcription in PC12 cells. J. Biol. Chem. 260:14101-14110.

Greene L.A. and E.M. Shooter (1980) The nerve growth factor: Biochemistry, synthesis and mechanism of action. Annu. Rev. Neurosci. 3:353-402.

Greengard P., Valtorta F., Czernik A.J., and F. Benfenati (1993) Synaptic vesicle phosphoproteins and regulation of synaptic function. Science 259:780-785.

Haas C.A., and L.J. DeGennaro (1988) Multiple synapsin I messenger RNAs are differentially regulated during neuronal development. J. Cell Biol. 106:195-203.

Haas C.A., DeGennaro L.J., Muller M., and H. Hollander (1990) Synapsin I expression in the rat retina during postnatal development. Exp. Brain Res. 82:25-32.

Hackett J.T., Cochran S.L., Greenfield L.J., Brosius D.C.Jr., and T. Ueda (1990) Synapsin I injected presynaptically into goldfish Mauthner axons reduces quantal synaptic transmission. J. Neurophysiol. 63:701-706.

Hall F.L., Mitchell J.P., and P.R. Vulliet (1990) Phosphorylation of synapsin I at a novel site by proline-directed protein kinase. J. Biol. Chem. 265:6944-6948.

Hamos J.E., DeGennaro L.J., and D.A. Drachman (1988) Synaptic loss in Alzheimer's disease and other dementias. Neurology 39:355-361.

Han H.-Q. Nichols R.A., Rubin M.R., Bahler M., and P. Greengard (1991) Induction of formation of presynaptic terminals in neuroblastoma cells by synapsin IIb. Nature 349:697-700.

Hansen L.A., DeTeresa R., Davies P., and R.D. Terry (1988) Neocortical morphometry, lesion counts, and choline acetyltransferase in the age spectrum of Alzheimer's disease. Neurology 38:48-54.

Hawkes R., Niday E., and A Matus (1982) MIT-23: A mitochondrial marker for terminal differentiation defined by a monoclonal antibody. Cell 28:253-258.

Hedreen J.C., Bacon S.J., and D.L. Price (1985) A modified histochemical technique to visualize acetylcholinesterase-containing axons. J. Histochem. Cytochem. 33:134-140

Henke P.G. (1990) Potentiation of inputs from the posterolateral amygdala to the dentate gyrus and resistance to stress ulcers formation in rats. Physiol. and Behav. 48:659-664.

Hersch S.M. and E.L. White (1981) Thalamocortical synapses involving identified neurons in mouse primary somatosensory cortex: A terminal degeneration and Golgi/EM study. J. Comp. Neurol. 195:253-263.

Heumann R. and H.Thoenen (1986) Comparison between the time course of changes in nerve growth factor protein levels and those of its messenger RNA in the cultured rat iris. J. Biol. Chem. 261:9246-9249.

Hinds J.W. (1968) Autoradiographic study of histogenesis in the mouse olfactory bulb. I. Time of origin of neurons and neuroglia. J. Comp. Neurol. 134:287-304.

Hine R.J. and G.D. Das (1974) Neuroembryogenesis in the hippocampal formation of the rat. An autoradiographic study. Z. Anat. Entwickl. Gesch. 144:173-186.

Hirokawa N., Sobue K., Kanda A., and H. Yorifuji (1989) The cytoskeletal architecture of the presynaptic terminal and molecular structure of synapsin I. J. Cell Biol. 108:111-126.

Hoff S.F., Scheff S.W., Benardo L.S., and C.W. Cotman (1982) Lesion-induced synaptogenesis in the dentate gyrus of aged rats: I. Loss and reacquisition of normal synaptic density. J. Comp. Neurol. 205:246-252.

Hoffman P.N. and D.W. Cleveland (1988) Neurofilament and tubulin expression recapitulates the developmental program during axonal regeneration: Induction of a specific β-tubulin isotype. Proc. Natl. Acad. Sci. U.S.A. 85:4530-4533.

Hjorth-Simonsen A. (1972) Projection of the lateral part of the entorhinal area to the hippocampus and fascia dentata. J. Comp. Neurol. 146:219-232.

Hjorth-Simonsen A. and B. Jeune (1972) Origin and termination of the hippocampal perforant patthway in the rat studied with silver impregnation. J. Comp. Neurol. 144:215-231.

Hjorth-Simonsen A. (1973) Some intrinsic connections of the hippocampus in the rat: An experimental analysis. J. Comp. Neurol. 147:145-162.

Hjorth-Simonsen A. (1977) Commissural connections of the dentae area in the rat. J. Comp. Neurol. 174:591-606.

Howland D.S., Hemmendinger L.M., Carroll P.D., Estes P.S., Melloni Jr. R.H., and L.J. DeGennaro (1991) Postive- and negative-acting promotor sequences regulate cell type-specific expression of the rat synapsin I gene. Mol. Brain Res. 11:345-353.

Huang K.-P. (1989) The mechanism of protein kinase C activation. Trends NeuroSci. 12:425-432.

Hubel D.H., Wiesel T.N., and S. LeVay (1977) Plasticity of ocular dominance columns in the monkey striate cortex. Philos. Trans. R. Soc. Lond. [Biol.] 278:377-409.

Huttner W.B. and P. Greengard (1979) Multiple phosphorylation sites in protein I and their differential regulation by cyclic AMP and calcium. Proc. Natl. Acad. Sci. U.S.A. 76:5402-5406.

Huttner, W.B., DeGennaro L.J., and P. Greengard (1981) Differential phosphorylation of multiple sites in purified protein I by cyclic AMP-dependent and calcium-dependent protein kinases. J. Biol. Chem. 256:1482-1488.

Huttner W.B., Schiebler W., Greengard P., and P. De Camilli (1983) Synapsin I (protein I), a nerve terminal specific phosphoprotein. III. Its association with synaptic vesicles studied in a highly purified synaptic vesicle preparation. J. Cell Biol. 96:1374-1388.

Hyman B.T., Van Hoesen G.W., Damasio A.R., and C.L. Barnes (1984) Alzheimer's disease: Cell specific pathology isolates the hippocampal formation. Science 225:1168-1170.

Hyman B.T., Van Hoesen G.W., Kromer L.J., and A.R. Damasio (1986) Enhanced acetycholinesterase staining in the hippocampal perforant pathway zone in Alzheimer's disease. Neurology 36(Suppl. 1):225.

Ilaria R., Wines D., Pardue S., Jamison S., Ojeda S. R., Snider J., and M. R. Morrison

(1985) A rapid microprocedure for isolating RNA from multiple samples of human and rat brain. J. Neuroscience Methods 15:165-174.

Irwin N., Perrone-Bizzozero N.I., and L.I. Benowitz (1991) GAP-43 mRNA binding proteins related to neural differentiation. Soc. Neurosci. Abstr. 17:1310.

Jahn R., Schiebler W., Ouimet C., and P. Greengard (1985) A 38,000-dalton membrane protein (p38) present in synaptic vesicles. Proc. Natl. Acad. Sci. U.S.A. 82:4137-4141.
Jones B.E. and R.T. Moore (1977) Ascending projections of the locus coeruleus in the rat. II. Autoradiographic study. Brain Res. 127:23-54.

Jones E.G., Coulter J.D., Burton H., and R. Porter (1977) Cells of origin and terminal distribution of cortico-striatal fibers arising in the sensory-motor cortex of monkeys. J. Comp. Neurol. 173:53-80.

Kahn D.W. and W.B. Besterman (1991) Cytosolic rat brain synapsin I is a diacylglycerol kinase. Proc. Natl. Acad. Sci. U.S.A. 88:6137-6141.

Kaplan M.S. and J.W. Hinds (1977) Neurogenesis in the adult rat: Electron microscopic analysis of light autoradiographs. Science 197:1092-1094.

Katz R. A., Erlanger B. F., and R. V.Guntaka (1983) Evidence for extrinsic methylation of ribosomal RNA genes in a rat XC cell line. Biochem. Biophys. Acta 739:258-264.

Kauer J.A., Malenka R.C., and R.A. Nicoll (1988) NMDA application potentiates synaptic transmission in the hippocampus. Nature 334:250-252.

Kennedy M.B. and P. Greengard (1981) Two calcium/calmodulin-dependent protein kinases, which are highly concentrated in brain, phosphorylate protein I at distinct sites. Proc. Natl. Acad. Sci. U.S.A. 78:1293-1297.

Kilimann M.W., and L.J. DeGennaro (1985) Molecular cloning of cDNAs for the nerve-cell specific phosphoprotein, synapsin I. EMBO J. 4:1997-2002.

Kirchgessner C.U., Trofatter J.A., Mahtani M.M., Willard H.F., and L.J. DeGennaro (1991) A highly polymorphic dinucleotide repeat on the proximal short arm of the human X chromosome: Linkage mapping of the synapsin I/A-*raf*-1 genes. Am. J. Hum. Genet. 49:184-191.

Klose J., and E. Zeindl (1984) An attempt to resolve all the various protein in a single human cell type by two-dimensional electrophoresis: I. Extraction of all cell proteins. Clin. Chem. 30(12):2014-2020.

Kohn D.T. and N.I. Perone-Bizzozero (1992) RNA-protein interactions between the 3'UTR of GAP-43 mRNA and cytosolic proteins from rat brain. Soc. Neurosci. Abstr. 18:605.

Kyhse-Anderson J. (1984) Electroblotting of multiple gels: A simple apparatus without buffer tank for rapid transfer of proteins from polyacrylamide to nitrocellulose. J. Biochem. Biophys. Methods 10:203-209.

Laatch R.G. and W.M. Cowan (1967) Electron microscopic studies of the dentate gyrus of the rat. II. Degeneration of commissural aferetns. J. Comp. Neurol. 130:241-262.

Laemmli E.K. (1970) Cleavage of structural proteins during the assembly of the head of bacteriophage T4. Nature 227:680-685.

Landis D.M.D. (1988) Membrane and cytoplasmic structure at synaptic junctions in the mammalian central nervous system. J. Electron Micros. Tech. 10:129-151.

Landis D.M.D., Hall A.K., and L.A. Weinstein (1988) The organization of cytoplasm at the presynaptic active zone of a central nervous system synapse. Neuron 1:201-209.

Lapchak P.A., Jenden D.J., and F. Hefti (1991) Compensatory elevation of acetylcholine synthesis in vivo by cholinergic neurons surviving partial lesions of the septohippocampal pathway. 11(9):2821-2828.

Laping N.J., Nichols N.R., Day J.R., and C.E. Finch (1991) Corticosterone differentially regulates the bilateral response of astrocyte mRNAs in the hippocampus to entorhinal cortex lesions in male rats. Mol. Brain Res. 10:291-297.

Laurberg S. (1979) Commissural and intrinsic connections of the rat hippocampus. J. Comp. Neurol. 184:685-708.

Lazarides E. and J. Nelson (1983) Erythrocyte form of spectrin in cerebellum: Appearance at a specific stage in the terminal differentiation of neurons. Science 222:931-933.

Laurberg S. (1979) Commissural and intrinsic connections of the rat hippocampus. J. Comp. Neurol. 184:685-708.

Laurberg S. and K.E. Sorenson (1981) Associational and commissural collaterals of neurons in the hippocampal formation (hilus fasciae dentatae and subfield CA3). Brain Res. 212:287-300.

Lenoir D., Battenberg E., Kiel M., Bloom F.E., and R.J. Milner (1986) The brain-specific gene 1B236 is expressed postnatally in the developing brain. 6(2):522-530.

LeVay S., Stryker M.P., and C.J. Shatz (1978) Ocular dominance columns and their development in layer IV of the cat's visual cortex: A quantitative study. J. Comp. Neurol. 179:223-244.

Levitt P., Rakic P., De Camilli P., and P. Greengard (1984) Emergence of cyclic guanosine 3':5'-monophosphate-dependent protein kinase immunoreactivity in developing rhesus monkey cerebellum: Correlative immunocytochemical and electron microscopic analysis. J. Neurosci. 4(10):2553-2564.

Lewis P.R. and C.C.D. Shute (1967) The cholinergic limbic system: Projections to hippocampal formation, medial cortex, nuclei of the ascending cholinergic reticular system, and the subfornical organ and supra-optic crest. Brain 90:521-540.

Lewis R.M., Wallace W.C., Kanazir S.D., and P. Greengard (1983) Expression of cell-type specific neuronal phosphoproteins. Cold Spring Harbor Symp. Quant. Biol. 48:347-354.

Lin J.-W., Sugimori M., Llinas R.R., McGuinness T.L., and P. Greengard (1990) Effects of synapsin I and calcium/calmodulin-dependent protein kinase II on spontaneous neurotransmitter release in the squid giant synapse. Proc. Natl. Acad. Sci. U.S.A.

87:8257-8261.

Lindenbaum M.H., Carbonetto S., Grosveld F., Flavell D., and W.E. Muchynski (1988) Transcriptional and post-transcriptional effects of nerve growth factor on expression of the three neurofilament subunits in PC12 cells. J. Biol. Chem. 263:5662-5667.

Lippa C.F., Hamos J.E., Pulaski-Salo D., DeGennaro L.J., and D.A. Drachman (1992) Alzheimer's disease and aging: Effects on perforant pathway perikarya and synapses. Neurobiol. of Aging 13:405-411.

Llinas R., McGuinness T.L., Leonard C.S., Sugimori M., and P. Greengard (1985) Intraterminal injection of synapsin I or calcium calmodulin-dependent protein kinase II alters neurotransmitter release at the squid giant synapse. Proc. Natl. Acad. Sci. U.S.A. 82:3055-3039.

Llinas R., Gruner J.A., Sugimor M., McGuinness T.L., and P. Greengard (1991) Regulation by synapsin I and Ca2+/calmodulin-dependent protein Kinase II of transmitter release in squid giant synapse. J. Physiol. 436:257-282.

Loesche J. and O. Steward (1977) Behavioral correlates of denervation and reinnervation of the hippocampal formation of the rat: Recovery of alternation performance following unilateral entorhinal cortex lesions. Brain Res. Bull. 2:31-39.

Lohmann S.M., Ueda T. and P. Greengard (1978) Ontogeny of synaptic phosphoproteins in brain. Proc. Natl. Acad. Sci. U.S.A. 75(8):4037-4041.

Lorente de No R. (1934) Studies on the structure of the cerebral cortex. II. Continuation of the study of the ammonic system. J. Psychol. Neur. 46:113-177.

Lorente de No R. (1938) Architectonics and structure of the cerebral cortex. In *Physiology of the Nervous System.* (ed. Fulton J.F.), pp. 291-325. Oxford University Press, New York.

Lu B., Greengard P., and M-m. Poo (1992) Exogenous synapsin I promotes functional maturation of developing neuromuscular synapses. Neuron 8:521-529.

Lund J.S. (1973) Organization of neurons in the visual cortex, area 17, of the monkey (Macaca mulatta). J. Comp. Neurol. 147:455-496.

Lynch G., Matthews D.A., Mosko S., Parks T., and C.W. Cotman (1972) Induced acetylcholinesteras-rich layer in rat dentate gyrus following entorhinal lesions. Brain Res. 42:311-318.

Lynch G., Mosko S., Parks T., and C.W. Cotman (1973) Relocation and hyperdevelopment of the dentate gyrus commissural system after entorhinal lesions in immature rats. Brain Res. 50:174-178.

Lynch G., Gall C., Rose G., and C.W. Cotman (1976) Changes in the distribution of the dentate gyrus associational system following unilateral or bilateral entorhinal lesion in the adult rat. Brain Res. 110:57-71.

Lynch G., Gall C., and C.W. Cotman (1977) Temporal parameters of axon "sprouting" in the brain of the adult rat. Exp. Neurol. 54:179-183.

Mailleux P., Takazawa K., Erneux C., and J.-J. Vanderhaeghen (1993) Distribution of the neurons containing inositol 1,4,5-triphosphate 3-kinase and its messenger RNA in the developing rat brain. J. Comp. Neurol. 327:618-630.

Maniatis T., Fritsch E.F., and J. Sambrook (1982) Molecular cloning: A laboratory manual, Cold Spring Harbor laboratory. New York: Cold Spring Harbor.

Mann D.A., Yates P.O., and B. Marcyniuk (1984) Changes in nerve cells of the nucleus basalis of meynert in Alzheimer's disease and their relationship to ageing and to the accumulation of lipofuscin pigment. Mech. of Ageing and Devel. 25:189-204.

Marqueze-Pouey B., Wisden W., Malosio M.L., and H. Betz (1991) Differential expression of synaptophysin and synaptoporin mRNAs in the postnatal rat central nervous system. J. Neurosci. 11:3388-3397.

Masco D. and W. Seifert (1990) Gangliosides in lesion-induced synaptogenesis: Studies in the hippocampus of rat brain. Brain Res. 314:84-92.

Mason C.A. (1986) Axon development in mouse cerebellum: Embryonic axon forms and expression of synapsin I. Neuroscience 19(4):1319-1333.

Matthews D.A., Cotman C.W., and G. Lynch (1976a) An electron microscopic study of lesion-induced synaptogenesis in the dentate gyrus of the adult rat. I. Magnitude and time course of degeneration. Brain Res. 115:1-21.

Matthews D.A., Cotman C.W., and G. Lynch (1976b) An electron microscopic study of lesion-induced synaptogenesis in the dentate gyrus of the adult rat. II. Reappearance of morphologically normal contacts. Brain Res. 115:23-41.

Maue R.A., Kraner S.D., Goodman R.H., and G. Mandel (1990) Neuron-specific expression of the rat brain type II sodium channel gene is directed by upstream regulatory elements. Neuron 4:223-231.

May P.C., Lamper-Etchells M., Johnson S.A., Poirer J., Masters J.N. and C.E. Finch (1990) Dynamics of gene expression for a hippocampal glycoprotein elevated in Alzheimer's disease and in response to exprimental lesions in rat. Neuron 5:831-839.

McCaffery C.A. and L.J. DeGennaro (1986) Determination and analysis of the primary structure of the nerve terminal specific phosphoprotein, synapsin I. EMBO J. 5(12):3167-3173.

McGuinness, T.L., Y. Lai, and P. Greengard (1985) Ca^{2+}/calmodulin-dependent protein kinase II (Isozymic forms from rat forebrain and cerebellum). J. Biol. Chem. 260:1696-1704.

McLean I.W., and. P.K. Nakane (1974) Periodate-lysine-paraformaldehyde fixative. A new fixative for immunoelectron microscopy. J. Histochem. Cytochem. 22:1077-1083.

McWilliams J.R. and G. Lynch (1981) Sprouting in the hippocampus is accompanied by an increase in coated vesicles. Brain Res. 211:158-164;.

Meibach R.C. and A. Siegel (1977a) Efferent connections of the septal area in the rat: An analysis utilizing retrograde and anterograde transport methods. Brain Res. 119:1-20.

Meibach R.C. and A. Siegel (1977b) Efferent connections of the hippocampal formation in the rat. Brain Res. 124:197-224.

Meirer R. (1988) A universal and efficient protocol for the isolation of RNA from tissues and cultured cells. Nucl. Acids Res. 16(5):2340.

Mellgren S.I. and B. Srebro (1973) Changes in acetylcholinesterase and distribution of degenerating fibres in the hippocampal region after septal lesions in the rat. Brain Res. 52:19-36.

Melloni Jr. R.H., Estes P.S., Howland D.S., and DeGennaro L.J. (1992) A method for the direct measurement of mRNA in discrete regions of mammalian brain. Anal. Biochem. 200:95-99.

Melloni Jr. R.H., Hemmendinger, L.M., Hamos, J.E., and DeGennaro, L.J. (1993) Synapsin I gene expression in the adult rat brain with comparative analysis of mRNA and protein in the hippocampus. J. Comp. Neurol. 327, 507-520.

Melloni Jr. R.H. and L.J. DeGennaro (submitted for publication) Temporal onset of synapsin I gene expression coincides with neuronal differentiation during the development of the rat nervous system.

Melloni Jr. R.H., Apostolides P.J., Hamos J.E., and L.J. DeGennaro (submitted for publication) Dynamics of neuron-specific gene expression during the establishment and restoration of functional synapses in the rat hippocampus.

Miller F.D., Mathew T.C., and J.G. Toma (1991) Regulation of nerve growth factor receptor gene expression by nerve growth factor in the developing peripheral nervous system. J. Cell Biol. 112(2):303-312.

Monaghan D.T. and C.W. Cotman (1982) The distribution of [^{3}H] kainic acid binding sites in rat CNS as determined by autoradiography. Brain Res. 252:91-100.

Moore R.Y. and A.E. Halaris (1975) Hippocampal innervation by serotonin neurons of the midbrain raphe in the rat. J. Comp. Neurol. 164:171-184.

Moore R.Y. and M.E. Bernstein (1989) Synaptogenesis in the rat suprachiasmatic nucleus demostrated by electron microscopy and synapsin I immunoreactivity. J. Neurosci. 9(6):2151-2162.

Morgan J.I., Cohen D.R., Hempstead J.L., and T. Curran (1987) Mapping patterns of *c-fos* expression in the central nervous system after seizure. Science 237:192-197.

Morgan J.I. and T. Curran (1989) Stimulus-transcription coupling in neurons: Role of cellular immediate-early genes. TINS 12:459-462.

Mori N., Stein R., Sigmund O., and D.J. Anderson (1990) A cell type-preferred silencer element that controls the neural-specific expression of the SCG10 gene. Neuron 4:583-594.

Mori N., Schoenherr C., Vandenbergh D.J., and D.J. Anderson (1992) A common silencer element in the SCG10 and type II Na^+ channel genes binds a factor present in

nonneuronal cells but not in neuronal cells. Neuron 9:45-54.

Mosko S., Lynch G., and C.W. Cotman (1973) The distribution of septal projections to the hippocampus of the rat. J. Comp. Neurol. 152:163-174.

Muglia L. and L.B. Rothman-Denes (1986) Cell type-specific negative regulatory element in the control region of the rat α-fetoprotein gene. Proc. Natl. Acad. Sci. U.S.A. 83:7653-7657.

Mullins L.J., Stephenson D.A., Grant S.G., and V.M. Chapman (1990) Efficient linkage of 10 loci in the proximal region of the mouse X chromosome. Genomics 7:19-30.

Nadler J.V., Cotman C.W., and G.S. Lynch (1973) Altered distribution of choline acetyltransferase and acetylcholinesterase activities in the developing rat dentate gyrus following entorhinal lesions. Brain Res. 63:215-230.

Nadler J.V., Cotman C.W., and G.S. Lynch (1977) Histochemical evidence of altered development of cholinergic fibers in the rat dentate gyrus following lesions. I. Time course after complete unilateral entorhinal lesion at various ages. J. Comp. Neurol. 171:561-577.

Nairn A.C. and P. Greengard (1987) Purification and characterization of Ca^{2+}/calmodulin-dependent protein kinase I from bovine brain. J. Biol. Chem. 262:7273-7281.

Navone F., Greengard P., and P. De Camilli (1984) Synapsin I in nerve terminals: selective association with small synaptic vesicles. Science 226:1209-1211.

Nedivi E., Basi G.S., and J.H.P. Skene (1991) Identification of *cis*-acting elements regulating GAP-43 promotor activity. Soc. Neurosci. Abstr. 17:1310.

Nedivi E., Basi G.S., Akey I.V., and J.H.P. Skene (1992) A neural-specific GAP-43 core promotor located between unusual DNA elements that interact to regulate its activity. J. Neurosci. 12(3):691-703.

Nestler E.J. and P. Greengard (1984) Protein phosphorylation in the nervous system. Wiley, N.Y.

Neve R.L., Perrone-Bizzozero N.I., Finklestein S., Zwiers H., Bird E., Kurnit D.M., and L.I. Benowitz (1987) The neuronal growth-associated protein GAP-43 (B50, F1): neuronal specificity, developmental regulation and regional distribution of the human and rat mRNAs. Mol. Brain Res. 2:177-183.

Nichols N.R., Laping N.J., Day J.R., and C.E. Finch (1991) Increases in transforming growth factor-β mRNA in hippocampus during response to entorhinal cortex lesions in intact and adrenalectomized rats. J. Neurosci. 28:134-139.

Nichols R.A., Chilcote T.J., Czernik A.J., and P. Greengard (1992) Synapsin I regulates glutamate release from rat brain synaptosomes. J. Neurochem. 58:783-785.

Nieto-Sampedro N., Lewis E.R., Cotman C.W., Manthorpe M., Skaper S.D., Barbin G., Longo F.M., and S. Varon (1982) Brain injury causes a time-dependent increase in neuronotrophic activity at the lesion site. Science 217:860-861.

Nir U., Walker M.D., and W.J. Rutter (1986) Regulation of rat insulin 1 gene expression: evidence for negative regulation in nonpancreatic cells. Proc. Natl. Acad. Sci. U.S.A. 83:3180-3184.

O'Leary J.L. (1941) Structure of the area striata of the cat. J. Comp. Neurol. 5:131-164.

Palkovitz,M., and M.J. Brownstein (1988) Maps and guide to microdissection of rat brain. Elsevier, N.Y.

Pauli U., Wright K., van Wijnen A., Stein G., and J. Stein (1991) In *Methods in Nucleic Acids Research* (ed. Karam J.D., Chao L., and Warr G.W.), pp. 227-250. CRC Press, Boca Raton, FL.

Peltz S.W., Brewer G., Bernstein P., Hart P.A., and J. Ross (1992) Regulation of mRNA turnover in eukaryotic cells. Crit. Rev. Euk. Gene Exp. 1:99-126.

Perdahl E., Adolfsson R., Alafuzoff I., Albert K.A., Nester E.J., Greengard P., and B. Winblad (1984) Synapsin I (Protein I) in different regions in senile dementia of alzheimer type and in multiinfarct dementia. J. Neural Trans. 60:133-141.

Perrone--Bizzozero N.I., Finklestein S.P., and L.I. Benowitz (1986) Synthesis of a growth-associated protein by embryonic rat cerebrocortical neurons in vitro. J. Neurosci. 6:3721-3730.

Perrone--Bizzozero N.I., and L.I. Benowitz (1987) Expression of a 48-kilodalton growth-associated protein in the goldfish retina. J.Neurochem. 48:644-652.

Perrone--Bizzozero N.I., Neve R.L., Irwin N., Lewis S.E., Fischer I., and L.I. Benowitz (1991) Post-transcriptional regulation of GAP-43 mRNA levels during neuronal differentiation and nerve regeneration. Mol. Cell Neurosci. 2:402-409.

Perrone--Bizzozero N.I., Cansino V.V., and D.T. Kohn (1993) Posttranscriptional regulation of GAP-43 gene expression in PC12 cells through protein kinase C-dependent stabilization of the mRNA. J. Cell Biol. 120(5):1263-1270.

Petrucci T.C. and J.S. Morrow (1987) Synapsin I: an actin-bundling protein under phosphorylation control. J. Cell Biol. 105:1355-1363.

Phillips L.L. and O. Steward (1990) Increases in mRNA for cytoskeletal protein in the denervated neuropil of the dentate gyrus: An in situ hybridization study using riboprobes for β-actin and β-tubulin. Mol. Brain Res. 8:249-257.

Poirer J., May P.C., Osterberg H.H., Geddes J., Cotman C.W., and C.E. Finch (1990) Selective alterations of RNA in rat hippocampus after entorhinal cortex lesioning. Proc. Natl. Acad. Sci. U.S.A. 87:303-307.

Poirer J., Hess M., May P.C., and C.E. Finch (1991a) Astrocytic apolipoprotein E mRNA and GFAP mRNA in hippocampus after entorhinal cortex lesioning. Mol. Brain Res. 11:97-106.

Poirer J., Hess M., May P.C., and C.E. Finch (1991b) Cloning of hippocampal poly(A) RNA sequences that increase after entorhinal cortex lesion in adult rat. Mol. Brain Res.

9:191-195.

Racamora N., Palacios J.M., and G. Mengod (1992) Limbic seizures induce a differential regulation of the expression of nerve growth factor, brain-derived neurotrophic factor and neurotrophin-3, in the rat hippocampus. Mol. Brain Res. 13:27-33.

Racine R.J., Milgram N.W., and S. Hafner (1983) Long-term potentiation phenomena in the rat limbic forebrain. Brain Res. 260:217-231.

Raisman G., Cowan W.M., and T.P.S. Powell (1965) The extrinsic afferent, commissural and association fibers of the hippocampus. Brain 88:963-966.

Raisman G., Cowan W.M., and T.P.S. Powell (1966) An experimental analysis of the efferent projection of the hippocampus. Brain 89:83-108.

Rakic P. (1976) Prenatal genesis of connections subserving ocular dominance in the rhesus monkey. Nature 261:467-471.

Rakic P. (1977) Prenatal development of the visual system in rhesus monkey. Philos. Trans. R. Soc. Lond. [Biol.] 278:245-260.

Rappolee D. A., Wang A., Mark D., and Z. Werb (1989) Novel method for studying mRNA phenotypes in single or small numbers of cells. J. Cell. Biochem. 39:1-11.

Rasool C.G., Svendesen C.N., and D.J. Selkoe (1986) Neurofibrillary degeneration of cholinergic and noncholinergic neurons of the basal forebrain in Alzheimer's disease. Ann. Neurol. 20:482-488.

Reeves T.M. and D.C. Smith (1987) Reinnervation of the dentate gyrus and recovery of alternation behavior following entorhinal cortex lesions. Behav. Neurosci. 101:179-186.

Reeves T.M. and O. Steward (1988) Changes in the firing properties of neurons in the dentate gyrus with denervation and reinnervation: Implications for behavioral recovery. Exp. Neurol. 102:37-49.

Rossor M.N., Svendsen C., and S.P. Hunt (1982) The substantia inominata in Alzheimer's disease: a histochemical and biochemical study of cholinergic marker enzymes. Neurosci. Letts. 28:217-222.

Sauerwald A., Hoesche C., Oschwald R., and M.W. Kilimann (1990) The 5' flanking region of the synapsin I gene. J. Biol. Chem. 265:14932-14937.

Savangner P., Miyashita T., and Y. Yamada (1990) Two silencers regulate the tissue-specific expression of the collagen II gene. J. Biol. Chem. 265(12):6669-6674.

Scheff S.W., Bernado L.S., and C.W. Cotman (1977) Progressive brain damage accelerates axon sprouting in the adult rat. Science 197:795-797.

Scheff S.W., and C.W. Cotman (1977) Recovery of spontaneous alternation following lesion of the entorhinal cortex in adult rats: possible correlation to axon sprouting. Behav. Biol., 21:286-293.

Scheff S.W., Anderson K.J., and S.T. DeKosky (1985) Strain comparison of synaptic density in hippocampal CA1 of aged rats. Neurobiol. of Aging 6:29-34.

Scheff S.W., Scott S.A., and S.T. DeKosky (1991) Quantitation of synaptic density in the septal nuclei of young and aged Fisher 344 rats. Neurobiol. of Aging 12:3-12.

Schiebler W., Jahn R., Doucet J.P., Rothein J., and P. Greengard (1986) Characterization of synapsin I binkding to small synaptic vesicles. J. Biol. Chem. 261:8383-8390.

Schlessinger A.R., Cowan W.M., and D.I. Gottlieb (1975) An autoradiographic study of the time of origin and the pattern of granule cell migration in the dentate gyrus of the rat. J. Comp. Neurol. 159:149-176.

Skene J.H.P. and M. Willard (1989) Axonal growth-associated proteins. Annu. Rev. Neurosci. 12:127-156.

Stanfield B.B. and W.M. Cowan (1979) The development of the hippocampus and dentate gyrus in normal and reeler mice. J. Comp. Neurol. 185:423-460.

Sheng M. and M.E. Greenberg (1990) The regulation and function of *c-fos* and other immediate early genes in the nervous system. Neuron 4:477-485.

Sihra T.S., Wang J.K.T., Gorelick F.S., and P. Greengard (1989) Translocation of synapsin I in response to depolarization of isolated nerve terminals. Proc. Natl. Acad. Sci. U.S.A. 86:8108-8112.

Sive H. L., Hattori K., and H.Weintraub (1989) Progressive determination during formation of the anteroposterior axis in Xenopus laevis. Cell 58:171-180.

Smale S.T. and D. Baltimore (1989) The 'initiator' as a transcription control element. Cell 57:103-113.

Smith T.W., Nikulasson S., De Girolami U., and L.J. DeGennaro (1993) Immunohistochemistry of synapsin I and synaptophysin in human nervous system and neuroendocrine tumors. J. Neuropath. Exp. Neurol. (in press).

Steward O., Cotman C.W., and G. Lynch (1973) Re-establishment of electrophysiologically functional entorhinal cortical input to the dentate gyrus deafferenteed by ipsilateral entorhinal lesions: Innervation by the contralateral entorhinal cortex. Exp. Brain Res. 18:396-414.

Steward O. (1976a) Topographic organization of projections from the entorhinal area to the hippocampal formation of the rat. J. Comp. Neurol. 167:285-314.

Steward O. (1976b) Reinnervation of the dentate gyrus by homologous afferents following entorhinal cortical lesions in adult rats. Science 194:426-428.

Steward O. and S.A. Scoville (1976) Cells of origin of entorhinal cortical afferents to the hippocampus and fascia dentata of the rat. J. Comp. Neurol. 169:347-340.

Steward O. (1981) Assessing the functional significance of lesion-induced neuronal plasticity. Int. Rev. Neurobiol. 23:197-254.

Steward O. (1983) Alterations in polyribosomes associated with dendritic spines during the reinnervation of the dentate gyrus of the adult rat. J. Neurosci. 3(1):177-188..

Steward O. and S.L. Vinsant (1983) The process of reinnervation in the dentate gyrus of the adult rat: A quantitative electron microscopic analysis of terminal proliferation and reactive synaptogenesis. J. Comp. Neurol. 214:370-386.

Steward O., Torre E.R., Phillips L.L., and P.A. Trimmer (1990) The process of reinnervation in the dentate gyrus of adult rats: Time course of increases in mRNA for glial fibrillary acidic protein. 10(7):2373-2384..

Stirling R.V. and T.V.P. Bliss (1978) Hippocampal mossy fiber development at the ultrastructural level. Prog. Brain Res. 48:191-198.

Storm-Mathisen J. and H.C. Guldberg (1974) 5-Hydroxytryptamine and noradrenaline in the hippocampal region: effect of transection of afferent pathways on endogenous levels, high affinity uptake and some transmitter-related enzymes. J. Neurochem. 22:793-803.

Sudhof T.C., Lottspeich F., Greengard P., Ehrenfried M., and R. Jahn (1987) A synaptic vesicle protein with a novel cytoplasmic domain. Science 238:1142-1144.

Sudhof T.C., Czernik A.J., Kao H.T., Takei K., Johnston P.A., Horiuchi A., Kanazir S.D., Wagner M.A., Perin M.S., De Camilli P., and P. Greengard (1989) Synapsins: mosaics of shared and individual domains in a family of synaptic vesicle phosphoproteins. Science 245:1474-1480.

Sudhof T.C. (1990) The structure of the human synapsin I gene and protein. J. Biol. Chem. 265:7849-7852.

Sudhof T.C.and R. Jahn (1991) Proteins of synaptic vesicles involved in exocytosis and membrane recycling. Neuron 6:665-677.

Swanson L.W. and W.M. Cowan (1975) Hippocampal-hypothalamic connections: Origin in the subicular cortex, not in Ammon's horn. Science 189:303-304.

Swanson L.W. and W.M. Cowan (1976) Autoradiographic studies of the development and connections of the septal area in the rat. In *The Septal Nuclei.* (ed De France J.W.) pp. 37-64. Plenum Press, New York.

Swanson L.W. and W.M. Cowan (1977) An autoradiographic study of the organization of the efferent connections of the hippocampal formation in the rat. J. Comp. Neurol. 172:49-84.

Swanson L.W., Wyss J.M., and W.M. Cowan (1978) An autoradiographic study of the organization of intrahippocampal association pathways in the rat. J. Comp. Neurol. 181:681-716.

Swanson L.W., Sawchenko P.E., and W.M. Cowan (1981) Evidence for collateral projections by neurons in Ammon's horn, the dentate gyrus, and the subiculum: a multiple retrograde labeling study in the rat. J. Neurosci. 1:548-559.

Taxt T. and J. Storm-Mathisen (1994) Uptake of D-aspartate and L-glutamate in excitatory axon termials in hippocampus: autoradiographic and biochemical comparison with γ-aminobutyrate and other amino acids in normal rats ansd in rats with lesions. Neuroscience 11:79-100.

Tagliavani F. and G. Pilleri (1983a) Neuronal counts in the nucleus of Meynert in Alzheimer's disease and in simple senile dementia. Lancet 2:469-470.

Tagliavani F. and G. Pilleri (1983b) Basal nucleus of Meynert: a neuropathological sutdy in Alzheimer's disease, simple senile dementia, Pick's disease and Huntington's chorea. J. Neurol. Sci. 62:243-260.

Tarelli F.T., Bossi M., Fesce R., Greengard P., and F. Valtorta (1992) Synapsin I partially dissociates from synaptic vesicles during exocytosis induced by electrical stimulation. Neuron 9:1143-1153.

Thomas P.S. (1980) Hybridization of denatured RNA and small DNA fragments transferred to nitrocellulose. Proc. Natl. Acad. Sci. U.S.A. 77:5201-5205.

Thomas L., Hartung K., Langosch D., Rehm H., Bamberg E., Franke W.W., and H. Betz (1988) Identification of synaptophysin as a hexameric channal protein of the synaptic vesicle membrane. Science 242:1050-1053.

Thompson M.A. and E.B. Ziff (1989) Structure of the gene encoding peripherin, an NGF-regulated neuronal-specific type III intermediate filament protein. Neuron 2:1043-1053.

Thiel G., Greengard P., and T.C. Sudhof (1991) Characterization of tissue-specific transcription by the human synapsin I gene promotor. Proc. Natl. Acad. Sci. U.S.A. 88:3431-3435.

Towbin H., Staehelin T, and J. Gordon (1979) Electrophoretic transfer of proteins from polyacrylamide gels to nitrocellulose sheets: Procedure and some applications. Proc. Natl. Acad. Sci. U.S.A. 76:4350-4354.

Trimble W.S., Gray T.S., Elferink L.A., Wilson M.C., and R.H. Scheller (1990) Distinct patterns of expression of two VAMP genes within the rat brain. J. Neurosci. 10:1380-1387.

Ueda T., Maeno H., and P. Greengard (1973) Regulation of endogenous phosphorylation of specific proteins in synaptic membrane fractions from rat brain by adenosine 3',5'-monophosphate. J. Biol. Chem. 248:8295-8305.

Ueda T. and P. Greengard (1977) Adenosine 3';5'-monophosphate regulated phosphoprotein system of neuronal membranes. I. Solubilization, purification and some properties of an endogenous phosphoprotein. J. Biol. Chem. 252:5155-5163.

Vulliet P.R., Hall F.L., Mitchell J.P., and D.G. Hardie (1989) Identification of a novel proline-directed serine/threonine protein kinase in rat pheochromocytoma. J. Biol. Chem. 264:16292-16298.

Walaas S.I., Browning M.D. , and P. Greengard (1988) Synapsin Ia, synapsin Ib, protein IIIa, protein IIIb, four related synaptic vesicle-associated phosphoproteins, share regional and cellular localization in rat brain. J. Neurochem. 51:1214-1220.

Walaas S.I., Nairn A.C., and P.Greengard (1983) Regional distribution of calcium- and cyclic adenosine 3';5'-monophosphate-regulated protein phosphorylation systems in mammalian brain. J. Neurosci. 3:291-301.

Weinberger J., Jat P.S., and P.A. Sharp (1988) Localization of a repressive sequence contributing to B-cell specificity in the immunoglobulin heavy-chain enhancer. Mol. and Cell Biol. 8(2):988-992.

Weiss S., Pin J.-P., Sebben M., Kemp D., Sladeczek F., Gabrion J., and J. Bockaert (1986) Synaptogenesis of cultured striatal neurons in serum-free medium: a morphological and biochemical study. Proc. Natl. Acad. Sci. U.S.A. 83:2238-2242.

Weissman J.D. and D.S. Singer (1991) A complex regulatory DNA element associated with a major histocompatability complex class I gene consists of both a silencer and an enhancer. Mol. and Cell Biol. 11(8):4217-4227.

West J., Deadwyler S., Cotman C.W., and G. Lynch (1975) Time-dependent changes in commissural field potential in the dentate gyrus following lesions of the entorhinal cortex in rats. Brain Res. 97:215-233.

Whitehouse P.J., Price D.L., and A.W. Clark (1981) Alzheimer disease evidence for selective loss of cholinergic neurons in the nucleus basalis. Ann. Neurol. 10:122-126.

Whitehouse P.J., Price D.L., and R.G. Struble (1982a) Alzheimer's disease and senile dementia: Loss of neurons in the basal forebrain. Science 215:1237-1239.

Whitehouse P.J., Struble P.G., and A.W. Clark (1982b) Alzheimer's disease: plaques, tangles and the basal forebrain. Ann. Neurol. 12:494.

Whittmore S.R., Larkfors L., Ebendal T., Holets V.R., Ericsson A., and H. Persson (1987) Increased β-nerve growth factor messenger RNA and protein levels in neonatal rat hippocampus following specific cholinergic lesions. J. Neurosci. 7(1):244-251.

Wiedenmann B. and W.W. Franke (1985) Identification and localization of synaptophysin, an integral membrane glycoprotein of Mr 38,000 characteristic of presynaptic vesicles. Cell 41:1017-1028.

Wilcock G.K., Esiri M.M., Bowen D.M., and C.C.C.T. Smith (1983) The nucleus basalis in Alzheimer's disease: Cell counts and cortical biochemistry. Neuropathol. Appl. Neurobiol. 9:175-179.

Wilkinson M. (1988) RNA isolation: A mini-prep method. Nucl. Acids Res. 16(22):10,933.

Wilkinson M. (1988) A rapid and comvenient method for isolation of nuclear, cytoplasmic and total cellular RNA. Nucl. Acids Res. 16(22):10,934.

Wise S.P. and E.G. Jones (1977) Cells of origin and terminal distribution of coticofugal pathways from the rat somatic sensory cortex. J. Comp. Neurol. 175:129-158.

Wong M.-L., Weiss S.R.B., Gold P.W., Doi S.Q., Banjeree S., Lincinio J., Lad R., Post R.M., and M.A. Smith (1992) Induction of constitutive heat shock protein 73 mRNA in the dentate gyrus by seizures. Mol. Brain Res. 13:19-25.

Xie C.-W., Mitchell C.L., and J.-S. Hong (1990) Perforant path stimulation differentially alters prodynorphin mRNA and proenkephalin mRNA levels in the entorhinal cortex-hippocampal region. Mol. Brain Res. 7:199-205.

Yeng-Feng T.L., DeGennaro L.J., and U. Francke (1986) Genes for synapsin I, a neuronal phosphoprotein, map to conserved regions of human and murine X chromosomes. Proc. Natl. Acad. Sci. U.S.A. 83:8679-8683.

Zimmer J. (1973) Extended commissural and ipsilateral projections in postnatally deentorhinated hippocampus and fascia dentata demonstrated in rats by silver impregnation. Brain Res. 64:293-311.

Zimmer J. and A. Hjorth-Simonsen (1975) Crossed pathways from the entorhinal area to the fascia dentata. II. provokable in rats. J. Comp. Neurol. 161:71-102.

Zimmer J. and F.-M.S. Haug (1978) Laminar differentiation of the hippocampus, fascia dentata and subiculum in developing rats, observed with the Timm sulphide silver method. J. Comp. Neurol. 179:581-618.

APPENDIX

RECENT PUBLICATIONS

ANALYTICAL BIOCHEMISTRY 200, 95–99 (1992)

A Method for the Direct Measurement of mRNA in Discrete Regions of Mammalian Brain

Richard H. Melloni, Jr.,*,† Patricia S. Estes,* David S. Howland,* and Louis J. DeGennaro*,†

*Departments of *Neurology and †Cell Biology, University of Massachusetts Medical Center, 55 Lake Avenue, North, Worcester, Massachusetts 01655*

Received March 25, 1991

A rapid and nearly quantitative method for the direct analysis of steady-state mRNA levels in microgram quantities of frozen mammalian brain is described. Briefly, tissue punches 0.5–1.0 mm in diameter were sampled from 250-μm-thick cryostat sections of rat brain (approximately 50–200 μg tissue). The samples were homogenized in 50 μl of a denaturing gel loading buffer and applied directly to a 2.2 M formaldehyde–agarose gel for electrophoresis and subsequent RNA blot analysis. The method is extremely rapid, results in excellent recovery of intact RNA, and allows the direct assay of mRNA levels in discrete subregions of the mammalian brain.

Hybridization analysis of steady-state mRNA levels as a reflection of differential gene expression is a procedure commonly used in molecular neurobiology. For such analyses to be truly quantitative and reproducible, RNA isolation and purification protocols typically must yield intact RNA with high efficiency and good recovery. Several difficulties arise in the application of current methods which meet these criteria to the study of gene expression in the discrete subregions of the mammalian brain. First, these methods invariably require moderate amounts of tissue, which precludes their use in the analysis of mRNA levels in tissue samples where quantities are limited. Furthermore, due to the elaborate nature of conventional RNA preparation protocols, the analysis of large numbers of RNA samples can be tedious and often very time consuming. Recently, several reports of rapid, small-scale preparations of nuclear, cytoplasmic, poly(A)$^+$, and total cellular RNA have been published (1–12). These reports detail RNA extraction protocols from both isolated- and cultured-cell suspensions and fresh tissues, using as little as 10^5 cells or 3 mg tissue, respectively. However, consistently poor yields indicate that many of these methods are unsuitable for the rapid analysis of multiple RNA samples from microgram amounts (approximately 50–200 μg) of intact tissue.

An alternate method of measuring mRNA levels in small amounts of tissue has recently been published by Sive *et al.* (13). The authors describe the use of a urea lysis buffer (7 M urea, 0.5% SDS,[1] 1× Mops) to solubilize small amounts of freshly dissected *Xenopus* embryo parts. To measure steady-state mRNA levels directly, the solubilized tissue samples were added to a formaldehyde–agarose gel for electrophoresis and subsequent RNA blot analysis. In our hands, however, complications with RNA degradation and incomplete denaturation proved this buffer unsuitable for use with small quantities of frozen mammalian brain tissue.

In this paper, we report a modified procedure for the direct analysis of mRNA levels in microgram quantities of frozen mammalian tissues, with particular emphasis on RNAs from brain. The punch-and-load procedure is extremely rapid, results in excellent recovery of RNA, and allows the direct assay of mRNA levels in discrete regions of cryostat cut tissue sections.

MATERIALS AND METHODS

Materials. All materials were molecular biology grade or of the highest purity. All glassware was baked at 180°C for >4 h to inactivate ribonucleases (14), and aqueous solutions were treated with 0.1% DEPC and autoclaved before use. The FUV-denaturing gel loading buffer was a modified urea lysis buffer (13). The FUV-buffer contained 2.2 M formaldehyde, 7 M urea, 20 mM ribonucleoside–vanadyl complexes (VRC) 0.5% SDS,

[1] Abbreviations used: SDS, sodium dodecyl sulfate; Mops, 3-(*N*-morpholino)propanesulfonic acid; DEPC, diethyl pyrocarbonate; VRC, vanadyl–ribonucleoside complex.

0003-2697/92 $3.00

and 1× Mops. A urea stock solution minus formaldehyde and VRC was made and stored at room temperature for no longer than 1 week. Formaldehyde (37%) and VRC were added just prior to sample processing.

Three-month-old male Wistar rats were anesthesized and killed by decapitation. Brains were removed, frozen in dry-ice-supercooled (−30 to −40°C) isopentane (Aldrich), and stored in plastic bags at −70°C. Just before use, the brains were warmed to −10°C and cryostat sections were cut to 250 μm in thickness. The sections were thaw-mounted on glass slides and then stored at −70°C for microdissection.

RNA analysis. Total RNA was extracted and purified from rat tissues by the method of Chirgwin *et al.* (15) or analyzed by the punch-and-load procedure described below.

Stainless-steel hypodermic tubing (Small Parts Inc., Miami, FL) was used to sample punches of tissue 0.5–1.0 mm in diameter from 250-μm-thick cryostat sections of rat brain, kidney, and liver (approximately 50–200 μg tissue (16)). The micropunches were immediately solubilized by pestle homogenization using a Kontes reusable CTFE/stainless-steel pestle attached to a Skiltwist cordless screwdriver motor unit. Homogenization was carried out in 50 μl FUV-buffer in Kontes 500-μl polypropylene microtubes and samples were placed on ice. Samples were then centrifuged in an Eppendorf microfuge for 15 s at room temperature, heated at 65°C for 20 min, and returned to ice. Ethidium bromide, to a final concentration of 25 ng/μl, and bromphenol blue (4%) loading dye were added to each tube, and the samples were applied directly to a 2.2 M formaldehyde–agarose (1.2%) gel for electrophoresis (14). The gel was then photographed under ultraviolet illumination to visualize the 28 S ribosomal RNA band as a qualitative measure of RNA integrity.

Hybridization. RNA was blotted onto Zetabind nylon membrane (American Bioanalytical) by capillary action using 10× SSC (1× SSC is 0.16 M NaCl, 0.015 M $Na_3C_6H_7 \cdot 2H_2O$, pH 7.0) as the transfer buffer. Membranes were uv cross-linked for 1 min (17) and baked at 80°C for 1 h. For prehybridization, membranes were incubated for 4–6 h at 50°C in hybridization buffer (50% formamide, 0.5 M Na_2HPO_4, pH 7.5, 7% SDS, and 250 μg/ml heat-denatured *Escherichia coli* DNA). Membranes were then hybridized to [^{32}P]dCTP random-primed labeled (Boehringer–Mannheim) synapsin I (18), α-tubulin (19), and/or 18 S ribosomal RNA (20) cDNA probes at 3–10 × 10^6 cpm/ml. Hybridizations were carried out in hybridization buffer at 50°C overnight (>16 h). Membranes were then washed at room temperature for 20 min in two changes of 2× SSC, 0.1% SDS, 0.1% $Na_4P_2O_7$; followed by 1× SSC, 0.1% SDS, 0.1% $Na_4P_2O_7$; and 0.3× SSC, 0.1% SDS, 0.1% $Na_4P_2O_7$, each preheated to 65°C. RNA blots were then exposed to Kodak XAR-5 film for >4 days at −70°C with a DuPont Cronex intensifying screen.

Standardization. Prior to tissue sampling, an unlabeled sense synapsin I synthetic RNA was added to the FUV-buffer to serve as external standard (21). Briefly, a 1.7-kb synapsin I sense RNA transcript was synthesized *in vitro* using a SP6/T7 Transcription Kit (Boehringer–Mannheim). The RNA was purified by repeated ethanol precipitation, and a known amount was added to punch samples to control for differences in RNA recovery, degradation, blotting, and hybridization.

RESULTS AND DISCUSSION

Figure 1A shows the ethidium bromide-stained 2.2 M formaldehyde–agarose (1.2%) gel of duplicate punches of rat brain frontal cortex. Punch samples of 0.5 mm in diameter (approximately 50 μg tissue, lanes 3 and 4) and 1.0 mm in diameter (approximately 200 μg tissue, lanes 5 and 6) were processed by the punch-and-load procedure and photographed under ultraviolet illumination. The 28 S ribosomal RNA band of the FUV-denatured punches comigrates with those of purified rat brain (lane 1) and liver (lane 2) RNA. This similarity in migration and band pattern signifies complete denaturation of intact RNA present in the lysed punches and demonstrates the suitability of this RNA for hybridization analysis. Subsequent densitometric and/or hybridization analysis of the 28 S ribosomal RNA offer alternative means of quantitating relative amounts of RNA present per FUV-denatured punch. The ethidium bromide fluorescence at the bottom of each sample most likely represents a mixture of transfer RNAs, solubilized proteins, and cellular debris, present since whole tissue homogenates are being applied directly to the formaldehyde–agarose gel.

Total RNA isolated by the method of Chirgwin *et al.* (15) and that isolated by the punch-and-load procedure have been used for the detection and quantitation of mRNAs of the neuron-specific rat synapsin I gene and 18 S ribosomal RNA. Figure 1B shows an autoradiogram of the formaldehyde–agarose gel depicted in Fig. 1A after hybridization to a ^{32}P-labeled rat synapsin I cDNA probe. Synapsin I mRNAs of both 3.4 and 4.5 kb (22) were identified with little or no smearing in each of the four punch-and-load samples (lanes 3–6). The sharp banding pattern seen in Fig. 1B indicates that the synapsin I mRNAs are intact and suggests efficient inactivation of cellular RNases during the homogenization step of the punch-and-load procedure. Liver RNA (lane 2), added as a negative control, shows no hybridization signal with synapsin I cDNA as probe. Figure 1C illustrates the same RNA blot rehybridized to a ^{32}P-labeled 18 S ribosomal RNA cDNA probe. Hybridization in the punch-and-load samples is detected as a single discrete band migrating at approximately 1.8 kb in length. No

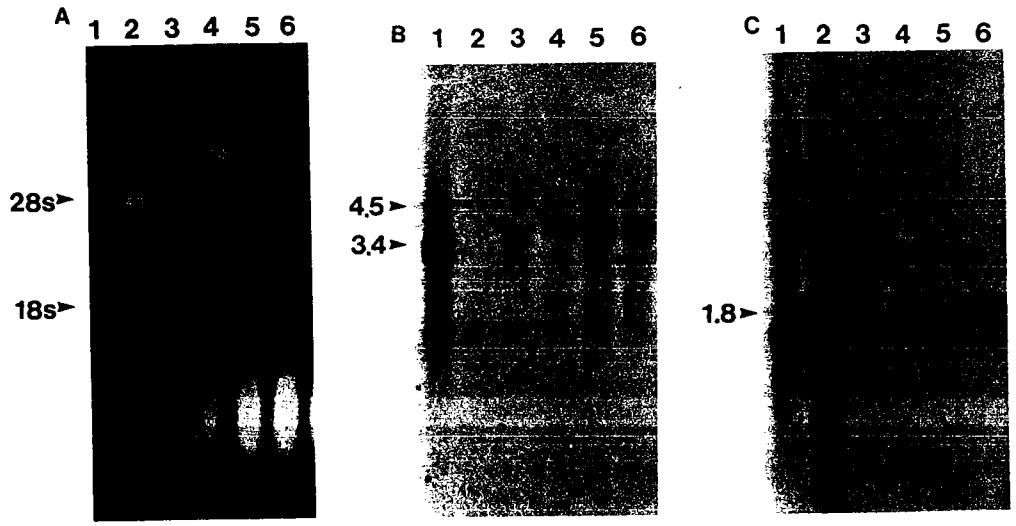

FIG. 1. Electrophoretic and RNA blot analysis of FUV-denatured punch samples from rat brain frontal cortex. Purified total rat brain RNA (1.0 μg, lane 1), rat liver RNA (4.0 μg, lane 2), and duplicate sample punches of rat frontal cortex, 0.5 mm in diameter (approximately 50 μg tissue, lanes 3 and 4) or 1.0 mm in diameter (approximately 200 μg tissue, lanes 5 and 6) ×250 μm in thickness, were solubilized in FUV-buffer and electrophoresed on a 2.2 M formaldehyde–agarose (1.2%) gel as described in the text. The gel (A) was photographed under ultraviolet illumination to visualize 28 S ribosomal RNA as a measure of RNA integrity, and then the RNA was transferred to the Zetabind nylon membrane and affixed by ultraviolet irradiation for 1 min and baking at 80°C for 1 h. The filter was hybridized to a rat synapsin I cDNA probe, washed as described, and exposed to Kodak XAR-5 film with a DuPont Cronex intensifying screen at −70°C. The filters were then stripped of synapsin I probe in two washes of 20 min each in boiling 0.1× SSC, 0.5% SDS, followed by a 0.1× SSC rinse, and rehybridized to a 18 S ribosomal RNA cDNA probe; both probes were labeled with [^{32}P]dCTP. The autoradiogram (B) shows both 3.4- and 4.5-kb rat synapsin I mRNA species in rat total RNA (lane 1) and in rapid punch-and-load processed rat brain frontal cortex samples (lanes 3–6) when hybridized with rat synapsin I cDNA as probe, and (C) a 1.8-kb 18 S ribosomal RNA when rehybridized with 18 S ribosomal RNA cDNA as probe.

hybridization signals were detected in the wells of the RNA blots with either the synapsin I or the 18 S ribosomal RNA cDNA probes. The above results demonstrate the capacity of the FUV-denaturing gel loading buffer to thoroughly and reproducibly solubilize and denature different RNA species within the same sample.

The punch-and-load procedure has been used in our laboratory to quantitate synapsin I mRNAs from discrete regions of rat brain. Figure 2 presents RNA blot analysis of duplicate 1.0-mm FUV-denatured punches from various regions of rat brain (lanes 2–7). Hybridization of synapsin I cDNA probes identified intact synapsin I mRNAs of 3.4 and 4.5 kb, respectively, and a 1.7-kb synapsin I external cRNA standard (20 pg) added to control for mRNA recovery. Consistent with the RNA blot results described earlier, sufficient RNA was present in one punch of 50–200 μg from each of the dissected brain areas to quantitate reproducible steady-state levels of synapsin I mRNA. Subsequent rehybridization of the blot to alternative probes of interest offers a quantitative measure of differential gene expression in focal, discrete subregions of the mammalian brain, a level of analysis previously hindered by a lack of rapid and reproducible RNA microisolation techniques.

The general applicability of the punch-and-load procedure for the analysis of mRNAs in tissues other than rat brain has also been tested. Figure 3A shows the ethidium bromide-stained gel of FUV-denatured punches of rat liver (lanes 2 and 3) and kidney (lanes 4 and 5) compared with purified rat liver RNA (lane 1). Both the 28 S ribosomal RNA band and the 18 S ribosomal RNA band are visible in the liver punch samples. Such clear banding patterns in liver suggests an increased solubilization efficiency of the FUV-buffer in this tissue. Since densitometric and hybridization analyses can be performed on both ribosomal RNA species, RNA quantitation and standardization per punch are even more reliable in this case. Figure 3B presents RNA blot analysis of the gel in Fig. 3A using a ^{32}P-labeled 18 S ribosomal RNA cDNA as probe. The results obtained are similar to those shown in Fig. 1C, where a sharp, distinct band of 1.8 kb in length representing intact 18 S ribosomal RNA was easily identified.

Significant problems surfaced in the analysis of mRNA levels from pancreatic and striated muscle tissue. In the pancreas, high levels of RNase activity overwhelmed the FUV-buffer, resulting in degraded mRNA, as evidenced by a smeared or often nonexistent hybridization signal obtained when punch samples were probed with an α-tubulin cDNA probe (data not shown). Striated muscle tissue presented considerable problems in the homogenization step of the technique, as indi-

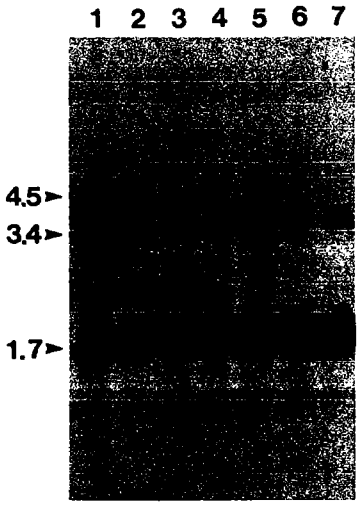

FIG. 2. RNA blot autoradiogram of RNA from punch-and-load processed samples from various regions of rat brain. Purified total rat brain RNA (3.3 μg, lane 1) and duplicate 1.0 mm × 250 μm sample punches (lanes 2–7) were processed, electrophoresed, and blotted as described in the text. The filter was hybridized to a rat synapsin I cDNA probe labeled with [^{32}P]dCTP. The filter was exposed to Kodak XAR-5 film with a DuPont Cronex intensifying screen for >4 days at −70°C. In all samples, intact synapsin I mRNAs of 3.4 and 4.5 kb were identified on the autoradiogram, along with a 1.7-kb synapsin I external cRNA standard (20 pg) added prior to sample homogenization to control for mRNA recovery. The rat brain regions sampled were frontal cortex (lanes 2 and 3), dentate gyrus (lanes 4 and 5), and the lateral and medial amygdaloid nuclei (lanes 6 and 7).

cated by a persistence of cellular precipitates after homogenization. Subsequent electrophoretic analysis showed incomplete denaturation of mRNAs on both the ethidium bromide-stained formaldehyde–agarose gel and the α-tubulin probed RNA blot (data not shown).

Variation in hybridization signal seen in lanes 3 and 4 of Fig. 1C and lanes 4 and 5 of Fig. 3B suggest different levels of 18 S ribosomal RNA in duplicate 1-mm punches. In general, we have found this variation to be due to inconsistent tissue sampling, where differences in cell number between duplicate punches translate into differences in RNA levels. To control for reproducible sampling of a cell cluster, punch positions that are similar in cell density and number, with defined boundaries and landmarks, should be chosen. Additionally, a punch whose internal diameter falls within the borders of the cell cluster should be chosen rather than one that samples the entire field.

We cannot rule out variation in hybridization signals which may be due to problems at the level of RNA blotting. Our results demonstrate that the punch-and-load method is reproducibly useful for the detection and quantification of relatively large mRNAs. However, smaller mRNAs which migrate near or within the smear of cellular debris present at the bottom of each formaldehyde–agarose gel may not transfer efficiently. Further, hybridization to these RNAs may be hindered by the presence of this same material on the RNA blot. Accordingly, to minimize problems inherent in RNA blot analysis and to control for differences in hybridization efficiencies, accurate normalization of RNA levels should be carried out with control probes which recognize RNA species of a size similar to that of the mRNA of interest.

Our objective was to develop a simple and reliable procedure for the direct analysis of mRNA levels in microgram quantities of frozen mammalian brain. The principal advantages of the punch-and-load procedure

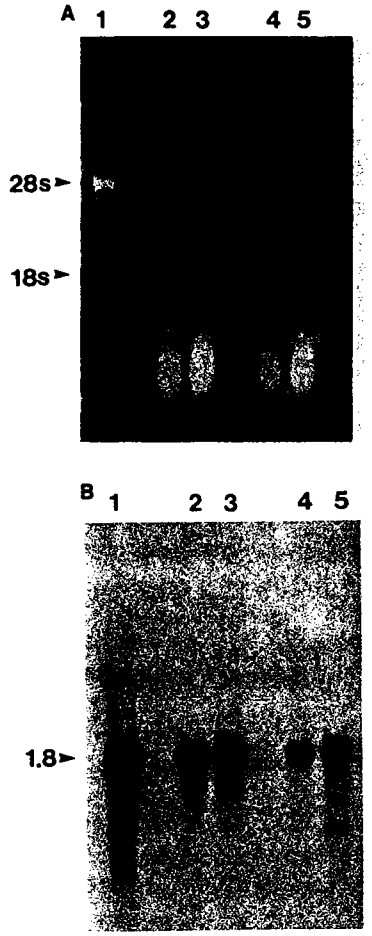

FIG. 3. Electrophoresis and RNA blot analysis of punch samples from tissues other than rat brain. Purified rat liver RNA (4.0 μg, lane 1) and duplicate 1.0 mm × 250 μm sample punches of rat liver (lanes 2 and 3) and kidney (lanes 4 and 5) were solubilized in FUV-buffer and electrophoresed as described in the text. The gel (A) was photographed under ultraviolet illumination as a measure of RNA quality. Note the integrity of both the 28 S ribosomal band and the 18 S ribosomal band present in the liver punch samples. The RNA was transferred to Zetabind nylon membrane and hybridized to a [^{32}P]-dCTP-labeled 18 S ribosomal RNA cDNA probe. Hybridization is detected as a single, discrete band of 1.8 kb in length with no apparent smearing on the autoradiogram.

over conventional methods are several. First, the procedure is extremely rapid. This minimizes time constraints inherent in conventional RNA preparation methods and becomes especially useful for the simultaneous processing of multiple samples. Second, it utilizes very small quantities of tissue, approximately 50–200 μg vs >3 mg for rapid procedures, and >1–2 g for most conventional RNA isolation and purification protocols. This is of particular significance to the molecular neurobiologist, since it affords the researcher the opportunity to compare specific mRNA levels in discrete brain areas or nuclei where tissue quantities are severely limited. Third, the procedure is quantitative and reproducible, as mRNA levels from duplicate samples can be easily normalized by hybridization to a known amount of added synthetic cRNA external standard and/or relative amounts of 18 and 28 S ribosomal RNA. Fourth, the procedure is sensitive and results in excellent recovery of intact RNA. In our hands, the punch-and-load technique can reproducibly detect on the order of 15–50 molecules of synapsin I mRNA per neuron. The degradation and loss of RNA are minimized by the limited processing of samples in this procedure. The lack of hybridization anywhere on the RNA blots other than to specifically targeted mRNAs suggests complete recovery of both exogenous and endogenous RNAs. Finally, because the rapid punch-and-load procedure is very simple, it circumvents the tedious and often difficult nature of conventional RNA preparation protocols. Electrophoresis of multiple samples can be underway within 30 min of tissue sectioning.

ACKNOWLEDGMENTS

We thank Drs. Paul R. Dobner and Robert H. Singer for providing the 18 S ribosomal and α-tubulin cDNA clones, respectively. We are grateful to Drs. Lisa M. Hemmendinger, Rodrigo Franco, Cordula U. Kirchgessner, and Erika L. F. Holzbaur for their critical reading of the manuscript. This work was supported by NIH Grants NS 25050 and NS 27833.

REFERENCES

1. Chen, C. L., Dionne, F. T., and Roberts, J. T. (1983) *Proc. Natl. Acad. Sci. USA* **80,** 2211–2215.
2. Dziadek, M. A., and Andrews, G. K. (1983) *EMBO J.* **2,** 549–554.
3. Ilaria, R., Wines, D., Pardue, S., Jamison, S., Ojeda, S. R., Snider, J., and Morrison, M. R. (1985) *J. Neurosci. Methods* **15,** 165–174.
4. Chomczynski, P., and Sacchi, N. (1987) *Anal. Biochem.* **162,** 156–159.
5. Badley, J. E., Bishop, G. A., St. John, T., and Frelinger, J. A. (1988) *Biotechniques* **6**(2), 114–116.
6. Birnboim, H. C. (1988) *Nucleic Acids Res.* **16**(4), 1487–1497.
7. Emmet, M., and Petrack, B. (1988) *Anal. Biochem.* **174,** 658–661.
8. Gough, N. M. (1988) *Anal. Biochem.* **173,** 93–95.
9. Meirer, R. (1988) *Nucleic Acids Res.* **16**(5), 2340.
10. Wilkinson, M. (1988) *Nucleic Acids Res.* **16**(22), 10,933.
11. Wilkinson, M. (1988) *Nucleic Acids Res.* **16**(22), 10,934.
12. Rappolee, D. A., Wang, A., Mark, D., and Werb, Z. (1989) *J. Cell. Biochem.* **39,** 1–11.
13. Sive, H. L., Hattori, K., and Weintraub, H. (1989) *Cell* **58,** 171–180.
14. Maniatis, T., Fritsch, E. F., and Sambrook, J. (1982) Molecular Cloning: A Laboratory Manual, Cold Spring Harbor Laboratory, Cold Spring Harbor, NY.
15. Chirgwin, J. M., Przybla, A. E., MacDonald, R. J., and Rutter, W. J. (1979) *Biochemistry* **18,** 5294–5299.
16. Palkovits, M., and Brownstein, M. J. (1988) Maps and Guide to Microdissection of Rat Brain, Elsevier, New York.
17. Pauli, U., Wright, K., van Wijnen, A., Stein, G., and Stein, J. (1991) *in* Methods in Nucleic Acids Research (Karam, J. D., Chao, L., and Warr, G. W., Eds.), pp. 227–250, CRC Press, Boca Raton, FL.
18. Kilimann, M. W., and DeGennaro, L. J. (1985) *EMBO J.* **4,** 1997–2002.
19. Cleveland, D. W., and Sullivan, K. F. (1985) *Annu. Rev. Biochem.* **54,** 331–365.
20. Katz, R. A., Erlanger, B. F., and Guntaka, R. V. (1983) *Biochem. Biophys. Acta* **739,** 258–264.
21. Heumann, R., and Thoenen, H. (1986) *J. Biol. Chem.* **261,** 9246–9249.
22. Haas, C. A., and DeGennaro, L. J. (1988) *J. Cell Biol.* **106,** 195–203.

THE JOURNAL OF COMPARATIVE NEUROLOGY 327:507–520 (1993)

Synapsin I Gene Expression in the Adult Rat Brain With Comparative Analysis of mRNA and Protein in the Hippocampus

RICHARD H. MELLONI, JR., LISA M. HEMMENDINGER, JAMES E. HAMOS, AND LOUIS J. DEGENNARO
Departments of Neurology (R.H.M., L.M.H., J.E.H., L.J.D.), Cell Biology (R.H.M., L.J.D.), and Anesthesiology (L.J.D.), University of Massachusetts Medical Center, Worcester, Massachusetts 01655

ABSTRACT

Synapsin I is the best characterized member of a family of neuron-specific phosphoproteins thought to be involved in the regulation of neurotransmitter release. In this report, we present the first extensive in situ hybridization study detailing the regional and cellular distribution of synapsin I mRNA in the adult rat brain. Both the regional distribution and relative levels of synapsin I mRNA established by in situ hybridization were confirmed by RNA blot analysis. Our data demonstrate the widespread yet regionally variable expression of synapsin I mRNA throughout the adult rat brain. The greatest abundance of synapsin I mRNA was found in the pyramidal neurons of the CA3 and CA4 fields of the hippocampus, and in the mitral and internal granular cell layers of the olfactory bulb. Other areas abundant in synapsin I mRNA were the layer II neurons of the piriform cortex and layer II and V neurons of the entorhinal cortex, the granule cell neurons of the dentate gyrus, the pyramidal neurons of hippocampal fields CA1 and CA2, and the cells of the parasubiculum. In general, the pattern of expression of synapsin I mRNA paralleled those encoding other synaptic terminal-specific proteins, such as synaptophysin, VAMP-2, and SNAP-25, with noteworthy exceptions. To determine specifically how synapsin I mRNA levels are related to levels of synapsin I protein, we examined in detail the local distribution patterns of both synapsin I mRNA and protein in the rat hippocampus. These data revealed differential levels of expression of synapsin I mRNA and protein within defined synaptic circuits of the rat hippocampus.

Key words: in situ hybridization, immunohistochemistry, regional distribution, entorhinal cortex, dentate gyrus

The specific molecular mechanisms underlying the release of neurotransmitter from the presynaptic nerve terminal remain unknown. To date a large number of neuron-specific proteins have been identified which perform various functions within the presynaptic terminal. Among these proteins are the synapsins. The synapsins are a distinct family of homologous neuronal phosphoproteins thought to play an integral role in the process of neural transmission. Synapsin I, the best characterized of the synapsins, is the collective name for two nearly identical neuron-specific proteins, synapsin Ia and synapsin Ib, which occur throughout the central and peripheral nervous systems (Ueda and Greengard, '77). Immunohistochemical studies have shown synapsin I to be concentrated in presynaptic terminals of virtually all neurons, regardless of transmitter type, where it is specifically associated with the cytoplasmic surface of small synaptic vesicles (De Camilli et al., '83a,b; Huttner et al., '83; Navone et al., '84; Schiebler et al., '86; Benfenati et al., '89). Synapsin I appears to possess specific domains capable of associating with components of the cytoskeleton (Bahler and Greengard, '87; Petrucci and Morrow, '87; Bahler et al., '89, '90) and others which are prominent cellular targets of several endogenous protein kinases, such as cAMP- and Ca^{2+}/calmodulin dependent protein kinases (Ueda et al., '73; Huttner and Greengard, '79; McGuinness et al., '85; Nairn and Greengard, '87). The affinity of synapsin I for synaptic vesicles has been shown to be phosphorylation dependent and regulated by conditions affecting neuronal activity (see review by Nestler and Greengard, '84). The phosphorylation state of synapsin I is intimately coupled to the release of neurotransmitter from presynaptic terminals, and it is generally thought that the protein functions as a regulator of the release process (Llinas et al., '85; De Camilli and Greengard, '86). Further,

Accepted September 25, 1992.

recent evidence establishing synapsin I as a diacylglycerol kinase suggests a second role for synapsin I in the nerve terminal, that of a potential regulator of protein kinase C-mediated extracellular signals (Kahn and Besterman, '91).

Synapsin I protein is widely distributed in nerve terminals throughout the mammalian central nervous system (De Camilli et al., '83a,b; DeGennaro et al., '89; Sudhof et al., '89; Apostolides et al., submitted). The pattern of distribution, however, is not uniform across the neuraxis, and it has been postulated that this differential distribution reflects differences in the functional properties of central synapses (Sudhof et al., '89; Apostolides et al., submitted). At present no data are available which detail the spatial distribution and comparative levels of expression of the synapsin I gene in the central nervous system. Such a map of the intensity of synapsin I gene expression would provide insight into the specific properties and functional requirements of those neurons whose termini comprise central synapses. In the present study, we have used in situ hybridization histochemistry employing radioactively-labeled synapsin I cDNA probes to examine the regional and cellular distribution of synapsin I mRNA in the adult rat central nervous system. Our data reveal widespread yet regionally variable levels of synapsin I gene expression throughout the adult rat brain. In addition, we focus on discrete brain regions which express high levels of synapsin I mRNA, and extend these studies by comparing relative levels of synapsin I mRNA and protein in these areas. These data reveal the differential expression of synapsin I mRNA and protein within defined synaptic circuits of the adult rat hippocampus.

MATERIALS AND METHODS

Animals and tissue preparation

Adult male Sprague-Dawley rats (n = 6) from Charles River Breeding Laboratories (Wilmington, MA), 90–120 days old and weighing 250–300 g, were used in this study. The animals were sacrificed by carbon dioxide asphyxiation and decapitation. Brains were removed, frozen in dry-ice-supercooled 2-methylbutane (Aldrich), and stored in plastic bags at −70°C. For in situ hybridization, the brains were warmed to −16°C, and 16 μm cryostat sections were cut in coronal, parasagittal, and horizontal planes. The sections were thaw-mounted on precooled slides coated with Vectabond® reagent (Vector Laboratories, Burlingame, CA) and stored at −20°C. For RNA blot analysis, rat brains were frozen as above and warmed to −9°C. Cryostat sections were cut at 250 μm, and the sections were used for brain punch microdissection (Palkovitz and Brownstein, '88) and punch-and-load RNA blot analysis (Melloni et al., '92).

Synthesis of cDNA probes

Synapsin I cDNA plasmid pSyn 5 (Kilimann and DeGennaro, '85) was cut with the restriction enzyme Eco RI (Boehringer Mannheim) and the digestion products displayed on a 1% agarose gel (Maniatis et al., '82). The 1,700 bp fragment, 5E2 (nucleotides 694–2,445 of the synapsin I cDNA sequence) was excised from the gel and purified with Gene-Clean (Bio 101, Inc., LaJolla, CA). For RNA blot analysis the synapsin I cDNA fragment was labeled with [α-^{32}P]dCTP by means of a random oligonucleotide priming kit (Boehringer Mannheim). For in situ hybridization, fragment 5E2 was purified and digested with the restriction enzyme Dde I (Boehringer Mannheim). The restriction products were then purified by ethanol precipitation and labeled in the presence of [α-^{35}S]dCTP by random priming. Unincorporated nucleotides were removed by chromatography over a Sephadex G25 spin column (Boehringer Mannheim).

RNA blot analysis

Total RNA was extracted and purified from rat brain by the method of Chirgwin et al. ('79) or analyzed by the punch-and-load method (Melloni et al., '92). Briefly, brain punches, 1 mm diameter × 250 μm thickness, were homogenized in 50 μl FUV-denaturing gel loading buffer (2.2 M formaldehyde, 7 M urea, 20 mM vanadyl ribonucleoside complex, 0.5% SDS, and 20 mM 3-(N-morpholino) propanesulfonic acid [MOPS]) and applied directly to a 2.2 M formaldehyde-agarose (1.2%) gel for electrophoresis (Maniatis et al., '82). The gel was rinsed 20 minutes each in two changes 10 × SSC (1 × SSC = 160 mM NaCl, 15 mM sodium citrate, pH 7.0) and blotted onto Zetabind nylon membrane (American Bioanalytical) as described by Thomas ('80). The membrane was hybridized for > 16 hours at 50°C in 50% (v/v) formamide, 7% (w/v) SDS, 0.5 M Na_2HPO_4, pH 7.5, 250 μg/ml heat-denatured *Escherichia coli* DNA and 10 ng/ml rat synapsin I cDNA fragment, labeled as described above. Membranes were then washed at room temperature for 20 minutes in two changes of 2 × SSC, 0.1% SDS, 0.1% $Na_4P_2O_7$; followed by 1 × SSC, 0.1% SDS, 0.1% $Na_4P_2O_7$, and 0.3 × SSC, 0.1% SDS, 0.1% $Na_4P_2O_7$, each preheated to 65°C. RNA blots were then exposed to Kodak XAR-5 film for > 4 days at −70°C with a Dupont Cronex intensifying screen.

Standardization: Prior to tissue sampling, an unlabeled synthetic synapsin I sense RNA was added to the FUV-buffer to serve as external standard (Heumann and Thoenen, '86). Briefly, a 1.7 kb synapsin I sense RNA transcript was synthesized in vitro with the aid of a SP6/T7 Transcription Kit (Boehringer Mannheim). The RNA was purified by repeated ethanol precipitation, and a known amount was added to punch samples to control for differences in RNA recovery, degradation, blotting, and hybridization.

In situ hybridization

Slide-mounted brain sections were warmed to room temperature, post-fixed in 4% paraformaldehyde in 0.1 M phosphate buffer (pH 7.4) for 5 minutes at 0°C, rinsed in phosphate buffered saline (PBS), and treated with 0.25% acetic anhydride (in 0.1 M triethanolamine, pH 8.0) for 10 minutes at room temperature. After rinsing in 2 × SSC and dehydration through a graded series of alcohols, the sections were delipidated in chloroform for 5 minutes at room temperature. The sections were subsequently rehydrated to 95% ethanol in descending concentrations of alcohols and then air dried. Each section was prehybridized with 150 μl of prehybridization buffer (50% formamide, 2 × Denhardt's solution [1 × Denhardt's solution is 0.02% Ficoll, 0.02% polyvinylpyrrolidone, 0.02% BSA], 50 mM dithiothreitol [DTT], 5 × SSC, and 0.1% SDS) at 50°C in a moist chamber for 1 hour. For hybridization, probe (2 × 10^6 cpm) was applied in 100 μl hybridization buffer (50% formamide, 10% dextran sulfate, 2 × Denhardt's solution, 5 × SSC, 50 mM DTT, 0.1% SDS, 100 μM dNTPs, and 0.1% $Na_4P_2O_7$), and the slides were coverslipped and incubated as above for > 12 hours. Following hybridization, coverslips were re-

moved in 2 × SSC, 0.1% $Na_4P_2O_7$ at room temperature. Slides were washed for 30 minutes each in two changes of 2 × SSC, 0.1% $Na_4P_2O_7$ at room temperature; 2 × SSC, 0.1% $Na_4P_2O_7$ at 42°C; 0.5 × SSC, 0.1% $Na_4P_2O_7$ at room temperature; 0.1 × SSC, 0.1% $Na_4P_2O_7$ at room temperature; and 0.1 × SSC, 0.1% $Na_4P_2O_7$ at 42°C. A final wash in 0.1 × SSC, 0.1% $Na_4P_2O_7$ for 15 minutes at room temperature was done, and the sections were dehydrated through a graded series of alcohols in which water was replaced by 0.6 M ammonium acetate. The slides were then air dried and exposed to Kodak XAR-5 film for 7–10 days at room temperature. For emulsion autoradiography, selected slides were coated with photographic emulsion (NTB2; Eastman Kodak, Rochester, NY; diluted 1:1 with 0.6 M ammonium acetate), exposed for 10–14 days at 4°C, developed in D19 (diluted 1:1 with water), and counterstained with 0.04% cresyl violet in 0.1 M ammonium acetate, pH 3.5.

Antibodies

Synapsin I polyclonal antibodies used in these experiments were contained in antisera prepared in rabbits against purified rat synapsin I protein. These antibodies have been extensively characterized (Kilimann and DeGennaro, '85), and previously used to localize synapsin I protein in a number of immunohistochemical studies (Hamos et al., '88; Smith et al., '92; Apostolides et al., submitted). At dilutions of 1:500–1:2,000, the synapsin I antiserum reacts specifically with synapsin I on Western blots of rat brain protein (Kilimann and DeGennaro, '85; and Fig. 6), and on rat and human brain sections processed for immunohistochemistry (Hamos et al., '88; Smith et al., '92; Apostolides et al., submitted).

Western blot analysis

Total protein was extracted from the neocortex of an adult rat brain by a modification of the method of Klose and Zeindl ('84). Briefly, brain punches, 1 mm diameter × 250 μm thickness, were homogenized in 500 μl of tissue extraction buffer [2% Nonidet P-40, 9.5 M urea, 1% β-mercaptoethanol, and 200 mM K_2CO_3 (pH 9.5)] and then centrifuged in an Eppendorf microfuge for 10 minutes at room temperature. The supernatant was collected and a Coomassie Plus protein assay (Pierce, Rockford, IL) was performed to determine protein concentration.

Western blots were performed according to the method of Towbin et al. ('79). Briefly, 8% polyacrylamide gels were run according to the method of Laemmli ('70). Gels were blotted onto Immobilon-P (Millipore, Bedford, MA) using the semidry blotting technique of Kyhse-Anderson ('84), washed with TBST (25 mM Tris [pH 8.0], 137 mM NaCl, 2.7 mM KCl, 0.05% Tween 20), and blocked with TBST containing 5% nonfat dry milk (NFDM). Synapsin I polyclonal antibody was diluted 1:1,000 in TBST containing 1% NFDM (antibody buffer) and incubated with the blot for 1 hour at room temperature. Blots were washed extensively in TBST and incubated with secondary antibody (alkaline phosphatase conjugated goat anti-rabbit IgG, Sigma) at a dilution of 1:3,000 in antibody buffer for 1 hour at room temperature. The blots were washed in three changes of TBST for 5 minutes each, rinsed in TBS, and then developed with the Immune-Lite chemiluminescent detection system (Bio-Rad, Richmond, CA) according to manufactures instructions.

Immunohistochemistry

Synapsin I protein was localized in sections of rat brain with a rabbit polyclonal antibody raised against purified rat synapsin I protein (Kilimann and DeGennaro, '85). Animals were perfused transcardially with a saline flush, followed by 0.01 M, periodate-0.075 M lysine-4% paraformaldehyde in 0.037 M phosphate buffer, pH 7.2 ("PLP fixative," McLean and Nakane, '74). Brains were postfixed for 2 hours at room temperature and passed through ascending concentrations of sucrose in 0.2 M phosphate buffer, pH 7.2 (PB), at 4°C. Horizontal sections were cut free-floating at 40 μm on a sliding microtome and placed in 0.1 M phosphate-buffered saline (pH 7.4) (PBS). Sections were pretreated in 0.01% H_2O_2 in methanol for 30 minutes, rinsed thoroughly in PBS, 0.03% Triton X-100 (Sigma) (PBST), and then incubated for 1 hour in blocking buffer [20% nonimmune goat serum in PBS containing 0.3% Triton X-100]. Immunostaining was carried out overnight, at 4°C, with the aid of a Vectastain ABC kit (Vector Laboratories), with the primary antibody diluted 1:1,000 in PBS, 0.3% Triton X-100, 3% nonimmune goat serum. On the following day, sections were rinsed twice for 30 minutes each in PBST, incubated for one hour in biotinylated goat anti-rabbit immunoglobulins (secondary antibody) in PBST, rinsed again twice for 15 minutes each in PBST, and incubated for 1 hour in avidin-biotin-peroxidase complex. The peroxidase label was revealed by using 3,3'-diaminobenzidine (DAB) (Sigma; 0.05% in 50 mM Tris, pH 7.4) as a chromogen. The immunostained sections were mounted on gelatin-coated slides, dehydrated in a graded series of alcohols and xylene, and coverslipped with Permount. Adjacent sections were stained with cresyl violet.

Experimental controls were performed on representative sections and included either the omission of the primary antibody, omission of the secondary antibody, or preabsorption of anti-synapsin I IgGs from total rabbit serum using a 100-fold excess of purified synapsin I.

RESULTS

RNA blot analysis and in situ hybridization of synapsin I mRNA

In rat brain, the gene encoding synapsin I directs the synthesis of two classes of mRNA of 3.4 kb and 4.5 kb in length, respectively (Haas and DeGennaro, '88). The 3.4 kb mRNA is comprised of two alternatively spliced transcripts encoding synapsin Ia and Ib polypeptides (Sudhof et al., '89). The complete sequence of the 4.5 kb mRNA has not been determined. To establish that the cDNA probes used in this study recognize only synapsin I mRNA and to compare the relative levels of expression of synapsin I mRNA in different areas of the adult rat central nervous system, we performed RNA blot analysis on RNA prepared from various subregions of rat brain. Figure 1A presents RNA blot analysis of duplicate 1.0 mm tissue punches from discrete regions of the adult rat brain. The synapsin I 5E2-fragment cDNA probe recognized exclusively synapsin I mRNAs of 3.4 kb and 4.5 kb, and a 1.7 kb synapsin I external RNA standard, in purified rat brain RNA (RB) and RNA from all brain areas sampled (Ctx-MS). The strength of the hybridization signal obtained varied in different brain regions, with the highest signal in the RNAs from the dentate gyrus and the neocortex and the lowest in the RNA from the caudate nucleus.

The hybridization signals obtained by RNA blot analysis (Fig. 1A) corresponded with the pattern and strength of synapsin I mRNA hybridization localized in discrete regions of rat brain by in situ hybridization (Fig. 1B,C). Strong radioactive labeling of granule cell neurons in the dentate gyrus (Fig. 1C) corresponded to the highest level of synapsin I mRNA detected by RNA blot analysis (Fig. 1A). Lower hybridization signals were obtained, in decreasing order of intensity, in the neocortex, central/lateral amygdala, medial septum, and the caudate nucleus. In these areas, as above, the strength of the hybridization signals revealed by in situ hybridization corresponded to the intensity of signals obtained by RNA blot analysis.

Emulsion autoradiography revealed that, throughout the brain, hybridization was restricted to neuronal profiles and was essentially absent in white matter fiber tracts, meninges, blood vessels, and the neuropil (Fig. 2). For example, a comparison of dark- and brightfield images of an emulsion autoradiogram of the dentate gyrus revealed hybridization over the somata of granule cell and hilar neurons in this region (Fig. 2A,B). Labeling was distributed evenly over neurons of the granule cell layer and appeared consistent along the entire length of the dentate gyrus. Examination of the cells of the hilus at high magnification showed labeling to be present over individual neuronal somata in this region (Fig. 2C).

To ensure that labeling of sections was specific to synapsin I mRNA, some sections were co-incubated with a mixture of radioactively-labeled synapsin I cDNA probe and a 100-fold excess of unlabeled synapsin I cDNA probe. In all control sections, no detectable hybridization signals were obtained (data not shown).

Mapping of synapsin I mRNA throughout the adult rat brain

To detail the distribution of synapsin I mRNA in the adult rat brain, we conducted several (> 7) in situ hybridization studies in coronal (Fig. 1B,C), horizontal (Fig. 3), and parasagittal (Fig. 4) planes of section. In the present study we have characterized the hybridization signals as light (+), moderate (++), high (+++), and intense (++++), as estimated by visual comparison of several autoradiographic films of sections hybridized to radioactively-labeled synapsin I cDNA probes of comparable specific activities (Table 1). In each in situ hybridization run, this relative scale was used to describe the intensity of the hybridization signals from the different rat brain regions. This scale consistently assigned the CA3 neurons of the rat hippocampus the highest hybridization intensities and the caudate nucleus the lowest. After visual inspection of autoradiographic films, selected slides were processed for emulsion autoradiography to examine more accurately synapsin I mRNA distribution and cellular localization.

Telencephalon

Olfactory bulb. Intense labeling was observed in discrete layers of the olfactory bulb (Figs. 3, 4). Intense labeling was seen over the cells of the mitral and internal granular layers (Figs. 3G, 4E). Light-to-moderate labeling was observed over cells of the glomerular layer (Figs. 3F,G). Little or no labeling was detected over the external plexiform and olfactory nerve layers.

Cortex. Synapsin I mRNAs were concentrated in the entorhinal, piriform, cingulate, and frontal cortices (Figs. 1, 3–5). High-to-intense synapsin I mRNA levels were detected in neocortical lamina II and the upper parts of lamina V (Figs. 3B, 5A,B). The parasubiculum was intensely labeled (Figs. 3B–E, 7B), as were the lamina II neurons of the piriform cortex (Figs. 3I, 4A, 5D) and laminae II and V of the entorhinal cortex (Figs. 3C, 5C, 7B). Moderate synapsin I hybridization signals were observed primarily in laminae III, IV, and VI of the neocortex (Figs. 3B–E, 5A,B).

Basal forebrain and basal ganglia. In the basal forebrain, labeling of synapsin I mRNA was high in the olfactory tubercle and moderate in the bed nucleus of the stria terminalis, diagonal band of Broca, and medial septum (Figs. 1B, 3F–H). Light hybridization was observed in the lateral septum (Fig. 3C–G). In the basal ganglia the caudate-putamen was among the lightest hybridizing areas of the rat brain (Figs. 1B, 3C).

Amygdala. Both the anterior basolateral and the lateral nucleus of the amygdala exhibited high levels of synapsin I mRNA (Figs. 1C, 3G–I, 4A), while the medial division of the central nucleus contained moderate amounts (Fig. 3F–I). The least pronounced hybridization in the amygdala came from the lateral division of the central nucleus (Fig. 3F–I).

Hippocampus. The large pyramidal neurons of hippocampal fields CA3 and CA4 consistently revealed the highest density of hybridization throughout the adult rat brain (Figs. 3, 5G, 7B). Similarly, high-to-intense levels of synapsin I mRNA were detected in the "mossy cells" or hilar neurons of the dentate gyrus (Fig. 2). Labeling of synapsin I mRNA was notably high over pyramidal cells in layers CA1 and CA2 and the granule cells of the entire dentate gyrus (Figs. 1C, 3D, 4C, 5E,F, 7B). Dentate granule neurons exhibited strong hybridization signals by both in situ hybridization and RNA blot analysis (Figs. 1A,C, 2A, 3D).

Diencephalon

Thalamus. High hybridization signals were present in the anterodorsal and paraventricular thalamic nuclei (Figs. 3C,D, 4D). In contrast, light-to-moderate labeling was generally observed in most remaining thalamic nuclei, including both the ventrolateral and the dorsomedial divisions of the anteroventral nucleus, and the parafasicular nucleus (Fig. 3E). Particularly light labeling was observed in the ventral posterolateral thalamic nucleus and the dorsal lateral geniculate nucleus (Fig. 4B).

Habenula. The medial habenula contained moderate-to-high levels of synapsin I mRNA (Fig. 3B), while the lateral habenula contained lesser amounts.

Hypothalamus. In the hypothalamus, high levels of synapsin I mRNA were observed in the ventromedial nucleus (Fig. 4E). Specifically, hybridization was high in the dorsomedial and ventrolateral divisions of the ventromedial nucleus (data not shown). Similarly high levels were seen in the ventral premammillary nucleus and in the subthalamic nucleus (Figs. 3H, 4C,E). Lower levels of synapsin I mRNA were present in most other hypothalamic regions, including the arcuate nucleus, the paraventricular nucleus, the lateral anterior nuclei, the lateral magnocellular nucleus, and the preoptic nucleus.

Midbrain

Moderate-to-high amounts of synapsin I mRNA were present in the red nucleus and in the substantia nigra pars compacta (Fig. 3G,H). Light-to-moderate levels of synapsin I mRNA were observed in most other midbrain regions. For example, the dorsal central gray (Fig. 4F) and the ventral

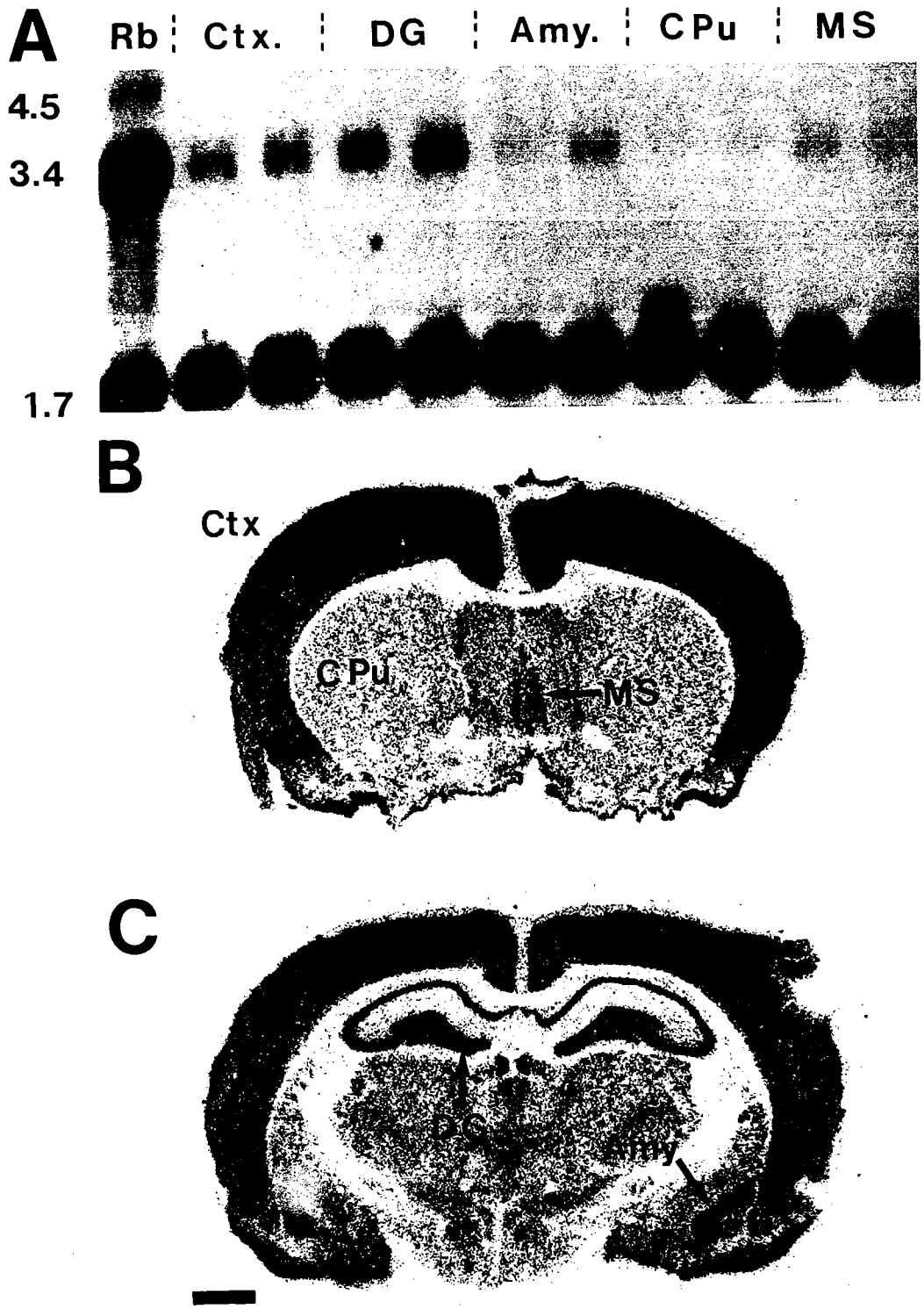

Fig. 1. RNA blot analysis and in situ hybridization of synapsin I mRNA in rat brain. **A:** RNA blot autoradiogram of synapsin I mRNA levels in different brain regions. Purified total rat brain RNA (3 μg) and RNAs prepared from various regions of brain were processed, separated by electrophoresis, blotted, and hybridized as described in text. The strength of the hybridization signal obtained varied in different brain regions, with the highest signal in the RNAs from the dentate gyrus and the neocortex and the lowest in the RNA from the caudate nucleus. **B,C:** X-ray autoradiograms of coronal sections of adult rat brain hybridized with ^{35}S-labeled synapsin I cDNA probes. In these sections, the strength of the hybridization signals revealed by in situ hybridization corresponded to the intensity of signals obtained by RNA blot analysis. Amy, central/lateral amygdala; CPu, caudate/putamen; Ctx, neocortex; DG, dentate gyrus; MS, medial septum; Rb, total rat brain RNA. Blots were exposed to Kodak XAR-5 film for 4 days. Sections were exposed to Kodak XAR-5 film for 10 days. Scale bar: B and C, 1.5 mm.

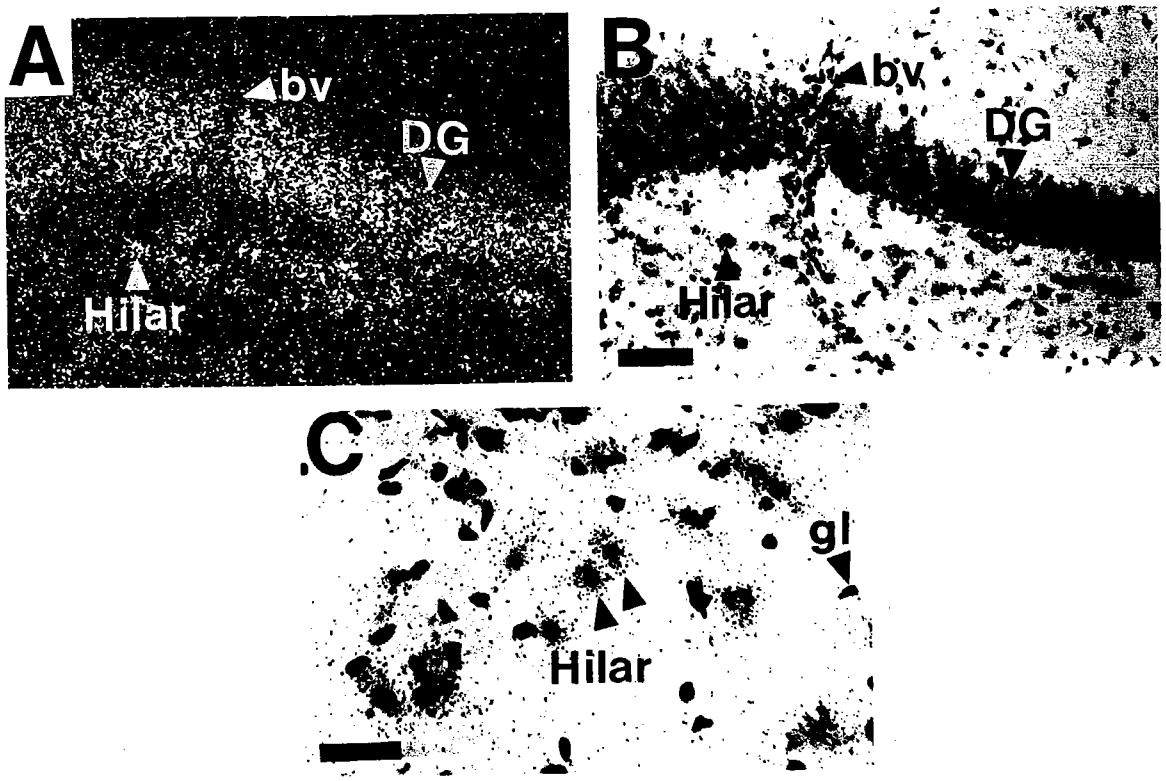

Fig. 2. Emulsion autoradiograms demonstrating specificity of synapsin I cDNA probes for neurons in the central nervous system. **A** and **B:** Darkfield and brightfield photomicrographs of an emulsion autoradiogram of granule cell neurons of the dentate gyrus hybridized to synapsin I cDNA probes. Synapsin I hybridization is specific for neuronal profiles of the granule cell layer and hilar region of the dentate gyrus. **C:** High magnification brightfield photomicrograph of an emulsion autoradiogram of cells of the hilar region of the dentate gyrus. Clusters of silver grains indicate hybridization to synapsin I probes is specific for neuronal somata and not glial components of the CNS. bv, blood vessel; DG, dentate gyrus; gl, glial cell; Hilar, dentate hilar neuron. Exposure time of the emulsion-coated sections was 2 weeks. Scale bars: A and B, 300 μm; C, 120 μm.

tegmental area (Fig. 4D) were moderately labeled. Synapsin I mRNAs were expressed uniformly across the inferior and superior colliculi. Here, both the dorsal cortex of the inferior colliculus and the superficial gray layer of the superior colliculus were lightly labeled (Figs. 3A, 4E).

Brainstem

In the brainstem, high levels of synapsin I mRNA were present in the pontine nucleus (Fig. 4D), the reticulotegmental nucleus (Fig. 4F), the ventral tegmental nucleus (Fig. 4F), the pontine central gray (Fig. 4D), and the facial nerve nucleus (Fig. 4C). Many brainstem nuclei, such as the ventral cochlear nucleus and the nucleus of the trapezoid body were moderately labeled.

Cerebellum

In the cerebellum, high-to-intense labeling was present over the cerebellar granule cells (Figs. 3A–D, 4B–F). The intense labeling of granule cells made it difficult to determine, on X-ray film and by emulsion autoradiography, how much of the synapsin I hybridization signal was attributable to Purkinje cells. Light-to-moderate labeling was observed over the remainder of the cerebellar layers (Figs. 3A–D, 4B–F), while the deep cerebellar nuclei showed moderate-to-high labeling over individual neurons scattered throughout the region (data not shown).

Synapsin I mRNA and protein: comparative analysis of expression

Previous studies employing endogenous phosphorylation assays (Walaas et al., '83, '88), radioimmunological assays (Goelz et al., '81), and immunocytochemistry (Bloom et al., '79; De Camilli et al., '83a,b; DeGennaro et al., '89; Apostilides et al., submitted) indicate that synapsin I protein is present in high levels in the hippocampus. No studies however, have been reported which correlate protein data with the cellular distribution and patterns of expression of synapsin I mRNA in these areas. To examine the distribution of synapsin I mRNA and compare the relative levels of synapsin I mRNA and protein in rat hippocampus, we performed in situ hybridization and immunohistochemistry on horizontal sections of adult rat brain (Fig. 7).

To ensure the specificity of the synapsin I polyclonal antibody, we performed Western blot with protein from adult rat neocortex (Fig. 6). At the dilutions used for immunohistochemistry, 1:500–1:2,000, the synapsin I antibodies recognized exclusively synapsin Ia and Ib polypeptides.

Immunohistochemistry using polyclonal antibodies to synapsin I revealed extremely low levels of synapsin I protein in the somata of all neurons, as evidenced by weak

TABLE 1. Relative Abundance of Synapsin I mRNA in Different Regions of Rat Brain[1]

Area	Abundance
Olfactory bulb	
Mitral cell layer	++++
Internal granular cell layer	++++
Glomerular cell layer	+
Cortex	
Layers II–III, neocortex	++–+++
Layer V, neocortex	+++–++++
Piriform, layer II	++++
Entorhinal, layer II and V	++++
Frontal/cingulate	+++/+++
Pre-/para-subiculum	++/+++–++++
Basal forebrain	
Bed nucleus of stria terminalis	++
Diagonal band of Broca	++
Olfactory tubercle	+++
Septum, medial	++
Septum, lateral	+
Basal ganglia, caudate/putamen	+
Amygdala	
Basolateral, anterior	+++
Central, lateral/medial divisions	+/++
Lateral	+++
Hippocampus	
CA1	+++
CA3	++++
CA4	++++
Dentate gyrus	+++
Hilar neurons	++++
Thalamus	
Anterodorsal nucleus	+++
Paraventricular nucleus	+++
Anteroventral nucleus, ventrolateral	++
Anteroventral nucleus, dorsomedial	++
Parafasicular nucleus	++
Geniculate nucleus	
Ventral lateral, magnocellular part	++
Medial	+
Precommisural nucleus	+++
Hypothalamus	
Ventromedial nucleus	+++
Paraventricular nucleus	++
Lateral anterior nuclei	++
Lateral, magnocelluular nucleus	++
Preoptic nucleus	++
Arcuate nucleus	++
Premammillary nucleus, ventral	++
Subthalamic nucleus	+++
Habenula, medial	++–+++
Colliculi	
Inferior	+
Superior	+
Red nucleus	+++
Central grey	
Dorsal	++
Pontine	+++
Substantia nigra pars compacta	+++
Tegmental nucleus	
Ventral	++
Anterior	+++
Pontine nucleus	+++
Reticulotegmental nucleus	+++
Ventral cochlear nucleus, anterior part	++
Cerebellum	
Granule cell layer	+++
Deep cerebellar nuclei	++–+++

[1]Hybridization signals were characterized as light (++), moderate (+++), high (++++), and intense (++++), as estimated by visual comparison of several autoradiographic films of sections hybridized to radioactively labeled synapsin I cDNA probes of comparable specific activities.

synapsin I immunostaining in the pyramidal cell layers of the hippocampus, the dentate gyrus, and the layer II cells of the entorhinal cortex (Fig. 7C). In the dentate gyrus, granule cells give rise to mossy fiber afferents which terminate solely upon neurons of the hilar zone and the proximal dendrites of the CA3–CA4 cells of the hippocampus. Here, in situ hybridization and immunohistochemistry revealed a direct correspondence between high levels of synapsin I mRNA in granule cell somata and intense synapsin I protein staining in their mossy fiber terminals (Fig. 7B,C). In contrast, in situ hybridization revealed intense levels of synapsin I mRNA in the somata of layer II neurons of the entorhinal cortex, while only moderate synapsin I protein staining was observed in the outer molecular layer of the dentate gyrus, the terminal field of these layer II neurons (Fig. 7B,C). These results suggest differential levels of expression of synapsin I mRNA and protein within neurons which compose a defined synaptic circuit in the adult rat brain.

DISCUSSION

In this paper, we present the first extensive in situ hybridization study describing the regional and cellular distribution of synapsin I mRNA in the central nervous system. We report the widespread but regionally variable distribution of synapsin I mRNA throughout the adult rat brain. Further, in the rat hippocampus we identify specific neurons in which the level of synapsin I mRNA in neuronal parikarya correlates directly with the level of synapsin I protein in the synaptic termini of those cells, and other neurons within the same synaptic circuit in which synapsin I mRNA and protein levels do not correspond.

Distribution of synapsin I mRNA in adult rat brain

Synapsin I cDNA probes revealed specific patterns of hybridization in different regions of the adult rat brain by RNA blot analysis and in situ hybridization. By RNA blot analysis, synapsin I cDNA probes recognized exclusively synapsin I mRNAs of 3.4 kb and 4.5 kb. The intensity of synapsin I mRNA hybridization varied in RNA prepared from different regions of the rat brain, suggesting differential levels of expression of synapsin I mRNAs in these areas. By in situ hybridization, similar patterns of hybridization emerged, and the intensity of synapsin I mRNA labeling in discrete subregions of the adult rat brain revealed by in situ hybridization corresponded with the strength of the hybridization signals obtained by RNA blot analysis (Fig. 1). Synapsin I mRNA labeling was clearly neuron-specific (Fig. 2), consistent with previous immunocytochemical and limited in situ hybridization data showing that synapsin I protein (De Camilli et al., '83a,b; Huttner et al., '83) and mRNA (Haas and DeGennaro, '88) are present only within neurons in the central nervous system. The greatest abundance of synapsin I mRNA was found in the pyramidal neurons of the CA3 and CA4 fields of the hippocampus, and in the mitral and internal granular cell layers of the olfactory bulb. Other areas notably abundant in synapsin I mRNA were the layer II neurons of the piriform cortex and layer II and V neurons of the entorhinal cortex, the granule cell neurons of the dentate gyrus, the pyramidal neurons of hippocampal fields CA1 and CA2, and the cells of the parasubiculum.

Synapsin I in situ hybridization patterns correlate with the distribution of mRNAs encoding other neuron-specific synaptic vesicle proteins

Immunohistochemical studies have shown that synapsin I and synaptophysin, a synaptic vesicle integral membrane protein, display similar distributions in the rat central nervous system (Sudhof et al., '89). Recently the distribution and cellular localization of synaptophysin mRNA in the rat brain has been reported (Marqueze-Pouey et al., '91). By

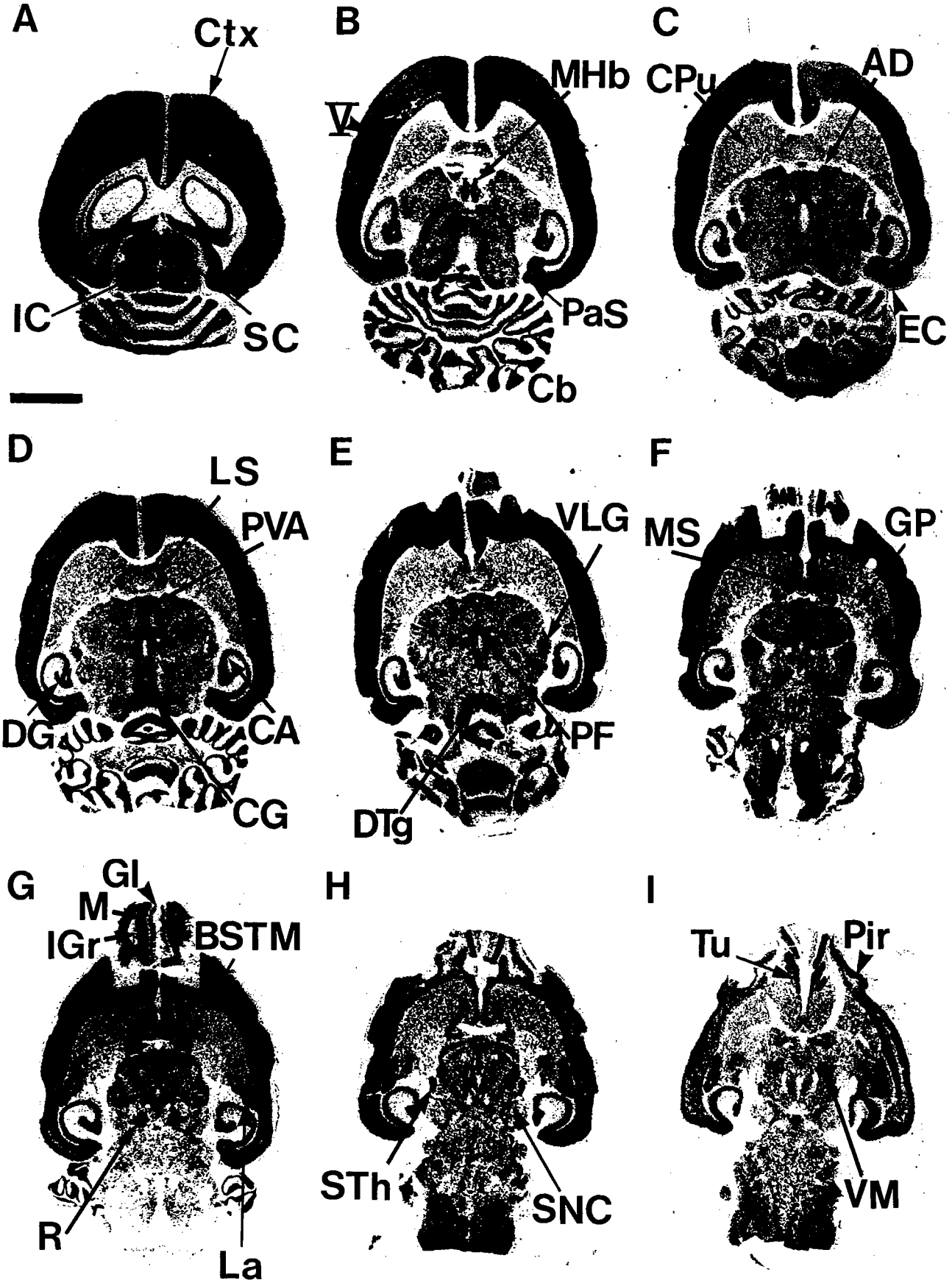
A
Ctx
IC
SC
B
MHb
V
PaS
Cb
C
CPu
AD
EC
D
LS
PVA
DG
CA
CG
E
VLG
PF
DTg
F
MS
GP
G
Gl
M
IGr
BSTM
R
La
H
STh
SNC
I
Tu
Pir
VM

Figure 3

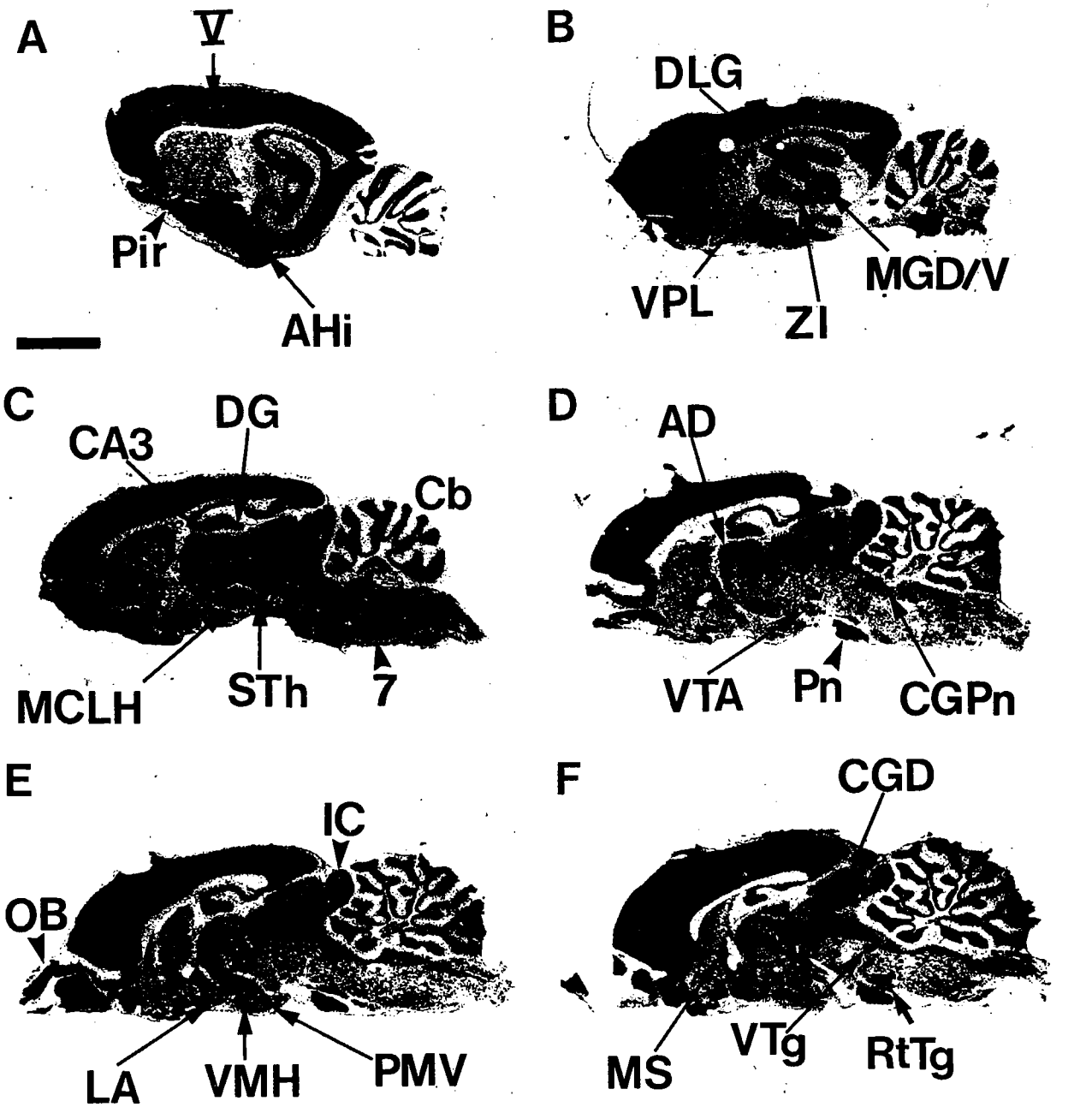

Fig. 4. In situ hybridization of synapsin I mRNA in parasagittal sections of adult rat brain. **A–F:** X-ray autoradiograms of sections hybridized to ^{35}S-labeled synapsin I cDNA probes. V, lamina V of the neocortex; 7, facial nucleus; AD, anterodorsal thalamic nucleus; AHi, amygdalohippocampal area; CA3, CA3 field of the hippocampus; Cb, cerebellum; CGD, central gray, dorsal part; CGPn, central gray of the pons; DG, dentate gyrus; DLG, dorsal lateral geniculate nucleus; IC, inferior colliculus; LA, lateroanterior hypothalamic nucleus; MCLH, magnocellular nucleus of the lateral hypothalamus; MGD/V, medial geniculate nucleus, dorsal and ventral parts; MS, medial septum; OB, olfactory bulb; Pir, piriform cortex; PMV, premammillary nucleus, ventral part; Pn, pontine nuclei; RtTg, reticulotegmental nucleus of the pons; STh, subthalamic nucleus; VMH, ventromedial hypothalamus; VPL, ventral posterolateral thalamic nucleus; VTA, ventral tegmental area; VTg, ventral tegmental nucleus; ZI, zona incerta. Sections were apposed to Kodak XAR-5 film for 10 days. Scale bar: 4 mm (for all panels).

Fig. 3. Distribution of synapsin I mRNA in horizontal sections of adult rat brain by in situ hybridization. **A–I:** X-ray autoradiograms of sections hybridized to ^{35}S-labeled synapsin I cDNA probes. V, lamina V of the neocortex; AD, anterodorsal thalamic nucleus; BSTM, bed nucleus of the stria terminalis, medial; CA, CA fields of the hippocampus; Cb, cerebellum; CG, central gray; CPu, caudate/putamen; Ctx, neocortex; DG, dentate gyrus; DTg, dorsal tegmental nucleus; EC, entorhinal cortex; Gl, glomerular layer; GP, globus pallidus; IC, inferior colliculus; IGr, internal granular layer; La, lateral amygdala; LS, lateral septum; M, mitral cell layer; MHb, medial habenula; MS, medial septum; PaS, parasubiculum; PF, parafasicular thalamic nucleus; Pir, piriform cortex; PVA, paraventricular thalamic nucleus, anterior part; R, red nucleus; SC, superior colliculus; SNC, substantia nigra pars compacta; STh, subthalamic nucleus; Tu, olfactory tubercle; VLG, ventral lateral geniculate nucleus; VM, ventromedial thalamic nucleus. Sections were exposed to Kodak XAR-5 film for 10 days. Scale bar: 4 mm (for all panels).

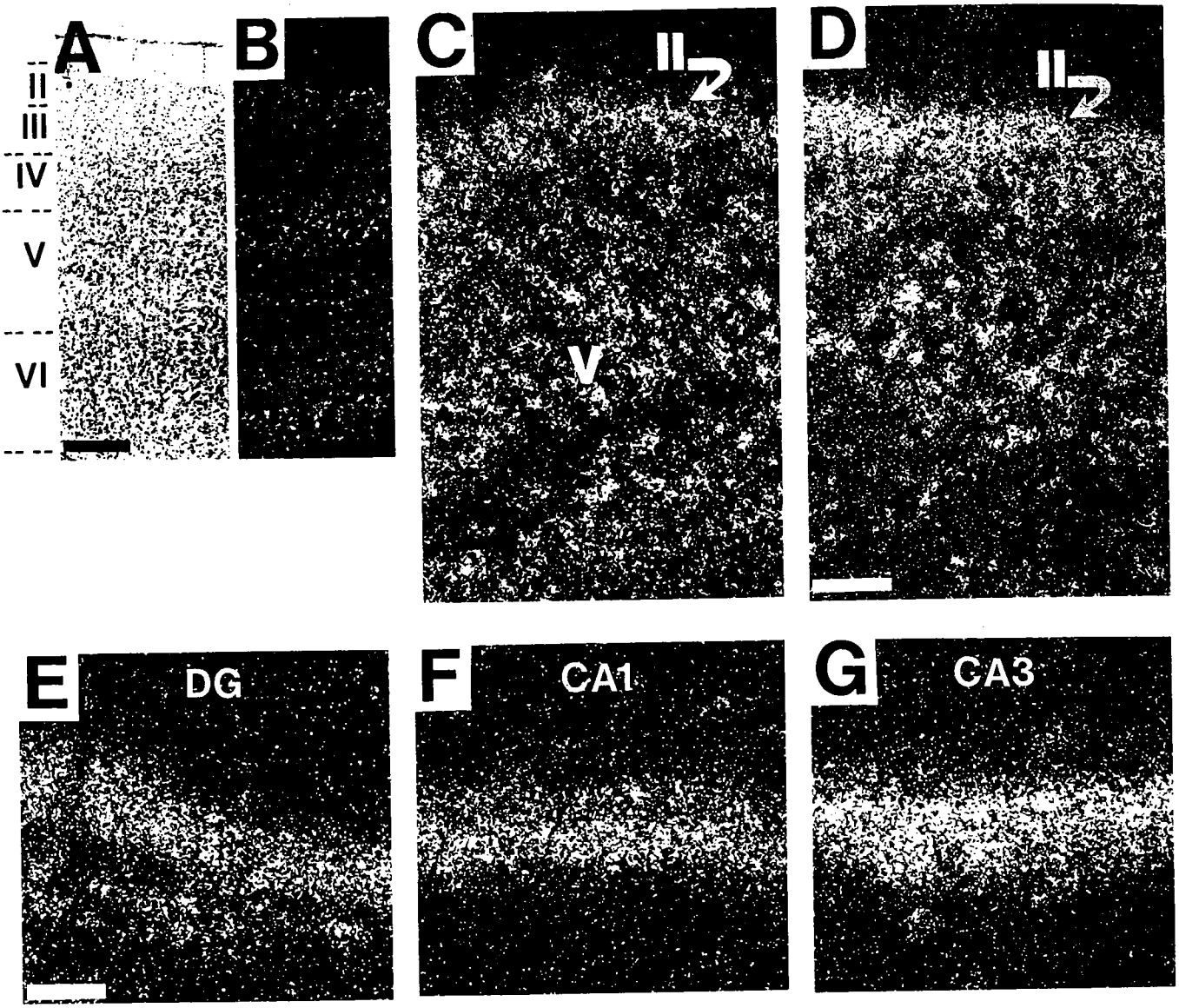

Fig. 5. High-magnification darkfield and brightfield photomicrographs of emulsion autoradiograms of cells of the parietal neocortex (**A** and **B**), entorhinal cortex (**C**), piriform cortex (**D**), dentate granule cell neurons of the dentate gyrus (**E**), and the pyramidal cells of the hippocampus (**F** and **G**) hybridized to ^{35}S-labeled synapsin I cDNA probes. Hybridization intensities were greatest in layer V of the parietal, layers II and V of the entorhinal, and layer II of the piriform cortex. The highest hybridization signals detected throughout the rat brain were present in the CA3 neurons of the hippocampus. I–VI, layers of the cerebral cortex; CA1, CA1 field neurons of the hippocampus; CA3, CA3 field neurons of the hippocampus; DG, dentate gyrus. Emulsion-coated sections were exposed for 2 weeks. Scale bars: A and B, 1 mm; C–G, 300 μm.

comparison, we observe a striking correlation between the patterns of expression of synapsin I and synaptophysin mRNAs in specific regions of the adult rat brain. High levels of both mRNAs are present in layers IV–V of the neocortex, in the mitral cell layer of the olfactory bulb, in all fields of the hippocampus proper and the dentate gyrus, the medial habenula, the paraventricular nucleus of the thalamus, and in the granule cells of the cerebellum. Additionally, light-to-moderate levels of both mRNAs were localized in the striatum, the basal forebrain, and in widespread areas of the thalamus. No correlation however, was observed between the localization of synapsin I and synaptophysin transcripts in the internal granule cell layer of the olfactory bulb. Here, synapsin I mRNAs were present at high levels, while little or no synaptophysin mRNAs were detected. In this cell layer however, a good correlation was observed between the localization of synapsin I and synaptoporin, a novel synaptophysin variant (Marqueze-Pouey et al., '91).

Synapsin I mRNA distribution correlates well with the pattern of expression of mRNAs encoding other synaptic vesicle proteins. VAMP-2 is another abundant synaptic vesicle protein whose mRNA expression pattern and distribution has been reported in rat central nervous system (Elferink et al., '89; Trimble et al., '90). Both the VAMP-2 and synapsin I genes express high levels of mRNAs in the substantia nigra pars compacta, the anterodorsal thalamus, the basolateral amygdala, the piriform cortex, and in all fields of the hippocampus proper and the dentate gyrus.

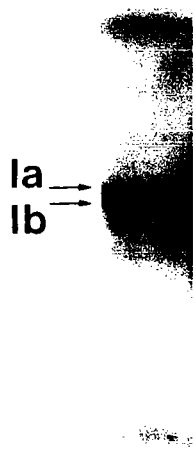

Fig. 6. Western blot demonstrating specificity of synapsin I polyclonal antibody. Purified rat total neocortical brain protein was prepared, electrophoresed, and blotted as described in text. Synapsin I polyclonal antibodies were bound and immunoreactive bands were visualized. Antibodies recognized exclusively synapsin Ia and Ib polypeptides, of 78 Kd and 74 Kd, respectively, and a small amount of synapsin I proteolysis products.

Similarly, the hippocampal localization and distribution of the mRNA for synaptosomal-associated protein, 25 kD, (SNAP-25), parallels that of synapsin I mRNA (Geddes et al., '90). In the adult rat hippocampus, the greatest abundance of SNAP-25 mRNA was in the large pyramidal neurons of CA3, with a lower density of hybridization signal in the CA1 pyramidal cells and in the granule cells of the dentate gyrus.

Heterogeneous distribution of synapsin I mRNA

Together the RNA blot and in situ hybridization data provide biochemical and histochemical evidence of regional variability in the level of synapsin I mRNA in the central nervous system. At least two possibilities exist to explain the heterogeneous distribution of synapsin I mRNA throughout the adult rat brain. One possibility is that strong hybridization signals reflect the number and density of neuronal somata per field. The mitral and internal granular cell layers of the olfactory bulb, the granule cell layer of the dentate gyrus, and the CA1 field of the hippocampus are all examples of densely packed layers of cells which exhibit high levels of synapsin I mRNA labeling. Densely packed nuclei also display strong labeling of synapsin I mRNA. The anterodorsal and paraventricular thalamic nuclei, the medial habenula, the subthalamic nucleus, and the substantia nigra pars compacta all display

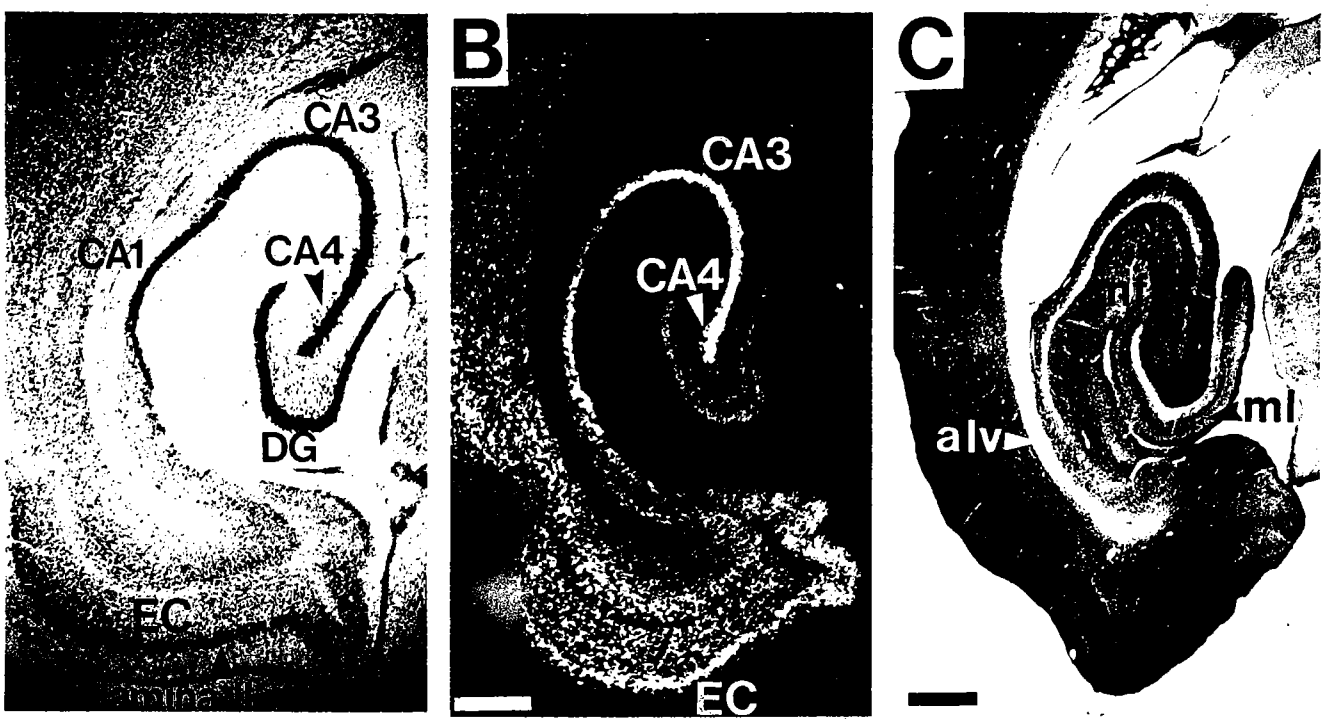

Fig. 7. Expression of synapsin I mRNA and protein in horizontal sections of the adult rat hippocampus. **A:** Cresyl violet stained section of rat hippocampal area to identify neuronal perikarya. **B:** Darkfield photomicrograph of an emulsion-coated section of the rat hippocampal area hybridized to ^{35}S-labeled synapsin I cDNA probes. Hybridization intensity is greatest over the pyramidal cells of CA3 and CA4, and the layer II neurons of the medial entorhinal cortex. **C:** Immunocytochemical localization of synapsin I protein in the rat hippocampus. Sections were immunostained with a polyclonal antibody raised against purified synapsin I protein. Intense immunoreactivity was apparent in the mossy fiber terminals, while moderate immunoreactivity was present in the molecular layer of the dentate gyrus. Immunoreactivity was weak in neuronal parikarya and in white matter fiber tracts. alv, alveus of the hippocampus; CA1, CA1 field neurons of the hippocampus; CA3, CA3 field neurons of the hippocampus; CA4, CA4 field neurons of the hippocampus; DG, dentate gyrus; EC, entorhinal cortex; mf, mossy fiber terminals; ml, molecular layer of the dentate gyrus. Emulsion-coated sections were exposed for 2 weeks. Scale bars: A, 55 μm; B, 65 μm; C, 70 μm.

similarly high hybridization signals by in situ hybridization. The cell types in each of these areas varies widely, from small spherical granule cells to large pyramidal neurons, densely packed in clusters forming a nucleus or tract of cells. In these regions, strong synapsin I mRNA hybridization signals are most probably related directly to cell packing.

A second possibility is that strong hybridization signals in discrete regions of rat brain reflect differences in the levels of synapsin I mRNA expressed in those cells. In these regions, hybridization intensity cannot be attributed solely to the number and packing density of neuronal perikarya. For example, Figure 5B shows high levels of synapsin I mRNA in the perikarya of neurons in layer V of the parietal neocortex. Although this region is low in cell number and packing density (Fig. 5A), these medium-sized neurons express high amounts of synapsin I mRNA, as evidenced by the sharp band of hybridization seen in Figures 3B–E, 4A–C, and 5B. Similarly, the small and medium-sized cells in layer V of the medial entorhinal cortex express notably high levels of synapsin I mRNA (Figs. 3C–E, 5C, 7B). Other examples of areas which appear to express levels of synapsin I mRNA not apparently related to packing density, are the pyramidal neurons of hippocampal field CA3, the layer II stellate cells of the entorhinal cortex, and the neurons of the parasubiculum. The large pyramidal neurons of CA3 are significantly less densely packed than the pyramidal neurons of the neighboring CA1 field and the granule cells of the dentate gyrus. The CA3 neurons, however, express appreciably higher levels of synapsin I mRNA (Fig. 5E–G) then cells in the other two regions. The layer II stellate neurons of the entorhinal cortex form a continuous layer of cells in the medial aspect of the parahippocampal gyrus. Here, although somewhat less densely packed than neurons of the dentate gyrus and CA1, the stellate cells display consistently higher hybridization signals (Fig. 7A,B). In fact, hybridization to synapsin I mRNA in these neurons was nearly equal in intensity to that in neurons of the CA3 field of the hippocampus (Fig. 7B). The parasubiculum lies adjacent to the medial entorhinal cortex and is characterized by a superficial layer of moderately packed medium-sized cells. The presubiculum lies next to the parasubiculum and is characterized typically by a lamina of densely packed small cells. Although significantly more densely packed, the presubiculum appears less labeled than its neighbor, suggesting different levels of expression of synapsin I mRNA between the two cell populations (Figs. 3B, 7B). The areas mentioned above contain neurons of various cellular profiles which form less densely packed and occasionally pale fields of neurons. These neurons however, exhibit strong hybridization to synapsin I cDNA probes by in situ hybridization. Thus, these data reflect differences in synapsin I mRNA levels in individual neurons representative of a specific region of the rat brain.

Dissimilar expression patterns of synapsin I mRNA and protein in the rat hippocampus

To address directly the possibility that high levels of synapsin I mRNA in discrete subsets of neurons may reflect the amount of synapsin I protein present in the presynaptic terminal fields of those neurons, we compared the pattern of expression of synapsin I mRNA and protein in the defined synaptic circuitry of the rat hippocampus. The rat hippocampus is a fold of cortex divided into four distinct fields, CA1–CA4, respectively (Fig. 7A). Accompanying the hippocampus is the dentate gyrus, a layer of densely packed granule cells whose dendritic arborizations ramify in a dense synaptic plexus in the molecular layer of the dentate gyrus. The major source of afferent inputs to the dentate granule cells is the large stellate cells of layer II of the medial entorhinal cortex (Desmond and Levy, '82). These afferents project ipsilaterally, via the perforant path, to the outer two-thirds of the molecular layer of the dentate gyrus. The dentate granule cells, then, extend mossy fiber axons locally to the mossy cells scattered throughout the hilus of the dentate gyrus and to the proximal dendritic field of ipsilateral CA3–CA4 neurons of the hippocampus.

Synapsin I mRNA and protein are present in neurons of the rat dentate gyrus and entorhinal cortex (Fig. 7). Synapsin I transcripts are expressed at notably high levels in granule cells of the dentate gyrus and at intense levels in the layer II neurons of the entorhinal cortex (Fig. 7B). Synapsin I protein, however, exhibits remarkably dissimilar patterns of expression in the presynaptic terminal fields of these two cell populations (Fig. 7C). Synapsin I protein is present in intense amounts in the mossy fiber terminal fields of dentate granule neurons. In contrast, the protein is present in only moderate amounts in the outer two-thirds of the molecular layer of the dentate gyrus, the terminal field of layer II entorhinal neurons. One possible explanation for the discrepancy between levels of synapsin I mRNA and protein in the somata and termini of specific neurons of the hippocampal region is that these levels may reflect simply the synaptic density or amount of terminal arborization of those cells. However, a review of synaptic density, as measured by quantitative ultrastructural analyses, suggests that the number of synapses per unit area is relatively invariant across the hippocampal neuraxis (Amaral and Dent, '81; Scheff et al., '85, '91). Therefore, local differences in synaptic density cannot adequately explain the variability in synapsin I protein staining in the terminal fields of neurons of the dentate gyrus and entorhinal cortex. Furthermore, the markedly dissimilar patterns of expression of synapsin I mRNA and protein in the neurons of the dentate gyrus and entorhinal cortex suggest that synapsin I mRNA levels cannot reflect simply the amount of synapsin I protein present in the terminal arborizations of central neurons. Alternatively, we propose that the differential levels of expression of synapsin I mRNA and protein in these synaptic circuits reflect differences in the functional properties and/or requirements of neurons which form these central synapses. For example, studies on the restoration of synaptic connections in response to selective nervous system lesions have demonstrated that the hippocampal formation possesses a robust potential for synaptic regrowth (see review by Cotman and Nieto-Sampedro, '84). In these studies, synapse replacement is achieved by the selective sprouting of residual inputs; in the case of unilateral entorhinal lesions, originating in hippocampal fields CA3c–CA4, layer II of the contralateral entorhinal cortex, and in the medial septum. Thus, locally high levels of synapsin I mRNA in hippocampal and entorhinal somata may reflect the ability of the system to be plastic and respond to injury and/or select environmental stimuli by producing long-term synaptic circuitry changes. Other neurons, in which synaptic plasticity is not a major necessity (i.e., dentate granule neurons), might still require locally high levels of synapsin I mRNA to maintain correspondingly high levels of synapsin I protein in their presynaptic terminal fields. In these neurons, high levels of synapsin I

gene expression (mRNA and protein) might be required to maintain high rates of activity that characterizes the circuits in which they participate.

In conclusion, we have shown that synapsin I mRNA exhibits widespread yet regionally variable levels of expression throughout the adult rat central nervous system. Further study, employing more quantitative in situ hybridization procedures and probes able to distinguish individual synapsin I mRNA subtypes, will be necessary to quantitate precisely the levels of the different isoforms of synapsin I mRNAs expressed in these areas. Additionally, we have demonstrated differential levels of expression of synapsin I mRNA and protein within the defined synaptic circuitry of the adult rat hippocampus. Studies invoking synaptic turnover and reorganization in this brain region may provide insight into the functional requirement for synapsin I gene expression in the restoration of synaptic contacts in the central nervous system.

ACKNOWLEDGMENTS

The authors thank Dr. Neil Aronin for suggesting the use of Dde I-digested DNA for in situ hybridization and Dr. Edward Fey for assistance with the Western blot analysis. R.H.M. would also like to extend special thanks to Dr. Mark J. Alexander for scientific guidance and expert technical assistance, to Drs. Erika L.F. Holzbaur and David S. Howland for their useful discussion and critical reading of the manuscript, and to K.A. Lonis for support and motivation.

This work was supported by NIH grants NS 25050 and NS 27833, and by the Departments of Anesthesiology and Neurology, University of Massachusetts Medical Center.

LITERATURE CITED

Amaral, D.G., and J.A. Dent (1981) Development of the mossy fibers of the dentate gyrus: I. A light and electron microscopy study of the mossy fibers and their expansions. J. Comp. Neurol. *195:*51–86.

Apostolides, P.J., L.J. DeGennaro, R.H. Melloni, Jr., D. Pulaski-Salo, and J.E. Hamos (1992) Localization of synapsin I in the adult rat central nervous system. Submitted.

Bahler, M., F. Benfenati, F. Valtorta, A.J. Czernik, and P. Greengard (1989) Characterization of synapsin I fragments by cysteine-specific cleavage: a study of their interactions with F-actin. J. Cell Biol. *198:*1841–1849.

Bahler, M., F. Benfenati, F. Valtorta, and P. Greengard (1990) The synapsins and the regulation of synaptic function. Bioessays *12:*259–263.

Bahler, M., and P. Greengard (1987) Synapsin I bundles F-actin in a phosphorylation-dependent manner. Nature *326:*704–707.

Benfenati, F., M. Bahler, M. Jahn, and P. Greengard (1989) Interactions of synapsin I with small synaptic vesicles: distinct sites in synapsin I bind to vesicle phospholipids and vesicle proteins. J. Cell Biol. *108:*1863–1872.

Bloom, F.E., T. Ueda, E. Battenberg, and P. Greengard (1979) Immunocytochemical localization, in synapses, of protein I, an endogenous substrate for protein kinase in mammalian brain. Proc. Natl. Acad. Sci. USA *76:*5982–5986.

Chirgwin, J.M., A.E. Przybyla, R.J. MacDonald, and W.J. Rutter (1979) Isolation of biologically active ribonucleic acid from sources enriched in ribonuclease. Biochemistry *18:*5294–5299.

Cotman, C.W., and N. Nieto-Sampedro (1984) Cell biology of synaptic plasticity. Science *225:*1287–1294.

De Camilli, P., R. Cameron, and P. Greengard (1983a) Synapsin I (protein I), a nerve-terminal specific phosphoprotein. I. Its general distribution in the synapses of the central and peripheral nervous system demonstrated by immunofluorescence in frozen and plastic sections. J. Cell Biol. *96:*1337–1354.

De Camilli, P., and P. Greengard (1986) Synapsin I: a synaptic vesicle-associated phosphoprotein. Biochem. Pharmacol. *35:*4349–4357.

De Camilli, P., S.M. Harris, W.B. Huttner, and P. Greengard (1983b) Synapsin I (protein I), a nerve terminal-specific phosphoprotein. II. Its specific association with synaptic vesicles demonstrated by immunocytochemistry in agarose-embedded synaptosomes. J. Cell Biol. *96:*1355–1373.

DeGennaro, L.J., P.J. Apostolides, D. Pulaski-Salo, and J.E. Hamos (1989) Localization of synapsin I in adult rat brain. Soc. Neurosci. Abstr. *15:*680.

Desmond, N.L., and W.B. Levy (1982) A quantitative anatomical study of the granule cell dendritic fields of the rat dentate gyrus using a novel probabilistic method. J. Comp. Neurol. *212:*131–145.

Elferink, L.A., W.S. Trimble, and R.H. Scheller (1989) Two vesicle-associated membrane protein genes are differentially expressed in the rat central nervous system. J. Biol. Chem. *264:*11061–11064.

Geddes, J.W., E.J. Hess, R.A. Hart, J.P. Kesslak, C.W. Cotman, and M.C. Wilson (1990) Lesions of hippocampal circuitry define synaptosomal-associated protein-25 (SNAP-25) as a novel presynaptic marker. Neuroscience *38:*515–525.

Goelz, S.E., E.J. Nestler, B. Chehrazi, and P. Greengard (1981) Distribution of protein I in mammalian brain as determined by a detergent-based radioimmunoassay. Proc. Natl. Acad. Sci. USA *78:*2130–2134.

Haas, C.A., and L.J. DeGennaro (1988) Multiple synapsin I messenger RNAs are differentially regulated during neuronal development. J. Cell Biol. *106:*195–203.

Hamos, J.E., L.J. DeGennaro, and D.A. Drachman (1988) Synaptic loss in Alzheimer's disease and other dementias. Neurology *39:*355–361.

Heumann, R., and H. Thoenen (1986) Comparison between the time course of changes in nerve growth factor protein levels and those of its messenger RNA in the cultured rat iris. J. Biol. Chem. *261:*9246–9249.

Huttner, W.B., and P. Greengard (1979) Multiple phosphorylation sites in protein I and their differential regulation by cyclic AMP and calcium. Proc. Natl. Acad. Sci. USA *76:*5402–5406.

Huttner, W.B., W. Schiebler, P. Greengard, and P. De Camilli (1983) Synapsin I (protein I), a nerve terminal specific phosphoprotein. III. Its association with synaptic vesicles studied in a highly purified synaptic vesicle preparation. J. Cell Biol. *96:*1374–1388.

Kahn, D.W., and W.B. Besterman (1991) Cytosolic rat brain synapsin I is a diacylglycerol kinase. Proc. Natl. Acad. Sci. USA *88:*6137–6141.

Kilimann, M.W., and L.J. DeGennaro (1985) Molecular cloning of cDNAs for the nerve-cell specific phosphoprotein, synapsin I. EMBO J. *4:*1997–2002.

Klose, J., and E. Zeindl (1984) An attempt to resolve all the various protein in a single human cell type by two-dimensional electrophoresis: I. Extraction of all cell proteins. Clin. Chem. *30(12):*2014–2020.

Kyhse-Anderson, J. (1984) Electroblotting of multiple gels: A simple apparatus without buffer tank for rapid transfer of proteins from polyacrylamide to nitrocellulose. J. Biochem. Biophys. Methods *10:*203–209.

Laemmli, E.K. (1970) Cleavage of structural proteins during the assembly of the head of bacteriophage T4. Nature *227:*680–685.

Llinas, R., T.L. McGuinness, C.S. Leonard, M. Sugimori, and P. Greengard (1985) Intraterminal injection of synapsin I or calcium calmodulin-dependent protein kinase II alters neurotransmitter release at the squid giant synapse. Proc. Natl. Acad. Sci. USA *82:*3055–3039.

Maniatis, T., E.F. Fritsch, and J. Sambrook (1982) Molecular Cloning: A Laboratory Manual. Cold Spring Harbor, NY: Cold Spring Harbor Laboratory.

Marqueze-Pouey, B., W. Wisden, M.L. Malosio, and H. Betz (1991) Differential expression of synaptophysin and synaptoporin mRNAs in the postnatal rat central nervous system. J. Neurosci. *11:*3388–3397.

McGuinness, T.L., Y. Lai, and P. Greengard (1985) Ca2+/calmodulin-dependent protein kinase II (isozymic forms from rat forebrain and cerebellum). J. Biol. Chem. *260:*1696–1704.

McLean, I.W., and P.K. Nakane (1974) Periodate-lysine-paraformaldehyde fixative. A new fixative for immunoelectron microscopy. J. Histochem. Cytochem. *22:*1077–1083.

Melloni, R.H., Jr., P.S. Estes, D.S. Howland, and L.J. DeGennaro (1992) A method for the direct measurement of mRNA in discrete regions of mammalian brain. Anal. Biochem. *200:*95–99.

Nairn, A.C., and P. Greengard (1987) Purification and characterization of Ca^{2+}/calmodulin-dependent protein kinase I from bovine brain. J. Biol. Chem. *262:*7273–7281.

Navone, F., P. Greengard, and P. De Camilli (1984) Synapsin I in nerve terminals: selective association with small synaptic vesicles. Science *226:*1209–1211.

Nestler, E.J., and P. Greengard (1984) Protein Phosphorylation in the Nervous System. N.Y.: Wiley.

Palkovitz, M., and M.J. Brownstein (1988) Maps and Guide to Microdissection of Rat Brain. N.Y.: Elsevier.

Petrucci, T.C., and J.S. Morrow (1987) Synapsin I: an actin-bundling protein under phosphorylation control. J. Cell Biol. *105:*1355–1363.

Scheff, S.W., K.J. Anderson, and S.T. DeKosky (1985) Strain comparison of synaptic density in hippocampal CA1 of aged rats. Neurobiol. Aging *6:*29–34.

Scheff, S.W., S.A. Scott, and S.T. DeKosky (1991) Quantitation of synaptic density in the septal nuclei of young and aged Fisher 344 rats. Neurobiol. Aging *12:*3–12.

Schiebler, W., R. Jahn, J.P. Doucet, J. Rothein, and P. Greengard (1986) Characterization of synapsin I binding to small synaptic vesicles. J. Biol. Chem. *261:*8383–8390.

Smith, T.W., S. Nikulasson, U. De Girolami, and L.J. DeGennaro (1992) Immunohistochemistry of synapsin I and synaptophysin in human nervous system and neuroendocrine tumors. J. Neuropathol. Exp. Neurol. (in press).

Sudhof, T.C., A.J. Czernik, H.T. Kao, K. Takei, P.A. Johnston, A. Horiuchi, S.D. Kanazir, M.A. Wagner, M.S. Perin, P. De Camilli, and P. Greengard (1989) Synapsins: mosaics of shared and individual domains in a family of synaptic vesicle phosphoproteins. Science *245:*1474–1480.

Thomas, P.S. (1980) Hybridization of denatured RNA and small DNA fragments transferred to nitrocellulose. Proc. Natl. Acad. Sci. USA *77:*5201–5205.

Towbin, H., T. Staehelin, and J. Gordon (1979) Electrophoretic transfer of proteins from polyacrylamide gels to nitrocellulose sheets: Procedure and some applications. Proc. Natl. Acad. Sci. USA *76:*4350–4354.

Trimble, W.S., T.S. Gray, L.A. Elferink, M.C. Wilson, and R.H. Scheller (1990) Distinct patterns of expression of two VAMP genes within the rat brain. J. Neurosci. *10:*1380–1387.

Ueda, T., and P. Greengard (1977) Adenosine 3′:5′-monophosphate regulated phosphoprotein system of neuronal membranes. I. Solubilization, purification and some properties of an endogenous phosphoprotein. J. Biol. Chem. *252:*5155–5163.

Ueda, T., H. Maeno, and P. Greengard (1973) Regulation of endogenous phosphorylation of specific proteins in synaptic membrane fractions from rat brain by adenosine 3′,5′-monophosphate. J. Biol. Chem. *248:*8295–8305.

Walaas, S.I., M.D. Browning, and P. Greengard (1988) Synapsin Ia, synapsin Ib, protein IIIa, protein IIIb, four related synaptic vesicle-associated phosphoproteins, share regional and cellular localization in rat brain. J. Neurochem. *51:*1214–1220.

Walaas, S.I., A.C. Nairn, and P. Greengard (1983) Regional distribution of calcium- and cyclic adenosine 3′;5′-monophosphate-regulated protein phosphorylation systems in mammalian brain. J. Neurosci. *3:*291–301.